Immune regulation in health and Juvenile Idiopathic Arthritis (JIA): molecular mechanisms and regulatory T cells

Anne Maria Pesenacker

This dissertation is submitted for the degree of

Doctor of Philosophy (PhD)

May 2013

University College London (UCL)

Rheumatology department - Institute of Child Health

Declaration

I, Anne Maria Pesenacker, confirm that this work presented here is my own. Where information or data has been derived from or produced by others, it has been indicated in this thesis.

Abstract

Immune regulation is essential to fighting pathogens and tolerance to self and non-harmful (food and commensal) antigens. The immune system has several mechanisms in place to keep the immune system in balance. In this study some of these mechanisms are more closely investigated in health and disease.

In autoimmune Juvenile Idiopathic Arthritis (JIA) immune regulation fails at the site of disease, with large pro-inflammatory cell infiltrates and inflammation. In the first part of this thesis potential mechanisms in regulating the severity of JIA are examined through analysis of previously acquired gene expression array data from oligoarticular JIA synovial fluid cells at the time of diagnosis, stratified by disease severity outcome after one year. Expression of three genes (SMAD3, ERRFI1 and VIPR1) was tested using RT-PCR. Particular focus was put on vasoactive intestinal peptide receptor type one (VIPR1), as it was expressed at lower levels and with an apparent variant at the inflamed site of JIA.

Regulatory T cells (Treg) are one essential part of immune regulation. Recent studies have suggested some pro-inflammatory potential by Treg producing cytokines including IL-17 and IFN-γ. In this thesis Treg cytokine production was linked to CD161 expression. CD161+ Treg were characterized in health, throughout development and in JIA.

CD161+ Treg showed a memory effector T cell like phenotype, including expression of transcription factors (Tbet, RORCv2). However CD161+ Treg were also potent suppressors *in vitro* and showed a predominantly demethylated Treg specific demethylated region (TSDR). CD161+ Treg appeared pathogen specific and behaved differently to TCR stimulation as CD161- Treg. Furthermore CD161+ Treg were highly enriched in the synovial fluid of JIA and correlated with disease.

This thesis suggests that immune regulation is influenced by the inflammatory environment and has more facets to it, with cytokine-producing Treg playing an important part in health and disease.

Acknowledgements

First of all I would like to thank my supervisor Lucy R Wedderburn. Her enthusiasm, guidance and knowledge always helped and encouraged me. I would also like to thank David Bending for scientific and non-scientific talks, and his expertise and help especially with epigenetic analysis. I'm grateful for advice and support in the lab throughout my PhD from Simona Ursu (especially her help with cloning) and Hemlata Varsani (in particular for her work on immunofluorescent histology); Anna Furmanski was helpful throughout investigations of thymocytes and I'm thankful to her; Patricia Hunter and Ebun Omoyinmi for their advice regarding gene expression array analysis and our summer student Qiong Wu for assistance in T cell receptor cloning and analysis. I would also like to thank my secondary supervisor Tessa Crompton for her scientific discussions and input. Ayad Eddaoudi, Ambika Angheluta and Anna Rose are thanked for their help with flow cytometry sorting. Furthermore I'm grateful to past and present lab and group members for guidance and support: Halima Moncrieffe, Kiran Nistala, Laura Kassamouri, Balathas Thirugnanabalan, Fiona Patrick, Natasha Makengo, Katie Arnold, Sophie B Gordon-smith and Chantal Duurland. I would like to thank everyone (past and present) from the infection and immunity department on the 5^{th} and 6^{th} floor for advice, discussions and company throughout the four years I enjoyed working with them.

Special thanks go to all the healthy volunteers, patients and their families and Great Ormond Street Hospital and Rheumatology lab staff for samples. I'm grateful to my funders: the Oliver Bird program from the Nuffield foundation.

Outside of the laboratory I would like to thank my family and friends, without whose encouragement and support my studies would not have been possible. I would especially like to thank Tonya Kueck who was always there for me.

Abbreviations

A

Ab	Antibody
AIDS	Acquired immunodeficiency syndrome
AKT	V-akt murine thymoma viral oncogene homolog 1 (also known as Protein Kinase B (PKB))
AMP	Adenosine-5'-monophosphate
ANOVA	Analysis of variance
AP-1	Activator protein 1
APC	Antigen Presenting Cell
APC	Allophycocyanin
APS	Ammonium persulfate
ATP	Adenosine-5'-triphosphate

B

BCR	B cell receptor
bp	Base pair
BSA	Bovine Serum Albumin

C

C	Celsius
C. albicans	*Candida albicans*
CCR	CC Chemokine receptor
CD	Cluster of Differentiation
cDNA	Complementary deoxyribonucleic acid
CDR	Complementarity determining region
CM	complete media (RPMI 1640 + 1% v/v P/S + 10% v/v FBS)
CpG islands	DNA region wit a cytosine - phosphate - guanine combination (here CpG islands are analyzed in context of DNA methylation)
CRP	C-reactive protein
CT	Cycle threshold
CTLA-4	cytotoxic T lymphocyte antigen 4

D

Da	Dalton
DC	Dendritic cell
DEAF1	Deformed epidermal autoregulatory factor 1
DMSO	Dimethylsulphoxide
DNA	Deoxyribonucleic acid
DPBS	Dulbecco's Phosphate Buffered Saline
DTT	Dithiothreitol

E

EAE	Experimental Autoimmune Encephalomyelitis
EDTA	Ethylenediaminetetraacetic acid
EGTA	Ethylene glycol tetraacetic acid
ERK	Extracellular signal-regulated kinases
ERRFI1	ERbB receptor feedback inhibitor
ESR	erythrocyte sedimentation rate

F

FACS	Fluorescence Activated Cell Sorting
FBS	Foetal Bovine Serum
Fc-R	Fc receptor
FITC	Fluorescein Isothiocyanate
FoxP3	Forkhead box P3
FSC	Forward scatter

G

g	Gravity
glu	Glutamine
Gy	Gray
GVHD	Graft-versus Host Disease

H

HCL	Hydrochloric acid
hCMV	*human Cytomegalovirus*
HIV	Human immunodeficiency virus
HT29	Human colon adenocarcinoma grade II cell line

I

IFN-γ	Interferon gamma
IL	Interleukin
IL-23R	Interleukin 23 receptor
ILAR	International League of Associations for Rheumatology
iNKT	invariant Natural Killer T cell
IPEX	Immunodysregulation Polyendocrinopathy Enteropathy X-linked syndrome

J

JIA	Juvenile Idiopathic Arthritis

L

LB agar	Luria-Bertani agar
LLT1	Lectin like transcript 1

K

kb	Kilo bases
KLRB1	Killer cell lectin-like receptor subfamily B, member 1: the gene encoding CD161

M

M	Molar
MAIT cells	Mucosal associated invariant T cells
MFI	Median Fluorescence Intensity
mg	Milligram

MHC	Major Histocompatibility Complex
mL	Milliliter
mM	Millimolar
mRNA	Messenger ribonucleic acid
MTX	Methotraxate
MW	Molecular Weight

N

NaCl	Sodium chloride
NaVO4	Sodium Orthovandate
NCBI	National Center for Biotechnology Information
ng	Nanograms
NF-κB	Nuclear Factor kappa B
NK	Natural killer
NKRP1 family	Natural killer receptor protein 1 family: CD161 is in humans the only member of this family; in mice there are several members
NOD mice	Non-obese diabetic mice
nTreg	Natural T regulatory cell

O

O-JIA	Oligoarticular JIA

P

p	Probability
PAC1	pituitary adenylate cyclase activating polypeptide receptor 1
pAKT	at serine 473 phosphorylated AKT
PB	Peripheral blood
PBMC	Peripheral blood mononuclear cells
PBS	Phosphate Buffered Saline
PBST	Phosphate Buffered Saline Tween20
PCR	Polymerase chain reaction
PE/RPE	R-Phycoerythrin

PE-Cy5	R-Phycoerythrin-cyanine 5
PeCy7/PC7	R-Phycoerythrin-cyanine 7
PerCP	Peridinin-chlorophyll-protein complex
PFA	Paraformaldehyde
PI3K	Phosphoinositide 3-kinase
P-JIA	Polyarticular JIA
PMA	Phorbol Myristate Acetate
P/S	Penicillin/ Streptomycin

R

RA	Rheumatoid Arthritis
RNA	Riboneucleic acid
rpm	Revolutions per minute
RPMI 1640	Roswell Park Memorial Institute 1640 (media)
RORCv2	Retinoic acid related orphan receptor C variant 2
RT	Room temperature
RT-PCR/qPCR	Real-time Polymerase chain reaction

S

SDS	Sodiumdodecylsulfate
SEM	Standard error of the mean
SF	Synovial fluid
SFMC	Synovial fluid mononuclear cells
sJIA	Systemic JIA
SMAD	Similar to Mothers Against Decapentaplegic
SNP	Single nucleotide polymorphism
S.O.C media	Super Optimal broth with Catabolite repression media
SSC	Side scatter
STAT	Signal transducer and activator of transcription

T

t	Time
Tbet	T-box expressed in T cells - protein
TBX21	T-box expressed in T cells - gene
TBE	Tris Borate EDTA buffer
TBS	Tris-Buffered Saline
TBST	Tris-Buffered Saline Tween-20
TCR	T cell receptor
TCRBJ	J region of the TCR beta chain
TCRBC	C region of the TCR beta chain
Tconv	conventional T helper cell
TEMED	Tetramethylethylenediamine
Tfh	T follicular helper cell
TGF-β	Tumor Growth Factor beta
Th	T helper
TLR	Toll-like receptor
TM	transmembrane spanning unit
TNF-α	Tumor Necrosis Factor alpha
Treg	T regulatory cell
TSDR	Treg specific demethylated region

U

U	Units

V

Vβ	Variable chain beta of the TCR
VIP	Vasoactive Intestinal Peptide
VIPR1	VIP receptor type one
VIPR2	VIP receptor type two
vs	Versus

µ

µg	Microgram
µL	Microlitre
µM	Micromolar

Table of Contents

Declaration **2**

Abstract **3**

Acknowledgements **4**

Abbreviations **5**

List of Figures **18**

Chapter 1

1. Introduction **22**

1.1. Immune system - Tolerance, Regulation, Autoimmunity 22

1.1.1. Autoimmunity 23

1.1.2. Tolerance and regulation 25

1.1.3. Alternative regulation of the NF-κB pathway by immune signaling 26

1.2. T cell development and T cell receptor (TCR) 29

1.3. CD4+ T cells and subsets 30

1.4. Plasticity of T cells 31

1.5. Th17 31

1.6. FoxP3+ regulatory CD4 T cells (Treg) 33

1.6.1. The emergence of regulatory T cells 33

1.6.2. Different subsets of Treg 34

1.6.3. Treg can have effector cell properties 36

1.7. Juvenile Idiopathic Arthritis (JIA) 40

1.7.1. Immunopathology of the joint in JIA 43

1.7.2. Immunopathology regarding Treg in JIA 44

1.7.3. Treatment of JIA - and how it affects Treg 47

1.8. Project aims 51

Chapter 2

2. Materials and Methods **53**

2.1. Sample collection 53

2.1.1. Preparation of Peripheral and Umbilical Cord Blood Mononuclear Cells (PBMC and UBC respectively) 53

2.1.2. Preparation of Synovial Fluid Mononuclear Cells (SFMC) 54

2.1.3. Preparation of thymocytes 54

2.1.4. Continuous Cell Culture 54
2.1.5. Counting viable cells 55
2.1.6. Freezing and thawing of cells 55
2.2. Protein expression by Western Blotting 56
2.2.1. Sample preparation 56
2.2.2. SDS-PAGE gel electrophoresis 58
2.2.3. Transfer 58
2.2.4. Blocking and Protein detection 59
2.2.5. Stripping of Western membranes 59
2.3. Flow cytometry 60
2.3.1. Buffers and Solutions 60
2.3.2. Antibodies 60
2.3.3. Antibody labelling 62
2.3.4. Fixable live-dead staining 62
2.3.5. Surface Marker staining for Flow cytometry 62
2.3.6. Intracellular Staining using PFA and PERM Buffers 63
2.3.7. Intracellular Staining using FoxP3 Buffers 63
2.3.8. pAKT staining 63
2.3.9. Cytokine capture assay 65
2.3.10. Flow cytometry Analysis 65
2.4. Cell sorting 66
2.4.1. Magnetic bead cell sorting – positive selection 66
2.4.2. Magnetic bead sorting – negative T cell or CD4+ T cell enrichment 66
2.4.3. Flow cytometry cell sorting 67
2.4.4. Sorting strategy for monocyte, B and T cells 67
2.4.5. Sort strategy for regulatory and conventional T cells (Treg and Tconv) 69
2.5. Functional cell culture assays 70
2.5.1. CFSE labelling 70
2.5.2. Inhibition of IL-2 induction through VIPR1 activation 70
2.5.3. *In vitro* proliferation and suppression assays 70
2.5.4. Treg expansion 71
2.5.5. CD161 expression control and stability 71

2.5.6. CD161 ligation 72
2.5.7. Antigen specific culture 72
2.6. Analysis of gene expression 73
2.6.1. RNA extraction 73
2.6.2. First strand copy DNA (cDNA) synthesis 74
2.6.3. PCR and Real Time (RT)-PCR 75
2.6.4. Analysis of PCR: Agarose gel electrophoresis 78
2.6.5. Analysis of RT-PCR 78
2.7. Molecular Cloning 80
2.7.1. TCR-Vβ2 CDR3 cloning 81
2.7.2. Genomic DNA extraction 82
2.7.3. *FOXP3* TSDR methylation analysis 82
2.8. Fluorescent microscopy 84
2.9. Statistical Analysis 84

Chapter 3

3. Gene expression array target finding, validation and investigation 86
3.1. Introduction 86
3.2. Results 88
3.2.1. Gene expression array data analysis using different approaches - IPA, DAVID, lists of different rankings 88
3.2.2. Gene expression of VIPR1, SMAD3, ERRFI1 by RT-PCR 96
3.2.3. Expression of VIPR1 protein 101
3.2.4. Potential mechanism of small VIPR1 isoform 104
3.2.5. VIPR1 functional assays: IL-2 inhibition by VIP 107
3.3. Discussion 109

Chapter 4

4. CD161+FoxP3+ CD4+ T cells: the subset of Treg capable of producing pro-inflammatory cytokines - characterisation and phenotype in health 114
4.1. Introduction 114
4.2. Results 116
4.2.1. CD161+ Treg in healthy adults, children, cord blood and thymus 116
4.2.2. CD161+ Treg produce pro-inflammatory cytokines 121
4.2.3. CD161+ Treg phenotype - similarities with effector memory Tconv 124

4.2.4. CD161+ Treg express Treg functional markers 127
4.2.5. CD161+ Treg use a diverse Vβ repertoire, but may have a distinct origin to CD161- Treg 129
4.3. Discussion 133

Chapter 5

5. Stability and function of CD161+ Treg 136
5.1. Introduction 136
5.2. Results 138
5.2.1. Treg specific functions of CD161+ Treg 138
5.2.2. CD161+ Treg are predominantly demethylated at the Treg specific demethylated region 143
5.2.3. CD161 stability and regulation of expression 145
5.2.4. CD161+ Treg with their cytokine-producing phenotype are stable in longer-term Treg expansion 149
5.2.5. CD161+ Treg function and CD161 as a functional receptor 151
5.3. Discussion 157

Chapter 6

6. CD161+ Treg in Juvenile Idiopathic Arthritis 161
6.1. Introduction 161
6.2. Results 163
6.2.1. CD161+ Treg are enriched in the joint of JIA 163
6.2.2. Joint Treg are potent cytokine producers and share an effector-like phenotype 167
6.2.3. The enrichment of CD161+ cells is not equal between different T cell subsets 171
6.2.4. Joint CD161+ Treg show distinct association to IL-17 producing T cells and clinical measurements 175
6.2.5. The CD161 ligand LLT1 is expressed on JIA synovium 177
6.3. Discussion 179

Chapter 7

7. Discussion 182
7.1. Cytokine-producing Treg - what does this mean for our view on Treg? 184
7.2. Is CD161 essential for the full phenotype of CD161+ Treg? 188

7.3. The environment of the arthritic joint as a factor for disease severity and progression - Is autoimmune inflammation a 'vicious circle'? 192

8. References 196

9. List of publications arising from this work or contributed to during this PhD programme 218

10. Appendices 219

Appendix I: VIPR1 isoform sequence alignment 220

Appendix II: Full list of pathways identified by IPA and DAVID 229

Appendix III: List of clone sequences found in CD161- and/or CD161+ Treg by CDR3 cloning and sequencing of TCR-Vβ2 233

List of Tables

Table 1.1: ILAR classification of Juvenile Idiopathic Arthritis subtypes 41
Table 2.1: Buffer for sample preparation 57
Table 2.2: Recipe for 10% SDS-PAGE gel 58
Table 2.3: Antibodies used for Western blotting 59
Table 2.4: Buffers and Solutions, final concentrations shown 60
Table 2.5: Antibodies used for flow cytometry 61
Table 2.6: Sorting Buffer, final concentrations shown 66
Table 2.7: Master Mix per sample for cDNA synthesis by random hexamers 74
Table 2.8: Master Mix per sample for standard PCR (A) and RT PCR (B) 75
Table 2.9: PCR programs used 76
Table 2.10: RT-PCR primers used 77
Table 2.11: PCR primers used for VIPR1 exon splicing investigation 77
Table 2.12: PCR master mix using High Fidelity *Taq* 81
Table 2.13: PCR programs used for amplification of TCR-Vβ2, *FOXP3* TSDR and cloning products 83
Table 2.14: PCR primers used for amplification of TCR-Vβ2, *FOXP3* TSDR and cloning products 83
Table 3.1: Top 20 functional in the categories immunity, signalling, transcription and cell proliferation and differentiation 91
Table 3.2: Top 10 differentially expressed genes ranked according to p-value and fold change 93

List of Figures

Figure 1.1: Schematic overview of the NF-κB pathway with proposed effects of ERRFI1, SMAD3 and VIPR1. 28
Figure 1.2: Schematic of different regulatory T cell families. 39
Figure 2.1: Sorting strategy for separation of mononuclear cells from SFMC and PBMC. 68
Figure 2.2: Sorting strategy for CD161+ CD4+ Treg. 69
Figure 3.1: Functional annotation by IPA and DAVID programmes of differential expressed genes by gene expression array. 90
Figure 3.2: Relative expression levels of ERRFI1, SMAD3 and VIPR1 genes in SFMC form patients with persistent and extended-to-be oligoarticular JIA. 95
Figure 3.3: Gene expression of SMAD3 (A), ERRFI1 (B) and VIPR1 (C) quantified by RT-PCR. 97
Figure 3.4: SMAD3, ERFFI1 and VIPR1 mRNA expression in sorted cell substes of healthy adult PBMC, JIA PBMC and SFMC quantified by RT-PCR. 99
Figure 3.5: Analysis of VIPR1 protein expression in synovial and peripheral blood cells. 103
Figure 3.6: PCR amplification products from a set of reactions using diagnostic primer pairs suggest different mRNA between healthy PBMC and JIA SFMC. 106
Figure 3.7: VIPR1 function in healthy PBMC and JIA SFMC by inhibition of PMA/ionomycin induced IL-2 in CD3+CD4+ cells by VIP and VIPR1-specific agonist. 108
Figure 4.1: Choice of clone of anti-FoxP3 monoclonal antibody does not affect quantification of CD161+ regulatory T cells or analysis of their phenotype. 117
Figure 4.2: CD161 expression by regulatory T cells. 118
Figure 4.3: CD161 expression by regulatory T cells in immunological inexperienced cells. 120
Figure 4.4: CD161+FoxP3+ regulatory T cells can produce pro-inflammatory cytokines *ex-vivo*. 122
Figure 4.5: Cytokines produced by CD161+ Treg arise from the CD127 low population and are actively secreted. 123

Figure 4.6: Transcription factor expression in CD161+FoxP3+ cells at protein and mRNA level. 125
Figure 4.7: CD161+FoxP3+ regulatory T cells share phenotypic features with memory effector T cells. 126
Figure 4.8: CD161+FoxP3+ regulatory T cells express CD39 and only a subpopulation of CD161+FoxP3+ cells express Helios.....128
Figure 4.9: CD161+ regulatory T cells do not express an invariant TCR. 130
Figure 4.10: CD161- and CD161+ Treg do contain small clonal populations within the TCR-Vβ2 expressing cells, but their repertoires are predominantly non-overlapping with each other. 132
Figure 5.1: CD161+FoxP3+CD4+ T cells are suppressive and anergic *in vitro*. 140
Figure 5.2: CD161+ Treg produce pro-inflammatory cytokine during the suppression assays. 142
Figure 5.3: Both CD161- Treg and CD161+ Treg contain a predominantly demethylated *FOXP3* TSDR region.....144
Figure 5.4: Regulation of CD161 expression during *in vitro* culture and on stimulation. 146
Figure 5.5: CD161+ regulatory T cells are stable during *in vitro* short-term culture....148
Figure 5.6: CD161+ regulatory T cells and cytokine-producing phenotype persist upon Treg expansion. 150
Figure 5.7: Antigen specific-Treg responses lie predominantly within the CD161+FoxP3+ subset. 152
Figure 5.8: CD161+ Treg have increased pAKT upon TCR stimulation. 153
Figure 5.9: Effects of CD161 ligation. 156
Figure 6.1: CD161 expression by regulatory T cells is enriched in the inflammatory environment. 165
Figure 6.2: SF conventional and regulatory T cells produce high levels of cytokine, in particular the CD161+ Treg population. 168
Figure 6.3: SF regulatory T cells are enriched in other effector molecules, predominantly by CD161+ Treg. 170
Figure 6.4: CD161 expression is highly enriched on CD4+ T cells in JIA synovial fluid (SF). 172

Figure 6.5: CD161+ Treg frequency is not associated with CD161+Tconv frequency in JIA synovial fluid (SF). 174
Figure 6.6: CD161+ and CD161- Treg frequencies have different correlations with Th17 frequencies and clinical disease activity. 176
Figure 6.7: CD161 ligand LLT1 is expressed on the synovium of JIA. 177

Chapter 1

Introduction

1. Introduction

1.1. Immune system - Tolerance, Regulation, Autoimmunity

The body employs several mechanisms to maintain immune homeostasis, and protect the individual from pathogens. The immune system can be divided into physical barrier function, performed by the skin, mucosal surfaces and many different neutralizing enzymes, and two key elements of immunity: innate and adaptive immunity. Innate immunity can eliminate, sense and recognize foreign particles or pathogens by a variety of pattern recognition receptors, which are highly conserved throughout different species [1-3]. In contrast, adaptive immunity uses highly variable receptors, which are generated by rearranging genes that code for specific antigen receptors expressed by T and B lymphocytes. These use a vast array of specific receptors to recognize and mount responses, and generate immunological memory to, specific antigens [4]. Innate and adaptive immunity collaborate and interact in every aspect of immune responses, both protective and autoreactive.

However, in recent years more overlap between the various functions previously assigned to either innate or adaptive immunity has been observed. Thus for example innate lymphoid cells have been demonstrated to produce cytokines in a population specific manner to “help” the immune response, rather akin to CD4+ T helper cells (see section 1.3), [5]. On the other hand, adaptive immune cells have been shown to express sensing molecules, which were previously associated with innate immune cells. T cells can express and mediate functions through a variety of natural killer cell associated receptors including killer inhibiting receptors (KIRs) and members of natural killer group 2 (NKG2A, C, D) [6-8]. Also of topical interest to this thesis, the natural killer (NK) cell lectin-like receptor CD161 can be found both on interleukin (IL)-17 producing CD4 T helper cells [9], and as described and investigated in chapters 4 to 6 on human regulatory CD4+FoxP3+ T cells [10], as well as on NK cells.

Thus the immune system has a variety of mechanisms with which to fight off pathogenic invading organisms, and to clear dead cells, while at the same time remain ‘tolerant’ to self and some foreign antigens, such as commensals and food particles. However the immune system also needs mechanisms in place to maintain and regulate

tolerance so that the body's immune cells do not attack self tissues, which could lead to autoimmunity.

1.1.1. Autoimmunity

Autoimmune reactions are responses of the immune system to self, resulting in inflammation and tissue destruction. There are many different types of autoimmune diseases. Sometimes specific tissues are affected, like the joints in autoimmune arthritis, or the nervous system in multiples sclerosis. On the other hand there are autoimmune diseases affecting a variety of tissues and organs including systemic lupus erythematosus and systemic juvenile idiopathic arthritis.

It is not clearly understood what triggers autoimmune diseases; some start during childhood, while others mainly occur in adults. There have been many genetic associations shown with different autoimmune diseases. Of these the strongest associations, those with the Major histocompatibility complex (MHC) class I and class ll loci, can be common to more than one autoimmune disease. In contrast some genetic associations appear to be more specific for particular diseases. Thus an individual's specific genetic background might predispose to the development or severity of more than one specific autoimmune disease. Interestingly many autoimmune conditions appear driven by CD4+ helper T cells. Data from several animal models have suggested that autoimmunity can be passed on to previously unaffected animals by transferring CD4+ T cells.

There are several hypotheses to explain how autoimmunity might be triggered. The four most common hypotheses are as follows:

- One concept is that autoimmunity could be caused by molecular mimicry. This means that an immune response could be mounted against a self-antigen, which has high similarity to another antigen, possibly pathogenic, encountered before [11,12].
- Another possibility is that self-antigens, which are usually not visible to the immune cells under natural conditions, e.g. due to cell (e.g. DNA, RNA) or organ

(central nervous system) location or posttranslational modifications, become 'available or 'apparent' to immune cells and elicit a response [13,14].

- A third theory is autoimmunity through bystander activation [15]. Thus an immune response to a pathogenic antigen present might surge and immune cells might attack self-tissue or cells nearby as a bystander effect.
- Finally it is possible that autoimmunity may be caused in part by a defect in central tolerance, such that self-specific immune cells escape into the periphery and mediate an autoimmune response upon encountering their antigen.

Since the necessary circumstances to initiate autoimmunity are unclear, and the environment might act as a catalyst, it is challenging to design strategies by which to target autoimmunity that could be preventative. Additionally different autoimmune diseases probably have different triggers in different individuals. Thus understanding the mechanisms and cell populations involved at the inflammatory site in autoimmunity might help to identify pathways which could be targeted in order to shut off autoimmune responses. In addition understanding what might cause a break in tolerance or failure to regulate the immune system in autoimmunity could lead to new therapies for a range of autoimmune diseases.

1.1.2. Tolerance and regulation

The immune system has numerous ways of insuring tolerance to minimize the chance of autoimmunity. Innate immune cells have a diverse but restricted set of pattern recognition receptors. Central tolerance includes both B cell antigen receptor tolerance and T cell receptor (TCR) selection in the thymus. As a result of thymic selection T cells with self reactive TCR will be eliminated [16,17]. However despite this process of negative selection, the fact that TCR are selected on self MHC during thymic development means that it is possible that some peripheral T cells will express TCR molecules, which have some autoreactive binding to self antigens. The concept of suppression of immune responses in the periphery and tissues, making an important contribution to maintenance of tolerance was first proposed over 40 years ago [18,19].

A variety of cells with immune regulatory potential have emerged in recent years. Monocytes/macrophages can have a more anti-inflammatory phenotype (M2) [20,21]. Tolerogenic dendritic cells (DC) are able to induce regulatory CD4+ T cells (typically identified by their expression of the transcription factor FoxP3), instead of effector CD4 helper cells [22-24]. Regulatory B cells (Breg) have recently emerged and been shown to have multiple regulatory roles. They are thought to suppress immune responses via IL-10 and possibly through cell-cell contact (reviewed in [25]).

In the CD4 helper T cell compartment several types of cells may be regulatory. CD4+ T cells expressing the transcription factor FoxP3 (referred to as Treg) are the most thoroughly studied, while CD4+ effector cells producing regulatory cytokines like IL-10 are known as Tr1 cells [26]. FoxP3+ Treg are discussed in detail in 1.6 within this chapter: these are an important subset of regulatory T cells, which affect many immune responses including those of T, B and dendritic cells.

Immune regulation is also performed on the molecular level. For example the inflammatory nuclear factor-kappa B (NF-κB) pathway is essential to many immune responses and induced by Toll-like receptor (TLR) and pro-inflammatory cytokine signaling [27-30]. It can be regulated within a cell not just by its direct negative feedback, inhibitors and activators but also by a range of signaling products not usually

viewed as connected to the NF-κB pathway. Here I will highlight three such processes, which are also highlighted in chapter 3 of this thesis.

1.1.3. Alternative regulation of the NF-κB pathway by immune signaling

It is widely accepted that NF-κB can inhibit the TGF-β pathway [31-33]. However, the effect of TGF-β signaling on NF-κB is less well described. TGF-β signaling acts downstream through SMAD3, a member of the SMAD (Similar to Mothers Against Decapentaplegic) family. Upon activation SMAD3 is phosphorylated, can dimerize with other SMADs and translocates to the nucleus. SMAD3 is a DNA binding molecule, which may co-activate and/or repress transcription [31,33]. Among other targets the *FOXP3* gene is co-activated by SMAD3, explaining its importance in Treg development [34-36].

In addition to their DNA binding properties, SMAD proteins interact directly with NF-κB [37,38]. SMAD3 and 4 can act on NF-κB binding sites to inhibit the transcription of IL-12 (p40 subunit) [39]. Accordingly TGF-β can act as an inhibitor of NF-κB [40,41]. On the other hand TGF-β1 intensifies the transcriptional activity of NF-κB and SMADs can act in partnership with NF-κB to co-activate transcription of for example AP-1 [38]. There is still a lot of controversy concerning the role of the TGF-β pathway and how SMAD3 can modulate the NF-κB pathway.

Vasoactive intestinal peptide (VIP) is a neuropeptide with immune-modulatory properties. Additionally immune cells also produce VIP [42-45]. VIP can signal through Vasoactive intestinal peptide receptors type one (VIPR1), type two (VIPR2) and PAC1 (pituitary adenylate cyclase activating polypeptide receptor 1) to lesser affinity [46]. VIPR1 is widely expressed including on neurons, epithelial cells and immune cells especially monocytes, macrophages and T lymphocytes [43,47]. The VIP-VIPR1 signaling cascade prevents the complex formation of DNA, NF-κB and co-factors by binding to DNA itself [48-50]. Additionally VIPR1 activation prevents IκB kinase (IKK) action and thus release and translocation of NF-κB is blocked [49-51]. The signaling pathway downstream of VIPR1 is best described in monocytes/macrophages, but it is

thought that other immune cells signal through a similar pathway [52]. This signaling downstream of VIPR1 can be cAMP dependent or independent.

Furthermore VIPR1 engagement can have various effects in different cell types. VIPR1 signaling has been shown to have effects on T cell activation, proliferation and cytokine production by T cells and monocytes in particular (comprehensive review by Gonzalez-Rey *et al* [53]). T cell lineage decision has been shown to be modulated by VIPR1 ligation rejecting Th1 development in favour for Th2 or Th17 cells [54-56] Furthermore Treg development and induction can be enhanced through VIPR1 signaling [57-61]. VIP-VIPR1 signaling has also been shown to down-regulate chemokine receptors [62] and pro-inflammatory cytokines and chemokines including IFN-γ, TNF-α, IL-2, IL-4, IL-6, IL-8, CCL2 and MMP-2 [48,63-66]. Hence the VIP-VIPR1 axis might be an important regulatory mechanism independent of a specific cell subset.

The NF-κB pathway can also be positively regulated by a variety of other molecules, not classically associated to the NF-κB pathway. The ERbB receptor feedback inhibitor (ERRFI1) is a receptor-proximal inhibitor specifically of the mitogenic and transforming signals of ErbB receptors, also known as MIG6, RALT or gene33. It is induced by stress and ERK activation but rapidly degraded within the cell. ERRFI1 inhibits ErbB induced cell proliferation, transformation and activation [67-73]. A low physiological level of ERRFI1 is sufficient for an inhibitory effect [69]. ERRFI1 can activate NF-κB via the IκB-dependent pathway [74]. ERFFI1 contains a domain highly homologous to the IκBα binding domain of NF-κB. In the cytoplasm NF-κB is bound to IκB and this binding prevents its translocation to the nucleus. Upon phosphorylation of IκB, NF-κB is released to translocate into the nucleus. NF-κB activation by ERRFI1 suggests another pathway since ERRFI1 competes with NF-κB for the same binding site at IκB. Thus when ERRFI1 is bound to IκB, NF-κB can translocate into the nucleus and induce transcription without phosphorylation of IκB. In addition the activation through ERRFI1 would override an inhibition of IκB phosphorylation [74]. Thus the net effect of ERRFI1 upon the NF-κB pathway would be to increase expression of NF-κB driven genes, including the transcription of the pro inflammatory genes IL-6, TNF-α and others.

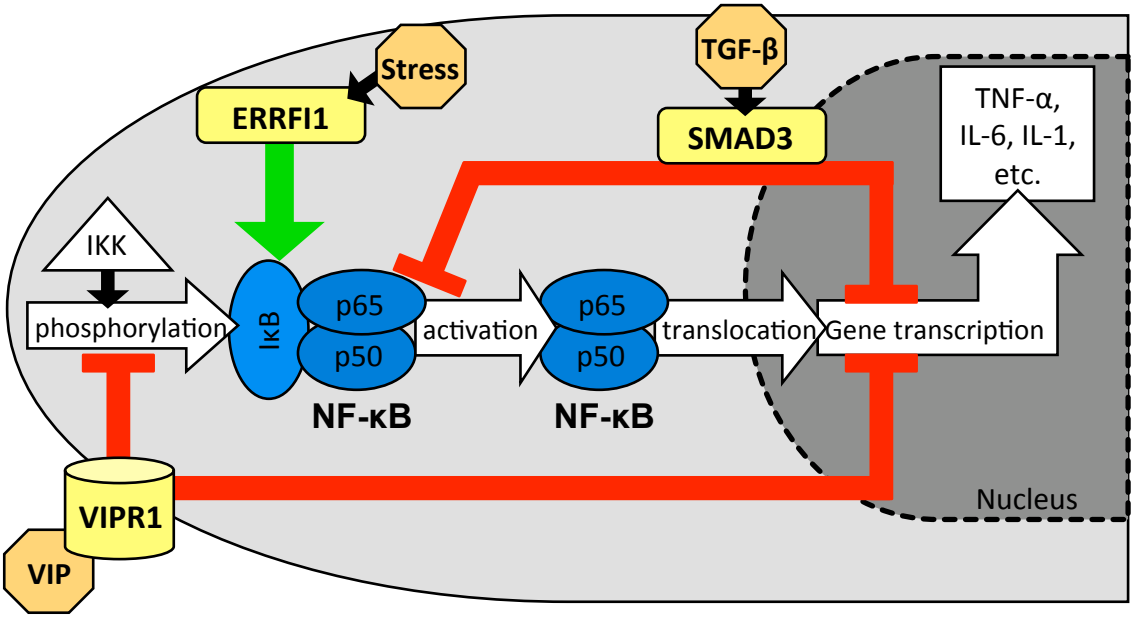

Figure 1.1: Schematic overview of the NF-κB pathway with proposed effects of ERRFI1, SMAD3 and VIPR1. The classical activation of the NF-κB pathway is through phosphorylation of IκB by the kinase IKK, leaving NF-κB free to activation, translocation and DNA binding to initiate gene transcription. Arrows are action. Green arrow indicates positive binding, red blunt arrows indicate inhibition.

These pathways may well contribute to modulate immunity through a variety of different cell types, but as yet there is overall no clear understanding of these processes.

1.2. T cell development and T cell receptor (TCR)

T cells develop within the thymus, and comprise CD4+ T helper cells, CD8+ and γδ T cells. T cell development occurs through positive and negative selection in the thymus, and their development yields a diverse repertoire of different TCR, of tens of thousands of different specificities. The TCR molecule has two protein chains: an alpha and a beta chain (or gamma and delta chain for γδ T cells). Each chain consists of a constant region, defined by the TCR-chain. At the antigen specific end of the molecule, each TCR chain has a variable region, which includes the highly variable complementarity determining regions (CDRs), CDR1, CDR2 and CDR3. Variability is achieved through rearrangement of different variable gene segments, the V, J and - in the case of the beta locus - D elements. During T cell development, DNA rearrangement takes place, bringing a V and J gene together (or for TCR beta chain V, D and J gene segments). The CDR3 region, coded for by the VDJ region, is a unique sequence for each rearranged TCR and therefore its sequence enables identification of different TCRs.

Unlike B cells, whose antigen specific receptor (immunoglobulin) undergoes somatic mutation in the periphery, the specific TCR sequence of a given T cell clone is not generally altered after emerging from the thymus and is therefore inherited by each daughter cell upon division. Therefore this allows tracking of T cell specificity. In order to study the diversity and repertoire of a population of T cells, mRNA species coding for the CDR3 (VDJ) region from a particular set for T cells can be amplified, cloned and sequenced. When comparing T cell populations by this approach the same CDR sequence indicates that the T cells were likely to have originated from the same parent T cell.

1.3. CD4+ T cells and subsets

In this thesis the central focus is on CD4+ helper T (Th) cells, which are identified by the co-stimulatory molecule CD4. As the name suggests, CD4 helper T cells, assist in the immune response. CD4+ Th cells interact with surrounding cells and tissue to produce cytokines, which then provide signals to other cells to direct their actions. For example CD4+ Th cells are crucial for B cells to mature and produce antibodies, through the production of IL-4, IL13 and other factors. CD4+ T cells are essential to protect against many pathogens and also to keep the immune system in homeostasis. However CD4+ T cells can also be linked to many autoimmune diseases and are sufficient to transfer disease in many animal models of autoimmune conditions.

CD4+ T cells can be divided into several subsets. Alongside CD4+FoxP3+ regulatory T cells (Treg), CD4+FoxP3- T cells (Tconv) represent the major Th subsets: Th1, Th2 and Th17, with IFN-γ, IL-4 and IL-13, and IL-17, respectively, as characteristic cytokines produced. T follicular helper (Tfh) cells are more recently revealed T cell subset, mainly present in secondary lymphatic organs, which provide help for B cell activation.
Each Th cell subset has at least one major or 'master' transcription factor, thought to be largely responsible for driving their phenotype. For Th1 cells this is T-box transcription factor *TBX21* (Tbet), while Th17 cells are driven by the transcription factor retinoic acid-related orphan receptor variant 2 (RORCv2 in human, or in mouse RORγt). There may well be more CD4+ Th cell subsets, for example Th9 (IL-9 producing) and Th22 (IL-22 producing) have been proposed [75-77], however it is not clear if these types of T cell truly represent separate subsets or site-specific phenotypes.

Transforming growth factor beta (TGF-β) with its signaling molecule SMAD3 is crucial in some Th lineage development [78]. Th lineages can be induced or skewed *in vitro* from naïve T cells by specific cytokines as follows: Th1: IL-12 and IFNγ, Th2: IL-4, and Th17: various combinations of TGF-β with IL-6, IL-1β or IL-23 and no IL-2. In some model systems Treg can be induced by TGF-β with IL-2 and no IL-6 [76,79,80]. Therefore the development of specific CD4+ T cell subsets is heavily influenced by cytokine present.

Other soluble factors, like vasoactive intestinal peptide (VIP) can also influence the lineage development [54,55], including Th17 skewing [56] and Treg development [57-61]. It is also noteworthy that Th17 and Treg (FoxP3+ regulatory CD4 T cells) are closely related [81], which might be an explanation for the similar induction conditions.

1.4. Plasticity of T cells

Originally it was thought that once a Th cell was committed to a specific cytokine profile, it would remain committed to this phenotype. However there has now been much evidence demonstrating so called plasticity of Th cytokine profiles, meaning that cells of a specific subset or phenotype may switch their cytokine profile to an alternative subset. One example of Th17 plasticity is further discussed below in 1.5. In general Th1 cells appear less plastic than the Th17 subset. Murphy and Stockinger introduced the concept that different CD4+ T cell subsets have different 'energy states' dictating their level of plasticity, similarly to the different energy levels of electrons in atoms. Accordingly Th1 are the most stable subset with he lowest 'energy state' and might represent a 'default final resting position' [76]. The stability of a Th lineage is influenced greatly by the strength of epigenetic modifications [75-77]. Plasticity seems to be driven in part by the microenvironment and can be replicated *in vitro* by different cytokines [79,82-84].

1.5. Th17

Th17 cells, as mentioned above, produce IL-17 and are driven by the transcription factor RORCv2. Th17 cells have been implicated in fighting extracellular and fungal pathogens in particular through the IL-17 pathway [85,86]. Th17 may produce both IL-17A and the closely related IL-17F, although much of the literature refers only to IL-17 (generally meaning Il-17A). Th17 are especially important in the intestines, and might be beneficial in gut inflammation, as IL-17 blockade or knockout typically worsens animal models of intestinal inflammation [87,88]. Commensal bacteria are essential drivers of Th17 development [89,90] and Th17 in turn might self-regulate in the gut [91]. Additionally it has been demonstrated that IL-17 might be involved in tight junction control of the intestinal epithelia [92].

Th17 cells characteristically express the chemokine receptor CCR6 (also called CD196) and the lectin-like receptor CD161. CD161 was been identified as a NK cell receptor, belonging to the NKRP1 family. CD161 is encoded by the gene *KLRB1* and its extracellular domain is a C-type lectin. Research has shown that CD161 expression is essential for Th17 cell development [93]. Within cord blood mononuclear cells, which only produce very low levels of cytokine *ex-vivo*, it has been shown that only CD161+ and not CD161- cells could be induced to produce IL-17 subsequently. A link to RORCv2 and CD161 expression was also established by this study [9].

IL-17 producing CD161+ cells can be modulated to express both IFN-γ and IL-17 together and subsequently even lose IL-17 production, but their CD161 expression remains. Thus CD161 expression does appear stable even when cytokine phenotype alters. This plasticity of CD4+CD161+ T cells has been found *in vivo* at the site of inflammation in juvenile idiopathic arthritis [82,83]. Interestingly, in asthma patients, CD4+CD161+ T cells producing both IL-17 and IL-4 also have been observed. Through clonal work it was established that CD161 expression was crucial to convert from IL-17 to IL-17 and IL-4 double producers [84]. Therefore CD161 expression links not just with IL-17, but also other cytokine production, like IFN-γ and IL-4.

1.6. FoxP3+ regulatory CD4 T cells (Treg)

1.6.1. The emergence of regulatory T cells

An early discovery suggesting T cells had regulatory capacity, demonstrated that inoculation of athymic (nude/nude) mice with CD4+ T cells, which had been depleted of CD25+ cells, led to severe autoimmunity, and this disease could be inhibited by addition of CD4+CD25+ cells [94]. Similarly *in vitro*, CD4+CD25+ cells could inhibit polyclonal CD4+CD25- T cells [95]. However even early studies demonstrated that not all CD4+CD25+ T cells have suppressive capacity [96].

Several groups then described CD4+CD25+ regulatory cells in human blood, which were functional *in vitro* [97-99]. It rapidly became clear that human CD4+CD25+ T cells are a heterogeneous population which may include both suppressive and non-suppressive cells, in part because CD25, the α–chain of the IL-2 receptor, is upregulated upon division or activation of human T cells. The demonstration that very high expression levels of CD25 correlated with good suppression [98,100], led to the proposal that the $CD25^{high}$ population contains the most suppressive cells.

Around this time, severe autoimmunity in the murine model scurfy was linked to mutations in a particular gene, *foxp3* [101] and in humans the *FOXP3* gene was shown to be mutated in the severe autoimmune condition IPEX (immunodysregulation polyendocrinopathy enteropathy X-linked syndrome) [102]. Further research showed that FoxP3 was crucial for the development of Treg and also their function [103-106]. Together these studies established FoxP3 as the master transcription factor for Treg. The development of specific monoclonal antibodies with which to identify FoxP3+ T cells, combined with the definition of other typical phenotypic features for these cells (such as the lack of IL-7Rα, CD127 [107]), has facilitated the huge growth of research in this area. More recently, evidence that the stable expression of FoxP3 is dependent upon demethylation at specific 5' non coding regions of the *FOXP3* locus, the so called Treg-specific demethylated region (TSDR), and that cells which express FoxP3 transiently are not predominantly demethylated at these regions, has led to a further method by which to identify *bona fide* regulatory T cells [108-110].

1.6.2. Different subsets of Treg

Regulatory T cells can develop in the thymus (so called natural Treg) or be induced in the peripheral immune system (induced or adaptive Treg). Natural Treg develop in the thymus, predominantly after birth. FoxP3 expression can be detected in mature CD4 single positive and a minority of double positive (CD4+CD8+) thymocytes [111,112]. To date there is no marker to distinguish between induced and natural Treg *ex-vivo*. The IKAROS family member Helios emerged as a possible marker to separate natural and induced Treg [113]. However upon further investigation, Helios expression could also be detected in induced Treg under certain conditions [114,115] and nTreg, which lacked Helios expression, were documented [116]. Both natural and induced Treg have important functions as investigated in different transgenic and adoptive transfer mouse models [117-120]. TGF-β and VIP are especially influential in Treg induction and development and are of particular relevance to this thesis [34-36,57-61].

It is increasingly clear that the CD4+ Treg population, typically 5-10 % of human peripheral blood CD4 T cells, is in fact a heterogeneous set of subpopulations, which differ both in terms of phenotypes and possibly functions. Various methods for dividing Treg into different subsets have been employed. One early sub-division proposed was by the expression of MHC class II molecule DR (HLA-DR), which is also expressed on activated T cells [121,122]. About a quarter (20-30%) of Treg express HLA-DR [123] and functional studies revealed that HLA-DR+ Treg exert early contact dependent suppression. HLA-DR- Treg however skew the cytokine production to a more Th2-like phenotype in the early stages, and at a later stage suppress through FoxP3-mediated contact-dependent mechanism [124].

Treg can also be defined by their expression of markers typical of naïve or memory T cells. For example memory Treg, with the phenotype CD45RA-CD45RO+, and expression of CCR6, have been described [125-127]. Memory Treg are high in the functional surface molecules CTLA4 and CD39, the effector memory marker CD44, but low in CD62L expression compared to naïve Treg. Compared to naïve Treg, memory Treg have a greater turnover, suggesting that a greater proportion is in the cell cycle and the population is self-renewing rapidly, both *in vitro* [125,127] and *in vivo* [128].

The surface molecules CTLA4 and CD39 have both been shown to be important in Treg function [129-131]. The exact role of CTLA4 in Treg function is not fully understood, but theories include that CTLA4 competes with CD28 for co-stimulatory receptors and then gives negative instead of CD28's positive signal, or that CTLA4 provides a direct signaling function, or that it may act in a T cell-extrinsic manner such as by stripping co-stimulatory molecules (CD80, CD86) from APC leaving them less able to stimulate naïve T cells [132].

CD39 is a potent cell-surface ecto-5'-nucleotidase ATPase, which breaks down extracellular pro-inflammatory ATP to AMP. Cell surface CD73 then breaks down extracellular AMP to adenosine. In mice, both of these enzymes are expressed on Treg [133]. In humans, however, there is conflicting evidence, whereas some report CD73 on Treg [134], we have observed that CD73 is not predominantly co-expressed with CD39 [135,136]. Due to the pro-inflammatory action of extracellular ATP [137,138], its breakdown is likely to contribute to Treg regulatory abilities.

CCR6 is an important chemokine receptor, expressed on many effector T cells. Next to IL-17 production, CCR6 expression is a hallmark characteristic of Th17 cells but is also important in directing Treg to the site of inflammation [139,140]. Treg can also express a variety of other chemokine receptors, associated with different Th lineages [141-145]. Specific chemokine receptor expression may enable specific co-localisation of certain Treg with specific T helper lineages [143,145].

Treg can express many activation markers, which may be shared with conventional FoxP3- T cells (Tconv), such as CD44, CD69 and GITR. Recently, however, a Treg-specific activation marker has been proposed, the Glycoprotein A repetitions predominant (GARP) protein [146,147]. GARP is expressed on Treg activated through the TCR, but not on Tconv, or TGF-β induced Treg. Interestingly, GARP serves as a receptor for latent TGF-β, a cytokine known to promote Treg development and stability [148]. GARP overexpression in helper T cells leads to an efficient reprogramming of effector T cells into Treg, however these reprogrammed cells are not fully demethylated at the TSDR regions [149].

1.6.3. Treg can have effector cell properties

As mentioned above, Treg can express a variety of memory markers as well as chemokine receptors associated with a Tconv phenotype. Interestingly, there is now increasing evidence that some Treg share some functional capabilities with Tconv, in particular the ability to produce pro-inflammatory cytokines. Due to the evolutionary and developmental links between Treg and Th17 [81], several groups have tested whether Treg can be skewed towards IL-17 production upon stimulation *in vitro*. Koenen *et. al*. found that IL-1β, antigen presenting cells and epigenetic modifications were necessary to induce Treg to IL-17 producers [150]. Others showed that TLR2 stimulation may contribute to conversion of Treg to Th17-like cells with lower levels of FoxP3 expression and reduced suppressive capacity [151]. The authors suggested that this cellular phenotype may represent an intermediate population, which are 'on their way' to losing Treg function and become Th17-like Tconv.

In vitro expansion and induction of Treg has been shown to lead to the development of a population of IFN-γ-producing Treg [152]. In this study the IFN-γ frequency within FoxP3+ cells was enhanced by addition of IL-12 in the culturing conditions. These cytokine-producing expanded Treg showed lower levels of demethylation at the TSDR, also suggesting an intermediate cell population. Furthermore, samples from patients with type 1 diabetes showed an increased frequency of IFN-γ+ Treg after expansion, implicating a connection between inflammation and cytokine-producing Treg. Similarly, in a mouse model of colitis, an intermediate IFN-γ-producing inducible Treg has been suggested, these IFN-γ producing Treg were nevertheless suppressive *in vivo* [153]. Recently it has been shown that Treg isolated during the early inflammatory response following surgery, were less suppressive than Treg isolated pre-surgery or a later time point post-surgery [154]. *In vitro* Treg anergy was not affected, indicating that Treg did not convert to Tconv functionality. Together these studies suggest that Treg may produce cytokines, perhaps under the influence of pro-inflammatory conditions, yet remain functionally suppressive. The precise expansion or induction system used to generate these cytokine-producing Treg may be crucial to their functionality. For example, Zheng *et. al.* showed that the stimulation ratio of B cells to

T cells was critical in yielding either functional Treg that produced cytokine or highly activated effector Tconv [144].

Treg isolated from several chronic inflammatory or autoimmune conditions have been demonstrated to be functional *in vitro*. Cytokine-producing Treg are increased in inflammatory environments [153,155,156], including juvenile arthritis as demonstrated in this thesis [10]. Such cytokine-producing Treg can also be found upon *ex-vivo* stimulation of healthy PBMC as a small proportion of all Treg [10,145,157-159]. The frequency of cytokine-producing Treg can be increased by cytokine treatments. For example IL-17 production by Treg was enhanced by IL-6, IL-1β, IL-21 alone or in various combinations. IL-23 alone had no effect, but could act synergistically in combination with cytokines above [155,157,158]. The frequency of IFN-γ+ Treg was increased by IL-12 treatment in several studies [153,156,160]. These data show that the polarization 'requirements' for cytokine- producing Treg closely mirror those that drive polarization of Th effector cells.

Within this thesis I demonstrate that the cytokine-producing Treg are contained within the CD161+ Treg population, data that are now published [10]. Furthermore this subset is characterized in detail and findings compared to other studies within this thesis.

Treg can share expression of transcription factors that are typically associated with expression of a specific Th cell subset (e.g. Tbet associated with Th1, and RORCv2 with Th17). It has been proposed that expression of a specific transcription factor, commonly associated with Tconv, may 'assist' specific Treg to target its suppressive capacity towards specific T effector cells and may even be absolutely required for such suppression. For example, Treg suppression of Th1 cells is dependent on Tbet expression [143], IRF4 expression is crucial for Th2-targeting Treg [161], while STAT3 has been demonstrated to be essential for Treg suppression of Th17 [162,163].

A beneficial role in the protection against infection has been proposed for cytokine-producing Treg [145,157,160,164], with some evidence for specific expansion and

cytokine production against certain pathogenic antigens [145]. Moreover, there is evidence that such Treg may have a beneficial role during transplantation. In two mouse models of transplantation Treg derived IFN-γ was essential: IFN-γ mRNa increased in CD25+ Treg after challenge with allogeneic cells to which the host was tolerized to, but not from another animal (not tolerized), which were consequently rejected. Additionally blocking IFN-γ by antibodies or using IFN-γ deficient Treg resulted in rejection [160,164].

Consequently cytokine-producing Treg may represent an important mechanism during immune challenge, and their further investigation is warranted. It also becomes clear that there might be four main 'flavours' of Treg (Figure 1.2): naïve, memory, activated memory and effector memory Treg might represent separate families of Treg.

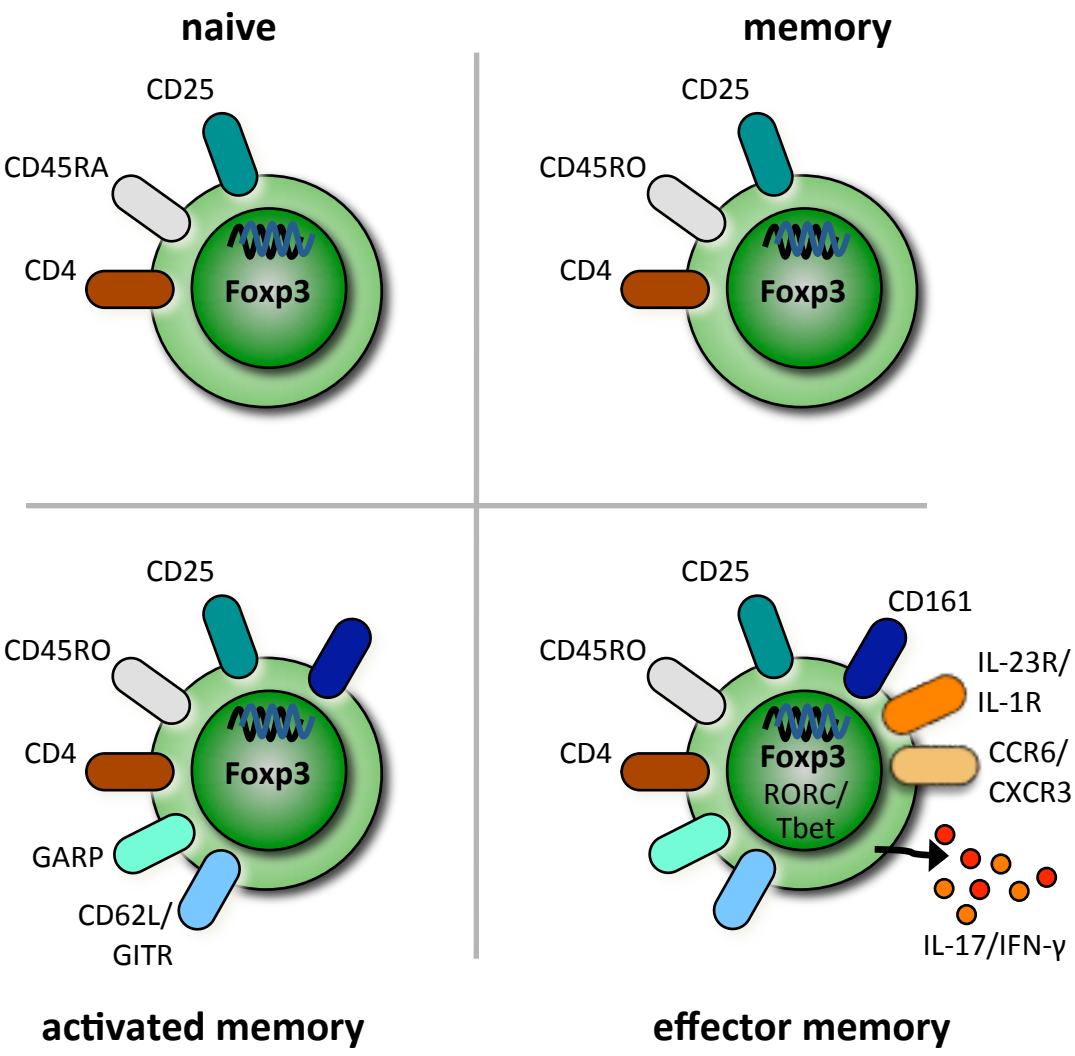

Figure 1.2: Schematic of different regulatory T cell families. Naïve, memory, activated memory and effector memory Treg.

1.7. Juvenile Idiopathic Arthritis (JIA)

JIA is the most common rheumatic disease in children affecting around 1 in 1000 children [165]. JIA is defined as arthritis in one or more joints lasting at least 6 weeks of no known cause, starting before the 16th birthday. The diagnosis of JIA is one of exclusion. The peak age when the disease occurs first is 2 to 4 years with a general predominance in girls in most but not in all forms of JIA [166,167].

There are seven main forms of JIA, see Table 1.1. Each subtype is clinically distinct from the others in respect to epidemiology, symptoms, complications and prognosis. Certain clinical features of one form are exclusion criteria for the other forms. Only the occurrence of arthritis is ubiquitous for all subtypes. Each subtype of JIA is complex and involves multiple parts of the immune system. The cause(s) of disease are unknown, but genetic components as well as environmental factors clearly play a role [168-174]. There have been different classifications over time making comparison of studies difficult: in 1994 the International League of Associations for Rheumatology (ILAR) formed a task force to agree on one international classification, which was approved in 1999 by The World Health Organization [173,175] and is now used widely across the world.

Table 1.1: ILAR classification of Juvenile Idiopathic Arthritis subtypes

Subtype	Definition	Exclusion criteria *
Systemic arthritis (sJIA)	An arthritis with or preceded by daily fever for at least 2 weeks, that has flares each day for at least three days and is accompanied by one or more of the following: 1. A short lived, non-fixed erythematous rash 2. A generalized lymph node enlargement 3. Enlargement of the liver and/or spleen 4. Serositis	a, b, c, d
Oligoarthritis (O-JIA)	An arthritis involving 1 to 4 joints within the first 6 months of disease. It has two subtypes 1. Persistent oligoarthritis – affects $\leq$ 4 joints through disease course 2. Extended oligoarthritis – affects > 4 joints after the first 6 months of disease	a,b,c,d,e
RF negative Polyarthritis (P-JIA)	An arthritis affecting 5 or more joints within the first 6 months of disease. RF is negative.	a,b,c,e
RF positive Polyarthritis	An arthritis affecting 5 or more joints within the first 6 months of disease. RF is positive.	a,b,c,e
Psoriatic arthritis	An arthritis with either psoriasis or at least two of the following: 1. Dactylitis 2. Nail pitting or onycholysis 3. Psoriasis in a first degree relative	b, c, d, e
Enthesitis related Arthritis (ERA)	An arthritis with enthesitis, arthritis or enthesitis with at least two of the following: 1. Sacroiliac joint tenderness and/or inflammatory lumbosacral pain 2. Presence of HLA B27 3. Age of onset above 6 years of age in a male 4. Ankylosing spondylitis, enthesitis related arthritis, sarcoilitis with IBD, Reiters syndrome or acute anterior uveitis in a first degree relative	a, d, e
Undifferentiated Arthritis	An arthritis that does not fulfill inclusion criteria of any category or is excluded by fulfilling criteria for more than one category	
* Exclusion criteria	a) Psoriasis in patient or first degree relative b) Arthritis in an HLA B27+ male with onset after 6 years of age c) Ankylosing spondylitis, enthesitis related arthritis, sacroiliitis with inflammatory bowl disease (IBD), Reiter syndrome or acute anterior uveitis in a first degree relative d) Presence of IgM RF on two or more occasions, more than three month apart e) Presence of systemic arthritis	

Oligoarthritis is the most common form of JIA. Around 50- 60% of all JIA cases are oligoarticular [166]. It has a female predominance. There are differences in the prevalence of oligoarticular JIA between different ethnic backgrounds and geographical locations, probably due to genetic differences or geographic, environmental and social factors [173,175,176]. Polyarticular JIA, comprising 30-35% of JIA, is the second most common subtype JIA [177]. This thesis will focus on oligoarticular and polyarticular JIA (O-JIA and P-JIA respectively), for the reason that these subtypes have no major systemic organ involvement (such as skin rashes or persistent fever).

The most common joints affected that are the knee with 56% of cases and the ankle with 20%. The small joints are less commonly involved. The joints involved usually show no symmetry. Before a diagnosis is made, some other diseases like infection, neoplasm, leukemia, or lyme disease need to be excluded [173,175].

As mentioned in Table 1.1, there are two forms of O-JIA, persistent and extended. There is no obvious clinical difference between the two types during the first six months. The disease presents with four or less joints affected. About 20 to 50% of ologoarthritis patients will extend, meaning an involvement of more than four joints, after six or more month, usually within two years of onset of the disease. Once extended there are several clinical differences between the two subgroups [165,173,175]. In particular, extended oligoarticular JIA can be severe and resistant to treatment. In the UK national registry for children with JIA treated with the anti-TNF agent Etanercept for their arthritis, over 15% of all children on Etanercept were of the extended oligoarticular JIA type [178].

1.7.1. Immunopathology of the joint in JIA

The joint undergoes subtle changes at the beginning of disease with increased synovial tissue cellular infiltrates and vascularity and an accompanying increase in synovial fluid (SF). At later stages the affected joints in JIA have increased synovial tissue thickness and increased surface of the synovial membrane, forming villi and folds of tissue, which is highly vascularised. Synovial fluid accumulation, synovial thickening and joint swelling leads to pain, stiffness and limitation of movement. A layer of immune and connective tissue cells might aggregate, forming a pannus, this may result in degradation of bone tissue by metalloproteinases and cytokines [173].

The amount of pro-angiogenic molecules is increased in the inflamed synovium of childhood arthritis. This is especially the case in polyarthritis [173], and has also been demonstrated by gene expression profiling for oligoarthritis [179]. Levels of inflammatory chemokines and adhesion molecules are also increased [180]. Macrophages and fibroblast-like synoviocytes congregate in the lining of the joint, while T cells are typically present in the sublining. Additionally many cells, including high numbers of CD4+ and CD8+ T cells, accumulate in the SF. The T cells found in the joint are highly activated, but hyporesponsive toward TCR signaling. Stimulation of JIA T cells with a human auto-antigen (Hsp60) lead to differential responses depending on disease severity [181,182]. Active O-JIA samples show high IL-10/IFN-γ ratios, driven by low IFN-γ production, whereas samples from patients in remission had high levels of IFN-γ, thus a low IL-10/IFN-g ratio. P-JIA samples showed no difference between active disease and remission, and overall low IL-10/IFN-γ ratios. This group has suggested that responses to self-hsp60, and in particular an enrichment of Treg that are specific for hsp60 correlate with good outcome in JIA [181,183].

The ratio of CD4+ to CD8+ T cells in the joint is low in oligoarthritis, when compared to peripheral blood T cells [179,184]. The response of synovial T cells is heavily skewed towards a Th1 response and has a high level of pro-inflammatory cytokines [185]. Th17 have also been linked to JIA. Hence Th17 cells are highly enriched within the T cell population of the inflamed joint and are correlated with disease severity [82,186,187]. Synovial effector T cells have also been shown to be able to switch from IL-17 to IFN-γ-

producers in the environment of the joint and *in vitro* [82,83]. The major cytokine found responsible for this plasticity was IL-12, which is also highly enriched within the joint. The addition of TGF-β could inhibit such conversion to some extent, but measurements showed very low levels of TGF-β in synovial fluid.

1.7.2. Immunopathology regarding Treg in JIA

The paradox of increased Treg numbers in the inflammatory joint (SF) of JIA has been known for some years [188]. Interestingly, Treg in the blood of children with O-JIA appear to be present at normal or even decreased frequency, compared to healthy children [186,189,190]. Thus, in JIA as in other inflammatory arthritis, there is a clear difference in Treg frequency between the inflamed synovial compartment and the peripheral circulation.

In an early study of the very severe form of JIA known as systemic JIA (sJIA; in addition to arthritis patients display systemic symptoms such as fever, rash and major organ involvement), Treg were shown to be reduced in peripheral blood in severe active disease, just before autologous stem cell transplantation. In these patients, the frequency of Treg was shown to recover upon successful treatment by autologous stem cell transplantation [191]. However a more recent study has suggested that while a difference in Treg frequency is observed between active and quiescent sJIA patients, the Treg numbers in quiescent sJIA disease were raised compared to healthy controls as well as compared to active sJIA. In this study the increase of total Treg, in the quiescent sJIA cases, appeared to come from an increase in CD45RO+ memory Treg subpopulation, perhaps indicating that a rise in Treg occurs as disease resolution takes place [192]. It has recently been shown that the very high inflammation in these patients, readily measureable in peripheral blood by the levels of the protein serum amyloid A (SAA) may directly impact upon Treg function, via the protein SAA, which reverses anergy in Treg without affecting their suppressive capacity [193].

As mentioned earlier, there are several genetic associations with JIA, some influence Treg biology. By far the strongest link with JIA and genetic variation is that of alleles of the HLA region on chromosome 6: in particular the class 2 alleles HLA_DRB1*0801 and

1101 have been shown to be risk alleles. Genetic associations with the *IL2* and *IL10* gene regions and the gene encoding CD25 (the IL-2R α-chain) have been demonstrated in JIA [194-197]; these genes are important in Treg maintenance and function. However no genetic association with any *FOXP3* SNP itself, or *CTLA4* could be found in more thorough studies [198,199]. Very recently the largest genetic study ever of JIA, which has included 2816 children with JIA and over 13,000 controls, has confirmed many of these associations at genome wide significance level and implicated many other immune loci including PTPN22, PTPN2, STAT4, RUNX1 and others [200].

The Wedderburn group and others have shown a relationship of Treg frequency and disease severity in oligoarticular JIA. Thus in the mild limited form of JIA known as persistent oligoarticular JIA (persistent O-JIA) the synovial fluid (SF) exudate has a higher frequency and absolute number of Treg compared to SF from children with the more severe extended O-JIA [186,188]. These data suggest that although immune tolerance has been broken in JIA, Treg frequency does correlate with disease severity and thus Treg might actively restrain inflammation.

When Treg in the joint were studied in the context of other cell types within the synovial fluid, it was demonstrated that Treg frequency correlates negatively with Th17 frequency [186]. This is also true for their transcription factors FoxP3 and RORCv2 (Th17) at message level [190]. Since Treg and Th17 have been associated in an evolutionary sense [81], the balance between Treg and Th17 might play a crucial role in JIA and local factors that impact upon this balance may correlate directly with clinical course and outcome. A study, highlighted in chapter 3, aimed to identify predictive biomarkers of extension to more severe disease early in oligoarticular JIA. It was observed that the difference in Treg frequency was present very early, even before extension, in those destined to go on to more severe arthritis (so called extended-to-be O-JIA) [179]. In addition, interestingly RORC2v2 was one of the gene transcripts found to be significantly differentially expressed between patients with persistent O-JIA and those with the extended-to–be OJIA phenotype [179].

Since Treg within the joint clearly do not resolve inflammation, many explorations into their phenotype and function have been undertaken, to determine if there is an intrinsic defect in Treg of JIA patients. Treg found in the inflamed joint are all of the memory phenotype and express CD45RO [188] and are activated, as demonstrated by high HLA-DR and GITR expression. CTLA4 and CD39 are also highly enriched on SF Treg [135,188]. Both CTLA4 and CD39 have been implicated in Treg function, as described above. Interestingly in the SF of JIA, in addition to CD39 on Treg, a population of CD39+FoxP3- cells has been demonstrated. Both Treg and non-Treg expressing CD39 are functional in breaking down ATP [135].

One hallmark test of Treg functionality is the ability to suppress Tconv *in vitro*. Several reports have found SF Treg to have potent suppressive activity [135,188,201-203]. However, more recently, there have been reports that SF Treg can suppress Tconv from the blood but not the effector cells obtained from the joint [204,205]. Together these studies suggest that Treg from patients with JIA do not appear to have an intrinsic defect, as they function well when taken out of the environment. However factors in the local joint microenvironment, or the effector T cells themselves may affect the function of regulatory cells such that they cannot control inflammation within the joint.

It has been shown that several cytokines can abrogate suppression by Treg by either affecting Treg directly or effector T cells. IL-2, IL-6, IL-7, IL-15 and TNF-α have all been implicated in diminishing the suppressive capacity of Treg *in vitro*, and these cytokines are also found in high levels in the synovial fluid of JIA [201,204,206]. Both TNF-α and IL-6 are now the targets of highly successful therapies for JIA. IL-6 and TNF-α have been shown to induce higher phosphorylation levels of PKB, thus activating signaling in effector T cells. This in turn renders effector T cells unresponsive to both TGF-β and Treg mediated suppression [204]. Given that SF Tconv are strong producers of higher levels of pro-inflammatory cytokines compared to Tconv from the blood, it is highly plausible that locally these effector T cells may contribute to a failure of regulation by Treg [205].

The recent description of pro-inflammatory cytokine-producing Treg in other autoimmune conditions, as described earlier, led to the investigation, presented in this thesis, to explore whether JIA Treg may also demonstrate this phenomenon. I found a clear enrichment of Treg with a pro-inflammatory potential, defined by CD161 expression, described in chapter 6 in detail, a factor that may also contribute to the apparent 'failure' by Treg to suppress ongoing inflammation in JIA [10].

Collectively, the findings suggest that the inflammatory environment of the joint plays an important role in the overall effect of regulatory cells at the site of inflammation. Thus cytokines and other inflammatory mediators may render T effector cells unresponsive to suppression. However, Treg should not be disregarded since they clearly also impact upon clinical outcomes and their manipulation may be possible to restore full functionality. With variable reports on Treg function, and the emerging knowledge of their capacity of making pro-inflammatory cytokines themselves, it will be crucial to investigate how these different Treg populations act at the site of inflammation, how stable they are and what the effects the local environment may have on Treg behavior and phenotype.

1.7.3. Treatment of JIA - and how it affects Treg

The first line of treatment of oligoarticular and polyarticular JIA is usually administration of anti-inflammatory medication and corticosteroid injections of the affected joints after aspiration of excess synovial fluid. This therapeutic intervention provides the special opportunity to study cells directly from the site of inflammation, by collecting the synovial fluid at joint injections and extracting mononuclear cells. Steroids may also be given orally or in severe cases intravenously at the start of therapy.

For around 50% of persistent oligoarticular JIA children, the disease or functional joint problems will persist over time, although some children will go into complete remission and live their adult lives with few residual functional problems. In general there is a lower remission rate in extended than in persistent O-JIA. Extended and polyarticular JIA patients often need more medication, like Methotraxate (MTX) or

other disease modifying agents [165,173]. While there is good evidence for efficacy of MTX in JIA [207], at least 40 % of children treated with MTX will ultimately fail this and require other medication [208]. The increasing availability of biologic agents to treat arthritis combined with the recognition that early control of inflammation is highly correlated with better long term outcomes, has led to a radical change in the management of sever JIA in the past 10 years [209].

For severe sJIA and P-JIA autologous stem cell transplantation (ASCT) has been successfully used as treatment [191,210-213]. After ASCT Treg numbers increased, relative to CD4+ T cells as a whole, suggesting a resetting of the immune system. However it has been established that adequate ablation of the immune system before transplantation is essential to prevent early relapse of disease in this approach.

The number of JIA patients treated with biologics is ever increasing, additionally new biologics, e.g. recombinant humanized monoclonal antibodies, are being developed continuously. Here I highlight how anti-TNF-α agents (Infliximab, Adalimumab, Etanercept), used as treatment for JIA and rheumatoid arthritis (RA), may affect Treg. Other biological treatment options in JIA include recombinant CTLA4-antibody complex (CTLA4-Ig, Abatacet, Belatacept), IL-1 blockade (e.g. Anakinra) and anti-IL-6 (e.g. Tocilizumab) treatment. CTLA4-Ig therapy has been successfully used in rheumatoid arthritis [214,215] and juvenile idiopathic arthritis [216]. Interestingly it has been suggested that in patients with RA, Abatacet lead to a fall in peripheral blood Treg numbers but a significant enhancement in Treg function, on a per cell basis [217]. No such differential study was possible on JIA samples so far. IL-1 blockade and anti-IL-6 therapy have been proven very successful in sJIA and some patients with P-JIA, but their mechanism implications are not discussed in detail here.

TNF-α has been implicated in pathogenesis of many forms of human inflammatory arthritis including JIA, where it has been shown to be highly enriched within the inflammatory joint [206]. There are several TNF-α blockade agents now being increasingly used to treat JIA. Infliximab and Adalimumab are both anti-TNF-α antibodies, whereas Etanercept is a soluble TNF-receptor fusion protein.

A third concept are TNF-kinoids [218], which are hybrid molecules used to vaccinate the recipient, such as TNF conjugated to a carrier protein (e.g. keyhole limpet haemocyanin), which induce the host to produce polyclonal self-antibodies against TNF. The theoretical advantage of this 'vaccination' approach would be that by inducing anti-TNF antibodies within the patient, the risk of anti drug antibodies is reduced.

Involvement of TNF-α in arthritis comes from several disciplines of research. Mice with TNF-α gene knocked in develop arthritis, and Treg at the peak of this disease model show only weak suppressive capacity [218]. In this study, treatment with anti-TNF-α (Infliximab) or a TNF-α-kinoid ameliorated disease and increased Treg frequency and function. *In vitro* treatment of healthy human Treg with TNF-α, rendered these less functional and decreased their level of FoxP3, mimicking the phenotype of Treg from RA patients. Treg function and FoxP3 could be restored by culture with anti-TNF-α antibodies. Treatment with Infliximab in RA patients can restore Treg levels and function and the population of Treg that develop upon Infliximab treatment have been shown to be a novel, induced Treg CD62L- population [219,220]. Others have suggested that Treg from RA patients actually have a high amount of TNF-α bound to their surface membrane, which impacts their functionality [221]. After anti-TNF-α treatment Treg with membrane bound TNF were decreased.

TNF-blockade alone is not as efficient in treating arthritis compared to combinational therapy with methotraxate (MTX) [222]. This synergy between MTX and anti-TNF treatment is also clear in humans, both in RA and JIA [216,223,224]. A placebo controlled study in RA showed a slight higher increase in Treg with anti-TNF plus MTX, compared to the placebo plus MTX group [225]. In another study, the ratio between Treg and Th17 frequency increased after treatment [226]. This would be useful to follow up in JIA patients on anti-TNF-α therapy, since the Treg to Th17 ratio already correlates with disease [186]. Others however did not find any prominent difference in Treg/Th17 between MTX alone or in combination of either Etanercept or Adalimumab [227,228]. A recent study looked at the mechanism of Treg in Adalimumab responding RA patients compared non-responders and active RA [229]. This study found that Treg

isolated from Adalimumab responding patients were able to suppress IL-17 production *in vitro*, by acting on monocytes, whereas non-responders or active RA samples did not. Interestingly this study also compared Treg from Etanercept treated patients, which did not suppress IL-17 *in vitro* independent of clinical response to the drug. Therefore different TNF-blockade treatments appear to exert different effects on Treg and Th17 balance.

A variety of anti-TNF blocking biological agents have been used with success in a large number of autoimmune conditions; however some patients developed a flare of psoriasis while on TNF-blockade treatment [230,231] and anti-TNF-α treatment exacerbated disease significantly in a mouse model of psoriasis [232]. Thus TNF-α has different roles in different disease settings, and cannot be used as a blanket treatment for all forms of arthritis.

Although biologics have dramatically improved treatment for many RA and JIA patients, not all patients respond in a similar way; these drugs are relatively expensive and to date are not widely available in all countries. Furthermore most of these studies have been performed on adult RA patients, whose disease is significantly different to JIA patients. But the rather small number of JIA patients at any centre and the young age group complicates big clinical studies, as several centers need to coordinate and work together with appropriate ethics in place. Further characterization and definition of different subgroups of disease will therefore be crucial, to develop biomarkers which can be used to help predict which treatment will be best for which patient.

1.8. Project aims

The overarching goal of this work was to gain further understanding into the fine balance between immune regulation and inflammation in health and disease using JIA as a model human autoimmune disease.

The specific areas of work presented in this thesis are:

1) Existing available gene expression array data were analyzed in detail to find and investigate possible mechanisms regulating disease severity in JIA. The array compared results from O-JIA synovial fluid cells at time of diagnosis stratified according to their disease status one year after diagnosis: persistent oligoarticular and patients who extended at 1 year (termed extended-to-be) were compared in this analysis [179].

2) Identification of a surface molecule identifying regulatory T cells (Treg) with the capacity to produce pro-inflammatory cytokines and thorough characterization of this subset throughout development and phenotype. It was hypothesized that CD161 might fit these criteria, due to its links to cytokine production and switch of cytokine production in effector CD4+ T cells [82-84].

3) Investigation of functions of CD161+ Treg as bona fide Treg and specific to this subset. To define the putative CD161+FoxP3+ subset as genuine Treg, anergy, suppression, and methylation status were tested. Existence of differences in pathogen specific and TCR signaling behaviour of CD161+ and CD161- Treg were hypothesized and ligation of CD161 receptor on Treg surface was attempted.

4) The hypothesis that CD161+ Treg might be enriched in JIA and thus contribute to disease was tested. CD161+ Treg frequencies and phenotype were investigated and associations to clinical readouts were addressed.

Chapter 2

Materials and Methods

2. Materials and Methods

2.1. Sample collection

Peripheral blood was taken from healthy adult volunteers with full informed consent from staff of the Institute of Child Health. Each subject was given a sample code with the prefix AW, for adult well, to anonymous their samples. Children with juvenile idiopathic arthritis (JIA) were recruited to this study as part of an ongoing study of pathogenesis of JIA with full informed parental consent, and assent where age appropriate. When blood sampling was clinically indicted, a small additional volume of peripheral blood was taken for the study. Synovial fluid was collected at the time of joint injections, as clinically indicated. Patients were allocated codes according to their subtype, PA for oligoarticular and PO for polyarticular JIA. Every patient and healthy volunteer gave fully informed consent (or age appropriate assent) in accordance with the local ethics approval (Great Ormond Street Hospital/ Institute of Child Health Research Ethics Committee ref 95RU04 and 07RU01). Samples were processed within 4h of collection, see below.

2.1.1. Preparation of Peripheral and Umbilical Cord Blood Mononuclear Cells (PBMC and UBC respectively)

Peripheral blood (PB) and umbilical cord blood (UBC) was collected into sterile tubes containing 35μL (=35U) of preservative free heparin (Wockhardt). All subsequent work and cell culture work was done in a sterile Gelaire BSB 4A category 2 laminar flow hood, following local safety regulations, using sterile and endotoxin-free reagents and equipment.

The blood was diluted with an equal volume of RPMI (Roswell Park Memorial Institute) 1640 medium (Life Technologies) with 1% v/v Penicillin (final concentration 100U/ml) and Streptomycin (final concentration 100μg/mL) antibiotic mix (P/S, Life Technologies), called medium hereafter. A maximum of 30mL of blood/medium mixture was layered over half the volume (e.g. 15mL) of LymphoprepTM (Axis-Shield), per tube. The samples were centrifuged at 800g for 20min with no brake in a Sorvall Legend RT centrifuge (Germany). The PBMC-containing interface was removed and

diluted with complete medium (CM: RPMI 1640 containing P/S as above plus 10% v/v heat inactivated foetal bovine calf serum (FBS, Life Technologies)), and centrifuged at 500g for 10min. The cell pellet was carefully resuspended in complete medium and counted according to section 2.1.3. Cell aliquots were then centrifuged at 300g for 7 min and resuspended in freezing medium, FBS containing 10% v/v dimethyl sulphoxide (DMSO, Sigma), or 1mL of TRIZOL (Life Technologies) and stored at -80°C for RNA extraction, as detailed in sections 2.1.5 and 2.2.1 respectively.

2.1.2. Preparation of Synovial Fluid Mononuclear Cells (SFMC)

Synovial fluid was processed as for blood to generate mononculear cells (SFMC), but before layering the synovial fluid/medium mixture onto lymphoprepTM, hyaluronidase (Sigma) was added at 1μL/1mL (final concentration 10U/ml) of synovial fluid medium mixture and incubated for 15-30min at 37°C. Following this, the same method as for the preparation of PBMC was followed, as detailed in 2.1.1.

2.1.3. Preparation of thymocytes

Human thymus tissue samples were obtained after surgical removal in children undergoing corrective cardiac surgery. Thymocytes were isolated by gentle tissue disruption followed by sieving through a mesh into CM and used immediately.

2.1.4. Continuous Cell Culture

HT29 is a human colon carcinoma cell line expressing the protein VIPR1 at a high level [233-235]. HT29 cells were grown as an adherent layer in T25 flasks with DMEM Glutamax (Life Technologies) containing 10% v/v FBS, 1% v/v P/S (as above) and 1% v/v non-essential amino acids (Sigma), called complete DMEM Glutamax medium hereafter, at 37 °C and 5% CO_2 in a humidified incubator (Jencons-PLS). At 70-80% confluency the medium was removed, the cells rinsed with PBS (Life Technologies) and 1.7mL 0.05% trypsin (Life Technologies) was added and incubated for 3min at 37°C and 5% CO_2. Adding excess complete DMEM Glutamax medium quenched the trypsin. The suspension was then centrifuged at 300g for 3min, the cell pellet resuspended in fresh medium and cells were split 1 in 10 into a new T25 flask.

2.1.5. Counting viable cells

Viable cells were enumerated by counting the cells in a Neubauer improved counting chamber (Hawskley) with Trypan blue (Sigma). The cell suspension was diluted with 0.4% Trypan blue at equal volumes, 10μL each. 10μL of this mixture was placed in a Neubauer counting chamber. Viable, clear, cells were counted in the 25-box field under a light microscope. The following formula was used to calculate the estimate number of viable cells in the entire cell suspension: Number of cells counted in the 25 squares x 2 (dilution factor) x 10^4 (factor for the counting chamber) x total volume of cell suspension = total viable cell count. Dead, blue, cells were also noted, and no sample with a viability of less than 90% was used.

2.1.6. Freezing and thawing of cells

To store viable cells over a prolonged period of time they were prepared as follows. The cell pellet was resuspended at 1-2 x 10^7 cells/mL of freezing medium, consisting of FBS with 10% v/v DMSO, and aliquoted into individual cryovials (NUNC) at 0.5-1mL. These were then frozen slowly in a freezing pot (Nalgene) containing isopropanol at -80°C for at least 24h (cooling at an average of 1C per minute) before being transferred to liquid nitrogen for long-term storage.

Frozen cells were recovered by thawing the aliquot quickly in a 37°C water bath and diluting the cell suspension into warmed CM. Viable cells were counted and the tube containing the cell suspension was centrifuged at 300g for 7min. The cell pellet was resuspended in an appropriate amount of CM, usually at 1-1.5 x 10^6 cells/mL.

2.2. Protein expression by Western Blotting

2.2.1. Sample preparation

Cell lysates were prepared using 1x Radio Immuno Precipitation Assay (RIPA) buffer (Table 2.1) pelleted cells were resuspended in 1x RIPA, 50 μL/ 1 x 10^6 cells, passed through a 27 gouge needle five times, to break the cells apart and incubated on ice for 30 min. The suspension was then centrifuged at 10000 rpm for 10 min. Supernatant was transferred to a new Eppendorf tube and stored at -20°C until further use. Before loading onto the gel, cell lysate was mixed with 6x Laemmli Buffer (Table 2.1) 1 in 6, e. g. 20μL lysate + 4μL 6x Laemmli Buffer, and boiled at 95°C for 5min to ensure protein denaturation.

Table 2.1: Buffer for sample preparation

Buffer	source	final concentration	amount
5x RIPA			for 500mL
Tris pH 7.4	Sigma	250mM	5.1g
Sodium chloride	Sigma	750mM	22g
NP-40	Sigma	5%	25g
SDS	Sigma	0.5%	2.5g
Sodium deoxycholate	Sigma	2.5%	12.5g
EDTA	Sigma	25mM	3.65g
EGTA	Sigma	5mM	0.95g
H_2O			top up to 500mL
-> store at RT			
For 1x RIPA add fresh			for 10mL
5x RIPA		1x	2mL
Sodium Orthovandate 1M	Sigma	10mM	100µL
Sodium fluoride	Sigma		Tip-dip
Protease inhibitor tablet complete mini	Roche		1
H_2O			top up to 10mL
-> store at -20 °C			
6x Laemmli Buffer			for 10mL
Tris 0.5M pH 6.8	Sigma	60mM lit-50mM	1.2mL
Glycerol	Sigma	47%	4.7mL
SDS	Sigma	12%	1.2g
DTT	Sigma	0.5M	0.93g
0.04 % Bromophenol blue	Fisher	0.005-0.01%	as needed
H_2O			top up to 10mL
-> store at -20 °C			

2.2.2. SDS-PAGE gel electrophoresis

The gel cassette was assembled and filled with the resolving gel, made up according to Table 2.2. The gel was topped with a thin layer of isopropanol and left to set for 30min at room temperature (RT). The isopropanol was washed off with plenty of water and the stacking gel (Table 2.2) was then poured onto the resolving gel. A 1.5mm comb was inserted and the gel is left to set for 20min at RT.

Table 2.2: Recipe for 10% SDS-PAGE gel

Resolving gel		amount
MilliQ filtered H_2O		4 mL
S-Buffer		2.5 mL
30 % Acrylamide	Sigma	3.5 mL
0.1 % APS	Sigma	100 μL
TEMED	Sigma	10 μL

S-Buffer		amount
Trizma base	Sigma	18.2 g
10 % w/v SDS	Sigma	4 mL
MilliQ filtered H_2O		100 mL
HCL	Sigma	-> pH 8.8

Stacking gel	
MilliQ filtered H_2O	2.2 mL
C-Buffer	1.2 mL
30 % Acrylamide	1.2 mL
0.1 % APS	120 μL
TEMED	10 μL

C-Buffer	
Trizma base	6.6 g
10 % w/v SDS	4 mL
MilliQ filtered H_2O	100 mL
HCL	-> pH 6.8

After setting, the comb was removed, the electrode assembly assembled and the buffer chamber was filled with 1x Running Buffer, with final concentration 25mM Trizma base, 192mM Glycine and 0.1% w/v SDS. Samples and SeeBlue Plus2 prestained standard 1x (Life Technologies) were loaded and the gel were run at 140V for about 1h. A Mini-Protean 3 gel tank system was used (BioRad).

2.2.3. Transfer

The gel was transferred to the wet blotting cassettes according to manufacturers instructions (BioRad), in direct contact with a Hybond C Nitrocellulose membrane (Amersham, GE Healthcare). The transfer was run under a current of 400mA for 30min with a cooling block in the tank in 1x Transfer Buffer: final concentrations 25mM Trizma base, 192mM Glycine and 5% v/v methanol.

2.2.4. Blocking and Protein detection

The membrane was blocked in 4% w/v milk proteins (Marvel) made up in TBST buffer (final concentrations 50mM Tris-HCL, pH 7.6, 0.15M Sodium Chloride, 0.1% Tween20, all Sigma) for 1h at RT on a shaker. The primary antibody (Ab) to detect specific proteins was made up in 5% w/v BSA (Sigma) TBST, at a specific dilution (Table 2.3), added to the membrane and incubated for 1h at RT or overnight at 4°C on a shaker. Following three 5min washes with PBST (1xPBS (Oxoid), 0.1% Tween20) the membrane was added to a new tube with the secondary Ab made up in 5% BSA TBST (Table 2.3) and incubated for 1h at RT on a roller. The membrane was then washed three times for 5min in PBST. To detect specific antibody binding to proteins enhanced chemiluminescence (ECL) plus Western Blotting detection reagents (Amersham, GE Healthcare) were used according to the manufacturers instructions. In short, the detection reagents A and B were mixed 40:1, distributed onto the membrane and incubated for 5min at RT without movement. The Hyperfilm ECL (Amersham, GE Healthcare) was placed onto the membrane in a darkroom and was exposed for 5s to 5min, depending on the outcome, for longer or shorter time periods for optimal detection of proteins. The films were developed in the compact x4 automatic x-ray film processor by Xograph imaging systems.

Table 2.3: Antibodies used for Western blotting

	Manufacturer	Clone	Dilution used
Mouse anti-humanVIPR1	Millipore	AS58	1:2000
Rabbit Anti-mouse HRP linked IgG	DAKO	polyclonal	1:2500
Rabbit anti human β-Actin	Biolabs	13E5	1:2000
Goat Anti-rabbit HRP linked IgG	Biolabs	polyclonal	1:2500

2.2.5. Stripping of Western membranes

After developing films for detection of proteins, the membrane was stripped using 0.2M Sodium Hydroxide (Sigma) twice for 5min on a shaker followed by 3 washes with PBS. Blocking and staining was then repeated as described in section 2.2.4 for β-Actin as a control for protein loading.

2.3. Flow cytometry

2.3.1. Buffers and Solutions

Table 2.4: Buffers and Solutions, final concentrations shown

FACS Buffer		PERM Buffer		PFA	
1x	PBS	1x	FACS Buffer	1x	PBS
1 %	FBS	1 %	Formaldehyde	4 %	Paraformaldehyde dissolved at 65°C for 45min under fume cupboard
0.1 %	Sodium Azide				

FoxP3 Fix/Perm working solution – freshly prepared before each experiment		
1 part	FoxP3 Fixation/permeabilization concentrate	(eBioscience)
3 parts	FoxP3 Fixation/permeabilization dilutent	(eBioscience)

1x FoxP3-Perm buffer – freshly prepared before each experiment		
1 part	Permeabilization Buffer	(eBioscience)
9 parts	Sterile MilliQ filtered H_2O	

For intracellular cytokine investigation standard stimulation was used: PMA 0.05μg/mL, ionomycin 0.5μg/mL and BrefeldinA of 5μg/mL (all final concentrations) in Complete media (CM, 2.1.1), incubation: 3h at 37°C in 5% CO_2.

2.3.2. Antibodies

Monoclonal antibodies against specific human proteins were used as direct conjugates to fluorescent colours or biotin plus secondary Streptavadin, see Table 2.5. Before use in experimental protocols, all antibodies were tested for staining, compared to previous batches and titrated to determine optimal dilution conditions. In some experiments, where indicated, isotype control reagents were used for comparison of staining to estimate background binding by antibody reagents.

Table 2.5: Antibodies used for flow cytometry

Target	Conjugate	Clone	Manufacturer
CD1a	FITC	HI149	eBioscience
CD3	PC7, V450	UCHT1	Beckman Coulter, BD
CD4	APC, PC7, Qdot605	SFCI12T4D11, S3.5	Beckman Coulter, Life Technologies
CD8	APC	SK1	eBioscience
CD14	FITC	UCHM-1	Sigma
CD19	PE	HIB19	BD
CD25	PE	M-A251	BD
CD45RO	FITC	UCLH1	Biolegend
CD127	FITC, biotinylated, Pe-Cy5	eBioRDR5	eBioscience
CD161	PE, APC, Pe-Cy7	HP-3G10	eBioscience
CCR6	AlexaFluor488	TG7/CCR6	Biolegend
IL-23R	Biotin	polyclonal	R&D Systems
LLT1	PE	402659	R&D Systems
TCR-Vβ	FITC, PE	IOTest® Beta Mark TCR V beta Repertoire Kit	Beckman Coulter
VIPR1	pure, PE labelled	AS58	Millipore
Isotype control	Biotin	N/A	R&D Systems
streptavadin	Qdot605, APC-Cy7	N/A	Life Technologies, eBioscience
IL-2	PE	MQ1-17H12	eBioscience
IL-17	AlexaFluor488, V450	EBIO64DEC, N49-653	eBioscience, BD
IFNγ	FITC, V450, V500	25723.11, B27	BD
FoxP3	AlexaFluor488, APC	PCH101, 236A/E7, 206D	eBioscience, Biolegend
RORC	PE	AFKJS-9	eBioscience
Tbet	PE	eBio4B10 (4B10, 4-B10)	eBioscience
pAKT (Ser473)	pure	193H12	Cell Signaling
Anti-rabbit (for p-AKT)	Alexa488	N/A	Life technologies

N/A = non applicable

2.3.3. Antibody labelling

Pure VIPR1 antibody was labelled using LYNX rapid RPE antibody conjugation kit (AbD serotec) according to Manufacturers guidelines. In short 1μL LYNX modifier was added per 10μL antibody, mixed and added to the lyopholyzed R-Phycoerythrin (RPE) mix and resuspended by gentle pipetting twice. The mixture was incubated in the dark overnight. The following morning 1μL LYNX quencher reagent was added per 10μL antibody and incubated for 30min before use, or storage at 4°C.

2.3.4. Fixable live-dead staining

For some experiments the LIVE/DEAD® Fixable Blue Dead Cell Stain (Life Technologies) was used before surface and intracellular staining according to manufacturers instructions. In short: cells were washed in culture grade DPBS (Life Technologies), spun at 300g, and stain was used at 1:250 in DPBS. 40μL staining was used per well, and after resuspension, incubated for 30min at 4°C in the dark. Then cells were washed once more with DPBS.

2.3.5. Surface Marker staining for Flow cytometry

PBMC or SFMC were plated out in a round bottom 96 well plate (VWR) at a cell concentration of 1.5 x 10^6 cells/mL in CM. After specific treatment and/or stimulation, depending on the specific experiment set up section 2.5, cells were spun down at 300g for 3min and washed with FACS buffer, see Table 2.4, and spun down again. Typically 100-300x10^3 cells were plated out per different antibody mixture for each experiment. The cell pellet was then resuspended in 25μL FACS Buffer containing the antibodies against specific cell surface proteins. These were incubated for 30min at 4°C in the dark. The cells were washed with 160μL FACS Buffer. Cells were then either washed once more, resuspended in 200μL FACS Buffer and transferred to FACS tubes for immediate analysis on the LSR II (BD) flow cytometer, or stained with fluorochrome labeled Streptavadin (to bind biotinylayed antibodies) in 25μL FACS Buffer for 15min at 4°C in the dark with an additional wash with FACS Buffer, or went on to fixing and intracellular staining with FoxP3 buffers as detailed in 2.3.6.

2.3.6. Intracellular Staining using PFA and PERM Buffers

To investigate cytokine production by T cells from PBMC or SFMC with or without pre-treatment, as detailed in section 2.5, cells were washed with FACS Buffer after stimulation. The cell pellet was resuspended in 100μL PFA (see Table 2.4) to fix the cell proteins, and incubated for 10min at RT in the dark. After spinning the cells down at 300g for 3min, cells were washed once with FACS Buffer, and then permeabilised by incubation in with PERM Buffer (see Table 2.4) to allow detection of intracellular proteins in cells. The cells were resuspended in 25μL PERM Buffer containing the relevant antibodies and incubated for 30min at 4°C in the dark followed by one wash with PERM Buffer and one wash with FACS Buffer. Cells were then resuspended in 300μL FACS Buffer, transferred to FACS tubes and analysed on the LSRII flow cytometer.

2.3.7. Intracellular Staining using FoxP3 Buffers

Surface molecules were stained as described in 2.4.5. After the wash with FACS Buffer, cells were resuspended in 100μL FoxP3 Fix/Perm working solution (Table 2.4) and incubated for 45min at 4°C in the dark. 100μL FoxP3-Perm Buffer was added and the cells were spun down at 300g for 3min followed by one wash with 200μL FoxP3-Perm Buffer. Intracellular antibodies were made up in 25μL FoxP3-Perm Buffer and the cells were resuspended in the antibody mix and incubated for 45min at 4°C in the dark followed by a wash with FoxP3-Perm Buffer. Cells were resuspended in 300μL FACS Buffer, transferred to FACS tubes and analysed on the LSR II flow cytometer.

2.3.8. pAKT staining

To detect phosphorylated AKT protein (V-akt murine thymoma viral oncogene homolog 1, also known as Protein Kinase B (PKB)), at serine 473 (Ser473), whole PBMC or CD4 T cell enriched cells (see section 2.4.2 Magnetic bead sorting – negative T cell or CD4+ T cell enrichment) were resuspended at 1-2x10^6 cells/mL in pure RPMI 1640, no FBS, aliquoted into Eppendorf tubes (500μL/tube) and cooled on ice. One tube per condition was used. A typical set-up contained following conditions:

1. unstimulated cells,

2. cells stimulated for 5min,

3. cells stimulated for 10min,

4. cells stimulated for 30min.

Additionally in some experiments CD161-ligating antibodies (clone DX12 (BD), clone 191B8.18.2 (Beckman coulter)) or isotype control IgG (BD) plus stimulation were included as conditions.

For T cell stimulation anti-CD3 (clone UCHT1, R&D systems, final concentration 1μg/mL) and anti-CD28 (clone CD28.2, BD, final concentration 1μg/mL) monoclonal antibodies +/- anti-CD161/isotype (final concentration 10μg/mL) were added. The cells incubated on ice for 45min. Goat anti-mouse $F(ab)_2$ protein fragment (Jackson Immuno Research) was diluted in pure RPMI1640 at 20μg/mL for cross-linking of antibodies and pre-warmed to 37°C. Then cells were spun down at 1500rpm for 5min at 4°C and supernatant was removed. Cells were resuspended in 200μL warm $F(ab)_2$ protein solution for stimulated cells, and 200μL warm RPMI1640 for unstimulated cells. Cells were incubated at 37°C in heated Eppendorf shaker at 900rpm for desired time (5, 10, 30min). The reaction was stopped by the addition of 200μL 2XFoxP3 Fix/Perm solution (eBiosciences) and cells were placed on ice. Tubes were spun at 10,000rpm for 5min at 4°C, supernatant discarded, resuspended in 100μL FACS buffer and transferred to a V-bottom 96-well plate. Cells were permeabilised by the addition of 100μL pure ice-cold methanol and incubation for 20min on ice. Cells were spun at 2200rpm for 4min and washed with FACS buffer. Non-specific binding was blocked by resuspending cells in 40μL of mouse IgG isotype antibody (20μg/mL) and incubation for 15min at RT. Staining antibodies were added, followed by 30min incubation at RT. Cells were washed in FACS buffer, then stained with a secondary anti-rabbit IgG antibody for 20min at RT. Cells were washed in FoxP3 Perm Buffer then resuspended in FACS buffer and run on the LSRII.

2.3.9. Cytokine capture assay

To investigate if cells secreted cytokine upon stimulation a cytokine capture assay was used. After CD4 T cell enrichment (2.4.2) cells were stimulated at $2x10^6$ cells/mL in RPMI1640 + P/S + 5% FBS by PMA (10ng/mL) and ionomycin (1000ng/mL, both final concentrations) for 2h on a MACSmix™ tube rotator (Milteny Biotech) at 37°C and 5% CO_2. As a negative control an aliquot was not stimulated, but treated the same throughout. Cold bead sort buffer (Table 2.6) was added, cell suspension was placed on ice to cool and then spun down to pellet at 4°C at 300g for 7min. Subsequently cells were resuspended in 90μL cold RPMI1640 + P/S + 5% FBS and 10μL IL-17 capture reagent (IL-17 Secretion Assay, Milteny Biotech) was added for around $1x10^7$ cells and incubated on ice for 5 min. The cell suspension with capture reagents was transferred to a 50mL Falcon tube, which was filled to 30mL with warm RPMI1640 + P/S + 5% FBS and directly transferred to the MACSmix™ tube rotator and incubated for 45min at 37°C and 5% CO_2. After incubation, cold bead sort buffer was added to the cell suspension, put on ice and centrifuged at 4°C at 300g for 7min. Cells were washed in cold bead sort buffer and then resuspended in 90μL bead sort buffer. 10μL of IL-17 detection PE reagent (IL-17 Secretion Assay, Milteny Biotech) and surface staining fluorochromes (CD4, CD3, CD161, Table 2.5) were added in the appropriate dilution and incubated for 10min on ice. Followed a wash with bead sort buffer, cells were fixed and stained intranuclear for FoxP3 according to 2.3.7 and analyzed on a LSR II flow cytometer. Alternatively this method can also be used to sort cytokine secreting cells, then additional fluorochromes might be necessary and no fixation is required, but cells would be resuspended in FACS sort buffer, filtered and live sorted (see end of 2.4.3).

2.3.10. Flow cytometry Analysis

Flow cytometric data were collected on a LSR II (BD) flow cytometer. Between 0.1-2 x 10^5 events were collected for each condition, gated on scatter properties of cells. Data were analyzed using FlowJo (Treestar Inc).

2.4. Cell sorting

Table 2.6: Sorting Buffer, final concentrations shown

Bead sorting Buffer			FACS sorting Buffer		
1x	DPBS	Life Technologies	1x	DPBS	Life Technologies
2%	FBS	Life Technologies	1%	FBS	Life Technologies
4mM	EDTA	Sigma (0.5M stock)	2mM	EDTA	Sigma (0.5M stock)

2.4.1. Magnetic bead cell sorting – positive selection

CD14 and CD4 positive selection kits from EasySep (StemCell Technologies) were used for magnetic bead cell sorting, performed according to manufacturers instructions. In brief, 10-30x10^6 cells were resuspended in 100-300μL Bead sorting Buffer (Table 2.6) and transferred to a polystyrene FACS tube (BD). The appropriate amount (10-30μL) of positive cell selection cocktail was added and incubated for 15min at 4°C, followed by addition of the well-mixed magnetic nanoparticles (5-15μL) and 10 min at 4°C incubation. The cell suspension was filled up to 2.5mL with Bead sorting Buffer and inserted into the magnet for 5min. In a smooth motion the negative portion was poured into a 15mL falcon. The positive fraction in the FACS tube was removed from the magnet and filled up to 2.5mL again to return to the magnet. This cycle was repeated leading to 3 times 5min in the magnet. After counting the positive and negative fractions (2.1.4) about 1 x 10^5 cells are used to check for purity using flow cytometry (section 2.3).

2.4.2. Magnetic bead sorting – negative T cell or CD4+ T cell enrichment

For no-touch T cell, or CD4+ T cell enrichment the kits from EasySep (StemCell Technologies) were used and performed according to manufacturers instructions. In brief, 10-80x10^6 cells were resuspended in 100-800μL Bead sorting Buffer (Table 2.6) and transferred to a polystyrene FACS tube (BD). The appropriate amount (5-40μL) of negative cell selection cocktail was added and incubated for 10min at RT, followed by addition of the well-mixed magnetic nanoparticles (10-80 μL) and incubation for 5min at RT. The cell suspension was filled up to 2.5mL with Bead sorting Buffer and inserted into the magnet for 5min. In a smooth motion the negative portion was poured into a

15mL falcon. The positive fraction in the FACS tube was removed from the magnet and filled up to 2.5mL again and mixed to return to the magnet for a further incubation and pour off. After counting and purity-check, the negative fraction, enriched for (CD4+) T cells, was used in the appropriate experiments.

2.4.3. Flow cytometry cell sorting

Magnetic bead enriched (negative or positive) cells, or total PBMC or SFMC were resuspended in 150μL FACS sorting Buffer (Table 2.6) with up to $30x10^6$ cells per 15mL falcon. Appropriate amounts of antibodies were added and incubated for 30min at 4°C in the dark. Cells were washed with FACS sorting Buffer and resuspended at $10\text{-}20x10^6$ cells/mL and put through a cell strainer (50-70μm) to remove any cell clumps. The MoFlow XDP cell sorter (Beckman Coulter) was used for cell sorting. DAPI was used to sort live cells and duplets (two or more cells stuck together) were excluded. Sorted cells were collected in complete medium. After all sorts, sorted cells were assessed for purity and yield.

2.4.4. Sorting strategy for monocyte, B and T cells

To determine mRNA expression (2.6) in specific subsets of white blood cells, the following sort strategy was used (Figure 2.1). Positive magnetic bead selection (2.4.1) was used for CD14+ monocyte selection, followed by flow cytometry sorting (2.4.3) of the CD14- fraction for B (CD19+) and T cells (CD3+CD4+ and CD3+CD4-). CD3+CD4- T cells mainly contain CD8+ T cells, but also a proportion of gamma delta (γδ) and NKT cells. Sorting of B cells on CD19+ by flow cytometry was performed only on large SFMC samples (typically with a cell number over $30x10^6$), because SFMC typically contain a small percentage of B cells. JIA PBMC samples have small cell numbers (peadiatric samples), thus no sorting for B cells was done from those; no sorting was performed on healthy child samples, due to small number of cells available. Mean sort purity was >90% for CD3+CD4+, CD3+CD4- and CD19+ cells as well as CD14+ healthy PBMC. JIA PBMC monocytes reached an average purity of >80% JIA SFMC CD14+ cells of >75%. The lower purity rates obtained for monocytes (CD14+) reflect the tendency of SFMC to clump together, thus trapping non CD14+ cells together with CD14+ cells and magnetic particles.

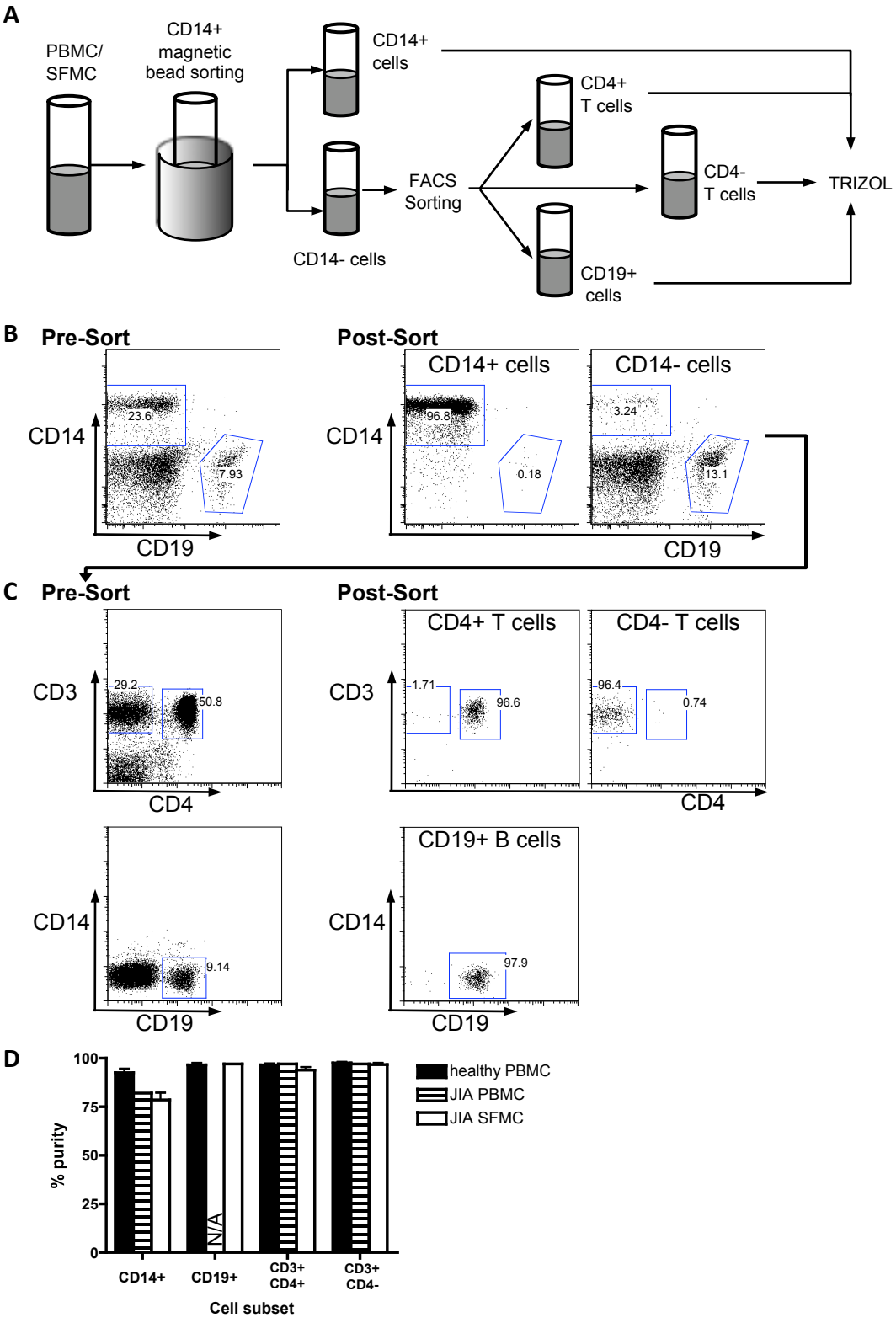

Figure 2.1: Sorting strategy for separation of mononuclear cells from SFMC and PBMC. (A) Schematic of sorting process. Cells were sorted either on magnetic bead or by flow cytometry (FACS); purified cells were stored for preparation of RNA (TRIZOL); (B, C) Representative flow cytometry plots of a healthy PBMC sample, (B) pre- and post-sorting with magnetic bead sorting for CD14+ cells, (C) followed by FACS sorting for CD4+ and CD4- T cells, and B cells. (D) Summary of available sorting data, bars represent mean, error bars standard error of the mean (CD14+: healthy PBMC n=11,

JIA PBMC n=2, JIA SFMC n=5; CD19+: healthy PBMC n=4, JIA SFMC n=3; CD3+CD4+: healthy PBMC n=7, JIA PBMC n=2, JIA SFMC n=9; CD3+CD4-: healthy PBMC n=8, JIA PBMC n=2, JIA SFMC n=9). N/A: not applicable.

2.4.5. Sort strategy for regulatory and conventional T cells (Treg and Tconv)

For mRNA expression (2.6) and functional assays (2.5) Treg and Tconv had to be separated. Following a negative CD4 T cell selection (2.4.2) cells were sorted using flow cytometry (2.4.3). Treg were defined as CD25+CD127lo and Tconv as CD25-CD127high, both on a live CD4+ gate with duplets excluded. For some assays Treg subsets had to be separated by CD161 expression. Purity was assessed by intranuclear staining of FoxP3 (2.3.7) on a small subset of the sorted cells. The sort strategy with representative sort purity is shown in Figure 2.2.

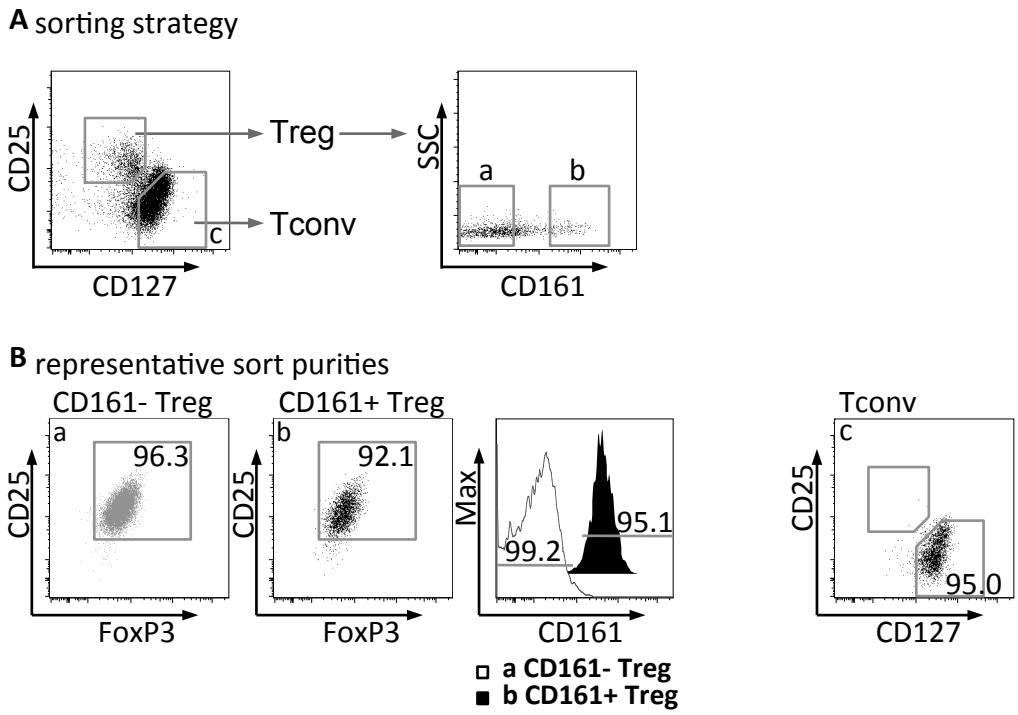

Figure 2.2: Sorting strategy for CD161+ CD4+ Treg. Treg and Tconv were sorted by flow cytometry. (A) Tconv defined by CD25-CD127high (c) and Treg by $CD25^{hi}CD127^{lo}$, with subpopulations by CD161 expression (a, CD161-; b, CD161+). (B) Representative sort purity of ≥90% for both subsets for FoxP3 and CD25 (dot plots) and CD161 staining (overlay histogram).

2.5. Functional cell culture assays

2.5.1. CFSE labelling

Cells were washed in PBS, labelled in 1μM CFSE solution (in DPBS, Life Technologies) for 10min at RT in the dark, followed by quenching of CFSE binding by addition of an equal volume of FBS for 10min at RT in the dark before multiple washes with medium. CFSE labeled cells were counted and placed into culture immediately after washing was completed.

2.5.2. Inhibition of IL-2 induction through VIPR1 activation

Whole PBMC, SFMC or (CD4) T cell enriched cells were plated out at a cell concentration of $1.5x10^6$ cells/mL in CM (2.1.1). Pretreatment, VIP, the VIPR1-specific agonist $^{[Ala\ 11,22,28]}$VIP (both Tocris) or Forskolin (FSK, Caltag) as non-specific cAMP inducer, was added to respective wells at final concentrations of 10^{-7} and 10^{-8}M, concentrations were chosen due to optimal effects shown in literature in that range [236-239]. Cells were incubated at 37°C, 5% CO_2 (time = 0h). At time = 21h standard stimulation for intracellular cytokine investigation (see 2.3.1) was added and incubated for an additional 3h. The cells were washed with FACS Buffer and the Intracellular Staining using PFA and PERM Buffer protocol was followed as detailed in 2.3.6. Data was analysed as IL-2 inhibition, where percent of CD3+CD4+IL2+ of stimulated cells without pretreatment is set as 100% and the %IL-2 in the stimulated samples with pretreatment from the same donor is calculated as a proportion of the sample without pretreatment. %IL-2 reduction was also calculated.

2.5.3. *In vitro* proliferation and suppression assays

To assess *in vitro* proliferation or anergy, sorted cells (2.4.5, CD161+ Treg (CD4+CD25^{hi}CD127^{lo}CD161+), CD161- Treg (CD4+CD25^{hi}CD127^{lo}CD161-) and/or Tconv, CD4+CD25-CD127^{hi}) were CFSE labelled (2.5.1). Labeled cells cultured at $5x10^4$/well in V-bottom 96-well plates (Corning CoStar) coated with 1μg/mL anti-CD3 (clone UCHT1, R&D systems) +/- 5μg/mL anti-CD28 (clone CD28.2, BD Biosciences) antibodies in CM at 37°C and 5% CO_2. After 5 days, cells were re-stimulated with standard stimulation

(2.3.1). CFSE dilution and IL-17A and IFN-γ production by live cells were assessed by flow cytometry (2.3.6).

Suppression assays were performed with $5x10^4$ CFSE labeled (2.5.1) Tconv and unlabeled CD161+ or CD161- Treg at a 1:1 ratio under the same conditions as the proliferation assay. Where cell numbers allowed 3:1 and 5:1 ratios were also tested. CFSE dilution and IL-17A and IFN-γ production by live cells were assessed by flow cytometry (2.3.6). Cytokine protein levels in culture supernatants were assessed by multiplex immunoassay (Luminex) for IL-2, IL-10, IFN-γ and IL-17A, kindly performed by Simona Ursu [240]. Suppression of proliferation was calculated using the FlowJo % divided function (Treestar Inc). The condition Tconv alone was defined as 0% suppression.

2.5.4. Treg expansion

For expansion of Treg, sorted Treg (2.4.5) were cultured at $5x10^4$ /well in V-Bottom 96-well plates (Corning CoStar), that had been pre-coated with 1μg/mL anti-CD3 and 5μg/mL anti-CD28 in culture medium with 100U/mL IL-2 (Roche) for 4, 6 and 10 days. IL-2 was renewed every 2 days. At the end of the culture standard stimulation for intracellular cytokine staining was performed and CD161, FoxP3 expression and cytokine production were assessed by flow cytometry (2.3.7).

2.5.5. CD161 expression control and stability

Whole PBMC were cultured at $1x10^5$cells/well in pre-coated U-bottom plates (1μg/mL anti-CD3, 5μg/mL anti-CD28) for 5 days in full culture medium (RPMI1640 + 10% FBS) with and without treatment. IL-1β, IL-2, IL-6, TNF-α (all BD), IL-12, IL-23 were used all at 10ng/mL and TGF-β (all R&D) was used at 2ng/mL. Synovial fluid serum was used at 5%. Synovial fluid serum-media mix was consequently measured by Luminex by Simona Ursu, but did not reach detection threshold for measured cytokines (IL-2, IL-10, IL-17A, IFN-γ). At the end of the culture, cells were re-stimulated with as above (2.3.1), and CD161, FoxP3 and cytokine expression were then assessed using flow cytometry (2.3.7).

Sorted CD161+ Treg or CD161- Treg subpopulations (2.4.5) were CFSE labeled (2.5.1) and spiked at a frequency of 5-7% into cultures of $1x10^5$ autologous PBMC in U-bottom 96-well plates (CoStar, pre-coated with 1μg/mL anti-CD3 and 5μg/mL anti-CD28. These cell mixtures were cultured in culture medium with either no cytokine or in the presence of cytokines as above, or a combination of IL-1β + IL-23 + TGF-β, at 37°C in 5% CO_2. After 3 days, cells were re-stimulated (2.3.1). CD161 expression and cytokine production by live CFSE+ cells were assessed by flow cytometry (2.3.7).

2.5.6. CD161 ligation

Two different specific clones of anti-CD161 antibody (DX12, BD Biosciences and 191B8.18.2, Beckman Coulter) were used, with an appropriate isotype IgG control antibody (BD Biosciences) to study the effect of CD161 ligation. These were used for pAKT analysis as described in 2.3.8.

Additionally U-bottom 96-well plates were coated at 10μg/mL of anti-CD161/isotype +/- anti-CD3 (1μg/mL) and anti-CD28 (5μg/mL). Sorted total Treg ($CD4+CD25^{hi}CD127^{lo}$) or Tconv ($CD4+CD25-CD127^{hi}$) (2.4.5) were cultured for 3 days at 37°C in 5% CO_2. At the end of the culture cells were re-stimulated (standard stimulation 2.3.1) and cytokine production was assessed using flow-cytometry (2.3.7).

2.5.7. Antigen specific culture

Whole PBMC were CFSE labeled as previously described (2.5.1), cultured at $1x10^5$ cells/well in CM with or without lysate of *Candida albicans* (Immunobiology unit, GOSH) or human cytomegalovirus (CMV, gift from Marianne Jacobson) for 6 days at 37°C in 5% CO_2. At day 6 cells were re-stimulated (2.3.1). CFSE dilution and cytokine production (IL-17A and IFN-γ) by CD161-FoxP3+ and CD161+FoxP3+ live CD4+ lymphocytes were assessed by flow cytometry (2.3.7). Responders were defined by antigen specific proliferation by CFSE dilution in FoxP3- Tconv, whereas non-responders did not show any specific proliferation in FoxP3- Tconv.

2.6. Analysis of gene expression

2.6.1. RNA extraction

To extract RNA from cell lines, PBMC or SFMC, cells were counted and $2x10^3$ - $5x10^6$ cells were resuspended in 800μL of TRIZOL reagent (Life Technologies) by strong pipetting up and down, and transferred to sterile 1.5mL Eppendorf tubes. These were incubated for 3-5min at RT and then stored at -80°C until further use for up to one month. To extract the RNA, aliquots were thawed rapidly and then 200μL of RNAse-free, molecular biology grade chloroform (VWR) was added, followed by 15s vigorous shaking and 2min incubation at RT. The tubes were centrifuged at 12,000g for 15min at 4°C in an Eppendorf centrifuge 5415R. The sample formed 3 layers, a pink bottom layer, a white interphase (containing protein/DNA) and a clear aqueous layer containing the RNA. This uppermost layer was taken off carefully, without touching any of the layers below, and transferred to a new sterile 1.5mL Eppendorf tube. 500μL RNAse- free, molecular biology grade isopropanol (propan-2-ol) (VWR) was added and mixed by inverting the tube twice, after incubation for 10min at RT the tubes were centrifuged at 12,000g for 10min at 4°C. The supernatant is discarded and 1mL of 75% v/v RNAse- free, molecular biology grade ethanol (VWR) was added to wash the pellet. A short vortex was followed by centrifugation at 7,500g for 5min at 4°C to precipitate the RNA. The supernatant was discarded and the pellet was air dried for 5-10min at RT. The pellet was not dried out completely to ensure good solubility in 10μL RNase free water (Severn Biotech ltd). The RNA was incubated at 55°C in a heat block to ensure the RNA was fully dissolved, before continuing with cDNA synthesis, as detailed in section 2.6.2, or storage at -80°C. Some samples were tested for RNA quality and quantity by spectrophotometer (Nanodrop machine, Agilent) by measuring absorbance at 260nm, and by gel electrophoresis (Bioanalyser Nanochip, Agilent). High quality RNA which had little contamination of other cellular molecules (especially proteins) had a ratio of the absorbances at A260/A280 close to 2.0 [241].

2.6.2. First strand copy DNA (cDNA) synthesis

Total RNA extracted as above was used to synthesize cDNA using random hexamers for priming. Random hexamers (Life Technologies), oligo nucleotides of 6 bases length and random sequences, 2.5μL at 100ng/mL were added to extracted RNA (optimal levels of 1-2μg), in a final volume of 11μL and incubated for 10min at 70°C in a heat block. Then 8.5μL of master mix, see Table 2.7, was added, and followed by incubation for 60min at 42°C, to allow reverse transcription to proceed. The reaction was terminated by incubation, at 70°C for 10mins. DNase/RNase free water was added in appropriate amounts to partially normalize for cell number, nothing for ≤ 0.01 x 10^6 cells, 25μL for ≤ 0.05 x 10^6 cells, 40μL for ≤ 0.5 x 10^6 cells, 80μL/ 1 x 10^6 cells, 140μL/ 2 x 10^6 cells, 200μL/ 3 x 10^6 cells and 300 μL/ 4 x 10^6 cells. cDNA samples were aliquoted and stored at -20°C.

Table 2.7: Master Mix per sample for cDNA synthesis by random hexamers

Solution	Manufacturer	Volume [μL]	Final concentration per reaction
5x First strand Buffer	Life Technologies	4	1x
0.1 M DTT	Life Technologies	2	10mM
10mM dNTP	Life Technologies	1	0.5mM
RNase out 40U/μL	Life Technologies	1	2U/μL
Superscript 200U/μL	Life Technologies	0.5	5U/μL
TOTAL VOLUME		20	

2.6.3. PCR and Real Time (RT)-PCR

Reagents for PCR protocols are shown in Table 2.8. Three PCR protocols, depending on application, were used as follows:

A. For standard PCR the BioMix Red (Bioline) containing dNTPs, *Taq* DNA polymerase and magnesium chloride ($MgCl_2$) was used, as detailed in Table 2.8A. The final reaction volume was 20μL and contained 2.0mM $MgCl_2$ and 0.5mM of each primer as final working concentrations. The PCR reaction was performed on a GeneAmp PCR system 9700 (PE Applied Biosystems) according to Table 2.9, with results analyzed according to section 2.6.4.

B. For Real Time PCR (RT-PCR) iQ SYBR green Supemix, containing dNTPs at 0.4mM each, 50U/mL i*Taq* DNA polymerase, 6 mM $MgCl_2$. SYBR Green I at 20nM (Biorad), served as a minor groove binding dye to determine the amount of double stranded DNA amplified quantitatively. The reagent mixes for RT PCR are shown in Table 2.8B. The total reaction volume was 20μL per reaction. The RT-PCR was performed using the iCycler (Biorad) or the Rotorgene 6000 (Corbett Life Science) according to Table 2.9, with results analyzed according to section 2.6.5.

C. For cDNA/DNA amplification pre-and post cloning, high fidelity Taq was used. Details are described in section 2.7.

Table 2.8: Master Mix per sample for standard PCR (A) and RT PCR (B)

A	Standard PCR		B	RT PCR	
	Mock	Control		Mock	Control
cDNA	2μL	2μL H_20	cDNA	5μL	5μL H_20
Primer forward (FW, 10nM)	1μL	1μL	Primer forward (FW, 10nM)	1μL	1 μL
Primer reverse (RV, 10nM)	1μL	1μL	Primer reverse (RV, 10nM)	1μL	1 μL
BioMix Red	10μL	10μL	iQ Syber green Supermix	10μL	10 μL
H_20	6μL	6μL	H_2O	3μL	3 μL

For high fidelity PCR master mix for cloning (C) see Table 2.12 in 2.7.

Table 2.9: PCR programs used

standard PCR (A)						
VIPR1 exon splicing investigation		45 cycles				
	94°C	95°C	60°C	72°C	72°C	
	5 min	30 s	30 s	1 min 45 s	7 min	
RT-PCR iCycler (B)						
ACTB, VIPR1, SMAD3, ERRFI1		45 cycles				
	95°C	95°C	60°C/56°C	72°C		plate read,
	3 min	30 s	30 s	45 s		melt curve
RT-PCR rotor6000 (B)						
ACTB, IL-23R, IFNG, IL17A, FOXP3, RORCv2, TBX21		45 cycles				
	95°C	95°C	60°C	72°C	72°C	plate read,
	5 min	30 s	30 s	30 s	5 min	melt curve

For high fidelity PCR programs for cloning see Table 2.13 in 2.7.

All PCR primers (Life Technologies, Qiagen) were used at 0.5mM, final concentration. Primers used for RT-PCR are shown in Table 2.10, primers for VIPR1 exon splicing investigation in Table 2.11 and primers for high fidelity PCR for cloning see Table 2.14 in 2.7. Primers were designed using the Primer 3 programme [242,243] to minimize primer dimers, hairpin loops and maintain best possible cytosine-guanine balance. All primers were checked for specific binding with NCBI Primer blast [244].

Table 2.10: RT-PCR primers used

Target	Direction	Primer sequence (5'-3')
ACTB (β-actin)	FW	AGA TGA CCC AGA TCA TGT TTG AG
	RV	AGG TCC AGA CGC AGG ATG
VIPR1	FW (Pr8)	ACAAGGCAGCGAGTTTGGAT
	RV (Pr9)	GTGCAGTGGAGCTTCCTGAAC
SMAD3	FW	ACGTCAACACCAAGTGCATC
	RV	CCAACACAGGAGGTAGAACTGG
ERRFI1	FW	GGAGCGCCTAATACCACT
	RV	ACCCCGTTCACAAAGAGG
IL-23R	FW + RV	Purchased from Qiagen (sequence not disclosed)
IFNG	FW	TGC CCA GAG CAT CCA AAA GA
	RV	TGT ATT GCT TTG CGT TGG AC
IL17A	FW	AAT CTC CAC CGC AAT GAG GA
	RV	ACG TTC CCA TCA GCG TTG A
TNF-α	FW + RV	Purchased from Qiagen (sequence not disclosed)
FOXP3	FW	ACC TGG AAG AAC GCC ATC
	RV	TGT TCG TCC ATC CTC CTT TC
RORC variant 2	FW	GAAGGACAGGGAGCCAAGGC
	RV	GCACCCCTCACAGGTGATAA
TBX21 (Tbet)	FW	CCC CAA GGA ATT GAC AGT TG
	RV	GGG AAA CTA AAG CTC ACA AAC

FW- forward primer, RV – reverse primer

Table 2.11: PCR primers used for VIPR1 exon splicing investigation

Primer Name	Sequence (5'-3')	Primer Name	Sequence (5'-3')
VIPR1 Pr 1 FW	CATGTGACCATTGGCAAGAC	VIPR1 Pr 9 RV	RT-PCR primer RV (Table 2.10)
VIPR1 Pr 2 FW	GCGGAGTATAAGCCCTACCC	VIPR1 Pr 7 RV	AGTCACACTCCTCCTGCAGC
VIPR1 Pr 3 FW	AATCAGAAGGGCACTGGAT	VIPR1 Pr 10 RV	GTGTCCCAGCACCCATAATC
VIPR1 Pr 4 FW	TCTTAGCTCTGGGGCCACA	VIPR1 Pr 11 RV	ACGACGAGCTCAAAGACCAT
VIPR1 Pr 5 FW	AGCGCCACTCTGCCAGGCT	VIPR1 Pr 12 RV	GTCAGACCAGGGAGACTTCG
VIPR1 Pr 6 FW	GCTGCAGGAGGAGTGTGACT		
VIPR1 Pr 8 FW	RT-PCR primer FW (Table 2.10)		

FW- forward primer, RV – reverse primer

For an alignment of VIPR1 primers to potential VIPR1 variants see Appendix I.

2.6.4. Analysis of PCR: Agarose gel electrophoresis

A 1-2% w/v agarose gel in 1x Tris Borate EDTA buffer (TBE, Sigma) was made, 10μL Gel Red (Biotum) was added per 100mL agarose gel to visualize DNA. The gel was then cast and left to set for about 30min at RT. 5μL Quick load 100bp DNA ladder (Biolabs) and 10μL of each PCR product was loaded. Gels were run under a current of 100V until the loading dye reached the bottom of the gel (typically 45 min).

2.6.5. Analysis of RT-PCR

Samples failed quantification if one or both duplicate for either the gene of interest or housekeeping gene was not possible to measure, did not amplify at all, or more than 2 log fold below the lowest standard, or if the melt curve did not fit its expected pattern. The correct melt curve pattern was confirmed when setting up the RT-PCR by running the product on a 2 % agarose gel (section 2.6.4) and the band size was verified as being correct. For each primer pair this procedure was done and verified.

2.6.5.1. ΔCT method

RT-PCR data gathered by the iCycler were analysed using the ΔCT method. The cycle threshold (CT) was recorded for each sample for the genes of interest (*VIPR1, SMAD3, ERRFI1*) and the housekeeping gene (*ACTB*: β-Actin). The mean of duplicate wells was taken and the following calculation was performed for each gene of interest for each sample: $\Delta CT=2^{-(CT(\text{gene of interest}) - CT(\text{housekeeping gene}))}$. Excel was used to calculate the mean of the duplicates and ΔCT. Samples with highly divergent duplicates or an inaccurate melt curve were excluded. A known cDNA (HT29 cells) was run at several dilutions in each run to verify the range of RT-PCR products.

2.6.5.2. Standard method

RT-PCR data generated on the Rotorgene6000 were analyzed using the standard method. A cDNA from stimulated healthy control cells was used as standard, which was diluted using 4 or 5 8-fold dilutions; these were run for each primer pair once in full and consequent experiments using the same primer pairs at least one of the standard points was run (usually 1:8 or 1:64). The chosen standards showed good

expression over the dilutions for the respective primer pairs. A standard curve was calculated using the threshold cycle of the dilutions, in duplicates, and the given concentration. The reaction from undiluted standard was set as 1 for each reaction. For each sample a relative concentration was calculated using the mean of the duplicates. This method enables the comparison of different reactions more accurately and removes inter-run variability, as the standard is used at the same concentration in each run, and the Rotorgene6000 software enables inter-run normalization. To normalize each expression value relative to amount of template material, the calculated concentration of the gene of interest was divided by the concentration of the housekeeping gene (β-Actin) of the same cDNA leading to a gene of interest concentration relative to a set standard normalized to a housekeeping gene.

The appropriate software for the Rotorgene 6000 was used to generate the standard curve and calculate sample concentration, excel was used to calculate the mean of the duplicates and normalize the gene of interest to the housekeeping gene. Samples with highly divergent duplicates, an inaccurate melt curve or well outside the range of the standard curve were excluded

2.7. Molecular Cloning

Sorted T cell populations (2.4.5) were used to prepare RNA, cDNA (2.6.1-2) and genomic DNA according to 2.7.2. The desired sequence was amplified using Platinum® *Taq* DNA Polymerase High Fidelity (Life Technologies) (Master mix Table 2.12) and PCR primers Table 2.14 and PCR programs in Table 2.13.

Cloning was performed using the TOPO-TA cloning system (kit, Life Technologies) according to manufacturer's instructions. In brief, PCR product (1μL for FoxP3 TSDR and 2μL for TCR-Vβ2 CDR3 to yield an insert to vector molar ratio of approximately 5:1 [e. g.: 10ng vector at ~4000bp, Zng PCR product at 336bp: 5 x (336/4000) = Z/10 -> Z=4.2ng PCR product], PCR product concentration was estimated on a 1% agarose gel (2.6.4)), vector (1μL), salt solution (1μL, both provided by the kit) and sterile water (2μL) were mixed gently, incubated for 30min at room temperature, followed by ice. Then 2μL of this ligation reaction mix was added to 1 vial of chemically competent cells (kit provided) and incubated 5min on ice, then heat shocked for 30s at 42°C and followed by 5min on ice. 250μL of room temperature S.O.C. media (Super Optimal broth with Catabolite repression media, kit provided) was added and the vial placed on a shaker at 200rpm in an 37°C incubator at 5% CO_2 for 1h. During this time ampicillin (Life Technologies, final concentration 50μg/mL) LB (Luria-Bertani) agar (Life Technologies) plates were warmed to 37°C. Plates were inoculated with 20-100μL and incubated overnight at 37°C and 5% CO_2. Appropriate amount of colonies were picked and amplified using M13 program and primers (Table 2.13 and 2.14), and the size checked on a 1% agarose gel (2.6.4). PCR products were cleaned using MultiScreen PCR micro 96 10/pk (Millipore) according to the manufacturer's instructions and sent for sequencing. Sequencing was performed on a 3730xl capillary sequencer (UCL genomics) and analyzed using Sequencher (Genestar) and Geneious 5.4.4 (Biomatters Ltd), in collaboration with UCL genomics

Table 2.12: PCR master mix using High Fidelity *Taq*

C	High Fidelity PCR		
	1st amplification	M13 amplification	
	(TCR-Vβ2 CDR3 and *FOXP3* TSDR)	TCR-Vβ2 CDR3 clones	*FOXP3* TSDR clones
template	5μL/ 5μL H_20	colony / empty tip	colony / empty tip
Primer forward (FW) (final concentration 0.5μM)	2μL	1μL	1μL
Primer reverse (RV) (final concentration 0.5μM)	2μL	1μL	1μL
High Fidelity Buffer	2.5μL	2.5μL	2μL
$MgSO_4$	1μL	1μL	0.8μL
dNTPs (stock concentration 10mM)	0.5μL	0.5μL	0.4μL
Platinum® *Taq* High fidelity	0.1μL	0.1μL	14.7μL
H_20	11.9μL	13.9μL	

2.7.1. TCR-Vβ2 CDR3 cloning

TCR CDR3 cloning and analysis was done with the assistance of an undergraduate summer student Qiong Wu and research assistant Simona Ursu. Complementarity determining region-3 (CDR3) TCR analysis was performed as previously described [245]. Briefly, sorted Treg subsets (CD161+ Treg and CD161- Treg) were used to prepare RNA and cDNA (2.6.1-2). TCR-Vβ2 mRNA was amplified by PCR (using master mix, program and primers as shown in Table 2.12, 2.13 and 2.14 respectively). The amplification products were cloned using the TOPO-TA cloning system, amplified using M13 primers and sequenced (details see above (2.7).

Sequence results were obtained, checked for quality, primer binding sites in the constant region and that the sequence in between is of similar sizes. Clones were grouped using Sequencher (Gene Codes Cooperation), then checked by eye in Geneious (Biomatters Ltd.) to confirm protein and nucleotide sequence were identical between clones.

2.7.2. Genomic DNA extraction

DNA was extracted from sorted cell subsets (purity of ≥80%) using the DNeasy blood and tissue kit (Qiagen) according to manufacturer's instructions. In short, sorted cell subsets (2.4.5) from male donors were washed in DPBS (Life Technologies) then were lysed, DNA was bound to spin columns, washed and eluted (reagents and spin columns provided by the kit). Postdoctoral fellow David Bending performed DNA extractions.

2.7.3. *FOXP3* TSDR methylation analysis

Analysis of the FOXP3 TSDR was done in cooperation with postdoctoral fellow David Bending in the group, including bisulfite conversion, cloning and sequence analysis. Extracted genomic DNA (2.7.2) was bisulfite-treated using the EpiTect Bisulfite Kit (Qiagen) according to the manufacturer's instructions. In brief, DNA and EpiTect reaction buffers (kit provided) were mixed and DNA converted in a thermocycler for 5 h (95°C - 5min, 60°C - 25min, 95°C - 5min, 60°C - 85min, 95°C - 5min, 60°C - 175min and 20°C - indefinitely). The converted DNA was transferred to a 1.5mL Eppendorf tube, Buffer BL was added, the DNA bound to spin columns, washed and desulfonated. Two additional washes were performed prior to elution (spin columns and reagents provided in the kit).

A 336bp segment containing the TSDR of *FOXP3* was amplified using published primers (Table 2.14) [108] using platinum high fidelity *Taq* (Life Technologies, master mix Table 2.12, PCR program Table 2.13, primers Table 2.14), followed by cloning of PCR products (TOPO-TA kit), as described above (2.7). 25-35 clones per subset were sequenced (details see 2.7) and from these the percentage of clones displaying methylated CpG for each site and total average was determined, with the presence of a C signifying a methylated and T a demethylated residue for each site.

Table 2.13: PCR programs used for amplification of TCR-Vβ2, *FOXP3* TSDR and cloning products

High Fidelity PCR

		35 cycles			
TCR-Vβ2	94°C	95°C	55°C	68°C	68°C
	5 min	30 s	30 s	60 s	5 min
		41 cycles			
FOXP3 TSDR	94°C	95°C	60°C	68°C	68°C
	2 min	30 s	30 s	60 s	15 min
		35 cycles			
M13	94°C	95°C	55°C	68°C	68°C
	2 min	30 s	30 s	60 s	5 min

Table 2.14: PCR primers used for amplification of TCR-Vβ2, *FOXP3* TSDR and cloning products

Target	Direction	Primer sequence (5'-3')
TCR-Vβ2	FW Vb	CACAACTATGTTTTGGTATCGTC
	RV Cb	GGGTGTGGGAGATCTCTGC
FOXP3 TSDR	FW	TGTTTGGGGGTAGAGGATTT
	RV	TATCACCCCACCTAAACCAA
M13	FW	GTAAAACGACGGCCAG
	RV	CAGGAAACAGCTATGAC

FW- forward primer, RV – reverse primer, V: variable beta region; Cb: constant beta region

2.8. Fluorescent microscopy

Staining for fluorescent microscopy was performed by Hemlata Versani, a research assistant in the group, according to standard technique. In brief, synovial biopsies were obtained from the hip at joint replacement surgery and snap frozen within 1h and stored at –80°C. All staining was carried out on acetone fixed 7μm cryostat sections. For fluorescence staining biopsies were labeled at 4°C overnight with anti-LLT1-PE antibody (1/10 Anti-human OCIL/CLEC2d, R&D systems). Sections were washed three times with PBS; slides were mounted with VECTASHIELD Mounting Medium with DAPI (Vector laboratories, DAPI at 1.5μg/mL) and analyzed by fluorescent microscopy. Pictures were taken at 40x magnification on a Leica DM LB microscope (Leica) with Image-Pro 6.2 (Media Cybernetics) software. Image composites were done in Image-J (public domain, designed at the National Institute of Health).

2.9. Statistical Analysis

Statistical analysis was performed using Prism 4 for Macintosh (GraphPad) software. Data are shown as mean +/- standard error of the mean (SEM) in bar graphs and as median in scatter plots, unless shown elsewhere. In chapters 4 through 6 CD161+Treg are defined by black symbols or bars and CD161- Treg as white symbols and bars, unless stated otherwise. The Mann-Whitney U-test, Wilcoxon matched pairs test or paired t-test were applied to compare 2 groups; the one-way ANOVA with Bonferroni or Dunn's posthoc tests was used to compare three or more means. Best fit of correlation was measured by the root mean square (Sy.x), with linear or non-linear regression. Correlation was assessed by spearman test. p values ≤ 0.05 were considered statistically significant. In the figures, p values are displayed according to the following scheme: ***≤ 0.001; **≤ 0.01; *≤ 0.05.

Chapter 3

Gene expression array target finding, validation and investigation

3. Gene expression array target finding, validation and investigation

3.1. Introduction

A gene expression profiling array was performed in the Wedderburn group to define differentially expressed genes in children with persistent and extended oligoarticular JIA at the site of inflammation at the point of diagnosis, i.e. before extension occurs [179]. Synovial fluid (SF) is routinely aspirated from swollen joints at therapeutic joint injections. In the Hunter study synovial fluid mononuclear cells (SFMC) from 21 oligoarticular JIA patients (in all cases the first SF aspirated and none of the children had had prior methotrexate (MTX) or steroids), were analysed by gene expression profiling and clinical outcome at one year (persistent, i.e. 4 or less joints involved or extended, 5 or more joints involved) was recorded. Children who had extended after one year were then called extended-to-be as they had not yet extended at the time of analysis. Of the 21 patients, 8 had extended at one-year follow up while 13 were persistent (i.e. still had 4 or fewer joints involved). This generated a list of 362 differentially expressed probe sets between persistent and extended-to-be with a cut off at an absolute fold change (FC) of 1.5 and a p-value of 0.05 [179]. These 362 probe sets identified 344 genes (Affymetrix data http://www.ncbi.nlm.nih.gov/gds). The results of this pilot study provided a starting point for further investigations into the mechanisms of severity in childhood arthritis. The general inflammatory profile due to joint involvement should be similar between persistent and extended-to-be cases, generating a list of differentially expressed genes between potential disease sub-groups and not just between health and inflammation. The list of genes that were differentially expressed between those who had a mild outcome (the persistent oligoarticular subgroup) and those children with a more severe outcome (extended-to be subgroup) was then examined with the overarching hypothesis that genes that are important in the mechanism of disease severity are expressed early in the more severe subtype.

In expression and functional data presented in 3.2.2.2 to 3.2.3.3, a total of 42 patients with JIA were included of which 7 were persistent, 6 extended-to-be and 25 extended oligoarticular JIA at time of sample. 4 cases had missing data for disease subtype. All experiments were run blind to the clinical status of patients. However in some of the

experiments presented here it was not always possible to stratify results by clinical subtype of JIA due to small numbers in some subsets, then patient data are referred to as 'JIA' in a combined group.

Specific aims of this chapter:

- Analysis of gene list generated by Hunter *et al* [179] by different bioinformatics tools and rankings.
- Finding gene candidates possibly involved in mechanism of extension/ protection and validate their expression levels in cell subsets from patient and healthy samples
- Functional investigation of candidate gene potentially involved in JIA

3.2. Results

3.2.1. Gene expression array data analysis using different approaches - IPA, DAVID, lists of different rankings

To drive examination of possible disease severity mechanisms, two different analysis tools, and various rankings were used to further analyse the list of genes differentially expressed between the two disease course groups: Ingenuity Pathway Analysis (IPA, http://www.ingenuity.com/ [246]) and Database for Annotation, Visualization and Integrated Discovery (DAVID, http://david.abcc.ncifcrf.gov/tools.jsp [246-248]). Both bioinformatics packages generated a list of functional annotations for groups of differently expressed genes, thus identifying pathways and biological functions, which may be contributing to disease severity subtypes.

Functional annotations (y-axis) ordered according to p-value on the upper x-axis in red (-log(p-value)), while the lower x-axis depicts the ratio (Figure 3.1). In both systems the p-value is then expressed as the negative logarithm to invert a small p-value to a high number. IPA and DAVID use different definitions for both of these parameters. In IPA (Figure 3.1A) the p-value, measures the enrichment of input genes in a functional pathway. It describes how many of the genes of the whole list belong to a certain pathway, a high -log(p-value) means a high proportion of all genes put in, belong to that particular functional annotation or pathway. DAVID (Figure 3.1B) defines the p-value as the enrichment of genes in this functional annotation within the genome, thus it compares the number of genes within the annotation from the input with the total number of genes belonging to that specific pathway. Hence a high -log(p-value) describes an enrichment of input genes in comparison to all possible genes from the genome for that particular annotation. The ratio is defined in IPA as the percentage of genes from the list compared to all possible genes in that pathway. Thus a ratio of 0 would indicate none of possible genes of the whole genome belonging to said pathway are among the input genes, whereas a ratio of 0.5 illustrates that 50 % of all possible genes involved in the pathway are among the input genes. DAVID defines the ratio as the number of genes within the functional annotation in relation to the total number of genes put into the analysis.

Results from IPA (Figure 3.1A) and DAVID (Figure 3.1B) showed several similarities. For example, in both methods, the complement pathway ranked high in the enrichment score. Thus in IPA the complement pathway had a -log(p-value) of 4.1, indicating that a large proportion of the input genes belong to this pathway. The ratio is 0.152, thus 15.2% of genes relating to the complement system in the whole genome are found among the gene list of differential expressed genes between persistent and extended-to-be cases. Other adaptive and innate immune responses were also implicated, including pattern recognition, TGF-β and IFN signaling as examples. The DAVID program generates more broad annotations, such as acute inflammatory response, lymphocyte mediated immunity and activation of immune response.

Both tools have their limitations. IPA is limited in connecting some genes to respective pathways, for example VIPR1 is an important inducer of cAMP, (a mediator that has itself been linked to Treg function) [249], yet it is not listed within the pathway cAMP-mediated signaling. DAVID in contrast generates very broad categories, often leaving some categories redundant, e.g. there are 6 groups comprised of the same genes involved in complement activation, which are all also summarized within the acute inflammatory response. Full pathway/annotation lists by IPA and DAVID are attached in Appendix II.

For this project, further analysis of gene lists generated was necessary. To rationalize the results obtained, redundant categories were removed, and the remaining functional annotations were grouped into categories, leading to a Top 20 functional annotations in the categories of Immunity, Signaling, transcription and cell proliferation and differentiation (Table 3.1), in both the IPA and DAVID analysis. In the work by Hunter *et al* a similar approach was taken [179].

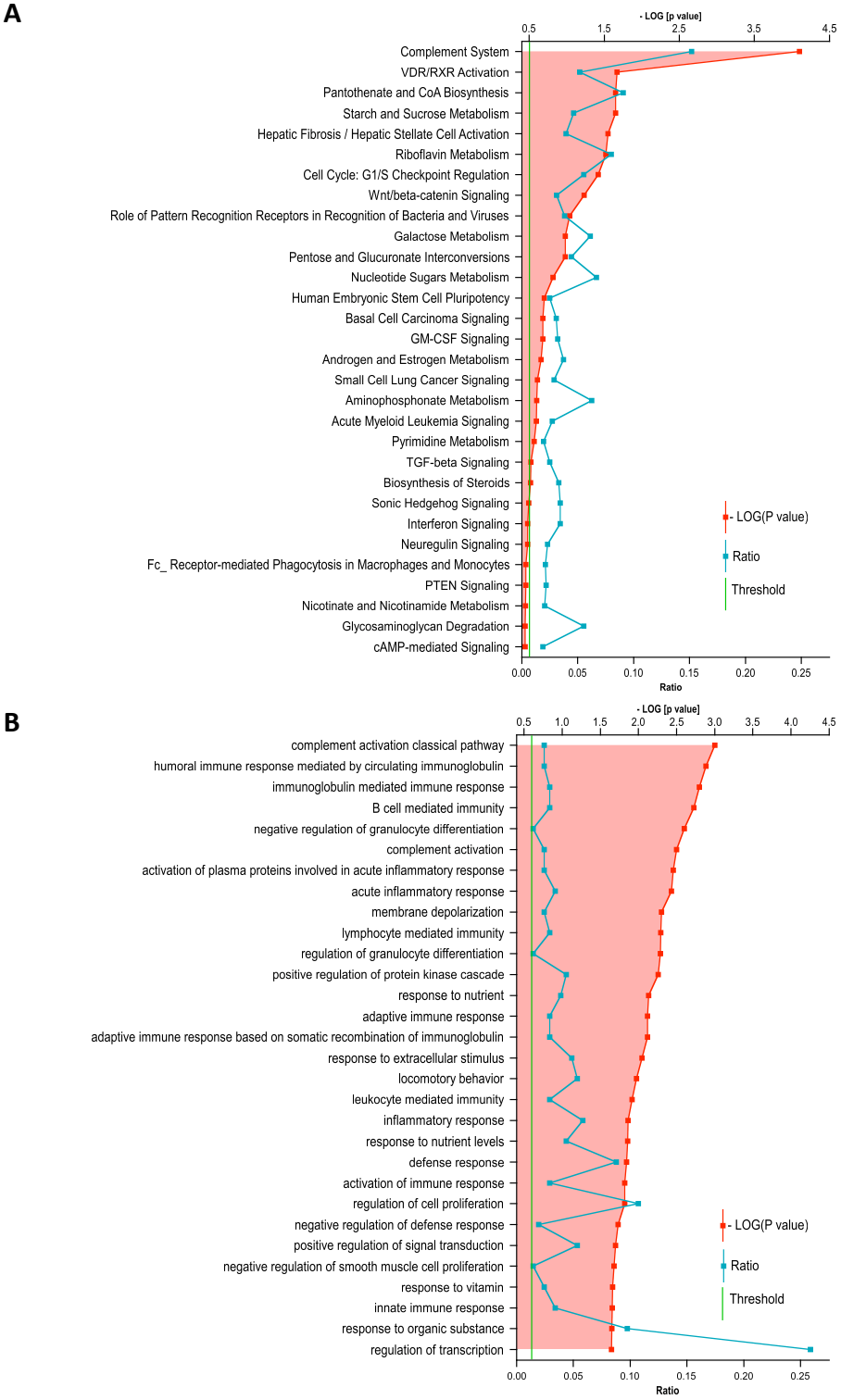

Figure 3.1: Functional annotation by IPA and DAVID programmes of differential expressed genes by gene expression array. Functional groups (y-axis) ranked according to –log (p-value) (upper x-axis), and respective ratio (lower x-axis). (A) IPA with p-value defined as the enrichment of the input genes in this functional annotation and the ratio as the percentage of genes from the uploaded list compared to all possible genes in that pathway (0.1 = 10% of possible genes are within the input gene list). (B) The p-value defined by DAVID describes the enrichment of a pathway in the genome (a high –log (p-value) describes a high proportion of all possible genes for this annotation are among the input genes) and ratio is defined as the number of genes

within the functional annotation compared to the total number of genes put into the analysis.

Table 3.1: Top 20 functional in the categories immunity, signaling, transcription and cell proliferation and differentiation; redundant annotations removed, functional annotations with gene names.

Immunity genes
Inflammatory response
CXCL9; IL8Rβ(CXCR2); CCR3; CCL18; NUPR1; AIMP1; SERPING1; complement C2; complement C1qA; complement C1qB; complement C1qC; fibronectin 1
negative regulation of inflammatory response
CD73; ADIPOQ; GHRL
lymphocyte mediated immunity
BCL10 (hypothetical LOC646626); SERPING1; complement C2; complement C1qA; complement C1qB; complement C1qC
regulation of interleukin-1 beta production
SMAD3; IFNγ; GHRL
positive regulation of immune system process
IFNγ; AQP3; BCL10 (hypothetical LOC646626); SERPING1; complement C2; complement C1qA; complement C1qB; complement C1qC
innate immune response
TBK1; BCL10 (hypothetical LOC646626); SERPING1; complement C2; complement C1qA; complement C1qB; complement C1qC
immune response
CXCL9; **VIPR1**; IFNγ; IL31RA; IFI6; CCL18; **SMAD3**; CD8b; TBK1; BCL10 (hypothetical LOC646626); ERAP2; HMHB1; SERPING1; complement C2; complement C1qA; complement C1qB; complement C1qC
Chemotaxis
IFNγ; CXCL9; CCR3; CCL18; IL8Rβ; PLD1; AIMP1
positive regulation of response to stimulus
SMAD3; BCL10 (hypothetical LOC646626); SEMA4C; GHRL; SERPING1; complement C2; complement C1qA; complement C1qB; complement C1qC
defense response
IFNγ; CXCL9; CCR3; CCL18; IL8Rβ; IL31RA; NUPR1; AIMP1; TBK1; BCL10 (hypothetical LOC646626); fibronectin 1; PLD1; TPSAB1, 2; SERPING1; complement C2; complement C1qA; complement C1qB; complement C1qC

Signaling genes
regulation of I-kappaB kinase/NF-kappaB cascade
TBK1; ADIPOQ; BCL10 (hypothetical LOC646626); TRIM13; TSPAN6
positive regulation of phosphorylation
IFNγ; IL31RA; ADIPOQ; BCL10 (hypothetical LOC646626); cyclin D1
regulation of protein kinase cascade
IFNγ; IL31RA; TBK1; ADIPOQ; BCL10 (hypothetical LOC646626); ERBB2; SEMA4C; TRIM13; TSPAN6
negative regulation of signal transduction
RGS7; RGS14; IGFBP-3; ADIPOQ; ERBB2; ARAP3; cyclin D1; TLE1
positive regulation of signal transduction
IFN; IL31RA; TBK1; ADIPOQ; BCL10 (hypothetical LOC646626); ERBB2; SEMA4C; GHRL; CDKN2B; TRIM13; TSPAN6
negative regulation of cell communication
RGS7; RGS14; KCNQ4; ADIPOQ; ERBB2; ARAP3; cyclin D1; TLE1; IGFBP-3

Transcription genes
regulation of transcription
IFNγ; IL31RA; VDR; RUNX1; ATF3; **RORC**; **SMAD3**; PKIA; PIAS2; NR4A2; SFPQ; ELL2; ELP2; TLE1; KLF4; ZNF193; ZNF550; ZNF436; ZNF44; ZNF260; ZNF354B; ZNF503; ZNF770; ZNF808; ZNF84; ZNF607; ZNF506; ZNF644; ZNF606; ZNF451; ZNF501; ZNF33A; ZNF518A; ZHF3; ZNF681; ALS2CR8; PBRM1; MORF4L2; MCTS1; PARP4; RAD54B; SOX7; CLOCK; BCL10 (hypothetical LOC646626); RHEBL1; RLF; cyclin C; FLI1; RAB18; FZD1; BRWD1; NEO1; HES7

Cell proliferation and differentiation
regulation of cell proliferation
IFNγ; **SMAD3**; **VIPR1**; IL8Rβ; IL31RA; IGFBP-3; VDR; ATF3; NUPR1; AIMP; KLF4; TSHR; FABP3; MCTS1; ERBB2; cyclin D1; GHRL; CUL1; PTCH1; FGFR2; LAMB1; CDKN2B
cell cycle arrest
IFNγ; **SMAD3**; GAS2L1; CDKN2B; CUL1
negative regulation of myeloid leukocyte differentiation
RUNX1; ADIPOQ; complement C1qC

Looking at both lists, the condensed Table 3.1 and the list previously generated by Hunter *et al,* the importance of T cell specific genes and regulatory molecules was evident [179]. Chemokines, cytokines and chemokine/cytokine receptors, CXCL9, CCR3, CCL18 and IFN-γ are some examples. In addition, numerous signaling molecules in the T cell compartment were identified, such as SMAD3 and CDKN2B, both induced by TGF-β; ATF3 and RORC are important transcription factors for Th1 and Th17 differentiation respectively. VIPR1 was highlighted in a more than one functional annotation. A literature search revealed the possible importance of VIPR1 in inflammatory processes and T cell immunology (see introduction 1.1.2). Furthermore several molecules (e.g. TBK1, BCL10, SMAD3, VIPR1) could be associated with the NF-κB pathway, a fundamentally important inflammatory signaling pathway. A schematic on how VIPR1 and SMAD3 might dampen NF-κB activity was drawn (see introduction Figure 1.1).

In order to narrow down the list of possible genes to be the focus of further investigation, the gene list extracted from the affymetrix data [179] was ranked in two ways, p-value and fold change (Table 3.2). Ranking by fold change generates a list according to large differences in expression levels. This describes the amplitude by how much the expression diverges on average between the two outcomes. To explore mechanistic differences between persistent and extended-to-be patients, thus identifying possible mechanisms of disease severity, the p-value is also very important as it describes the significance of the difference between persistent and extended-to-be cases.

Table 3.2: Top 10 differentially expressed genes ranked according to p-value and fold change, genes in bold investigated further.

p-value			Fold change		
6.98E-04	HIST1 H2AG-M	Histone cluster H2	5.997	TPSAB1	tryptase α/β 1
7.41E-04	RP4-692D3.1	hypothetical protein	4.469	SLC2A5	Solute carrier family 2 member 5
8.34E-04	**ERRFI1**	ERBB receptor feedback inhibitor	4.250	IFI27	interferon-α-inducible protein 27
9.32E-04	**VIPR1**	Vasoactive Intestinal Peptide receptor type 1	4.236	CHI3L1	Chitinase 3-like 1
9.86E-04	ZNF436	Zinc finger protein 436	3.951	C1QC	Complement C1qA
0.00102	**SMAD3**	SMAD family member 3 (TGF-β signaling)	3.636	RNASE1	Ribonuclease, RNase A family 1
0.00131	SSX2IP	synovial sarcoma, X breakpoint 2 interacting protein	3.537	C1QB	Complement C1qB
0.00165	ERBB3	v-erb-b2, erythroblastic leukemia viral oncogene homolog 3	3.372	**RORC**	Retinoic acid–related orphan receptor C
0.00201	LOC285628	hypothetical protein	3.215	C2	Complement
0.00228	ZNF84	Zinc finger protein 84	3.098	MARCO	Macrophage receptor with collagenous structure

To identify mechanistic important genes a very high significance (p-value) was considered to be more important than a great fold change, since regulatory molecules may be expressed at low level but have high potency. In the top 10 genes according to p-value are two zinc finger proteins (ZNF436, ZNF84), two hypothetical proteins with unknown function, two genes (SSX2IP, ERBB3), which have mainly been associated with cancer, and the Histone cluster H2, DNA binding histones. Among the remaining genes were SMAD3, VIPR1 and ERRFI1. SMAD3 and VIPR1 were also highlighted in several functional annotations in Table 3.1, and were introduced in the introduction (1.1.2)

SMAD3 is an important signaling molecule downstream of TGF-β and evidence suggests that it is essential in development of natural Treg and induced Treg [34-36]. VIPR1 signaling has been shown to act as an anti-inflammatory molecule and to have a role in the control of the ratio of different T cell subsets [54-56,250-253]. Both molecules are also able to inhibit the NF-κB pathway at different points (see introduction Figure 1.1) [37-41,48-50]. These two genes were both more highly

expressed in persistent, than extended-to-be oligoarticular JIA patients see Figure 3.2. Thus it is possible to hypothesize that these two molecules could play a role in a protective mechanism, which helps to maintain a mild level of inflammation.

ERRFI1 is a stress response protein, regulating the homeostasis of cells, but it has not been well investigated in the context of immunology. Moreover ERRFI1 has been associated with the NF-κB pathway in a potentially activating mode by occupying IκB binding sites and leave NF-κB free to translocate without IκB phosphorylation [74], thus potentially leading to pro-inflammatory signatures. Thus ERRFI1 was added to Figure 1.1 to show at what stage it might enhance NF-κB activity. ERRFI1 was more highly expressed in extended-to-be cases (Figure 3.2). It is possible that this gene might be involved in a more inflammatory mechanism. Thus SMAD3, ERRFI1 and VIPR1 were investigated in more detail as first part of possible molecules involved in regulation of disease severity (3.2.2).

Interestingly, RORC expression had a high fold change and was increased in persistent samples. The Wedderburn group has previously demonstrated that Th17 CD4+ cells, driven by RORC, are at higher frequency in patients with the more severe, extended oligoarticular JIA than those with mild persistent oligoarticular JIA [186]. With many T cell lineage associated genes and regulatory functional annotation, and the fact that RORC seems to be expressed early in a protective environment, the relationship between Treg and Th17 features was more closely explored in this thesis: this work is described in chapter 4 to 6.

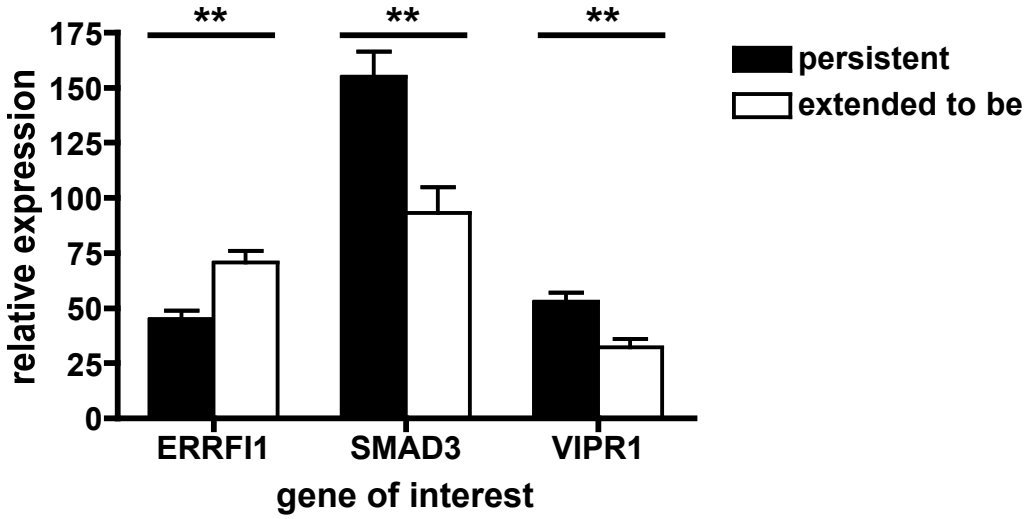

Figure 3.2: Relative expression levels of ERRFI1, SMAD3 and VIPR1 genes in SFMC form patients with persistent and extended-to-be oligoarticular JIA. (affymetrix data from Hunter *et al* 2010 [179]. Bars represent means +/- SEM with Man-Whitney test (p values: **<0.01).

3.2.2. Gene expression of VIPR1, SMAD3, ERRFI1 by RT-PCR

In order to investigate the possible relevance in disease of genes and their products implicated by the gene expression array analysis, real time PCR (RT-PCR, 2.6) validation was performed. The three genes initially chosen were SMAD3, ERRFI1 and VIPR1. All three can be associated with the NF-κB pathway and SMAD3 and VIPR1 facilitate other independent immunoregulatory functions (2.2.1, 1.1.2).

Gene expression was analysed by RT-PCR for unsorted healthy adult, child and JIA PBMC and SFMC (Figure 3.3). Additionally, where data was available, JIA samples were split into persistent (fewer than 4 joints), extended-to-be (fewer than four joints at time of sample, but has extended at a later time) and extended (more than 4 joints) at time of sample (Figure 3.3 right panel). No significant difference could be observed in SMAD3 and ERFFI1 expression between any of the groups. However when splitting the JIA samples according to their clinical status, a similar pattern to the gene expression array was seen (Figure 3.2). SFMC from extended-to-be cases had a lower median expression of SMAD3 compared to SFMC form persistent cases. At time of sample both SFMC and PBMC from children with extended oligoarticular JIA had a lower median expression of SMAD3 than either extended-to-be or persistent cases. A slight trend for increased levels of ERRFI1 in JIA compared to healthy as well as extended-to-be compared to persistent SFMC was suggested. VIPR1 mRNA was significantly decreased in JIA SFMC (Figure 3.3C), and this was significantly lower than healthy adult, healthy child or JIA PBMC.

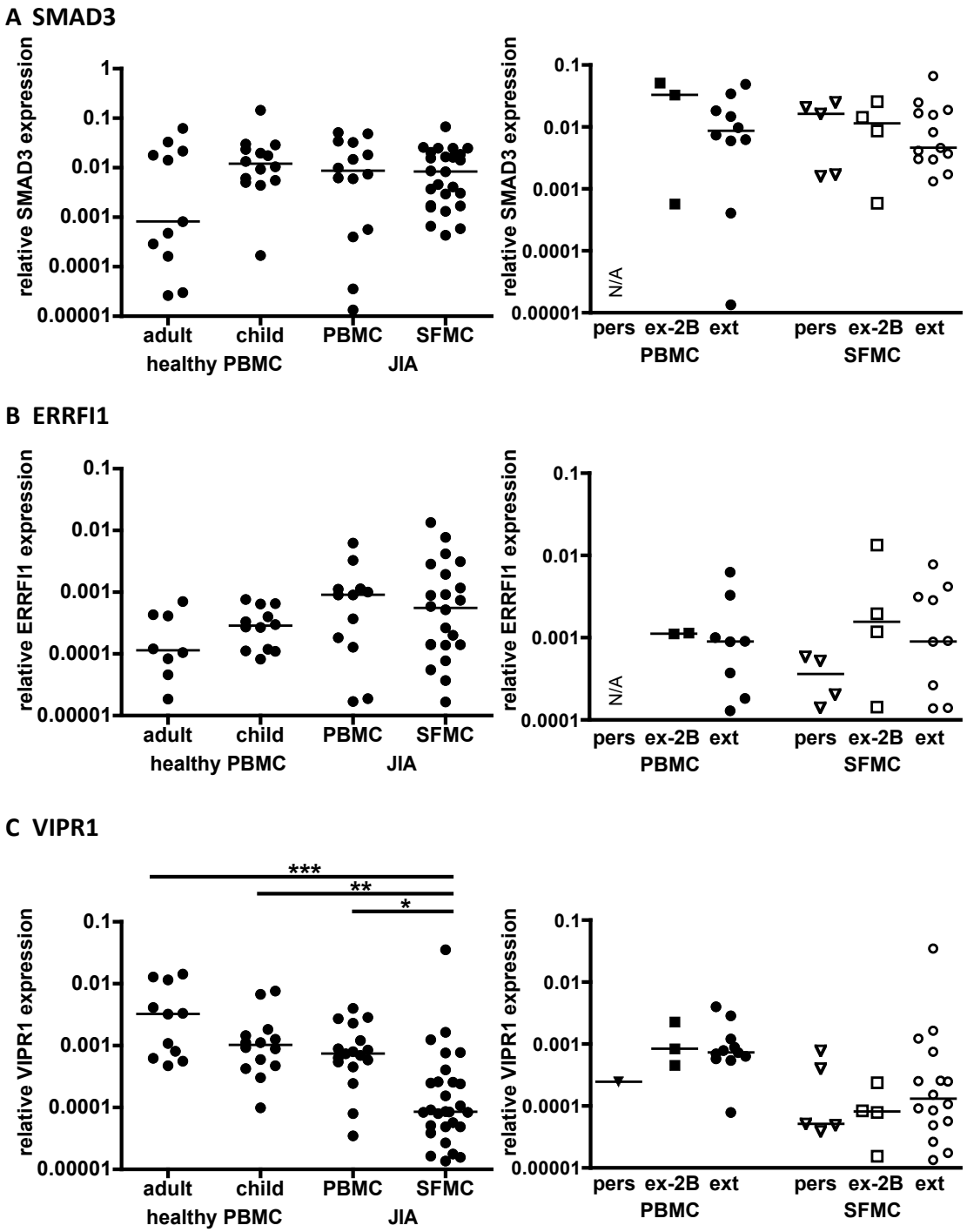

Figure 3.3: Gene expression of SMAD3 (A), ERRFI1 (B) and VIPR1 (C) quantified by RT-PCR. Comparing JIA PBMC and SFMC with healthy adult and child PBMC on the left; and JIA samples split into extension status on the right (triangle: persistent (pers), square: extended-to-be (ex-2B), circle: extended (ext); filled: PBMC, open: SFMC). Expression calculated using ΔCT method and normalized for amount of cDNA with β-actin, on logarithmic axis; horizontal lines represent median, p-values non-parametric one-way ANOVA with Dunn's multiple comparisons test (*≤0.05, **≤0.01, ***≤0.001) unsorted: SMAD3: healthy adult PBMC n=11, healthy child PBMC n=14, JIA PBMC n=14, JIA SFMC n=25; ERRFI1: healthy adult PBMC n=8, healthy child PBMC n=12, JIA PBMC n=12, JIA SFMC n=22; VIPR1: healthy adult PBMC n=11, healthy child PBMC n=14, JIA PBMC n=17, JIA SFMC n=28; N/A: non applicable.

Additionally the expression at mRNA level was measured in various cell subsets from healthy adult controls and JIA PB and SF samples. CD14+ Monocytes, CD19+ B cells and CD3+CD4+ and CD3+CD4- T cells were sorted. The CD4- T cell population will contain mainly CD8+ T cells but also gamma delta (γδ) T cells and NKT cells (sort strategy: 2.4.4, Figure 2.1).

Overall the gene expression was very variable and no significant difference between cell subsets or sample groups could be seen for most (Figure 3.4). ERRFI1 and VIPR1 mRNA was very low in B cells. VIPR1 expression in healthy monocytes (CD14+) was significantly increased compared to monocytes from the joint).

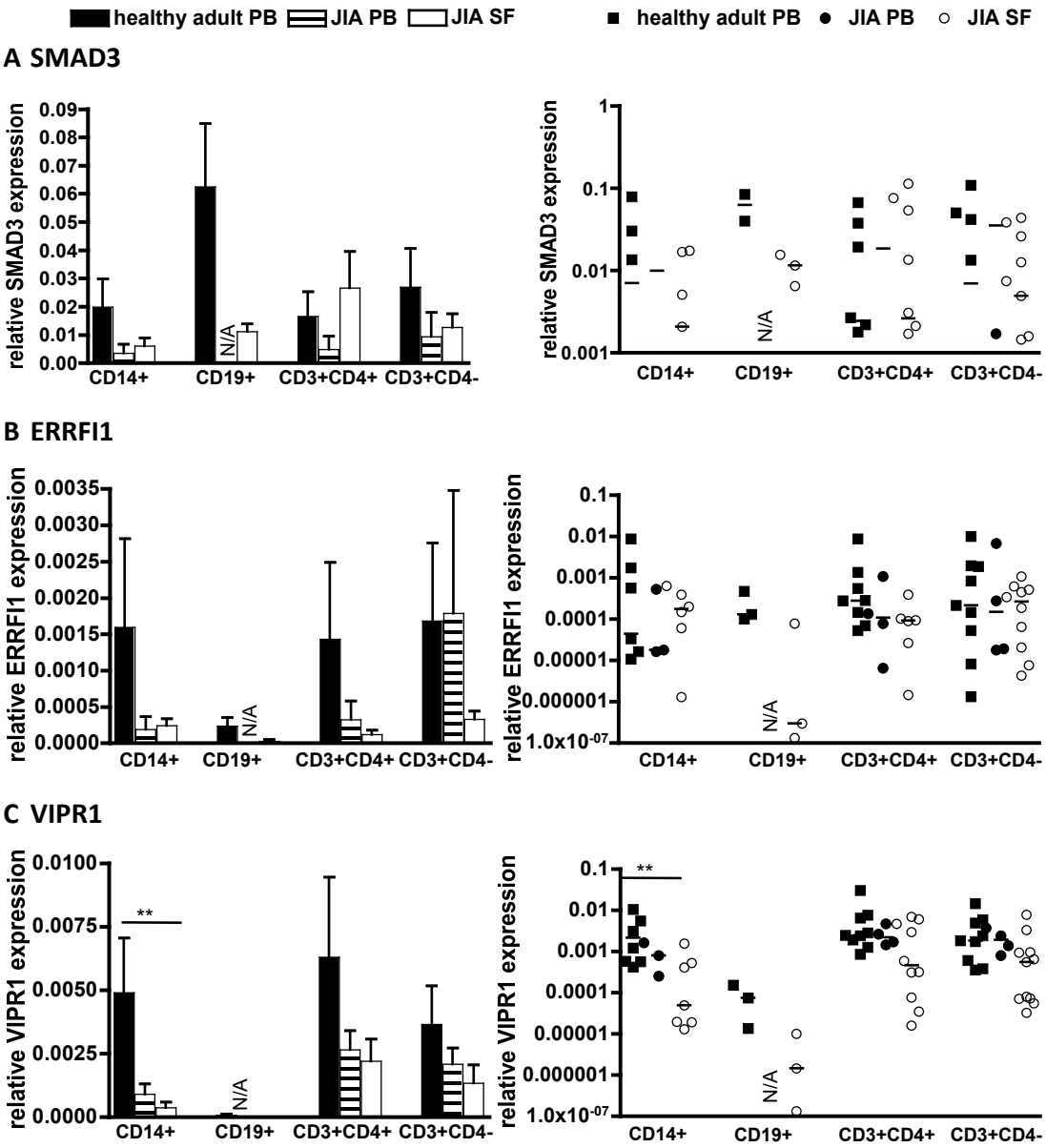

Figure 3.4: SMAD3, ERFFI1 and VIPR1 mRNA expression in sorted cell subsets of healthy adult PBMC, JIA PBMC and SFMC quantified by RT-PCR. Expression normalized for amount of cDNA with β-actin using CT-method ($2^{-(\Delta CT(SMAD3)-\Delta CT(\beta\text{-actin}))}$); linear axis on the left, logarithmic axis on the right. Relative SMAD3 (A), ERRFI1 (B) and VIPR1 (C) expression as bar graph showing mean with SEM on the left and scatter plot (each dot represents mean of duplicate wells) with median on the right for healthy PB (black bar/square), JIA PB (striped bar/black circle) and SF (white bar/open circle) for sorted subsets (CD14+, CD19+, CD3+CD4+, CD3+CD4-); p-values according to non-parametric One-way ANOVA with Dunn's multiple comparisons test (**≤0.01,). SMAD3: healthy adult PB: CD14+ n=8, CD19+ n=2, CD3+CD4+ n=8, CD3+CD4- n=8; JIA PB: CD14+ n=3, CD19+ N/A, CD3+CD4+ n=4, CD3+CD4- n=4; JIA SF: CD14+ n=7, CD19+ n=3, CD3+CD4+ n=10, CD3+CD4- n=11; ERFFI1: healthy adult PB: CD14+ n=7, CD19+ n=3, CD3+CD4+ n=8, CD3+CD4- n=9; JIA PB: CD14+ n=3, CD19+ N/A, CD3+CD4+ n=4, CD3+CD4- n=4; JIA SF: CD14+ n=6, CD19+ n=3, CD3+CD4+ n=6, CD3+CD4- n=10; VIPR1: healthy adult PB: CD14+ n=8, CD19+ n=3, CD3+CD4+ n=9, CD3+CD4- n=9; JIA PB: CD14+ n=3, CD19+ N/A, CD3+CD4+ n=4, CD3+CD4- n=4; JIA SF: CD14+ n=7, CD19+ n=3, CD3+CD4+ n=10, CD3+CD4- n=11; N/A: non applicable.

Taken together these data suggest that VIPR1 is downregulated within the joint of JIA compared to JIA PBMC, and healthy PBMC. I hypothesise that VIPR1 might play a role in distinct disease pathogenesis in different subtypes of arthritis. VIPR1 was therefore chosen as a candidate for protein analysis and functional work. Although SMAD3 showed no significant differences between joint and blood, there was a trend towards lower levels of SMAD3 expression in subgroups with more severe disease (extended compared to extended-to-be and persistent oligoarticular JIA). It would therefore be interesting to study functional SMAD3 in the context of JIA in the future. ERRFI1 did not show any differences therefore it was not investigated further.

3.2.3. Expression of VIPR1 protein

VIPR1 protein expression was investigated by two methods, western blotting (WB, 2.2) and flow cytometry (2.3). In parallel with the mRNA data shown earlier, CD14+ monocytes and CD4+CD3+ cells showed strong expression of VIPR1, while CD4- T cells showed moderate VIPR1 expression and expression on CD19+ B cells was below the limit detection in healthy PBMC. β-Actin was used as loading control. Densitometry confirmed this differential expression of VIPR1 (Figure 3.5A). Sorted SFMC (CD14+, CD3+CD4+ and CD3+CD4- cells) also showed expression on WB (Figure 3.5B), although these gels could not be evaluated by densitometry due to saturated β-actin bands, and would not give an accurate normalization.

In SFMC lysates the band for VIPR1 appeared to run at a slightly lower point than in healthy PBMC lysates (~48kDa versus ~52kDa). Running SFMC and healthy PBMC of the same cell type side by side on the same gel, revealed an apparent size difference in the band detected for VIPR1, of about 4kDa (Figure 3.5C). In the blot shown in Figure 3.5C (top and middle) the β-actin loading control was not detected for all samples equally, most likely due to technical reasons. The size difference was noted in at least three different experiments. However in some additional samples two VIPR1 bands were detected, one at the predicted size and a second weaker band at a lower size (Figure 3.5C bottom (1x ~52kDa, 1x ~48kDa)). The two JIA PBMC samples investigated, both showed two VIPR1 bands. Additionally there might be some hint of a faint second band in some healthy CD3+CD4+ lysates.

Additionally a pure monoclonal antibody against human VIPR1 and an appropriate isotype control were labelled with a fluorochrome *in vitro* using LYNX rapid RPE antibody conjugation kit (2.3.3), a commercially conjugated VIPR1 antibody did not yield any staining on the control cell line (data not shown). Titration was initially performed using the control cell line HT29. However, when staining of HT29 from several experiments was re-analysed it was apparent that the labelled VIPR1 antibody yielded variable results (Figure 3.5D). And that over time VIPR1 staining decreased perhaps due to instability of the Ab-conjugate. In addition very inconsistent results were obtained on PBMC samples despite various attempts to block background or

false positive staining (data not shown). Therefore staining VIPR1 using flow cytometry was discontinued.

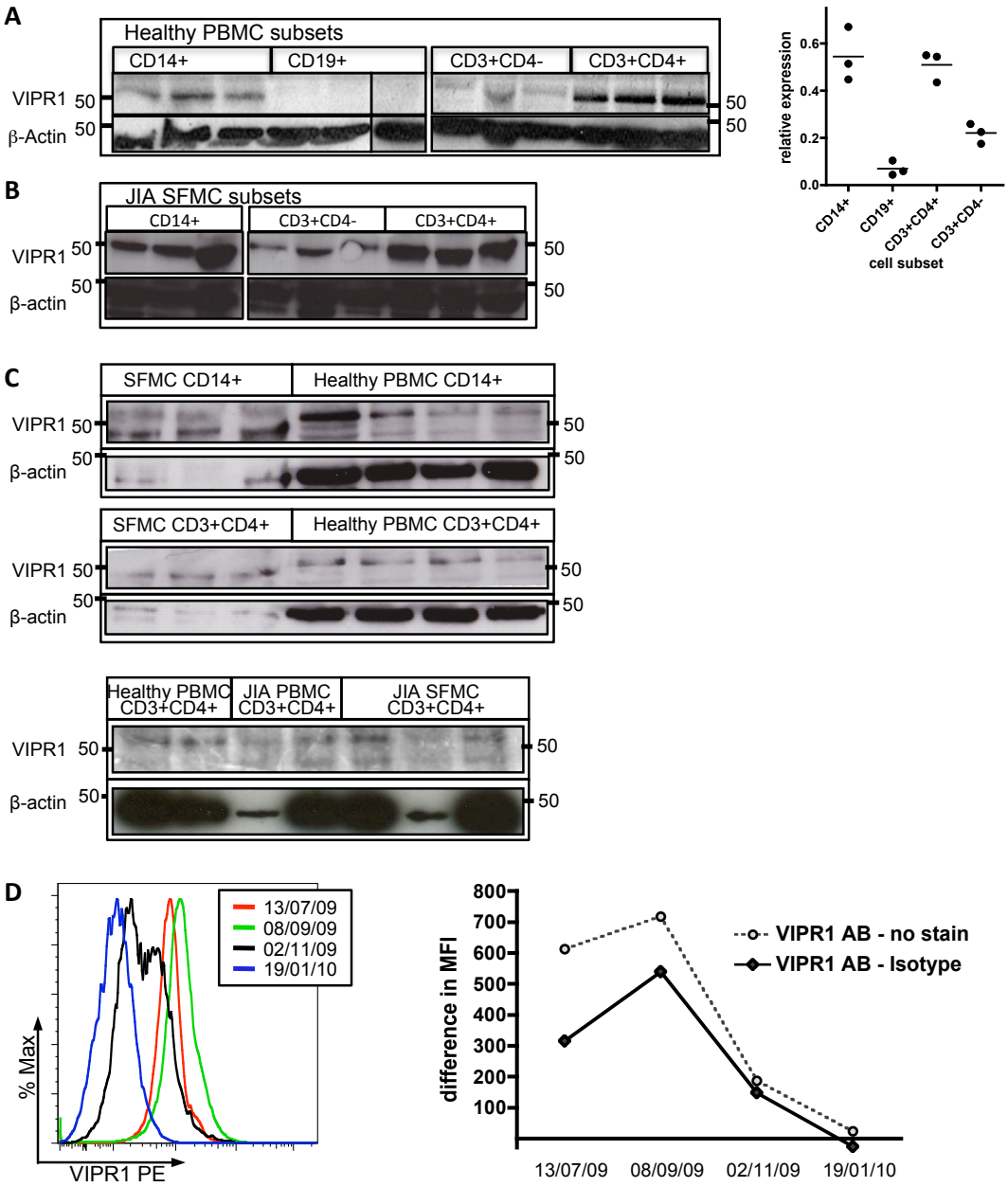

Figure 3.5: Analysis of VIPR1 protein expression in synovial and peripheral blood cells. (A-C) VIPR1 protein by western blot. (A) Expression profile of VIPR1 (~52kDa) on healthy PBMC subsets: CD14+, CD19+, CD3+CD4-, CD3+CD4+ each n=3, with β-actin (~45kDa) as loading control, with densitometry results (VIPR1/β-actin) (B) VIPR1 expression on CD3+CD4-, CD3+CD4+ and CD14+ JIA SFMC each n=3 with β-actin as loading control. (C) Size difference between JIA SFMC (n=3 each) and healthy PBMC (n=4 each) on CD14+ (top) andCD3+CD4+ cells (middle) CD3+CD4+ cell lysates from healthy PBMC (n=2), JIA PBMC (n=2) and SFMC (n=3) showing VIPR1 double bands (bottom) all with β-actin as loading control. Position of standard ladder proteins (in kDa) shown to right and left of each blot. (D) Variability of flow cytometry staining using PE-labelled VIPR1 antibody. Overlay of VIPR1-PE staining on HT29 cells on various days on the left. The difference of mean fluorescence intensity (MFI) of VIPR1-PE staining and no staining (grey, dotted) and VIPR1-PE staining and isotype-PE staining (black, line) for the same dates on the right.

3.2.4. Potential mechanism of small VIPR1 isoform

The apparent difference in molecular weight of VIPR1 protein observed in some JIA SFMC could be due to a variety of biological reasons, including posttranslational modification of the VIPR1 protein such as glycosylation, acetylation or phosphorylation. Alternatively the size difference of ~4kB might be the result of a splicing variant of VIPR1. A literature search revealed a known VIPR1 splice variant with five instead of seven transmembrane units (TM) [254]. However the 5TM VIPR1 has a predicted molecular weight of about 39kDa, thus smaller than the observed band in SF samples. The protein database UniProt (www.uniprot.org/) listed a long isoform, of 55kDa compared to VIPR1 regular isoform of 51.5kDa. The listed transcripts on e!Ensembl (www.ensembl.org) identified six transcripts encoding a protein (Table 3.3, Protein size in kDa was calculated using the molecular weight calculator using protein sequence by EnCor Biotechnology Inc (http://www.encorbio.com/protocols/Prot-MW.html)).

Table 3.3: VIPR1 transcripts encoding a protein according to e!Ensembl, protein size [kDa] calculated using molecular weight calculator by EnCor Biotechnology Inc

Name (e!Ensembl)	Transcript ID	length [bp]	Protein ID	length [aa]	size [kDa]	biotype
VIPR1-001 (ref seq)	ENST00000325123	2773	ENSP00000327246	457	51.56	Protein coding
VIPR1-002	ENST00000433647	3161	ENSP00000394950	416	47.21	Protein coding
VIPR1-011	ENST00000450274	743	ENSP00000415013	126	13.83	Protein coding
VIPR1-013	ENST00000439731	770	ENSP00000403478	219	23.70	Protein coding
VIPR1-201	ENST00000438259	1393	ENSP00000415371	247	28.18	Protein coding
VIPR1-202	ENST00000543411	1502	ENSP00000445701	409	46.29	Protein coding

bp: base pairs, aa: amino acids, kDa: kilo dalton

According to the protein size calculated for the transcript variants listed by e!Ensembl two transcripts (VIPR1-002 at 47.21kDa and VIPR1-202 at 46.29kDa) matched roughly the size of the band for VIPR1 seen in some JIA SF samples.

To test this hypothesis a PCR approach was used to investigate whether SFMC showed alternative splicing of VIPR1 at mRNA level. The regular transcript (VIPR1-001/ref seq) and transcripts VIPR1-002 and VIPR1-202 were aligned using Biology WorkBench 3.2

((www.workbench.sdc.edu); CLUSTAL W module[255]) (Appendix I). A total of 12 primers were designed to span VIPR1 exons including VIPR1-002 and VIPR1-202 regions sequences (Figure 3.6A for a schematic overview, Appendix I for detailed sequence). The exploratory PCR confirmed different behaviour in JIA SFMC than healthy PBMC (1 representative set (healthy PBMC, JIA SMC, no template control) of at least 3 samples tested Figure 3.6B).

Other primer pair combinations did either result in the same or no PCR product for both healthy PBMC and JIA SFMC cDNA (data not shown). Suboptimal primer design, PCR settings, high primer-dimer formation or no binding to transcript of primers might all be reasons for non-amplifying PCR. Further primers could be designed to investigate the differences around exon 1, 2, 8 and 9, and 11 and 12 seen in the PCR described.

There is some evidence that JIA SFMC might have variable splicing compared to healthy PBMC. However, due to variability between samples, low cDNA yields and missing bands no conclusive statement can be given and due to other projects this was not taken forward.

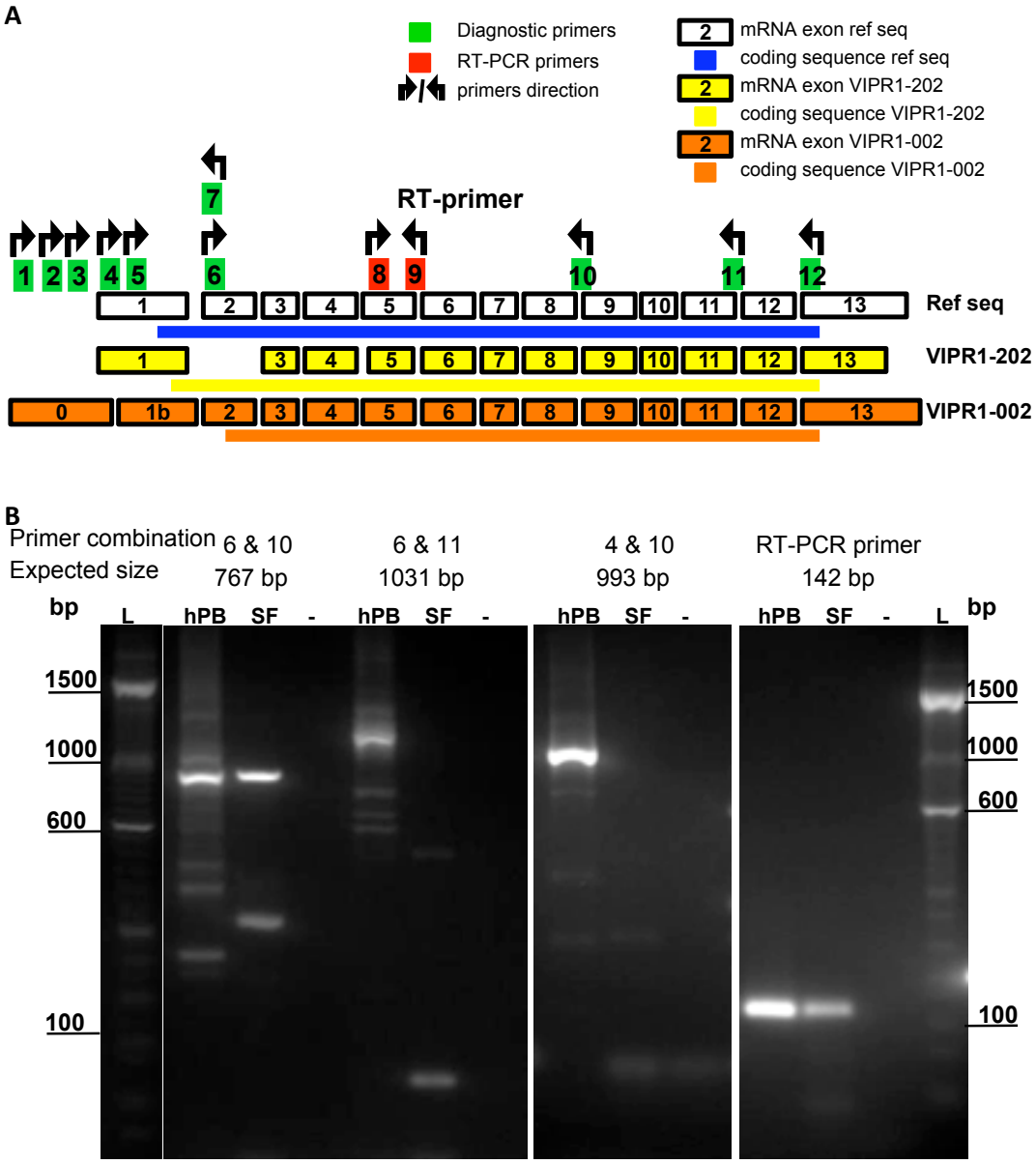

Figure 3.6: PCR amplification products from a set of reactions using diagnostic primer pairs suggest different mRNA between healthy PBMC and JIA SFMC. (A) Exon structure of VIPR1 gene with white blocks with numbers: reference sequence (ref seq); yellow filled blocks: VIPR1-202; orange filled blocks: VIPR1-002; green blocks: diagnostic primer, red blocks: RT-PCR primers, line: coding sequence (blue: ref seq, yellow VIPR1-202, orange: VIPR1-002). (B) Representative gel images of PCR products of primers 6 and 10 (767bp), 6 and 11 (1031bp), 4 and 10 (993bp) and VIPR1 RT primers (142bp) on a 2 % agarose gel stained with GelRed. In each case lanes are as follows: lane 1: healthy PBMC cDNA (hPB), lane 2: JIA SFMC cDNA (SF), lane 3: no template negative control (-); L: ladder.

3.2.5. VIPR1 functional assays: IL-2 inhibition by VIP

It was hypothesised that relative reduction of VIPR1 mRNA or protein expression or altered form of VIPR1 protein in JIA SFMC could lead to reduced or altered function of VIPR1 protein. Evidence suggests that VIPR1 has an inhibitory effect on immune responses like cytokine production, in part by reduction of IL-2 production after binding of VIP to VIPR1, and downstream signaling in mice and human [236-239,256,257]. In the Affymetrix gene expression data VIPR1 was expressed at higher levels in a milder clinical phenotype group of patients, but both groups do have clinical arthritis. The RT-PCR data suggest that in SFMC this immunoregulatory molecule VIPR1 is expressed at lower levels than in equivalent blood cells. Finally the western blot protein and splice variant PCR data suggest altered VIPR1 at the inflammatory site (SFMC). Together these data lead to the hypothesis that VIPR1 low expression or lack of function may contribute to inflammation in JIA.

The functionality of VIPR1 protein was investigated by taking advantage of its downstream signaling effect of decreased IL-2 production. VIPR1 can signal through cAMP dependent and independent pathways, but it is not yet clear which leads to reduced IL-2 production in T cells. To test VIPR1 function, healthy PBMC or JIA SFMC were incubated with or without either VIP, VIPR1-specific agonist $^{[11,22,28Ala]}$VIP or forskolin (FSK), a VIPR1 independent cAMP inducer (2.5.2). Representative FACS plots for healthy PBMC and JIA SFMC gated on CD3+CD4+ T cells of unstimulated, stimulated without pretreatment and stimulated with specified pretreatment (VIP or VIPR1 agonist) at 10^{-7}M are shown in Figure 3.7A.

Incubation of healthy PBMC with VIP confirmed suppression of IL-2 production with reduction in the IL-2+ percentage of cells for most samples tested. Pretreatment with VIPR1-specific agonist showed some IL-2 inhibition, though with a smaller effect than VIP pretreatment. In contrast SFMC samples showed no inhibition of IL2 production upon treatment with VIP or VIPR1-specific agonist. FSK pretreatment (cAMP Inducer) resulted in IL-2 reduction in only a minority of samples (data not shown), which suggests that IL-2 inhibition in T cells is not due to cAMP induction.

Hence this data suggest that there is some difference in VIPR1 function on whole SFMC cultures, which might be due to low expression or true functional difference of VIPR1 in the joint.

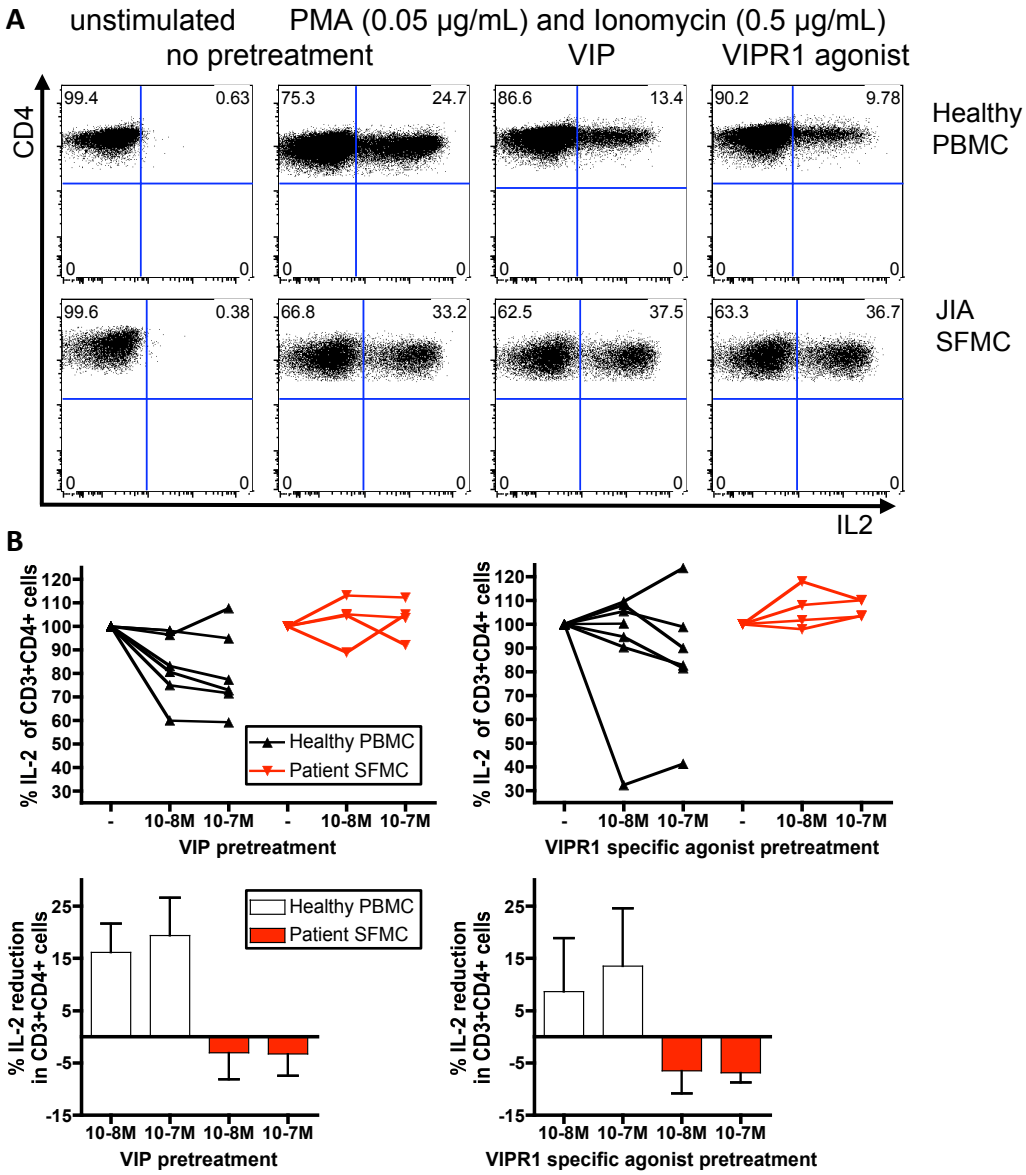

Figure 3.7: VIPR1 function in healthy PBMC and JIA SFMC by inhibition of PMA/ionomycin induced IL-2 in CD3+CD4+ cells by VIP and VIPR1-specific agonist. (A) Representative FACS plots showing IL-2 production from healthy PBMC (top) and JIA SFMC (bottom) gated on CD3+CD4+ cells, in unstimulated, PMA/ionomycin stimulated untreated, 10-7M VIP or 10-7M VIPR1-specific agonist pretreatment conditions. (B) Summary of IL-2 inhibition and reduction for VIP and VIPR1-specific agonist pretreatment in healthy CD3+CD4+ PBMC (black/ white bar) and JIA CD3+CD4+ SFMC (red), no pretreatment was set at 100%, pretreatment was calculated as proportion (top), and reduction of pretreatment (bottom).

3.3. Discussion

The gene expression array by Hunter *et al* [179] used whole SFMC samples at the time of diagnosis of JIA and first joint injection. The patients were followed up one year and disease state at 1 year (persistent and extended) was used to group the array analysis into persistent and extended-to-be. A total of 21 patients were recruited and followed up. With 8 extended-to-be and 13 persistent samples, thus the sample size for the gene expression array was small. Furthermore samples used were whole SFMC samples, thus not taking into account different cell frequencies and thus predominant expression profiles biasing the gene expression array. To address different cell frequencies, the group performed additional validations. Monocyte and T cell populations were sorted, being the most predominant cell types in SFMC, and used for NanoString analysis. NanoString nCounter gene expression system is an RNA capture assay, measuring single mRNA strands present in the sample without amplification bias [258]. Patricia Hunter used different patient samples, and some samples used in the affymetrix approach for NanoString. NanoString and affymetrix data correlated well, additionally monocyte and T cell signatures seen in affymetrix were also seen in the respective subset. NanoString was a more targeted approach with the expression of 150 chosen genes to be investigated. In those some similarity was observed in the top 20 gene rankings (personal communications with Patricia Hunter).

The analysis of the gene list generated by the affymetrix gene expression-profiling array gave rise to many molecules and pathways potentially involved in the mechanism of disease severity. Three molecules were chosen to be investigated further: SMAD3, ERRFI1 and VIPR1. SMAD3 and VIPR1 emerged from analysis using IPA and DAVID and are linked to regulatory T cells [34-36,57-61]. Additionally all three of these genes influence the NF-κB pathway [37-41,48-50,74].

RT-PCR analysis of gene expression gave varied levels. Cell subset analysis was only performed on a small number of samples, and did not yield significance. No significant difference between healthy and JIA samples, or within disease subsets were seen for SMAD3 or ERFFI1. There was an overall trend that ERFFI1 expression was increased in patient samples compared to healthy samples. SMAD3 levels appeared lower in SFMC

from more severe cases. VIPR1 mRNA was significantly decreased in JIA SFMC, compared to all three PBMC subsets (healthy adult, healthy child, JIA).

All three molecules might still be important in disease severity of JIA. SMAD3 needs to be phosphorylated to be active [31,78], thus the basal expression level of mRNA might not be the only level of control of SMAD3 function. It is known that the TGF-β concentration, which facilitates SMAD3 phosphorylation downstream of its receptors, is very low in the joint of JIA [259]. Additionally phosphorylated SMAD3 must translocate, in conjunction with SMAD4, into the nucleus for DNA binding activity. Hence SMAD3 might not be activated in the same manner in JIA SFMC than in a healthy environment. Phosphorylation, location and possible DNA binding could be investigated to further examine if SMAD3 plays a role in JIA pathogenesis or severity.

ERRFI1 is a stress response protein, which inhibits cell proliferation and differentiation through ErbB. It is rapidly transcribed, translated and degraded again, to work in a negative feedback loop only when necessary [67,69,71,72,260]. Thus the time of sample, or treatment of sample might be crucial for detection of ERRFI1 mRNA expression.

VIPR1 has been implicated in immune-regulation, especially for T cells, at multiple levels (comprehensive review by Gonzalez-Rey *et al* [53]). Lower expression of VIPR1 has also been detected in rheumatoid arthritis (RA) and been associated with lower anti-inflammatory function in synovial cells and fibroblasts [261,262].

VIPR1 investigation was taken forward. Western blotting confirmed the expression pattern across different cell subsets (present in monocytes and T cells, below detection in B cells). Interestingly the location of the VIPR1 protein bands for JIA SFMC suggested a slightly smaller size (~48kDa) than the reference protein size (~52kDa), with some variability. Such a variation in detected VIPR1 size might indicate that VIPR1 alteration is present under certain conditions, for example during inflammation, in a subset of samples. A size difference of around 4kDa could be explained by several circumstances. First, it is possible that inflammatory signaling induces variable

posttranslational modifications, including glycosylation and phosphorylation. VIPR1 does have four glycosylation sites. Alternatively a different mRNA splicing might occur. Some known isoforms were excluded due to size; two E!ensembl transcripts were investigated using a set of different diagnostic primer pairs, the mRNA from healthy PBMC and JIA SFMC amplified differently in preliminary data. However these did not concur with the expected PCR products for either of the E!ensembl transcripts investigated.

The exact nature of a possible splice variant remains elusive. Variations in both protein and mRNA between samples mean that a screening of several samples is necessary. Further primer design all along the VIPR1 mRNA, especially around exon 1 and 2, 8 and 9, and 11 and 12, with consequent sequencing of variable products could elucidate transcript variations. However the possibilities of suboptimal primer binding and PCR settings, including temperature, cycling and salt concentrations of the PCR-mix might have interfering with amplification, need to be taken into account. An alternative approach would be to perform an exon-array, or a 5-prime extension followed by PCR and sequencing. However due to high variability, and other projects no further investigation was taking in the course of this work.

VIPR1 signaling has been implicated in a variety of immune-regulating functions in mice and human. Thus it was important to investigate functionality of VIPR1 dependent processes in JIA SFMC compared to healthy PBMC. One known function of VIPR1 signaling in T cells is to reduce IL-2 expression and secretion [236-239,256,257]: this was therefore used to develop an *in vitro* assay to test VIPR1 function. This effect of VIPR1 has been suggested to be dependent on cAMP [238,239]. However, the VIPR1 independent cAMP inducer forskolin (FSK) [263,264] did not yield consistent IL-2 reduction, indicating VIP dependent IL-2 reduction is independent of cAMP. Alternatively FSK might not induce the same signaling cascade through cAMP as is utilized by VIP signaling.

Healthy donor samples showed varied responses. VIP itself showed most consistent inhibition of IL-2 secretion, however two samples did not show much change in IL-2.

The VIPR1-specific agonist $^{[11,22,28Ala]}$VIP displayed some reduction of IL-2, but to a lesser extend than VIP. Thus some of the effect by VIP could be attributed to the second VIP receptor VIPR2. On the other hand, the chemical modifications in $^{[11,22,28Ala]}$VIP could have lead to slightly altered kinetics in primary human cells, although in a transfected CHO cell line, kinetics were comparable with native VIP [265]. To ask whether levels of VIPR1 at mRNA levels correlate with functional activity of the VIPR1 assay, the data were insufficient.

In contrast to healthy control cells most JIA SFMC showed no IL-2 inhibition after VIP or VIPR1 agonist stimulation, in this assay. Interestingly the data generated so far suggest that cells from JIA synovial samples might be less responsive to VIP and VIPR1-specific agonist $^{[11,22,28Ala]}$VIP. Hence VIPR1 function might be impaired in SFMC or the level of VIPR1 is too low to elicit a function above background. Interestingly a genetic variant of VIPR1, which is associated with a lower functional capacity of VIPR1, has been associated with rheumatoid arthritis in adults [61].

Here it has been demonstrated that VIPR1 mRNA expression is lower in the synovial cell compartment compared to healthy blood. Additionally both the size of protein expressed, and VIPR1 function appeared to be decreased in most JIA SFMC samples. Together these indicate that there could be a defect in VIPR1 in arthritis. VIPR1 expression and function might be important in amelioration of inflammation within the joint, which is supported by the association with RA and the successful treatment of disease in the collagen induced arthritis model with VIP [57,59,266,267]. More work needs to be done to increase the sample size and define the potential variant of VIPR1 found in JIA SFMC and its role in pathogenesis, amelioration or severity of JIA.

Chapter 4

CD161+FoxP3+ CD4+ T cells:

the subset of Treg capable of producing pro-inflammatory cytokines

- characterisation and phenotype in health

4. CD161+FoxP3+ CD4+ T cells: the subset of Treg capable of producing pro-inflammatory cytokines - characterisation and phenotype in health

4.1. Introduction

The maintenance of immune tolerance is a key function of the immune system, mediated in part by the proper functioning of regulatory cells. One important population of regulatory CD4+ T cells (Treg) is defined by expression of the transcription factor FoxP3, which is essential for their suppressive capacity towards effector cells, as described in further detail in 1.4.

Furthermore many links between Treg and Th17 cells have been established, possibly indicating their co-evolutionary development [81]. Interestingly the gene expression array analysed in chapter 3 determined that the Th17 transcription factor RORC was enriched in the SFMC of continued persistent oligoarthritis JIA patients, compared to samples from individuals who extended to more severe disease, after one year of disease (Figure 3.3). At first this seemed contrary to previous findings by our group that Treg and Th17 cells have a reciprocal relationship at the site of inflammation in autoimmune childhood arthritis [186], and a higher frequency of Treg is associated with a milder disease course [188]. This therefore raised an interesting question about the cell source of the RORC mRNA detected by gene expression array.

The presence of Treg does not always ensure tolerance, since functionality and ability to fully control inflammation are vital. A central function of Treg is suppression of inflammatory responses, and it was previously thought that a hallmark of Treg was their lack of cytokine production [106,124]. However, recent studies have demonstrated that a small proportion of Treg are able to produce pro-inflammatory cytokines including IFN-γ or IL-17 [152,155-157].

These interesting observations imply that the boundaries between Tconv and Treg programmes may be more blurred than previously thought, and raise several important questions; in particular, how such cells arise *in vivo* in humans and their functional relevance in health and disease. In addition, a marker with which to identify such 'hybrid' Treg would be of great interest.

The transcription factor RORC is tightly linked to production of IL-17. RORC has also been shown to drive the lectin-like receptor CD161, which expression has previously been tightly linked to Th17 cells [93]. However RORC might not only drive IL-17 in effector cells, but also in Treg that can make cytokines. In this chapter CD161 expression is definitively linked to the population of Treg that display inflammatory signatures. Here their occurrence in healthy samples throughout the development and their specific phenotype is described.

Specific aims of this chapter:

- Defining the novel CD161+FoxP3+ Treg population throughout development
- Linking CD161 expression with cytokine production in Treg
- Determination of the phenotype associated with CD161+ Treg

4.2. Results

4.2.1. CD161+ Treg in healthy adults, children, cord blood and thymus

CD161 expression has not been typically associated with Treg. During my study of human Treg, a subpopulation of Treg was observed, which also express CD161. Using flow cytometry (2.3) this was further investigated. Given previous reports that some monoclonal antibody (Ab) clones specific for FoxP3 may produce high background staining [268,269], several clones of anti FoxP3 Ab were compared. Comparable results were seen with three different FoxP3 Ab clones and CD161+FoxP3+ cells were $CD25^{hi}CD127^{lo}$ (Figure 4.1). CD161 was expressed at a median frequency of 14% of FoxP3+CD4+ peripheral blood T cells in healthy adult donors. Interestingly, this population was also observed in the blood of healthy children, although at a significantly lower frequency (median 8.1%) than in adults (Figure 4.2A). It has been previously shown that expression of FoxP3 protein in human T cells may be induced by cell activation, and that recently activated 'FoxP3 intermediate' CD4+ T cells may not have suppressive function [268,270]. The mean expression of FoxP3 protein was compared in the two populations (CD161- and CD161+) to investigate whether the CD161+FoxP3+ population had lower expression of FoxP3 compared to CD161-FoxP3+ cells. FoxP3 staining intensity (assessed by mean fluorescent intensity (MFI)) represents the amount of FoxP3 protein per cell. In adult donors, there was no difference in intensity of FoxP3 staining between CD161+ and CD161-FoxP3+ cells, while in healthy child donors CD161+FoxP3+ cells actually had a slight but significantly higher median level of FoxP3 protein than CD161- cells (Figure 4.2B).

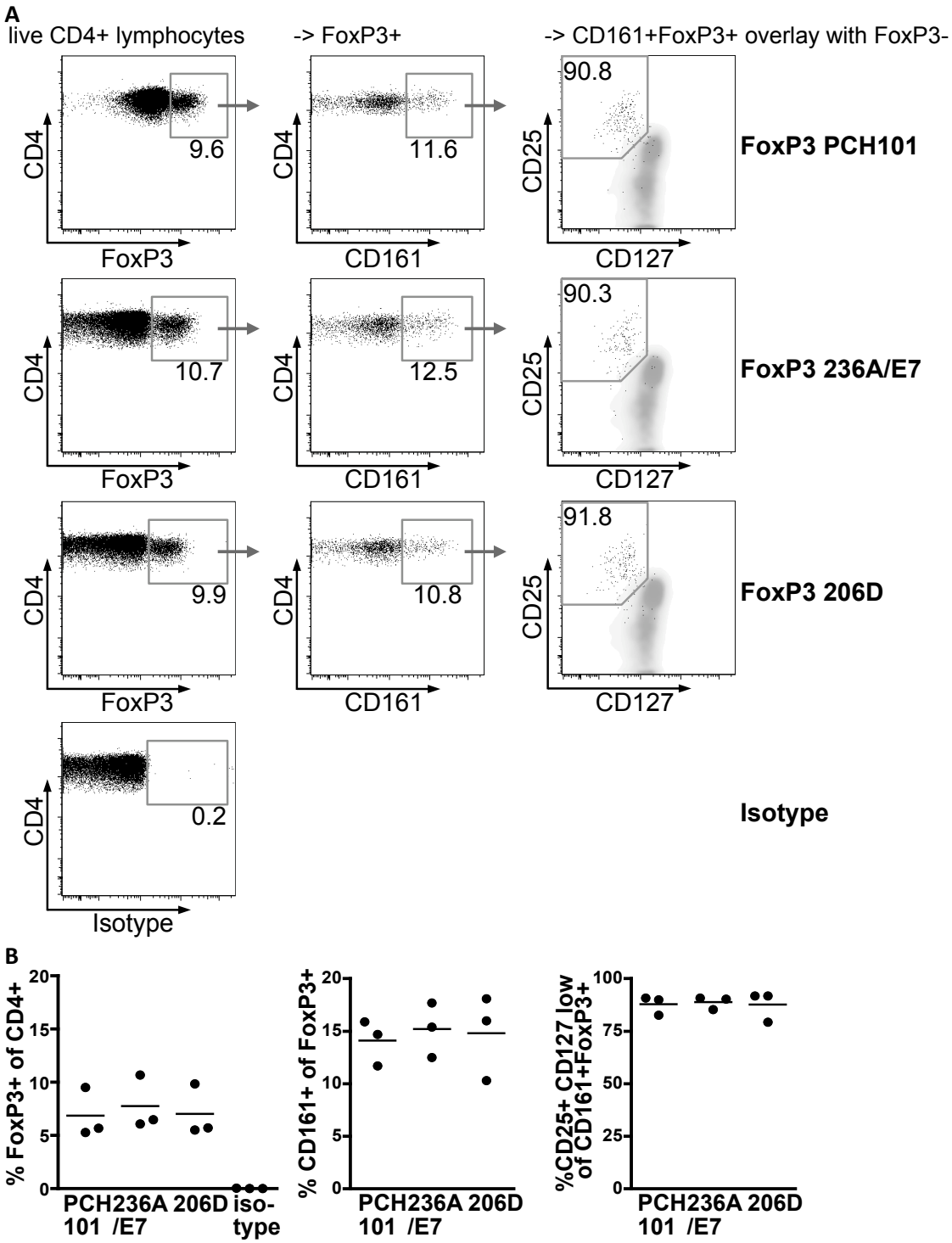

Figure 4.1: Choice of clone of anti-FoxP3 monoclonal antibody does not affect quantification of CD161+ regulatory T cells or analysis of their phenotype. (A) Representative flow cytometry plots for each FoxP3 monoclonal antibody (from top to bottom: PCH101, 236A/E7, 206D, isotype control) showing CD4+ lymphocytes vs FoxP3 (left), FoxP3+ gated cells vs CD161+ (middle), and CD161+FoxP3+ (dots) overlaid with FoxP3- population (density plot) showing CD25 vs CD127 expression (right). (B) Summary plots: horizontal lines represent median (n=3).

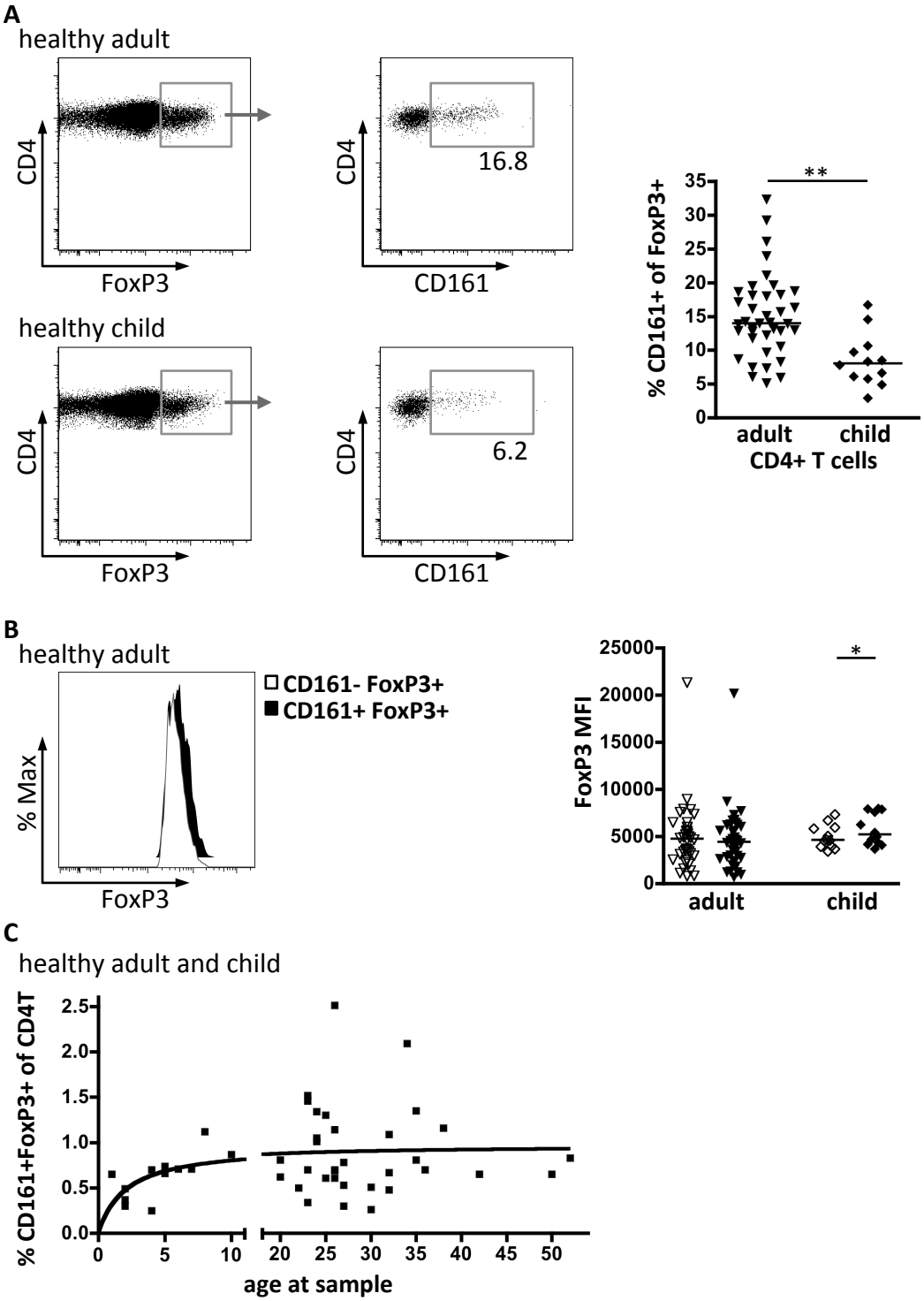

Figure 4.2: CD161 expression by regulatory T cells. (A) Representative flow cytometry plots of FoxP3 expression gated on CD4+ lymphocytes (left) and CD161 gated on FoxP3+CD4+ lymphocytes (right) in healthy adult (n=39; left panels) and healthy child (n=12; bottom) samples, with summary plot. (B) No difference in FoxP3 protein levels between CD161-FoxP3+ and CD161+FoxP3+ Treg. Representative histograms overlay, left (white symbols: CD161-FoxP3+, black symbols: CD161+FoxP3+) with summary plot, of FoxP3 staining intensity (MFI) on CD161-FoxP3+ (clear symbols) and CD161+FoxP3+ (filled symbols) CD4+ lymphocytes for healthy adult (n=37) and healthy child (n=12) samples. (C) Non-linear regression between CD161+ Treg and age in healthy child and

adult samples (n=31), one-side binding hyperbola. Horizontal bars represent medians. Statistical analysis by Wilcoxon matched pairs test (p values: **≤0.01; *≤0.05).

When these data were analysed by frequency of CD161+FoxP3+ cells within the CD4+ population, across the whole age range, a rise in frequency was seen through childhood, which plateaued during adult years; these data were best described by a one site-binding hyperbola (Figure 4.2C). In the paediatric age range %CD161+FoxP3+ cells correlated significantly with age (spearman correlation r=0.81, p≤0.01), but not in adults (r=-0.01, p=ns).

To assess when these CD161+FoxP3+ cells arise during development of the immune system, mature thymocytes and umbilical cord blood (UCB) were analysed as sources of immunological inexperienced and neonatal peripheral T cells. CD161+FoxP3+ cells were clearly demonstrated in both cord blood CD4+ T cells and also in mature CD4 single positive thymocytes (defined by CD1a-CD3+CD4+CD8-, Figure 4.3). Together these data show that CD161+FoxP3+ cells are present within the CD4 T cell population at different stages of development.

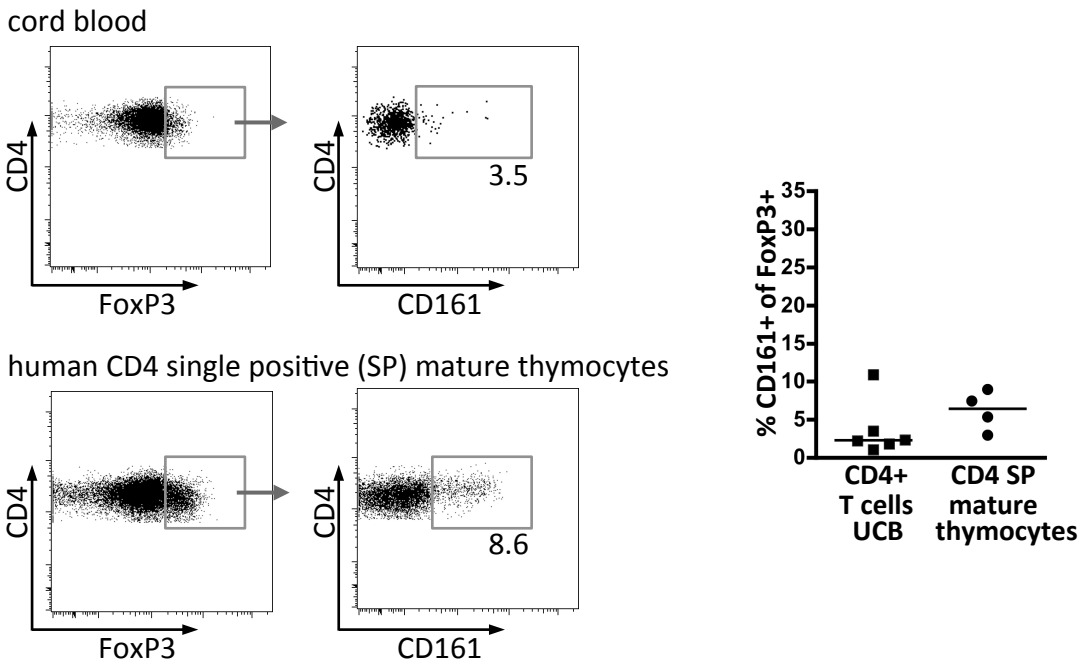

Figure 4.3: CD161 expression by regulatory T cells in immunological inexperienced cells. Representative flow cytometry plots of FoxP3 expression gated on CD4+ lymphocytes (left) and CD161 gated on FoxP3+CD4+ lymphocytes (right) in cord blood (UCB; n=5; top) and mature CD4 single positive thymocytes, defined by CD1a-CD3+CD4+CD8- (n=4; bottom) with summary plot. Horizontal bars represent medians.

4.2.2. CD161+ Treg produce pro-inflammatory cytokines

As part of their phenotype, Treg typically are not pro-inflammatory. However some reports suggest that a small proportion of Treg can make pro-inflammatory cytokines [155-158]. Interestingly, *ex-vivo* cytokine staining of healthy PBMC showed a higher frequency of cells producing pro-inflammatory cytokines within the CD161+FoxP3+ population than the CD161-FoxP3+ population (Figure 4.4). The CD161+FoxP3+ population had a significantly higher proportion of cells that produce IL-17A, IFN-γ, and surprisingly IL-2, with low or absent cytokine production within the CD161-FoxP3+ population. A proportion of CD161+FoxP3+ cells expressed more than one cytokine (Figure 4.4D). In the representative individual shown, 2.5% of CD161+FoxP3+ cells co-expressed IL-17A and IFN-γ, this combination of cytokines expressed by the same cells has been shown previously in Tconv in the inflamed environment of the joint [82,83]. Interestingly about half of all IFN-γ positive CD161+FoxP3+ cells co-expressed IL-2 (5.7% IFN-γ+IL-2- and 5.2% IFN-γ+IL-2+). These distinct functional features were clearly apparent in blood from both adults and children, where the majority of cytokine-producing Treg were defined by CD161 expression. CD127 has been shown to inversely correlate with FoxP3 expression and suppressive functions in Treg [271]: cytokine-producing CD161+FoxP3+ cells were also CD127low (Figure 4.5A). Since intracellular cytokine staining may not correlate precisely with secretion, the capacity of Treg to release the pro-inflammatory cytokine IL-17 was investigated. To address this a cytokine capture approach was used (2.3.9). An unstimulated condition was used as negative control to the PMA/ionomycin stimulated cells. Following cytokine-capture, intracellular FoxP3 staining was performed and cells were analysed based on their expression of CD161 (Figure 4.5B). Captured IL-17A amount was comparable with intracellular cytokine staining, showing that IL-17A is produced and secreted by FoxP3+CD161+ cells.

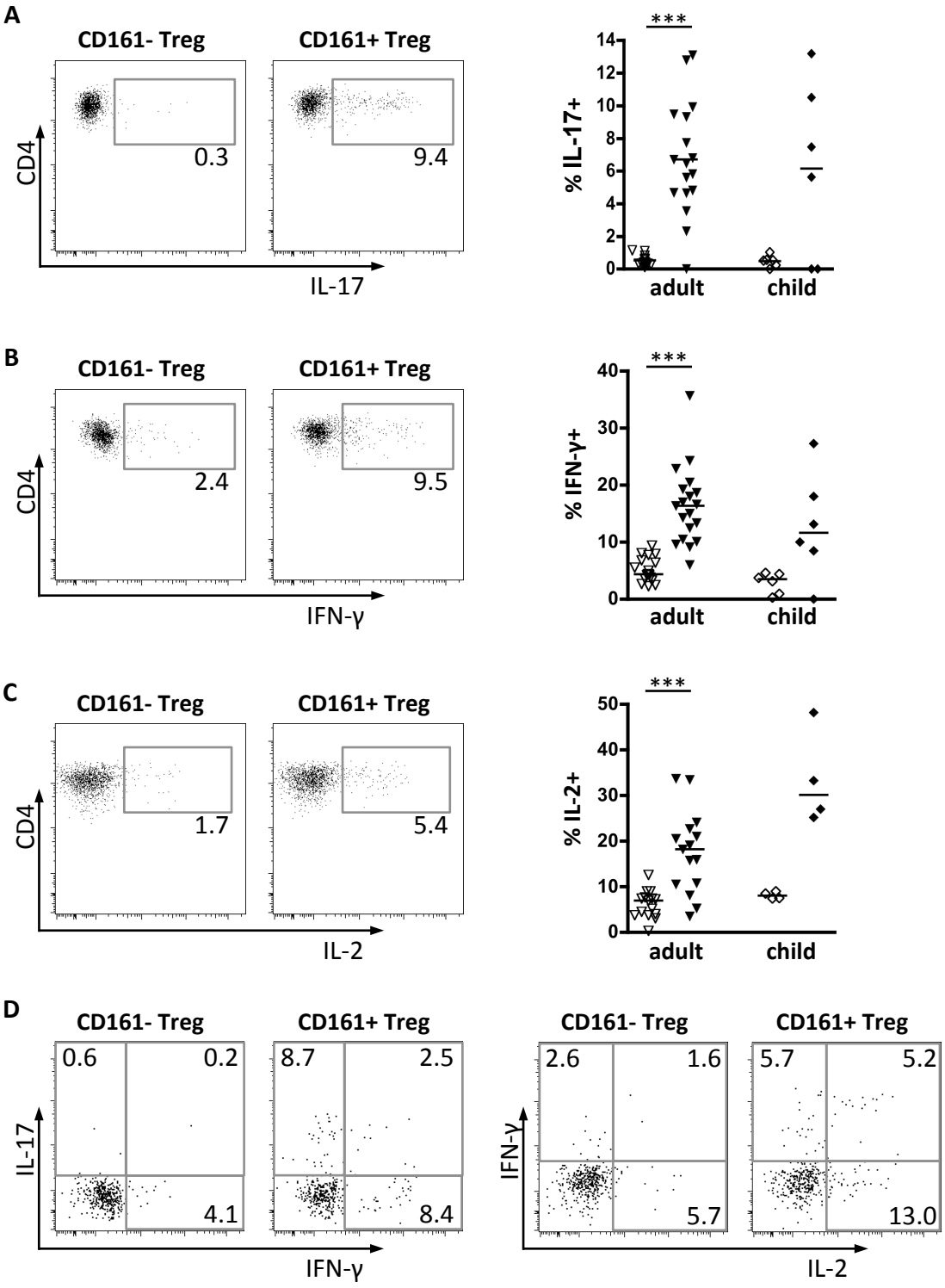

Figure 4.4: CD161+FoxP3+ regulatory T cells can produce pro-inflammatory cytokines *ex-vivo*. Dot plots show intracellular cytokine staining for IL-17A (A), IFN-γ (B) and IL-2 (C) gated on FoxP3+CD161- (white symbols) and FoxP3+CD161+ (black symbols) peripheral blood Treg respectively in one representative healthy adult, with respective summary for healthy adult (n=13-19) and child (n=4-6) peripheral blood samples. (D) Representative staining showing double positive cytokine production (left: IL-17A vs IFN-γ; right: IFN-γ vs IL-2) comparing CD161-FoxP3+ to CD161+FoxP3+ cells. Horizontal bars represent medians. Statistical analysis by Wilcoxon matched pairs test (p values: ***≤0.001; **≤0.01).

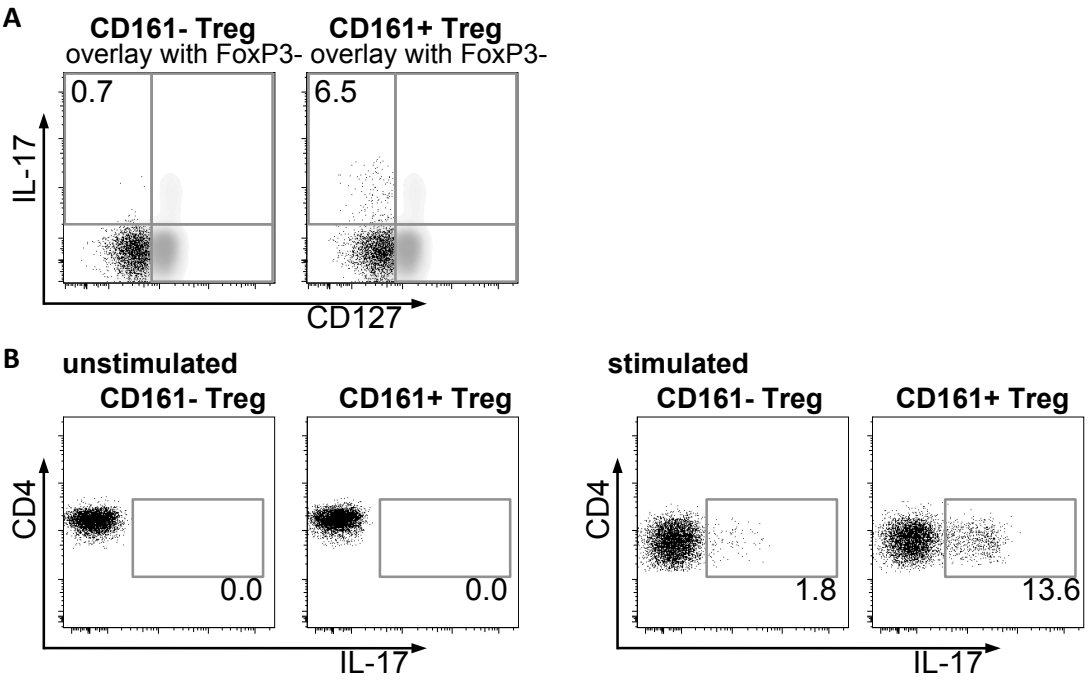

Figure 4.5: Cytokines produced by CD161+ Treg arise from the CD127 low population and are actively secreted. (A) Representative flow cytometry plots for IL-17A production of CD161-FoxP3+CD127low (left plot, dots) and CD161+FoxP3+CD127low Treg (right plot, dots) for IL-17A vs CD127 overlain over FoxP3- population (grey density plot). (B) Representative flow cytometry plots gated on FoxP3+CD4+ lymphocytes and CD161- or CD161+ showing frequency of captured IL-17 in unstimulated (left) and stimulated (right) cells, one representative of two individuals tested.

4.2.3. CD161+ Treg phenotype - similarities with effector memory Tconv

Next it was investigated whether the pro-inflammatory potential of CD161+FoxP3+ cells was associated with expression of transcription factors typical of Th1 (Tbet) or Th17 (RORCv2) cells. Expression of Tbet and RORC were analysed at mRNA level by RT-PCR (2.6) and protein level by flow cytometry (2.3). Significant increases in protein levels of both RORCv2 and Tbet in CD161+FoxP3+ cells were seen by flow cytometry (Figure 4.6A). In order to amplify mRNA transcripts, CD161+ and CD161- Treg were first sorted into pure populations (2.4.5, Figure 2.2). RT-PCR data was normalized and a fold change between CD161+ and CD161- Treg was calculated. RT-PCR for *TBX21* (Tbet) and *RORCv2* revealed a significant increase of the Th17-associated transcription factor *RORCv2* (mean fold increase of 6.4, $p<0.05$), and a trend towards increased Tbet mRNA (mean fold increase 2.0), linked to IFN-γ production, in CD161+FoxP3+ compared to CD161-FoxP3+ cells (Figure 4.6B). There was no difference in amount of *FOXP3* mRNA between the two populations.

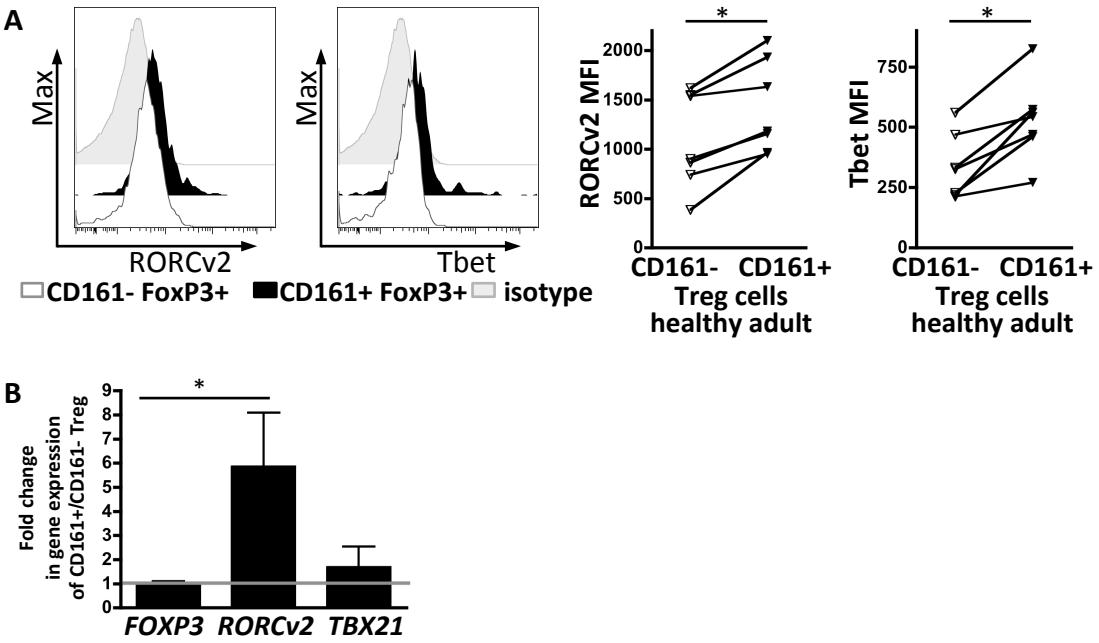

Figure 4.6: Transcription factor expression in CD161+FoxP3+ cells at protein and mRNA level. (A) RORCv2 and Tbet protein expression by flow cytometry *ex-vivo*. Representative flow cytometry plots of expression of RORCv2 (left) and Tbet (right) in CD161-FoxP3+ (white) compared to CD161+FoxP3+ cells (black) and isotype (grey), with summary graphs (n=7). (B) Fold change in mRNA expression of *FOXP3*, *RORCv2* and *TBX21* (Tbet) in cDNA samples from sorted CD161+ Treg relative to sorted CD161- Treg assayed by RT-PCR n=3-6, bars represent mean +/- SEM, Wilcoxon matched pairs test between cell subsets, between groups one-way non-parametric ANOVA (Kruskal-Wallis with Dunn's test) (p values: *$\leq$0.05).

Other groups have associated cytokine production with a memory Treg phenotype [125,126]. CD161+ Treg were found to be almost exclusively in the memory population, as defined by CD45RO expression, even in the blood of young children (Figure 4.7A). CCR6 has also been used to define cells of a memory phenotype, but is also an important chemokine receptor present on the majority of Th17 cells. Th17 cells are also known to express the cytokine receptor IL-23R, which is important for consolidation of their IL-17 producing phenotype [272]. The expression of CCR6 and IL-23R were therefore investigated on CD161+ Treg. In both adults and children, proportions of cells expressing CCR6 and IL-23R were significantly increased in CD161+FoxP3+ compared to CD161-FoxP3+ cells (Figure 4.7B and C). IL-23R mRNA expression as assessed by PCR was also enriched in sorted CD161+ Treg compared to sorted CD61- Treg from three healthy adults (Figure 4.7D).

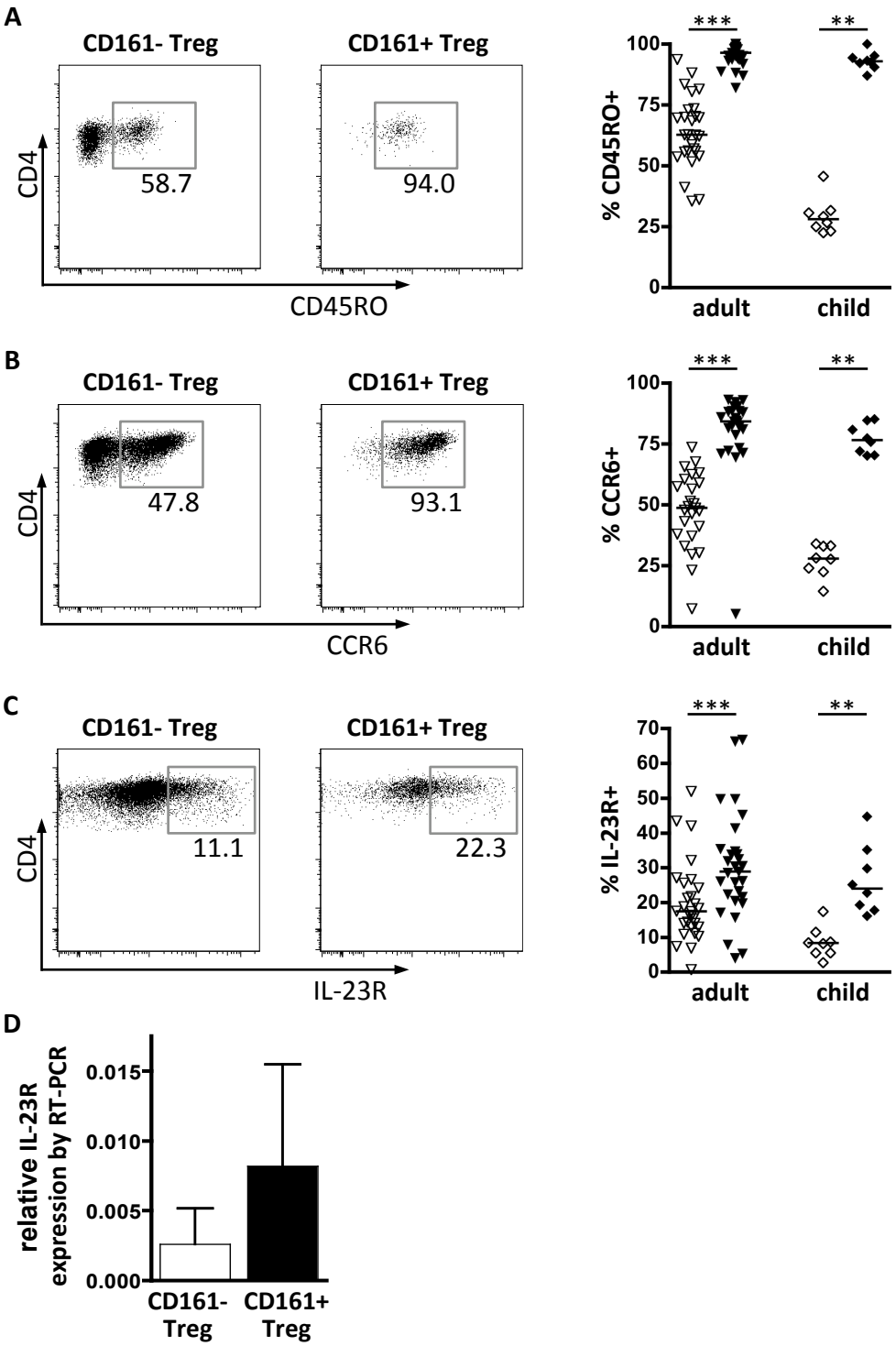

Figure 4.7: CD161+FoxP3+ regulatory T cells share phenotypic features with memory effector T cells. Representative flow cytometry plots showing expression of (A) CD45RO (B) CCR6 and (C) IL-23R on FoxP3+CD161- (white symbols) and FoxP3+CD161+ Treg (black symbols) respectively, with summary plots (right) for healthy adult (n=16-28) and child (n=6-8) peripheral blood samples. (D) Relative expression of IL-23R mRNA by RT-PCR on sorted CD161- and CD161+ Treg (n=3). Horizontal bars represent medians, bar graph shows mean with SEM. Statistical analysis by Wilcoxon matched pairs test (p values: ***$\leq$0.001; **$\leq$0.01).

4.2.4. CD161+ Treg express Treg functional markers

Treg implement their regulatory function through various mechanisms, besides FoxP3 driven suppression. One of these mechanisms is thought to include the action of the surface ectonucleotidase, CD39. CD39 is a potent cell-surface ATPase, which breaks down pro-inflammatory ATP to AMP [133,135,136]. Due to the pro-inflammatory action of ATP extracellular, the breakdown of ATP is thought to contribute to Treg regulatory abilities. As expected, Treg showed a significant number of cells that expressed CD39 and this proportion was higher in adults than child donors (Figure 4.8A). However there was no significant difference in CD39 expression between CD161- and CD161+FoxP3+ cells (Figure 4.8A).

The IKAROS family member Helios has recently been proposed as a possible marker to separate natural and induced Treg when it was reported to be expressed on all thymic derived Treg but not on induced Treg [113]. However upon further investigation, Helios expression could also be detected in induced Treg in mice lacking thymic derived Treg and *in vitro* [114,115]. Furthermore new research showed Helios negative natural thymic derived Treg in humans [116]. Helios is an important transcription factor and it has since been shown that Helios binds the *FOXP3* promoter and is involved in the Treg program [273,274]. Helios protein expression was therefore investigated in the CD161- and CD161+ Treg populations by flow cytometry. CD161+FoxP3+ expressed significantly lower levels of Helios both in adult and paediatric samples (Figure 4.8B). CD161-FoxP3+ cells were almost exclusively Helios+, whereas only about 50% of CD161+FoxP3+ cells expressed Helios.

Therefore CD161+ Treg might employ a diverse transcriptional profile partly independent of Helios. However CD161- and CD161+ Treg utilize similar levels of the functional protein CD39, giving them equal ability to break down ATP.

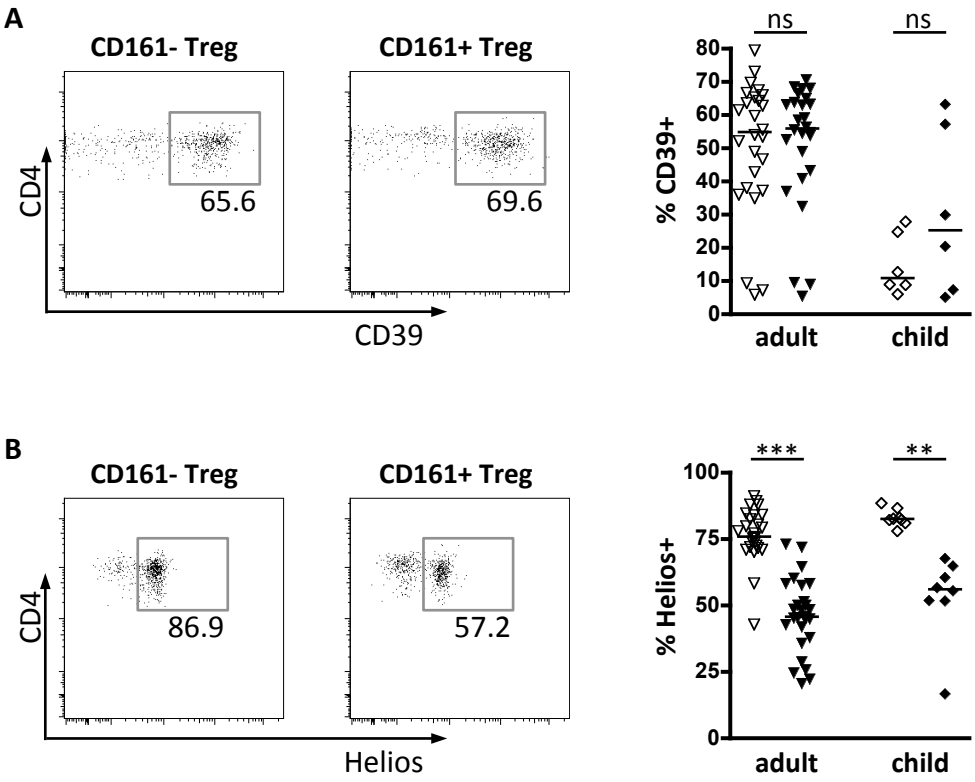

Figure 4.8: CD161+FoxP3+ regulatory T cells express CD39 and only a subpopulation of CD161+FoxP3+ cells express Helios. Representative flow cytometry plots showing expression of (A) CD39 and (B) Helios on FoxP3+CD161- (white symbols) and FoxP3+CD161+ Treg (black symbols) respectively, with summary plots (right) for healthy adult (n=26-27) and child (n=6-8) peripheral blood samples. Horizontal bars represent medians. Statistical analysis by Wilcoxon matched pairs test (p values: ***≤0.001; **≤0.01, ns= not significant).

4.2.5. CD161+ Treg use a diverse Vβ repertoire, but may have a distinct origin to CD161- Treg

CD161 expression has been associated with invariant TCR expression on NKT cells and some CD8+ T cell populations, which express a limited range of TCR-Vβ chain proteins [275,276]. Therefore, it was of interest to investigate the diversity of TCR repertoire used by the CD161+ Treg population. To test the TCR-Vβ repertoire on CD161+FoxP3+ cells, flow cytometry staining for TCR-Vβ families was first performed. The expression of twenty-four different TCR-Vβ families was investigated within five different T cell subsets: total CD4+, CD161-FoxP3+CD4+, CD161+FoxP3+CD4+, CD161-FoxP3-CD4+ and CD161+FoxP3-CD4+ lymphocytes (Figure 4.9). An example staining for three TCR-Vβ families in those populations is shown in Figure 4.9A. TCR-Vβ families examined by the panel of available antibodies covered a mean of 70.18% (+/- SD 8.268) of all analysed cells, representing the majority of cells within each subset investigated. The TCR-Vβ repertoire was comparable between all subsets tested, indicating that CD161+FoxP3+ do not express an invariant TCR, but have a diverse repertoire comparable with CD161-FoxP3+ and Tconv.

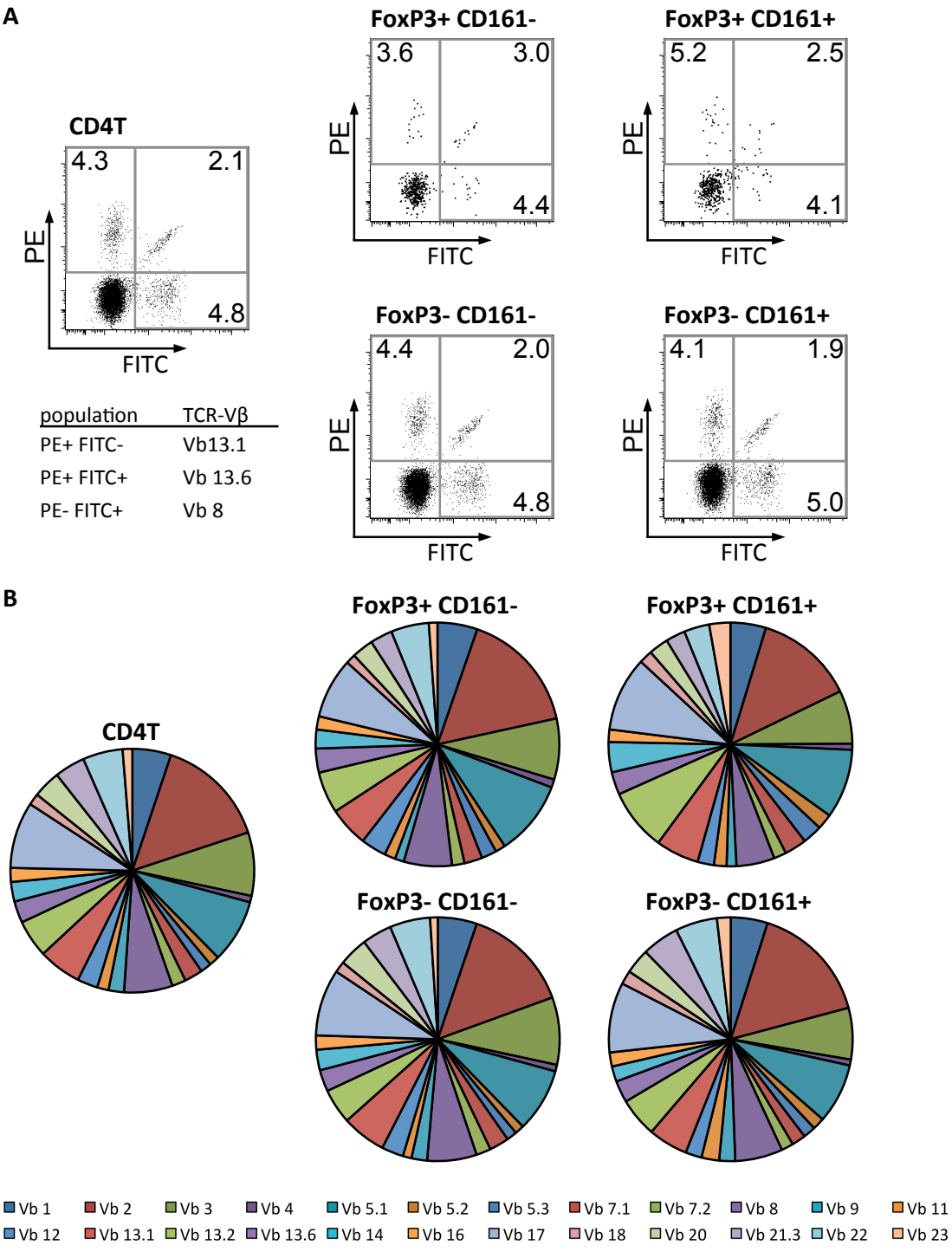

Figure 4.9: CD161+ regulatory T cells do not express an invariant TCR. Frequency of TCR-Vβ expression was assessed using a flow cytometry panel to detect 24 Vβ families, in healthy adult CD4+ T cells, CD161-FoxP3+CD4+, CD161+FoxP3+CD4+, CD161FoxP3-CD4+ and CD161+FoxP3-CD4+ cell populations as shown in representative flow cytometry plots (A) and summary pie charts (B, n=5). Data were gated on the specific population and then each TCR-Vβ. Pie charts show proportion of all cells positive for a specific TCR-Vβ (which identify a mean of 70.18% of all cells within respective subset).

To further investigate possible relationships between the CD161+ and CD161- Treg populations, the clonality of TCR was tested by sequence analysis across the VDJ-junction [245]. This work was done with assistance of Qiong Wu, undergraduate summer student, and Simona Ursu, a postdoctoral Research Assistant in the lab. CD161+ and CD161- Treg were sorted to high purity (2.4.5, Figure 2.2) and CDR3 regions of TCR-Vβ2 family were amplified using primers specific for the constant region and TCR-Vβ2 primers (2.7, Table 2.14). Amplification products were then cloned and sequenced. Although both Treg populations had a diverse repertoire, both subsets did show clonality (Figure 4.10). Clones here being defined as T cell populations sharing their TCR, which are present at a higher frequency than the majority of individual specific TCRs and as indicated by the finding of a specific nucleotide CDR3 sequence being present more than once in the set of sequences. A total of 345 sequences (170 CD161- Treg, 175 CD161+ Treg), were analysed: the sequences as nucleotide sequences and predicted protein sequences from this analysis are shown in Appendix III as a table. Among the 345 sequences analysed, there were 122 clonal sequences (identified 2 or more times out of the total) for CD161- and 118 clonal sequences for CD161+ Treg. The large majority of these clonal sequences were non-overlapping and none of the unique TCR sequences found in CD161+ were also in the CD161- TCR set, or vice versa. However there were 2 sequences that were found in both the CD161- and CD161+ subsets (Figure 4.10, indicated by thin red slice in the green pie chart or green slice in the red pie chart).

Together these data raise the possibility that CD161+ Treg may have a distinct origin from CD161- Treg or at least that they arise as separate subpopulations early and that either they cannot interconvert or, do so only very rarely.

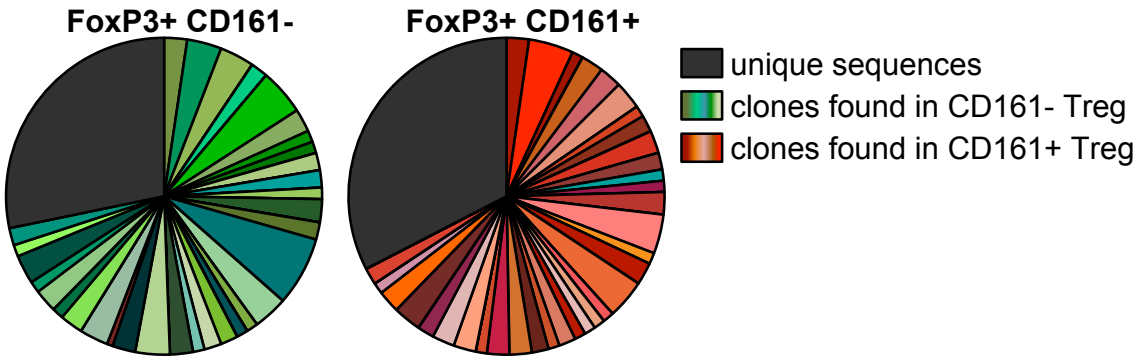

Figure 4.10: CD161- and CD161+ Treg do contain small clonal populations within the TCR-Vβ2 expressing cells, but their repertoires are predominantly non-overlapping with each other. TCR-CDR3 region sequencing of TCR-Vβ2 for CD161- Treg (170 sequences in total: 122 clones in shades of green, and 48 other unique sequences in grey) and CD161+ Treg (175 sequences in total: 118 clones in shades of red, and 57 other unique sequences in grey) revealed some clonality in both populations, but only 2 overlapping sequences, of the total 345 sequences (data from one healthy adult).

4.3. Discussion

It is widely considered that an important function of Treg is the suppression of disproportionate immune responses. Thus Treg and their role in health and disease are appealing to investigate. Additionally they might present a potential strategy to use therapeutically for diseases where an inappropriate immune response itself drives pathology. However, there are still many unknown elements to Treg-therapy. Of topical relevance, is the controversy surrounding the pro-inflammatory potential of Treg, particularly in inflammatory settings.

In this chapter, I have demonstrated the existence of a distinct population of FoxP3+CD4+ Treg, defined by the expression of the Th17-associated marker CD161, which show pro-inflammatory potential. This population can be demonstrated throughout life; CD161+FoxP3+ cells can be found already within the immunological inexperienced lymphocyte population of umbilical cord blood, and emerge as mature single positive thymocytes along with natural Treg. Although always a small population, the size of the CD161+ Treg population changes with age in childhood, and plateaus in adulthood.

The data presented here demonstrate that CD161+ Treg share some characteristics with Tconv phenotypes, with shared cytokine and chemokine receptors, memory markers, as well as the expression of Tconv-associated transcription factors RORCv2 and Tbet. CD161+ Treg have high levels of CD39 and about half of CD161+ Treg express the transcription factor Helios. Furthermore CD161+ Treg and CD161- Treg are diverse in their TCR-Vβ family repertoire. Therefore CD161 defines a population of 'hybrid Treg', the major source of cytokine-producing FoxP3+ T cells.

These data are supported by recent findings of cytokine-producing Treg that were generated by *in vitro* stimulation, expansion or cloning, which were still suppressive [152,155-157]. However, in those studies no potential origin or definitive way of identifying these cells without *ex-vivo* stimulation or permeabilisation was given. Interestingly, recent studies found that Helios- Treg produce more cytokine than Helios+ Treg [116,277], which correlates with the fact that fewer CD161+ Treg express

Helios. Thus I suggest here that CD161 defines the major source of Treg with inflammatory potential. CD161-expressing Tconv are the precursors for Th17 cells [93], and Th1 cells that have converted from Th17 cells are exclusively within the CD161+ population [82,83]. The data in this thesis again support a link between CD161 and IL-17 production, which appears to be the case in Treg as well.

Since their discovery, Treg have been subdivided into various groups. One functionally distinct Treg subset described was based on HLA-DR expression [124]. Different mechanisms of suppression were shown and the authors demonstrated the importance of both subsets, with DR+ Treg initiating early contact-dependent and DR- late FoxP3-associated suppression. It was subsequently identified that IL-17-secreting Treg are found within the DR- population [157]. However in healthy individuals most Treg are DR- (mean of 83%). Here I have demonstrated that CD161 expression accounts almost exclusively for IL-17A producing Treg. Another basis for defining Treg subsets is by memory markers [125,126]. CD161+ Treg fall within the CD45RO+CD45RA- population (so called population II and III by Miyara *et al*[126]) and the CCR6+ population described by Kleinewietfeld *et al* [125], and therefore can be considered memory Treg.

In conclusion, I report the novel discovery that CD161 defines the major source of inflammatory cytokines by Treg. CD161+FoxP3+ T cells can be found throughout development and show an effector-like phenotype. The functional capabilities of CD161+ Treg will be investigated in the next chapter (chapter 5: CD161+ Treg stability and function).

Chapter 5

Stability and function of CD161+ Treg

5. Stability and function of CD161+ Treg

5.1. Introduction

In chapter 4 I demonstrated the existence of CD161+FoxP3+ Treg in healthy peripheral blood and in the thymus, indicating that this population is present throughout development. Data were presented defining the phenotype of this subset, showing that CD161+ Treg are enriched as a population for markers typically associated with memory T cells and Th17 cells and showing that these cells have a high frequency of pro-inflammatory cytokine production compared to CD161-Treg. However, FoxP3 expression is only one of several characteristics for defining T regulatory cells. In this chapter the stability and function of CD161+ Treg are further explored. This chapter will present data on the suppressive function of CD161+ Treg, the methylation status of their *FOXP3* locus, the stability of CD161 expression during culture or expansion *in vitro*.

Treg stability has been linked to the demethylation status of the Treg specific demethylated region (TSDR) of the *FOXP3* locus [108,109]. The TSDR is a non-coding sequence located in the 1st intron of the *FOXP3* gene. Classic Treg have a series of demethylated C nucleotides (CpG islands) in this region, while effector cells are fully methylated at these positions: in most studies, between ten and fifteen CpG islands are usually analysed. Evidence has suggested that cytokine-producing Treg, when analysed directly *ex-vivo*, as well as T cell clones can be functionally suppressive [155-157] and are demethylated at the TSDR [156,160]. However there is also evidence of Treg, with cytokine production induced by expansion *in vitro*, which show an intermediate methylation profile [152]. Thus, in order to investigate whether CD161+ Treg can be classified as bona-fide Treg it was important to define the suppressive abilities and the methylation status of the TSDR in CD161+ Treg.

As well as *FOXP3* locus methylation status, the stability of CD161 expression under various conditions was investigated, and experiments were performed to ask whether CD161+ Treg have distinct responses and/or functions compared to CD161- Treg upon stimulation. Additionally it was attempted to understand the role of CD161 itself by

ligating it with monoclonal antibodies. The natural ligand for CD161 lectin like transcript one (LLT1) can be expressed on a variety of cells upon activation [278,279].

Previous studies on NK, CD8 or total CD3 T cells have suggested a link between CD161 ligation and change in cytokine production [280-282]. For example Aldemir *et al* suggested that upon CD161 and TCR ligation in polyclonal T cells, IFN-γ secretion is increased [282]. However there has also been some conflicting evidence, in part because it is not clear if the commercial antibodies that are available have a stimulatory or inhibitory function: both have been reported under different conditions using different tests [275,280,282-285]. With this conflicting evidence from different experimental set ups, research in animal models may in some situations provide data to help understand the function of specific molecules. However in the case of CD161 there is no direct homologue found in the mouse. To date, CD161 is the only NKRP1 family member in human. In mouse, there are many NKRP1 family members, but these only show a maximum of 40% homology to human CD161 [286] and exercise divergent functions [287,288]. Thus it is not possible to explore CD161 function using genetically modified animal models. For these reasons, *in vitro* assays testing CD161 ligation on Treg could be valuable to discern the specific functions of CD161 in this T cell subset.

Specific aims of this chapter:

- Ascertain whether CD161+ Treg are bona-fide Treg
- Investigate CD161 expression and stability in *in vitro* systems
- Establish persistence and functional phenotype of CD161+ Treg
- Examine pathogenic antigen specificity of CD161+ Treg
- Investigate effects of CD161 ligation on Treg

5.2. Results

5.2.1. Treg specific functions of CD161+ Treg

Since the demonstration that human blood contains CD4+ T cells that are suppressive *in vitro*, it has been known that Treg cultured alone without IL-2 are anergic, and that in co-culture they suppress the proliferation of conventional T cells (Tconv) [97,123,289]. In order to investigate the functional suppressive capacity of Treg, divided according to their expression of CD161, cells were sorted by flow cytometry to high purity (according to the methods detailed in 2.4.5 and Figure 2.2) to generate T conv (CD4+CD25-CD127^{hi}) and two populations of putative Treg: CD4+CD25^{hi}CD127^{lo}CD161+ and CD4+CD25^{hi}CD127^{lo}CD161-.

Initially, anergy of the two Treg populations was assessed by stimulating each subset on their own with anti-CD3 antibody (crosslinking achieved by antibody coating to plastic) for 5 days (2.5.3). Both CD161+ and CD161- Treg populations were profoundly anergic (proliferation assessed by CFSE dilution, Figure 5.1A).

Suppression of proliferation of Tconv by Treg is considered to be a definitive property of classic Treg. Therefore the regulatory capacity of CD161- and CD161+ Treg was tested (2.5.3). The capacity of CD161- Treg and CD161+ Treg to suppress proliferation at a 1:1 ratio was equivalent as assessed by CFSE dilution of Tconv (Figure 5.1B). Furthermore to test whether this suppressive capacity was equal at lower ratios of Tconv: Treg for both CD161+ and CD161- Treg, experiments were repeated using ratios of 3:1 and 5:1 (Figure 5.1D). Upon titration of Treg no difference was seen between CD161+ and CD161- Treg populations in their potency to suppress Tconv proliferation (Figure 5.1D). In addition, both Treg subpopulations suppressed the production of IFN-γ, but not IL-17A, by T conv: this was tested both by intracellular cytokine staining (Figure 5.1B) and by measuring cytokine secreted into the supernatants (Figure 5.1C). Amount of cytokine suppression was variable between samples, but clear in four out of five experiments. In other studies, successful suppression of IL-17 production from T conv by Treg using *in vitro* assays has been linked to the presence of antigen presenting cells [229,290], whereas in this experimental set up only CD4+ Tconv and

Treg were present with crosslinked anti-CD3 +/- anti-CD28 for stimulation. Thus some additional signal might be required for definitive IL-17 suppression.

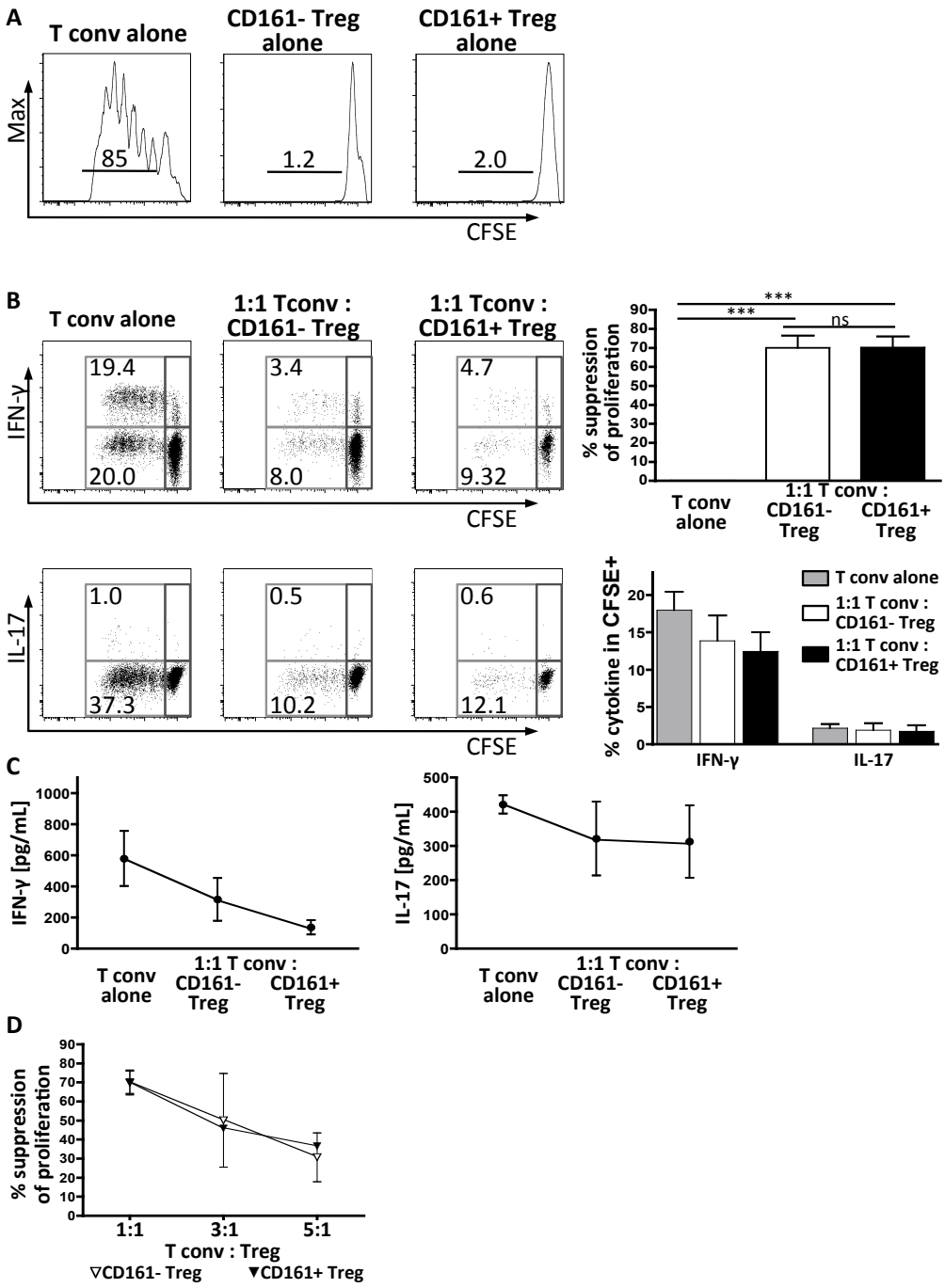

Figure 5.1: CD161+FoxP3+CD4+ T cells are suppressive and anergic *in vitro*. (A) Both CD161+ and CD161- Treg are anergic *in vitro*. Cells were sorted, labelled with CFSE and stimulated *in vitro* for 5 days with anti-CD3. Representative histograms showing CFSE dilution of sorted CD161- Treg (middle), CD161+ Treg (right) and conventional T cells (Tconv, left) from one healthy adult (of 2). Numbers above the bars represent the percentage of divided cells. (B-D) CD161+ Treg suppress proliferation and cytokine production. Sorted Tconv were labelled with CFSE, mixed with unlabelled Treg subpopulations as shown, and stimulated with anti-CD3 +/- anti-CD28 for 5 days as described, before analysis by flow cytometry. (B) Representative plots show CFSE dilution, and the production of IFN-γ (upper panels) or IL-17A (lower panels) by Tconv; summary plots at day 5 for the %suppression of division of Tconv in the various cultures at (1:1 Tconv:CD161- Treg (white) or CD161+ Treg (black)) top. % cytokine (IFN-γ, left; IL-17, right) in CFSE+ fraction (Tconv) under following conditions: Tconv

alone (grey), 1:1 Tconv:CD161- Treg (white) or CD161+ Treg (black) bottom (n=5; statistical analysis, one-way ANOVA). (C) IFN-γ and IL-17A protein levels were assessed in the supernatants from co-cultures by Luminex assay. (D) No difference between CD161- and CD161+ Treg suppressive capacity upon Treg titration (n=2-4); all summary plots show mean +/-SEM (p values: ***≤0.001; ns: not significant).

Interestingly CD161+ Treg themselves produced some cytokines during suppression assays (Figure 5.2A). The frequency of cytokine-producing CD161+ Treg in the *in vitro* suppression assay was decreased compared to when these cells were analysed *ex-vivo*, whereas the low cytokine frequency in CD161- Treg was similar in the suppression assay as to *ex-vivo* CD161- Treg. These data suggest that CD161+ Treg might suppress their own cytokine production (both IFN-γ and IL-17, but especially IL-17) in this *in vitro* setting.

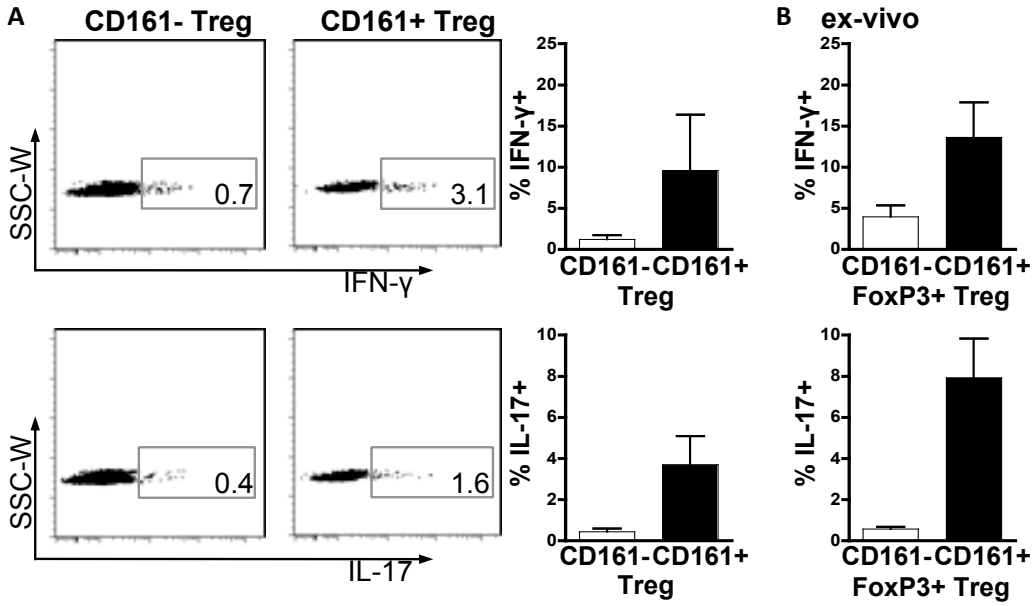

Figure 5.2: CD161+ Treg produce pro-inflammatory cytokine during the suppression assays. (A) Representative flow cytometry plots showing CD161- Treg (left) and CD161+ Treg (right) cytokine production (IFN-γ top, IL-17A bottom) gated on CFSE negative fraction (where Tconv were CFSE labelled, Treg were CFSE negative) of day 5 of suppression assay at 1:1 (Tconv:Treg); with summary plots at the right (n=5). (B) Cytokine production of corresponding individuals *ex-vivo* (n=4). Bars represent mean +/- SEM.

Together these data suggest that the proposed CD161+ Treg population that have been identified in this work, with the phenotype CD161+FoxP3+CD127^{lo}CD25^{hi}CD4+ can be classified as regulatory in that they show both suppressive capacity and anergy *in vitro*.

5.2.2. CD161+ Treg are predominantly demethylated at the Treg specific demethylated region

Recently, the importance of epigenetic modifications for Treg stability has emerged [108,109]. DNA demethylation at the Treg specific demethylated region (TSDR) of the *FOXP3* locus has been deemed crucial for Treg stability, stable FoxP3 expression and implementation of the Treg program [291]. TSDR methylation in sorted Tconv, CD161- and CD161+ Treg from healthy peripheral blood was therefore assessed by generation of bisulfite converted DNA, PCR amplification and sequencing, according to 2.7.2 and 2.7.3 in partnership with the postdoctoral fellow David Bending in the group. CD161- Treg and CD161+ Treg both showed a predominantly demethylated TSDR (Figure 5.3). Twelve CpG islands within the TSDR of the *FOXP3* locus were analysed for sorted Tconv, CD161- Treg and CD161+ Treg (top to bottom, purity >80%). Male donors were used for this analysis, since the *FOXP3* locus is on the X-chromosome and males therefore have only one copy of *FOXP3* gene. Thus the cloned locus in males will be from the active locus, whereas female samples (which have two X-chromosomes) would pose a 50% chance of cloning the inactive locus. Across three male individuals the TSDR of Tconv showed full methylation (96.4% (+/-0.8)). As expected, CD161- Treg were predominantly demethylated at the TSDR, although showed a small residual methylation (7.4% (+/-2.5)), while CD161+ Treg had 28.5% (+/-2.1) methylation. Analysis of the individual strands that had been cloned and sequenced was carried out to define the source of the partially methylated TSDR in CD161+ Treg. The increased overall methylation seen in the CD161+ Treg compared to CD161- Treg, was not due to an increase in fully methylated clones, but due to a proportion of CD161+ Treg clones being partially methylated.

These data suggest that CD161+ Treg are a stable subset with regulatory properties and predominantly demethylated TSDR at the *FOXP3* locus, thus fulfill the criteria that are widely accepted to indicate true regulatory T cells.

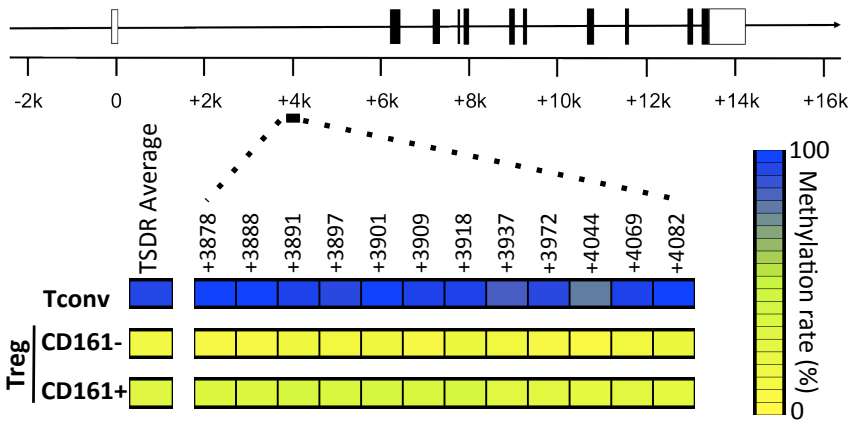

Figure 5.3: Both CD161- Treg and CD161+ Treg contain a predominantly demethylated *FOXP3* TSDR region. DNA was extracted from sorted Tconv, CD161- Treg and CD161+ Treg (purity >80%), bisulfite treated, and the TSDR region was amplified and then cloned. 20-35 individual clones were sequenced and the percentage of methylated CpG islands determined. Schematic of the *FOXP3* locus representing the location of the 12 CpG islands analysed top (positions +3878 to +4082), with mean %methylation of each CpG island displayed (left) and average for all islands (right; blue 100%, yellow 0%; one of three representative individuals shown).

5.2.3. CD161 stability and regulation of expression

To assess the stability of CD161 expression *in vitro*, whole PBMC were cultured with a variety of cytokines or synovial fluid (2.5.5). Synovial fluid (SF) was chosen as a culture condition because in childhood arthritis CD161 expression is increased on CD4+ T cells (described in chapter 6). 5% Synovial fluid (n=4, with no measured IL-17A, IFN-γ, IL-10 or IL-2 by Luminex) did result in an increase in CD161 frequency in both total CD4+ T cells and FoxP3+ Treg when accompanied by TCR stimulus (Figure 5.4A). Five day culture alone, with or without stimulation did not change CD161 frequency. However in the synovial fluid condition cells appeared visually less viable than in other conditions, thus it is possible that SF might not directly affect CD161 expression. Rather, it is possible that CD161+ cells have a survival advantage under culture conditions in the presence of synovial fluid. Final cell counts were not performed at day 5, meaning that this proposed decrease of cell survival was only estimated by the size of the cell pellet observed. To reduce possible effects on viability by unknown factors in the SF and to illuminate which factors might be important in CD161 expression cytokines were used as additional stimulus (Figure 5.4B). Cytokines were chosen due to their high (IL-6, IL-12, TNF-α) or low concentration (TGF-β) in SF from patients with JIA, as previously demonstrated in the Wedderburn lab [82,206]. Additionally both IL-2 and TGF-β have also been shown to be important in Treg generation and/or maintenance [292-295]. Additionally it has been suggested that both IL-12 and IL-2 have an effect increasing CD161 expression [296,297]. Furthermore IL-12 is linked to IFN-γ production by T cells [298] and IL-6 has been implicated in IL-17A production [299]. In the total CD4+ T cell gate no change of CD161 frequency with any of these cytokines was detected without TCR stimulus (Figure 5.4B left). In the FoxP3+ gate IL-2 appeared to increase and TGF-β decrease CD161 frequency slightly, although these differences were not statistically significant (Figure 5.4B right). Additional TCR stimulus revealed a trend to slightly reduced CD161 frequency in CD4+ T cells in TGF-β and IL-2 treated cells (Figure 5.4C left). Within the FoxP3+ gated population the trend towards reduced CD161 with TGF-β treatment was still apparent with TCR stimulus, whereas IL-2 did not change CD161 frequency when accompanied with TCR stimulus (Figure 5.4C right). Thus no cytokine candidate was found to be regulating CD161 expression definitively.

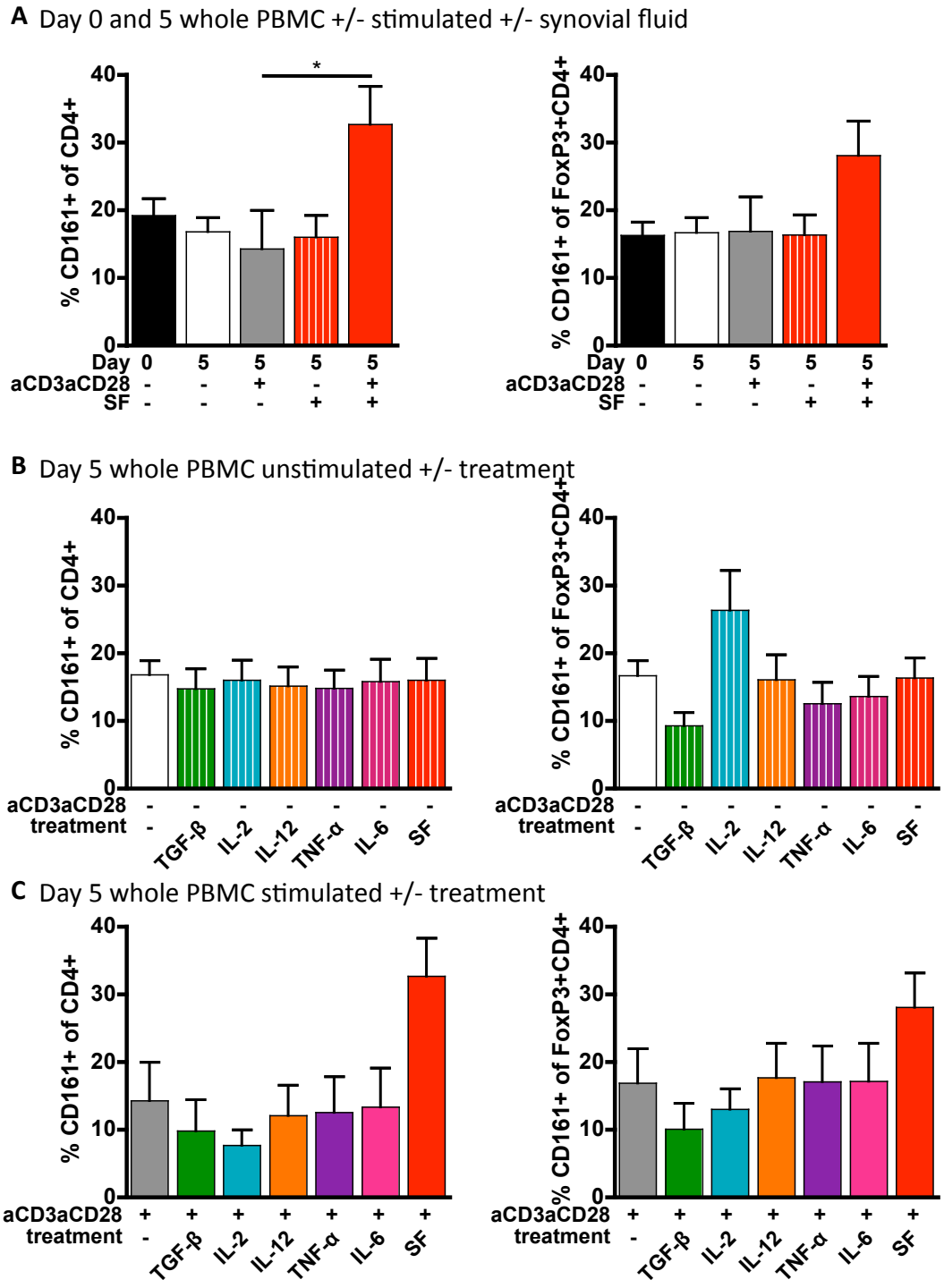

Figure 5.4: Regulation of CD161 expression during *in vitro* culture and on stimulation. (A-C) CD161+ cell frequency within CD4+ T cell population (left plots) and FoxP3+CD4+ Treg population (right plots), after culture of whole PBMC for 5 days under different conditions as shown. (A) T cell stimulation or culture alone does not affect CD161 expression; stimulation in the presence of synovial fluid (SF, red) increases CD161+ cell frequency. Cytokines have little effect on CD161 expression without (B) or with anti-CD3 and anti-CD28 stimulation (C). Conditions: Day 0- black bars; day 5 no stimulus- white bars; day 5 stimulated- grey bars. Throughout all plots, cytokines without stimulus- striped bars; cytokines with stimulus- solid bars. Cytokines added: +TGF-β green; +IL-2 turquoise; +IL-12 orange; +TNF-α purple; +IL-6 pink. All bars represent

mean +/-SEM. One-way non-parametric ANOVA (Kruskal-Wallis with Dunn's test; p values: *≤0.05; n=4-9).

However these experiments were performed by culturing whole PBMC: thus changes of CD161 expression cannot be tracked on specific cells and effects of specific cytokines might be lost. To further investigate the effects on either CD161- or CD161+ cells alone, I therefore tested how labeled CD161- and CD161+ Treg behave when cultured in PBMC conditions. For this set of experiments, CD161- and CD161+ Treg were sorted to high purity (2.4.5) labeled with CFSE (2.5.1), spiked back at 5-7% of cells into autologous PBMC and cultured for 3 days with or without anti-CD3 and anti-CD28 stimulation (2.5.5). The same cytokine conditions as in Figure 5.4B and C were used plus the additional condition of combined IL-1β + IL-23 + TGF-β, for Th17 skewing conditions [300], were used.

No differences in cell viability or survival between conditions were seen at day 3 (data not shown). CD161+ Treg (filled histogram and bars) retained expression of CD161 (Figure 5.5B, C), while CD161- cells (clear histograms and white bars) did not acquire CD161 expression (Figure 5.5B, C, D). CD161 expression was stable under all conditions. CD161 staining was performed using two different fluorochromes on Day 0 compared to Day 3, thus the slightly decreased CD161 expression per cell (as measured by MFI) at day 3 could be a technical artifact or a real decrease in protein per cell (Figure 5.5B, C). Addition of cytokine to the culture did not alter the stability of CD161 expression (Figure 5.5C shows IL-2, IL-6, IL-12 and IL-1β + IL-23 + TGF-β; no change in CD161 expression or cytokine production was seen with TNF-α, IL-1β or IL-23 alone). However, a trend towards increased CD161 levels was demonstrated when IL-12 was present (Figure 5.5C, top). Additionally, CD161+FoxP3+ cells maintained their cytokine phenotype, producing IL-17A and IFN-γ readily with PMA/Ionomycin without TCR stimulation during the 3 day culture (Figure 5.5B right and far right) and after T-cell activation (Figure 5.5C, bottom) in all culture conditions. Addition of cytokines to the culture system showed that, as expected, IL-12 enhanced IFN-γ production and limited IL-17A production, whereas other cytokines had little effect on the cytokine-producing phenotype of the two Treg populations (Figure 5.5C bottom).

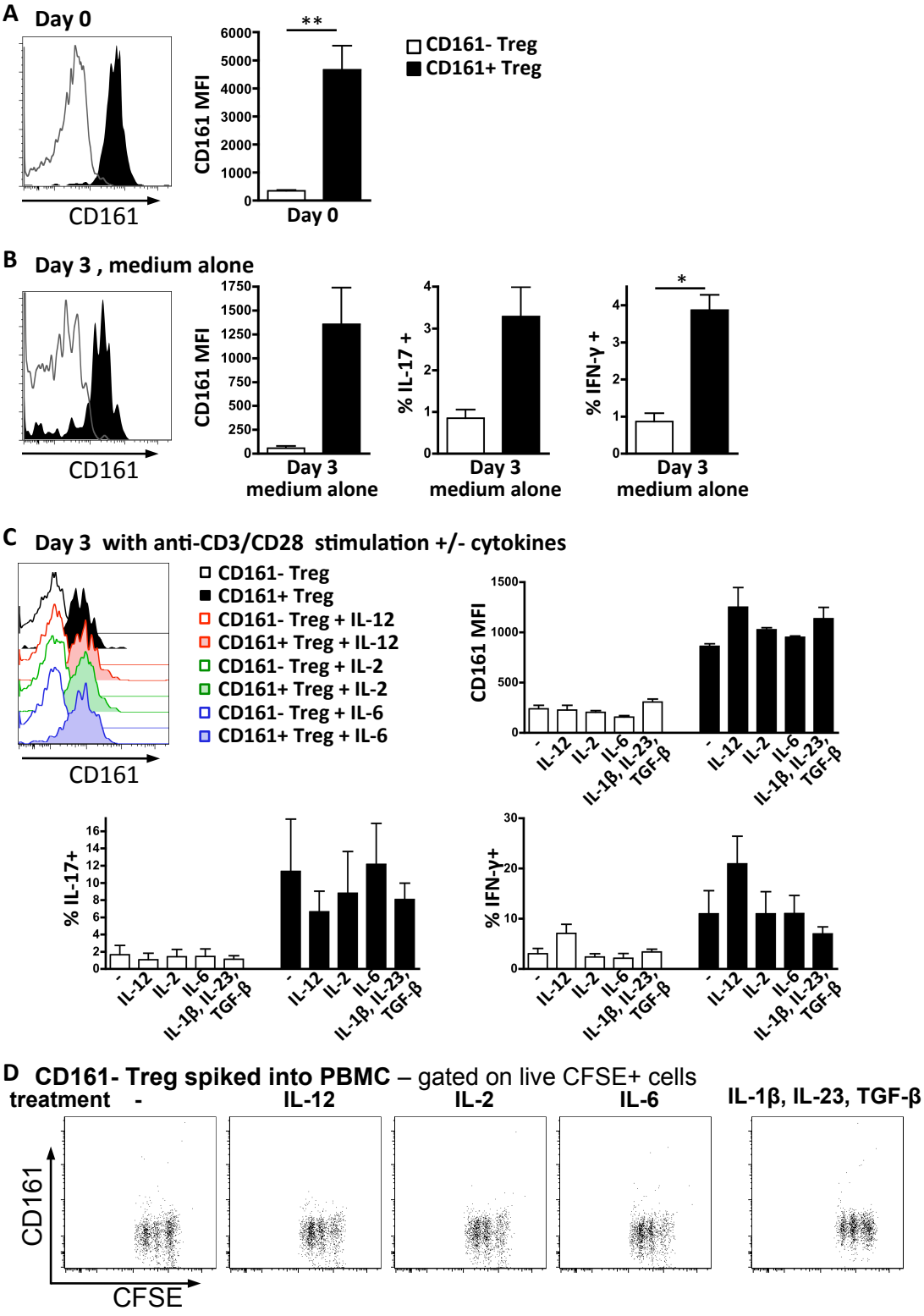

Figure 5.5: CD161+ regulatory T cells are stable during *in vitro* short-term culture. Sorted Treg subpopulations were labelled with CFSE, 'spiked' back into autologous PBMC (at 5-7%) and cultured for 3 days. Representative overlay histograms of CD161 expression gated on CFSE+ cells and summary plots of CD161 MFI at day 0 (n=5, A), after 3 day culture in medium alone (n=3, B), and after 3 day culture on anti-CD3/ anti-CD28 coated plates +/- cytokines (IL-12, IL-2, IL-6 or IL-1b+IL-23+TGFb as shown, n=3, C top); cytokine production by labelled CD161- or CD161+ Treg was also assessed on day 3 (B, C bottom). (D) CD161-Treg do not gain CD161 expression; representative flow

cytometry plots showing CD161 vs CFSE on day 3 with conditions, from left to right: no added cytokines, IL-12, IL-2, IL-6 or TGF-β+IL-1β+IL-23 treatment as shown (representative of n=4). Data are gated on CD4+CFSE+ live cells. For both histograms and graphs, clear/white symbols represent CD161- Treg, filled/black symbols CD161+Treg. In bar graph, bars represent means +/- SEM with Wilcoxon matched pairs test between cell subsets, between groups one-way non-parametric ANOVA (Kruskal-Wallis with Dunn's test) (p values: **<0.01; *<0.05).

5.2.4. CD161+ Treg with their cytokine-producing phenotype are stable in longer-term Treg expansion

To test CD161+ Treg characteristics in longer-term culture and in a possibly used for therapeutic application for Treg (Treg expansion for adoptive transfer to assist transplant tolerance or treat autoimmunity), total Treg ($CD25^{hi}CD127^{lo}$) were sorted to high purity (2.4.5) and cultured under Treg expansion conditions (2.5.4) with or without cytokines (IL-12 for Th1-like skewing; TGF-β+IL-1β+IL-23 as IL-17A skewing conditions). There was no difference in FoxP3 stability between Treg gated on CD161- or CD161+ and the frequency of CD161+FoxP3+ cells was constant throughout the 10-day culture, irrespective of culture conditions (Figure 5.6A, B). Furthermore CD161+FoxP3+ cells maintained their capacity to produce IL-17A and IFN-γ, whereas cytokine production remained negligible in CD161-FoxP3+ cells. Addition of cytokines to these cultures had little effect, with a small increase in IFN-γ and slight decrease in IL-17A in the presence of IL-12 (Figure 5.6C). This demonstration of persistence of CD161+FoxP3+ Treg pro-inflammatory potential should be of interest to investigators attempting to expand Treg *ex-vivo* for potential therapeutic applications. In inflammatory settings this profound pro-inflammatory phenotype could be harmful, whereas in other settings, such as transplantation, cytokine production by Treg has been suggested to be essential [160,164].

Taken together, these data suggest that CD161 expression and the phenotype of the CD161+ Treg subset appear stable, and that these features were not readily induced or reduced by the conditions tested. However the control of CD161 expression with its associated phenotype is still unclear and would require further investigation.

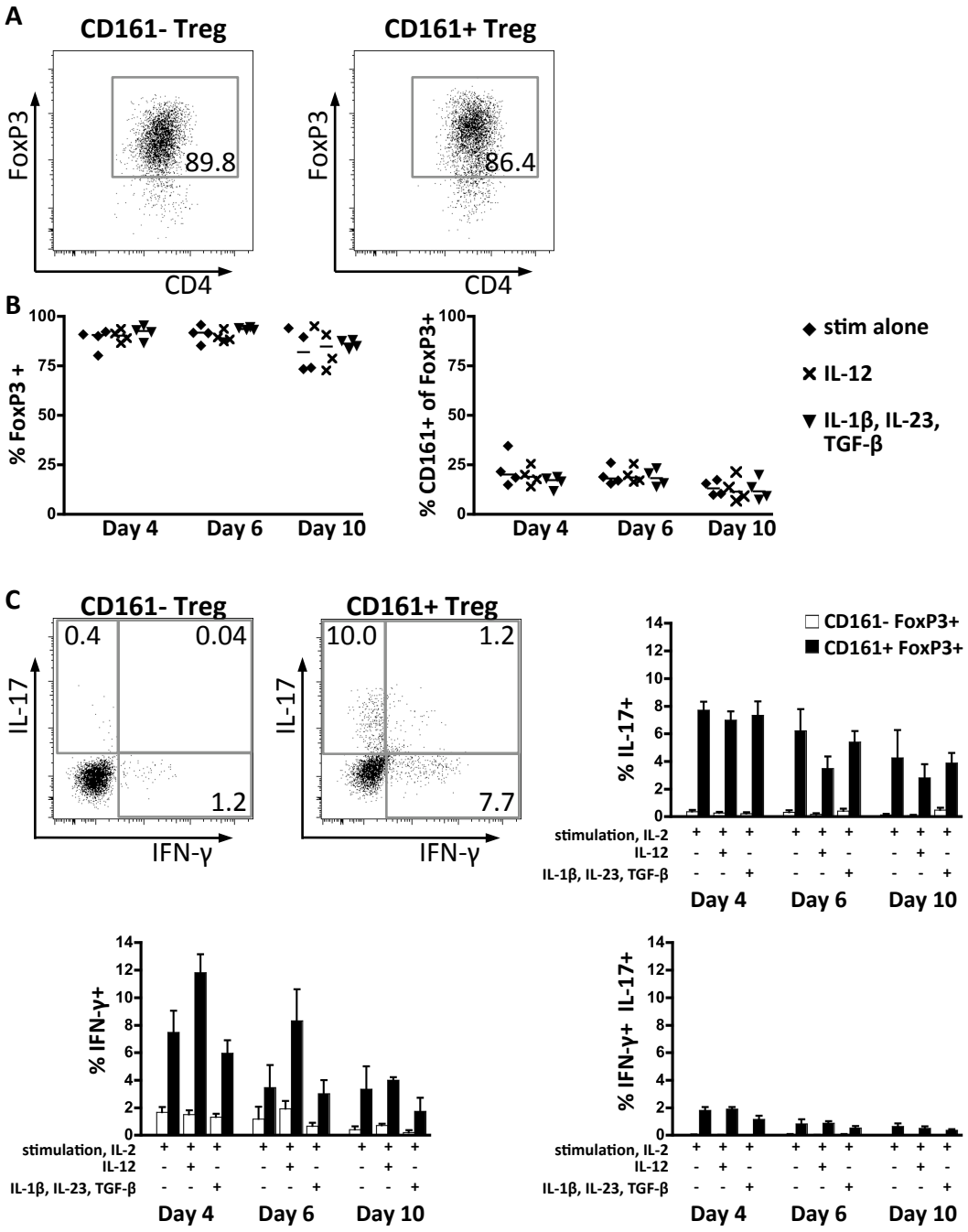

Figure 5.6: CD161+ regulatory T cells and cytokine-producing phenotype persist upon Treg expansion. Sorted Treg (CD4+CD25^{hi}CD127^{lo}) were expanded with IL-2 and anti-CD3 and anti-CD28 stimulus over 10 days with or without cytokine treatment as shown (n=4). (A) Representative flow cytometry plots of FoxP3 expression at day 10 with stimulation alone for CD161- and CD161+ cells (left). (B) Summary plots for FoxP3 expression overall (left) and frequency of CD161 in FoxP3+ cells (right), horizontal lines representing median; diamonds stimulation alone; crosses +IL-12; triangles +TGF-β, IL-1β and IL-23. (C) Representative flow cytometry plots showing cytokine production (IL-17A vs IFN-γ) of CD161-FoxP3+ (left) and CD161+FoxP3+ cells (right) with summary plots showing mean +/- SEM for IL-17A single, IFN-γ single and IL-17A+IFN-γ double producing cells for CD161- (white bars) and CD161+FoxP3+ (black bars).

5.2.5. CD161+ Treg function and CD161 as a functional receptor

To test the functional consequences of CD161 expression on Treg, and the effects of CD161 ligation by its ligand on T cells, two different strategies where used: functional assays (antigen specific responses and pAKT phosphorylation) comparing behaviour of CD161- and CD161+ Treg; and as a second approach use of monoclonal antibodies against CD161 to ligate CD161 directly and analyze the effects

5.2.5.1. CD161+ Treg are pathogen-specific

There is some evidence that cytokine-producing Treg might be important in infection, and may be pathogen specific [145]. To test the responses of CD161+ Treg to specific antigens, I performed an *in vitro* antigen challenge with *Candida albicans* and *human Cytomegalovirus (hCMV*) antigens using whole PBMC (2.5.7). In individuals with Tconv (FoxP3- cells) reactive to either pathogen, proliferation and cytokine-polarised responses were elicited to antigens in CD161+FoxP3+ but not CD161-FoxP3+ cells (Figure 5.7A). In non-responders, without any proliferation in FoxP3- cells, both CD161- and CD161+FoxP3+ T cells remained non-proliferative and produced similar amounts of IL-17A and IFN-γ as the same cells directly *ex-vivo* (Figure 5.7B). These data indicate that the CD161+ Treg population contains cells that are responsive to pathogens and might have arisen together with pathogen specific Tconv.

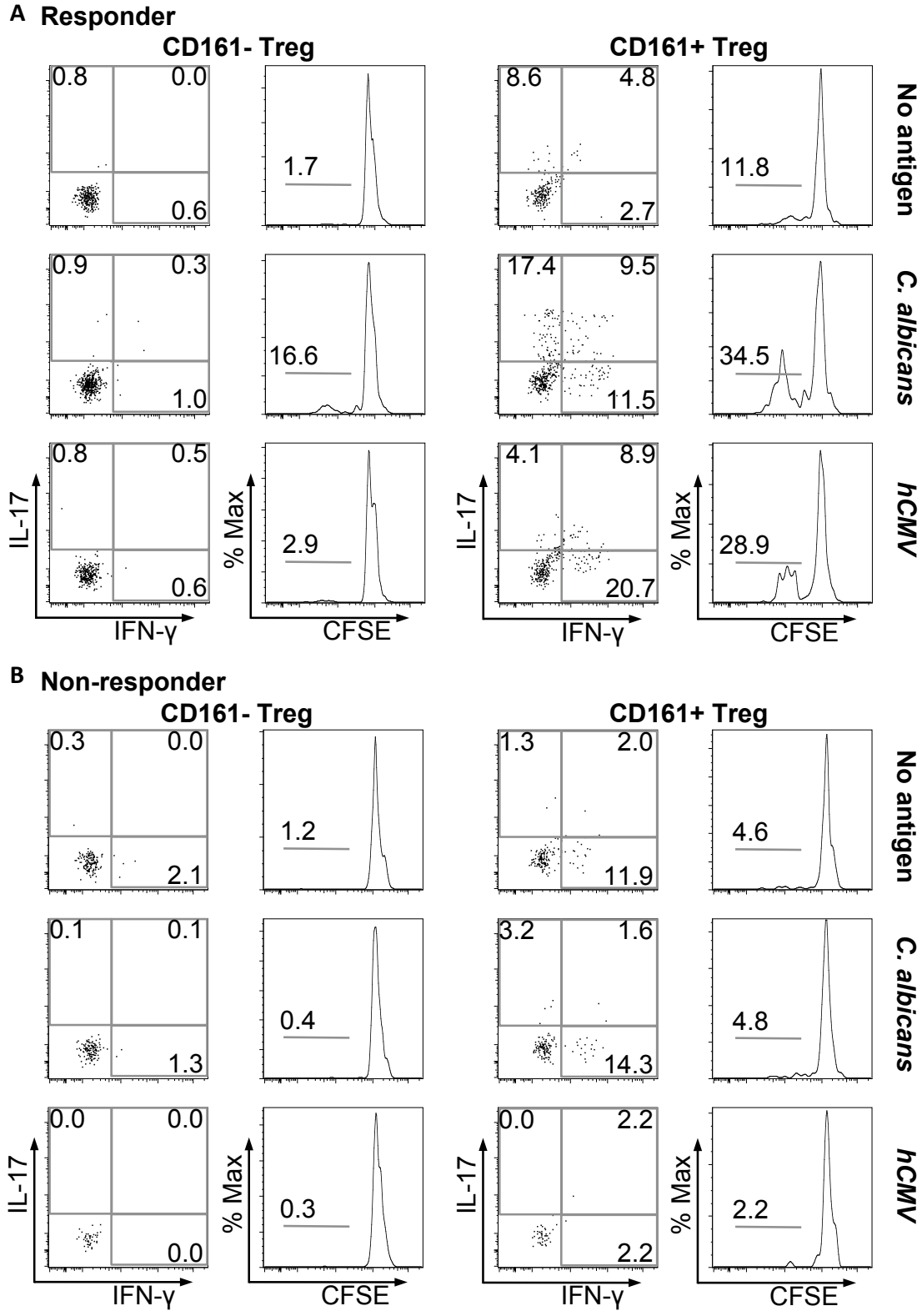

Figure 5.7: Antigen specific-Treg responses lie predominantly within the CD161+FoxP3+ subset. Representative flow cytometry plots gated on CD161-FoxP3+ (left) and CD161+FoxP3+ cells (right), showing each cytokine production (IL-17A vs IFN-γ) and proliferation by CFSE dilution in histograms; whole PBMC culture with or without lysate for *Candida albicans* (*C. albicans*) or *human CMV* (*hCMV*) for a responder (A) and non-responder (B); (representative of n=5 (3 responder (to one or both pathogens), 2 non-responder).

5.2.5.2. A role of AKT phosphorylation in CD161+ Treg upon TCR stimulation

It has been previously shown that Treg show a different signaling cascade after TCR stimulation compared to Tconv [301]. Treg show reduced phosphorylation of the protein kinase B, known as AKT (V-akt murine thymoma viral oncogene homolog 1), at serine 473 (pAKT), which was critical for *in vitro* suppressive function. Interestingly, transducing *ex-vivo* CD4+CD25+ Treg with a constantly active kinase resulted in IFN-γ production by those Treg in this study.

Hence the hypothesis was proposed that CD161+ Treg might have an altered pAKT status compared to CD161- Treg. A similar stimulation and staining protocol to the study performed by Crellin *et al* was used, with the addition of CD161 staining (2.3.8). CD161+FoxP3+ cells appeared to have a higher phosphorylation of serine 473 of AKT upon anti-CD3 and anti-CD28 stimulation compared to CD161-FoxP3+ cells at multiple time points (Figure 5.8). These data suggest that increased phosphorylation could be relevant for the cytokine production by CD161+ Treg and not CD161- Treg.

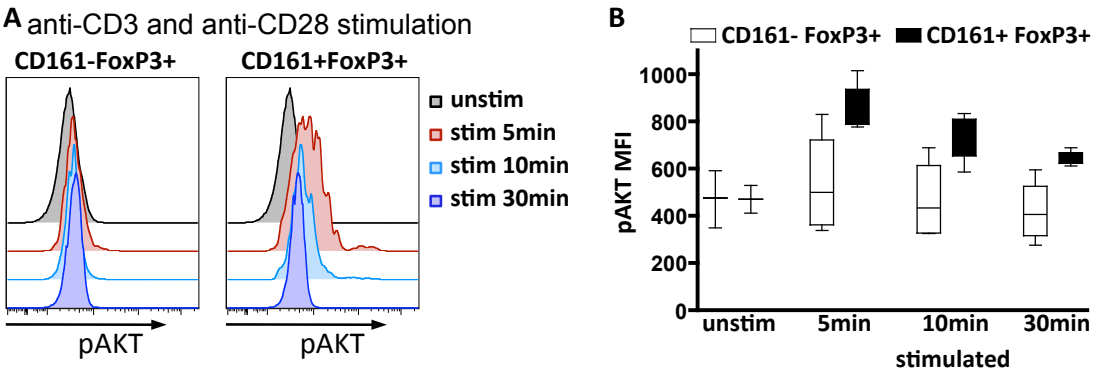

Figure 5.8: CD161+ Treg have increased pAKT upon TCR stimulation. (A) Representative overlay histograms gated on CD161-FoxP3+ (left) and CD161+FoxP3+ cells (right) showing unstimulated (grey), 5 (red), 10 (light blue) and 30min (blue) anti-CD3 and anti-CD28 stimulation. (B) Summary plot of the pAKT MFI in both Treg populations, after different times of stimulation (mean +/- SEM, CD161-: white, CD161+: black, n=4).

5.2.5.3. CD161 as potential perpetrator of some function of CD161+ Treg

To study the role of CD161 further, two commercially available ligating monoclonal antibody (Ab) clones specific to CD161 (DX12 and 191.B8.192) were used. It is still not clear which CD161 ligating antibodies show a activating effect and which an inhibitory effect, as studies using the same antibodies (DX12 and 191.B8.192, or clone DX1) have found variable effects [275,280-285]. However when interpreting these studies, care has to be taken to be sure whether inhibition was measured by inhibition of ligand binding, or actual outcome. Inhibition measured by inhibition of ligand binding, could still activate positive signaling through CD161. Thus the decision was made two use two different antibodies clones to potentially test the action of the different Ab clones.

It was first investigated whether CD161 ligation would affect pAKT in Treg. Ligating antibodies specific to CD161 were used in addition to anti-CD3 and anti-CD28 antibodies; all were cross-linked for a variety of time points followed by staining (2.3.8). In preliminary experiments ligation of CD161 using these two different antibody clones, showed little effect on pAKT in total FoxP3+ cells (Figure 5.9A). During these studies I noticed that the ligating and staining antibodies for CD161 inhibit each others binding, possibly due to sterical hindrance; thus a potential effect would have to be seen on the total Treg population (as no CD161 staining could be performed in this assay), where only a minority of cells express CD161. Thus the lack of noticeable change in pAKT could be real or might be due to the fact that only a minority of cells are affected and the 'noise' is too high to allow a detection of a change in signal.

Change in cytokine production has been linked to CD161 ligation in other cell subsets, such as total T cells and NK cells [280-282,302]; therefore this functional readout was tested here. Various time points, stimulation and cell subset cultures were assessed. However considerable noise-to-signal issues became apparent. In Figure 5.9B and C IFN-γ and TNF-α frequency on sorted Tconv (B) and Treg (C) (2.4.5) is shown after 3 days of TCR stimulation and CD161 ligation with the two different Ab clones (2.5.6). CD161 frequency was measured in a small separate cell aliquot after sorting (Figure 5.9B, C the far right). In Tconv CD161 ligation tended to increase both IFN-γ and TNF-α

positive cell frequencies; this increase reached statistical significance when ligation was performed using anti-CD161 Ab clone 191.B8.182. In Tconv from healthy adult donors, there is a higher frequency of CD161+ cells compared to Treg. Treg showed variable results in these experiments. TNF-α positive cell frequency did not change with CD161 ligation, and in some individuals tested IFN-γ frequency actually decreased with CD161 ligation, however no significance was reached, as others individuals showed an increase in cytokine positive cell frequency. Both anti-CD161 monoclonal Ab clones showed similar trends in any one individual.

Taking these data together, CD161 appears to mark a Treg subset with pathogen-specific responses and increased intracellular levels of pAKT. CD161 ligation might be involved in regulation of cytokine production directly. However more robust *in vitro* assays need to be designed to address this question further.

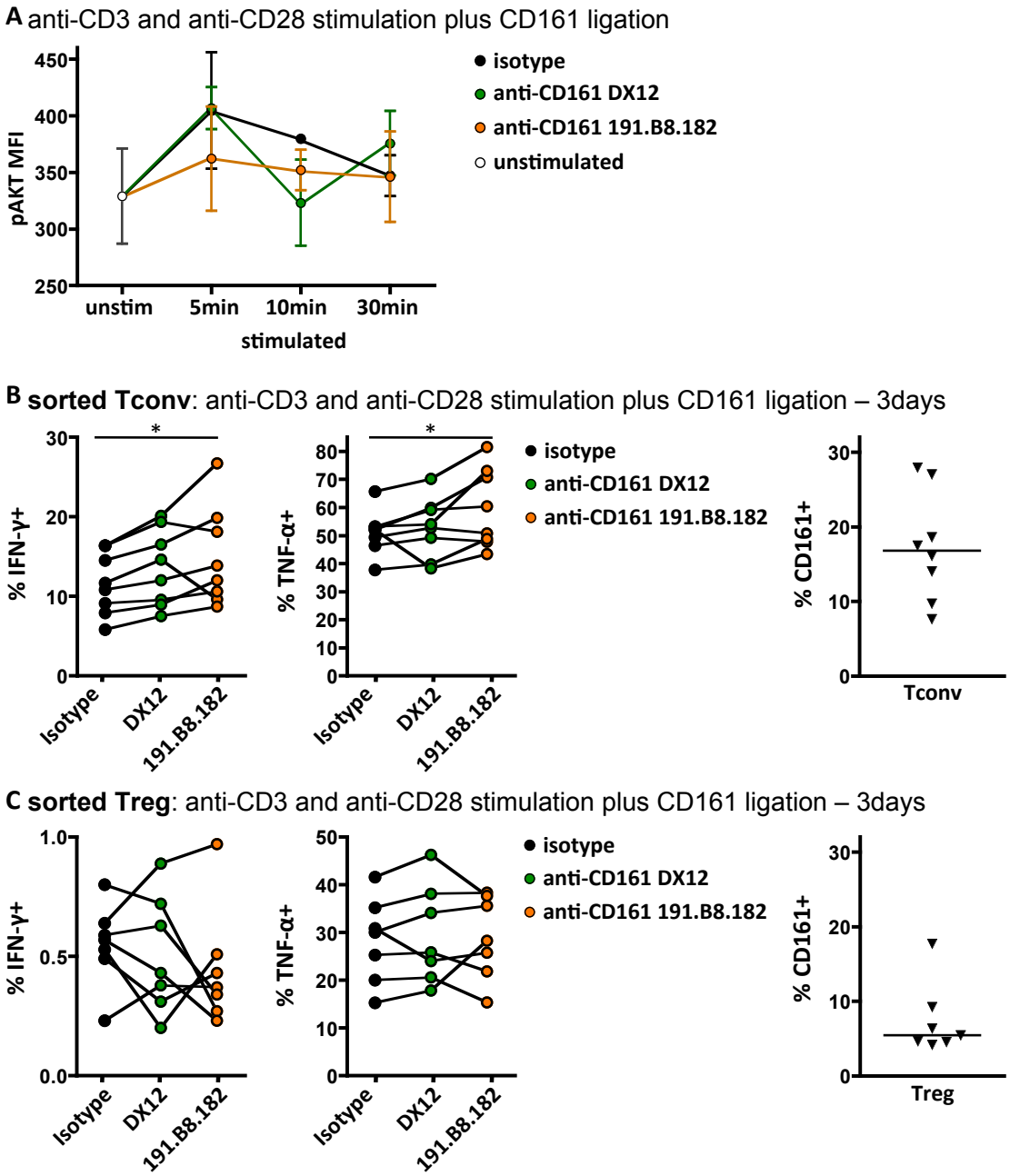

Figure 5.9: Effects of CD161 ligation. (A) Ligation of CD161 with TCR stimulus does not affect pAKT on total FoxP3+ Treg. Cells were stimulated as shown and gated on CD4+FoxP3+ (mean +/- SEM, isotype IgG: black, anti-CD161 clone DX12: green, clone 191.B8.182: orange, n=2). (B-C) CD161 ligation affects cytokine production in 3 day stimulation of sorted Tconv (B) and Treg (C). IFN-γ (far left) and TNF-α (left) frequencies at day 3 (isotype IgG: black, anti-CD161 clone DX12: green, clone 191.B8.182: orange, n=7) with CD161 frequency in sorted populations at day 0 (far right). Repeated measures ANOVA with Bonferroni multiple comparison test (p-value: *<0.05).

5.3. Discussion

It is widely considered that an important function of Treg is the suppression of disproportionate immune responses. However, there are still many unknown elements. Of topical relevance, is the controversy surrounding the pro-inflammatory potential of Treg, which is present in the CD161+ Treg population (as described in chapter 4), particularly in inflammatory settings. Here I have shown that CD161+ Treg fulfill the hallmark features of classic Treg as they are anergic in culture alone and they suppress the proliferation of Tconv to the same extent as CD161- Treg. Interestingly CD161+ Treg still produced some cytokine themselves in suppression assays.

CD161+ Treg show a predominantly demethylated TSDR region of the *FOXP3* locus. Overall methylation levels were in keeping with those for previously published Treg populations [108,126,204]; however in the three individuals tested, CD161+ Treg displayed a less demethylated TSDR region overall, with an altered methylation pattern compared to CD161- Treg. The functional consequences of this altered demethylation warrant future investigation. Interestingly Baecher-Allen *et al* recently observed a mixed methylation pattern in IL-17 producing CD73+ Treg clones [303]. In that study half of the CpG islands were methylated, some partially methylated and others not at all. These Treg clones had some CD127 expression and were HLA-DR-. The authors found that cells could switch between either producing IL-17 or suppressing Tconv. A more in depth analysis of which CpG islands were demethylated in these clones would be interesting, since in that publication exact CpG were not given. These findings, and my own data, suggest that cytokine production, partial methylation and potential to be suppressive might be linked.

These data are supported by recent findings of cytokine-producing Treg that were generated by *in vitro* stimulation, expansion or cloning, which were still suppressive [152,155-157].

Furthermore CD161+ Treg and their cytokine-producing phenotype appear stable in short and longer term cultures, while CD161-FoxP3+ cells do not up-regulate cytokine production, even in Th1- or Th17-skewing conditions. What controls CD161 expression

or cytokine production could not yet be fully defined and further investigation is required.

The growing recognition that Treg may have pro-inflammatory potential, has significant implications for therapeutic adoptive transfer of human Treg, since standard sorting methods to purify Treg would include such cells. These data suggest that the inclusion of a depletion step, to remove CD161+ Treg, in protocols designed to prepare Treg for cell therapy, could reduce the dangers of such pro-inflammatory cells to recipients, particularly in some inflammatory conditions. However so-called 'specialized Treg' have been shown to have the ability to regulate specific T helper cell responses in mouse models and thus may have potential benefit in some conditions [304]. Recently IFN-γ producing Treg were demonstrated to be essential in mouse models of transplantation to inhibit graft-versus-host disease [160,164] and high frequency of IFN-γ+CD25+ Treg in renal transplant patients have been associated with good graft function [305].

Moreover my data suggest a possible role in response to pathogens for CD161+ Treg. Only CD161+FoxP3+, not CD161-FoxP3+, responded with increased cytokine and proliferation to two model pathogenic antigens (*C. albicans* and *hCMV*). A possible role for cytokine-producing Treg in infection has been proposed previously [145,157,160], with Duhen *et al* showing antigen specific responses in Treg in a manner that was parallel to these data. CD161 has been seen at decreased levels and frequency in HIV and AIDS T cells [306,307]. Treg expressing CD161 have not been considered in these studies as a potentially important contributor, and may warrant future attention.

It remains unclear which signals direct the nature of the cytokines produced by CD161+FoxP3+ cells, but it is likely that the cytokine milieu is central in determining their cytokine-production profile, as demonstrated for some Treg [156,157]. However, within this study, using *in vitro* culture and a range of conditions, cytokines had only limited affects upon the skewing of responses *in vitro*. Similarly, it remains to be seen what the direct effects of CD161 ligation are on Treg and whether this is involved in the manifestation of the pro-inflammatory profile. The data generated here, indicate a positive effect of CD161 ligation on cytokine production in Tconv, however the data on

Treg are less clear. To address the effect of CD161 ligation in the *in vitro* setting is technically challenging since the antibody against CD161 is sterically hindered by the antibodies used for sorting, which means that functional analysis on purified populations with present reagents is very limited. Since CD161+ Treg are a minor population, stimulation on bulk Treg cultures might not constitute a sensitive enough assay to determine the functionality of CD161, and more robust *in vitro* modeling systems will need to be established to address this area. Furthermore there needs to be more thorough analysis of the specific action of available antibodies against CD161. Some reports used the inhibition of ligand binding as an indication of an inhibitory antibody, however, as others show the antibody might still be activating signaling through CD161 [275,280,282-285].

An *in vivo* system to test CD161+ Treg functionality would be valuable. Unfortunately this is not readily available, since human CD161 does not have an exact equivalent in mouse. Whilst CD161 is the only NKRP1 family member encoded in humans, in mouse there are several different and functionally diverse Nkrp1 receptors, with different expression profiles, divergent functions and a maximum of 40% homology compared to human CD161 (reviewed in Yokoyama *et al*)[286-288]. It therefore remains to be determined whether similar or related markers of Treg with pro-inflammatory potential exist – if at all – in other species.

To conclude this part of the work, the data suggest that CD161 defines a population of 'hybrid Treg' that have both inflammatory and suppressive potential. The precise role and control of cytokine-producing CD161+FoxP3+ cells *in vivo* is worthy of further characterization.

Chapter 6

CD161+ Treg in Juvenile Idiopathic Arthritis

6. CD161+ Treg in Juvenile Idiopathic Arthritis

6.1. Introduction

Juvenile idiopathic arthritis (JIA) is the most common inflammatory rheumatic disease of children. Worldwide it affects around 1 in every 1000 children [165]. JIA can be distinguished in several clinical subgroups (1.5). This study is focused on the following subtypes according to the International League of Associations for Rheumatology (ILAR) classification: oligoarticular (O-JIA; persistent O-JIA (children whose affected joint count remains <5 joints) and extended O-JIA (children whose disease starts with 4 or less joints involved, but whose affected joint count increases to ≥5 after 6 or more month of disease)) and the more severe clinical subtype polyarticular (P-JIA (at onset, or within the first 6 months ≥5 joints involved)); these JIA subtypes show localized inflammation restricted to the joints without systemic or major organ involvement [308].

A consistent finding in several studies of children with JIA has been a clear enrichment of Treg within the synovial fluid (SF) infiltrate of the joints compared to the level observed in peripheral blood of the same children [186,188,201]. The presence of high numbers of Treg in the joint appears to present a paradox, since arthritis is still ongoing suggesting that the immune regulatory function of these Treg is inadequate to control disease. One theory to explain this paradox is that the pro-inflammatory milieu of the joint may inhibit the ability of regulatory T cells to abrogate inflammation efficiently. Interestingly, persistent O-JIA SF has a higher frequency (as proportion of CD4+ T cells), and absolute number of Treg compared to SF from children with the more severe extended O-JIA [186,188]. Thus, Treg frequency does correlate with disease severity, and thus Treg might actively restrain inflammation at least to some extent.

The expression of the surface protein CD161 has been linked to JIA within effector T cell populations. For example, Th17 cells express CD161 and it was established that in the JIA joint many effector T cells which express CD161 may gain IFN-γ and lose IL-17 (so called ex-Th17 cells), and these cells continuously expressed CD161 [82,83]. Additionally it was demonstrated that Treg frequency inversely correlates with Th17

frequency [186,190]. This difference in Treg frequency was also shown to be present very early, even before extension, in children who then go on to have more severe arthritis, affecting more joints compared to persistent O-JIA. The children destined to have more severe arthritis, but whose disease has not yet fully manifested, have been designated extended-to-be O-JIA [179]. Interestingly the transcription factor linked to IL-17 and CD161 [9], retinoic acid related orphan receptor C variant 2 (RORC2v2), was one of the gene transcripts found to be significantly differentially expressed between patients with persistent O-JIA and extended-to–be O-JIA at time of diagnosis. However somewhat surprisingly this gene transcript was increased in the group with persistent outcome, not the extended-to-be patients [179].

Given the above data, and my findings about expression of CD161 on a subset of Treg, which I showed to have both regulatory and inflammatory capacity, I investigated a possible implication of CD161+ Treg in JIA. Great Ormond Street Hospital is Europe's largest centre for JIA patients; during therapeutic joint injections synovial fluid (SF) is aspirated, which gives the unique opportunity to study cells from the site of inflammation and compare these to peripheral blood (PB) samples from the same disease and in some cases even the same individual child at the same time point.

Specific aims of this chapter:

- Ascertain CD161+ Treg frequency and phenotype in JIA
- Investigate relationships of CD161+ Treg with IL-17 producing cells and clinical measurements of JIA
- Examine a role for the CD161 ligand lectin like transcript one (LLT1) in the joint of JIA

6.2. Results

6.2.1. CD161+ Treg are enriched in the joint of JIA

Synovial fluid mononuclear cells (SFMC) have different properties compared to PBMC. Thus, in SFMC the majority cell type is typically the T cell with smaller populations of B cells; monocyte numbers are very variable. The T cell size is typically greater than that of matched T cells form PBMC, which influences the appearance and staining of cells in the joint (Figure 6.1A PB left, SF right). Thus care must be taken when setting gates to define populations in SF cells.

It has been previously shown that Treg are greatly enriched within the highly inflammatory environment of the synovial space in JIA. I hypothesized that Treg expressing CD161 may be present within the synovial Treg population. Therefore CD161 expression was investigated in JIA using flow cytometry (2.3). Representative flow cytometry plots for FoxP3 on CD4+ T cells and CD161 staining on FoxP3+ cells are shown for JIA PB (Figure 6.1B top left) and JIA SF (Figure 6.1B top right). FoxP3+ Treg were, as expected, highly enriched in the joint (Figure 6.1B bottom left). PBMC of JIA patients showed no difference to age matched healthy control children in FoxP3 frequency, nor in CD161+ frequency within the FoxP3+ population (Figure 6.1B bottom). However, cells from the synovial fluid of affected joints had also a significantly higher CD161+ frequency within the FoxP3+ population (median: 23.7%) compared to JIA PBMC (median: 10.8%), and healthy samples (median adult: 14.0%, child: 8.1%; Figure 6.1B bottom right), concurring with our previous findings in JIA, of skewed CD4+ T populations at the inflamed site [82,135,179,186].

In children with an extended O-JIA disease course, there are fewer Treg than in those with the mild self-remitting persistent O-JIA [186,188]. When patients were analysed according to these clinical subgroups, data in this study replicated these previous findings for both CD161-FoxP3+ and CD161+FoxP3+ cells (Figure 6.1C). Thus, although all patients had an enrichment of Treg in SFMC compared to PBMC, both CD161- and CD161+ Treg populations frequencies were decreased in extended O-JIA (mean frequency SF persistent O-JIA for CD161- Treg 15.24%, CD161+ Treg 5.6% and SF extended O-JIA for CD161- Treg 13.2%, CD161+ Treg 4.1% respectively) compared to

persistent O-JIA. Both Treg populations were however increased in the SFMC compared to the PBMC of the respective subset, as expected. Analyzing the fold increase of the CD161+ Treg frequency in SFMC compared to PBMC, showed that this fold increase was much greater than the change for CD161- Treg. Figure 6.1D shows the fold change (proportion in SFMC/proportion in PBMC) across a large set of JIA samples for each Treg subset, in paired samples. The same finding held true for each clinical subset across all samples, with a fold change (SFMC/PBMC) for CD161+FoxP3+ persistent O-JIA of 7.6, extended O-JIA 5.4 and P-JIA 11.0 and a lower fold change for CD161- Treg (2.6, 2.5, and 3.0 respectively). These data demonstrate that CD161+FoxP3+ Treg are highly enriched within an inflammatory environment either through preferred migration of CD161+ Treg into the joint or increased expansion or survival within the joint, compared to CD161- Treg.

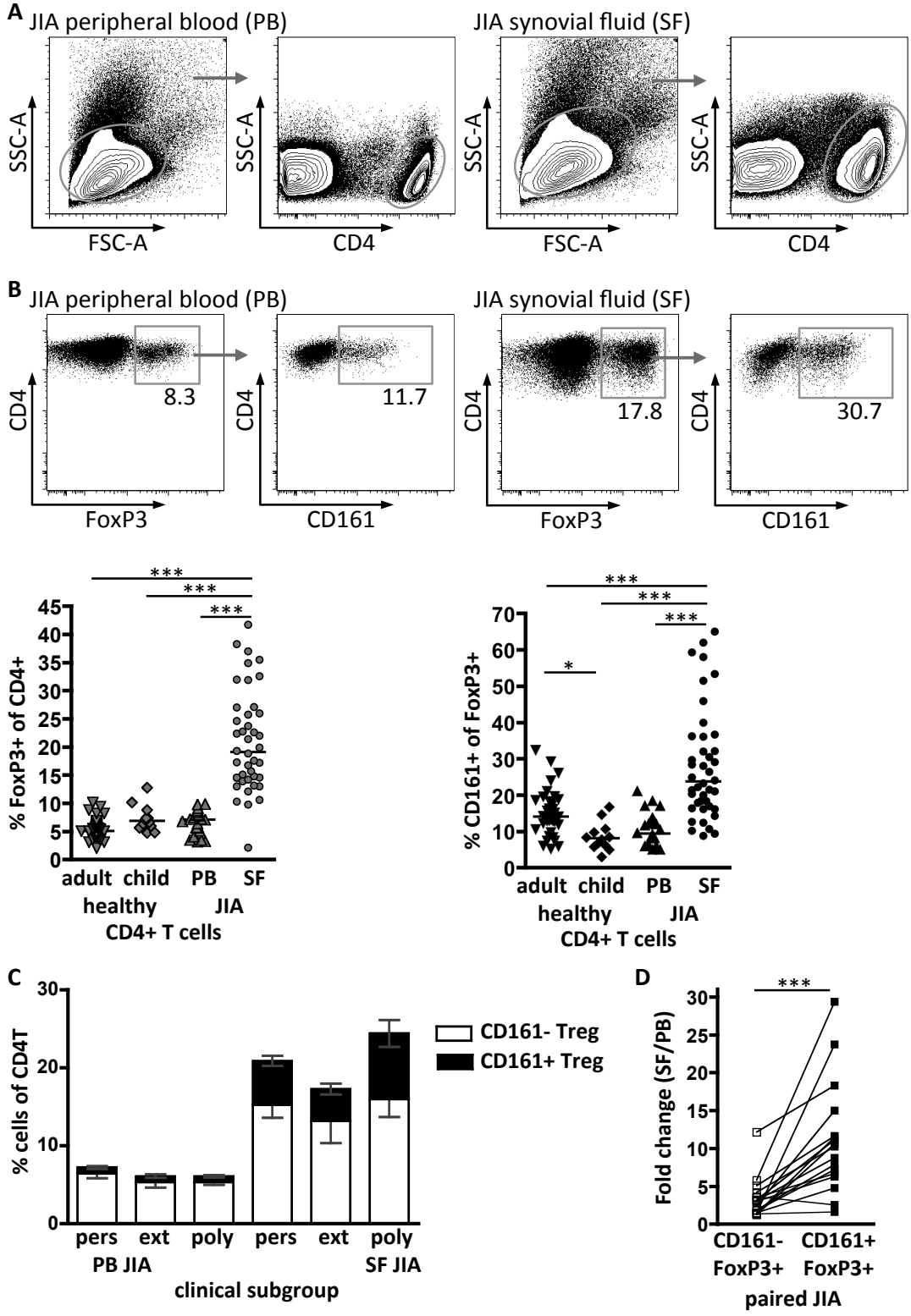

Figure 6.1: CD161 expression by regulatory T cells is enriched in the inflammatory environment. (A) Representative flow cytometry plots showing lymphocyte gate and CD4+ T cell gate for JIA peripheral blood (PB, left) and synovial fluid (SF, right). (B) Representative flow cytometry plots of FoxP3 expression on CD4+ lymphocytes and CD161 staining on FoxP3+CD4+ lymphocytes from JIA PB (left) and SF (right); summary plot for FoxP3 frequency (bottom, left) and CD161 frequency within FoxP3+ (bottom, right) shows data for healthy adult PB (n=39), healthy child PB (n=12), JIA PB (n=24) and JIA SF (n=41) samples; horizontal lines represent median with Kruskal-Wallis test

with Dunn's multiple comparison test. (C) Frequency of CD161+ Treg in different clinical JIA phenotypes was analysed by flow cytometry. Frequency of CD161- Treg (clear) and CD161+ Treg (black) within CD4+ T cells; data are divided into clinical subgroups, persistent O-JIA (pers), extended O-JIA (ext) and polyarticular P-JIA for PB (n=8, n=8 and n=5 respectively) and SF (n=15, n=11 and n=11 respectively) samples. Bars represent mean +/- SEM. (D) CD161+ Treg have a greater fold change between SF and PB than CD161- Treg. Frequency of CD161-FoxP3+ (clear) and CD161+FoxP3+ (filled) in SF divided by concordant frequency in PB of paired JIA samples (n=17) non-parametric paired t test; throughout p values: ***<0.001; **<0.01; *<0.05.

6.2.2. Joint Treg are potent cytokine producers and share an effector-like phenotype

It has been shown previously that synovial fluid from children with JIA has high levels of pro-inflammatory cytokines [206], including TNF-α, IL-6 and IL-12, and JIA effector Tconv have a high frequency of pro-inflammatory cytokine-producing cells, including IFN-γ and IL-17 [82,83,185]. I did confirm this with higher frequencies of IL-17A, IFN-γ and IL-2 producing T cells in SFMC non-Treg (FoxP3- cells) compared to JIA PBMC (representative plots Figure 6.2A). Additionally these flow cytometry plots show a high frequency of cytokine positive FoxP3+ Treg among SF Treg. Overall in Treg from the joints of JIA patients, I observed significantly more FoxP3+ cytokine+ (IL-17A, IFN-γ or IL-2) compared to JIA and healthy PB (Figure 6.2A, summary data below). This indicates that in the inflammatory environment of the joint Treg may also be highly inflammatory. Next, this study investigated whether in the joint CD161+ Treg account for the majority of cytokines produced by regulatory T cells as a whole. IL-17 production was almost exclusively within the CD161+ Treg population (Figure 6.2B). Interestingly, in the joint CD161- Treg were found to be more capable of producing IFN-γ compared to PB CD161- Treg, indicating an effect of the joint microenvironment on both Treg subsets (Figure 6.2B). Nevertheless the frequency of cytokine-producing cells was significantly higher in CD161+ Treg compared to CD161- Treg of both JIA PB and JIA SF (Figure 6.2B). However, to account for the high frequency of FoxP3+ cytokine+ cells among SF CD4+ T cells, it was not the case that more of the CD161+FoxP3+ cells produced cytokine. Rather, the higher proportion of Treg expressing CD161 was found to be driving this difference in synovial fluid (see Figure 6.1).

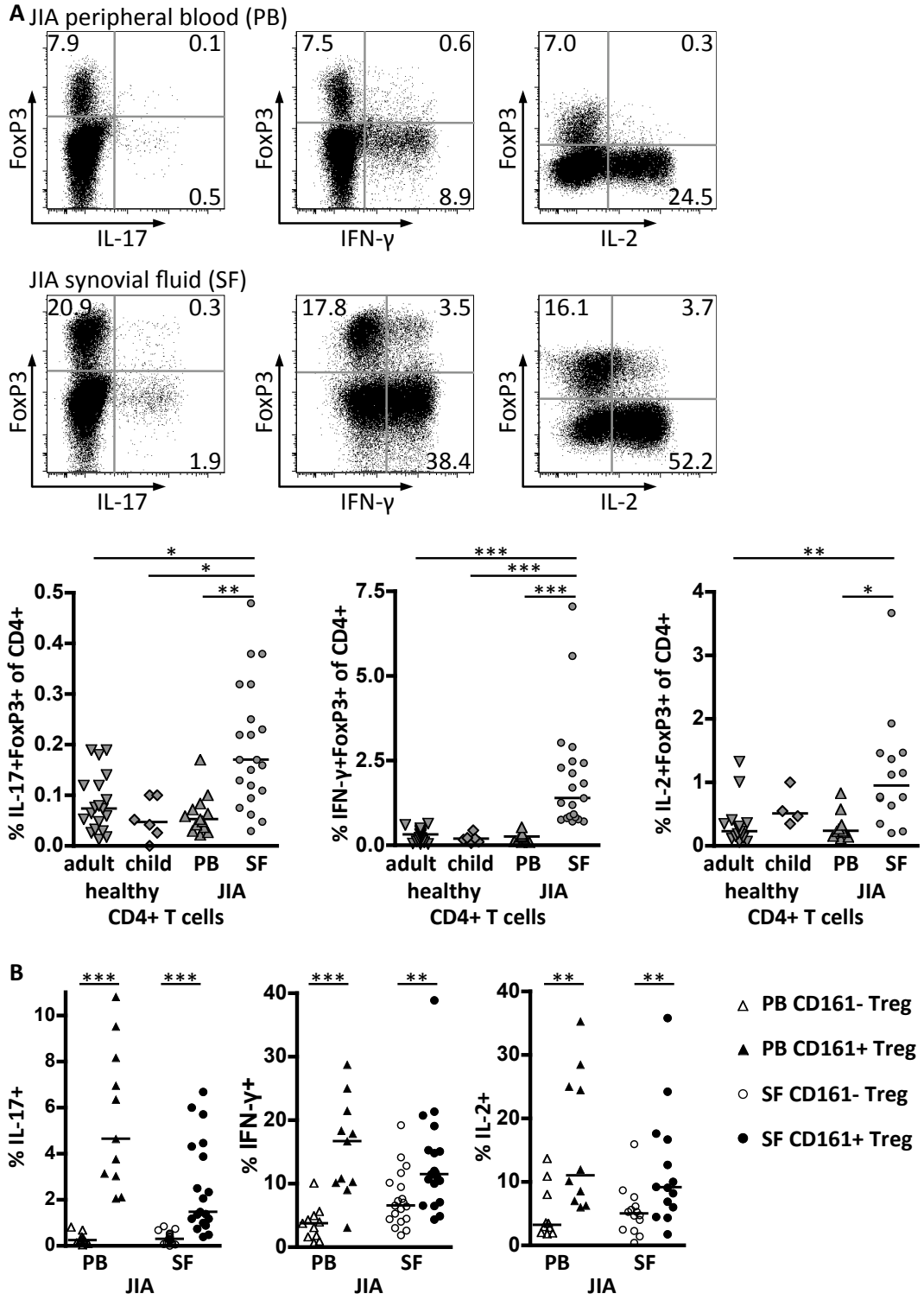

Figure 6.2: SF conventional and regulatory T cells produce high levels of cytokine, in particular the CD161+ Treg population. (A) Representative flow cytometry plots of FoxP3 (y-axis) and cytokine (x-axis: IL-17 left, IFN-γ middle, IL-2 right) expression on CD4+ lymphocytes from JIA peripheral blood (PB, top) and JIA synovial fluid (SF, middle); summary plots (bottom) shows FoxP3+cytokine+ data for healthy adult PB (n=15-19), healthy child PB (n=4-6), JIA PB (n=10-13) and JIA SF (n=14-21) samples; horizontal lines represent median, data tested with Kruskal-Wallis test with Dunn's multiple comparison test. (B) Frequency of cytokine+ cells (IL-17 left, IFN-γ middle, IL-2 right) within CD161- (clear symbols) and CD161+ Treg (filled symbols) in JIA PB (n=10-

11) and SF (n=14-19) by flow cytometry; horizontal lines represent median with non-parametric paired t test between cell subsets. Throughout p values: ***≤0.001; **≤0.01; *≤0.05.

The environment of the inflamed joint might also affect other surface molecules on Treg, or might favour the infiltration of specific subsets. Thus the surface molecules identified as differentially expressed between CD161- and CD161+ Treg in chapter 4 were next analysed in JIA PBMC and SFMC. Interestingly an overall enrichment of CD45RO+, CCR6+ and CD39+ cells was seen in both FoxP3+ and FoxP3- populations (Figure 6.3A). In the joint almost all CD4+ T cells are of a memory phenotype expressing CD45RO. The chemokine receptor CCR6 was expressed in over half of the FoxP3- Tconv, and most of the FoxP3+ cells, indicating that it might be important for the cells to locate to the site. CD39 is a functional surface molecule breaking down pro-inflammatory ATP. Analysis of CD39 expression in these samples showed increased CD39+ FoxP3+ and FoxP3- cells, confirming a previous finding by the group [135]. Interestingly, in addition, the majority of SF Treg express the transcription factor Helios.

Therefore both CD161- and CD161+ Treg from the inflamed joint were enriched for all these surface molecules (CD45RO, CCR6, CD39) compared to PBMC. However, SF CD161+ Treg were still statistically significantly different to SF CD161- Treg in their expression (Figure 6.3B) with increased memory phenotype (CD45RO+), increased CD39 and IL-23R expression and decreased Helios expression. CCR6 expression did not differ between CD161+ and CD161-FoxP3+ cells in the joint.

Taking this data together the phenotype of CD161+ Treg, characterized in chapter 4 on healthy PB, is preserved in the joint CD161+ Treg. Interestingly SF CD161- Treg are also enriched for effector memory markers. Thus the microenvironment of the joint might affect also CD161- Treg to match the phenotype of CD161+ Treg to some extent.

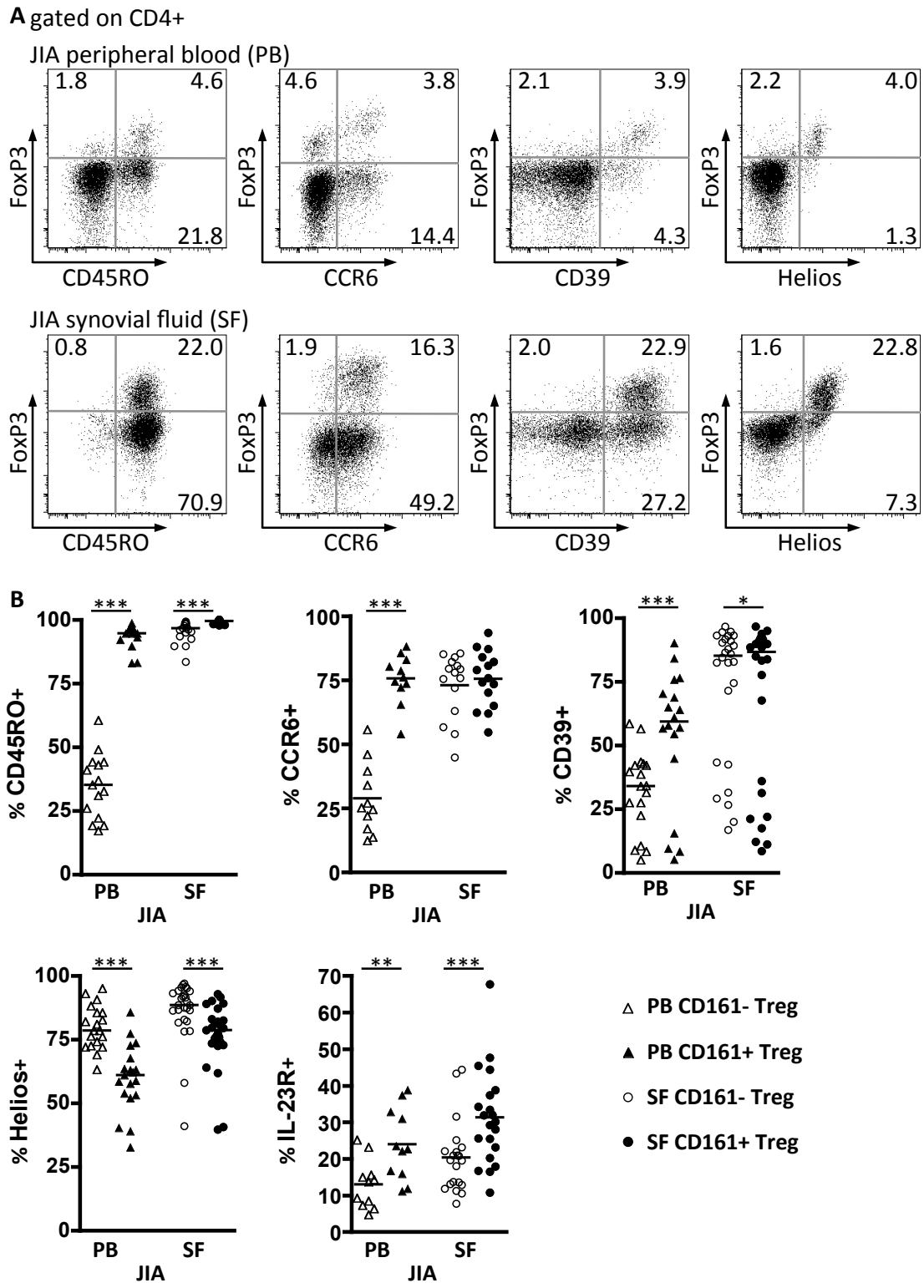

Figure 6.3: SF regulatory T cells are enriched in other effector molecules, predominantly by CD161+ Treg. (A) Representative flow cytometry plots of FoxP3 (y-axis) and effector molecules (x-axis: CD45RO far left, CCR6 left, CD39 right, Helios far right) expression on CD4+ lymphocytes from JIA peripheral blood (PB, top) and JIA synovial fluid (SF, bottom). (B) Frequency of effector molecule+ cells (CD45RO top left, CCR6 top middle, CD39 top right, Helios bottom left and IL-23R bottom middle) within CD161- (clear symbols) and CD161+ Treg (filled symbols) in JIA PB (n=11-19) and SF (n=15-27) by flow cytometry; horizontal lines represent median with non-parametric paired t test between cell subsets, p values: ***≤0.001; **≤0.01; *≤0.05.

6.2.3. The enrichment of CD161+ cells is not equal between different T cell subsets

The data presented thus far demonstrate an enrichment of CD161+ Treg in the joint. To investigate if this might be an overall increase of CD161+ cells other T cell subsets were analysed for their CD161 expression. As expected, JIA SF CD4+ T cells were highly enriched for CD161 expression compared to healthy and JIA PB (Figure 6.4). A trend towards increased CD161 expression on CD8+ T cells could be observed, however did not reach significance. Interestingly, within the CD4-CD8- population the level of CD161 was significantly decreased in the joint compared to healthy adult PB, and showed the same trend with healthy child and JIA PB. The CD4-CD8- T cell population comprises mainly γδ and NKT cells, both previously shown to have a high CD161 expression under normal conditions [275,283,309]. Thus it appears the enrichment for CD161 is mainly within the CD4+ T cell population.

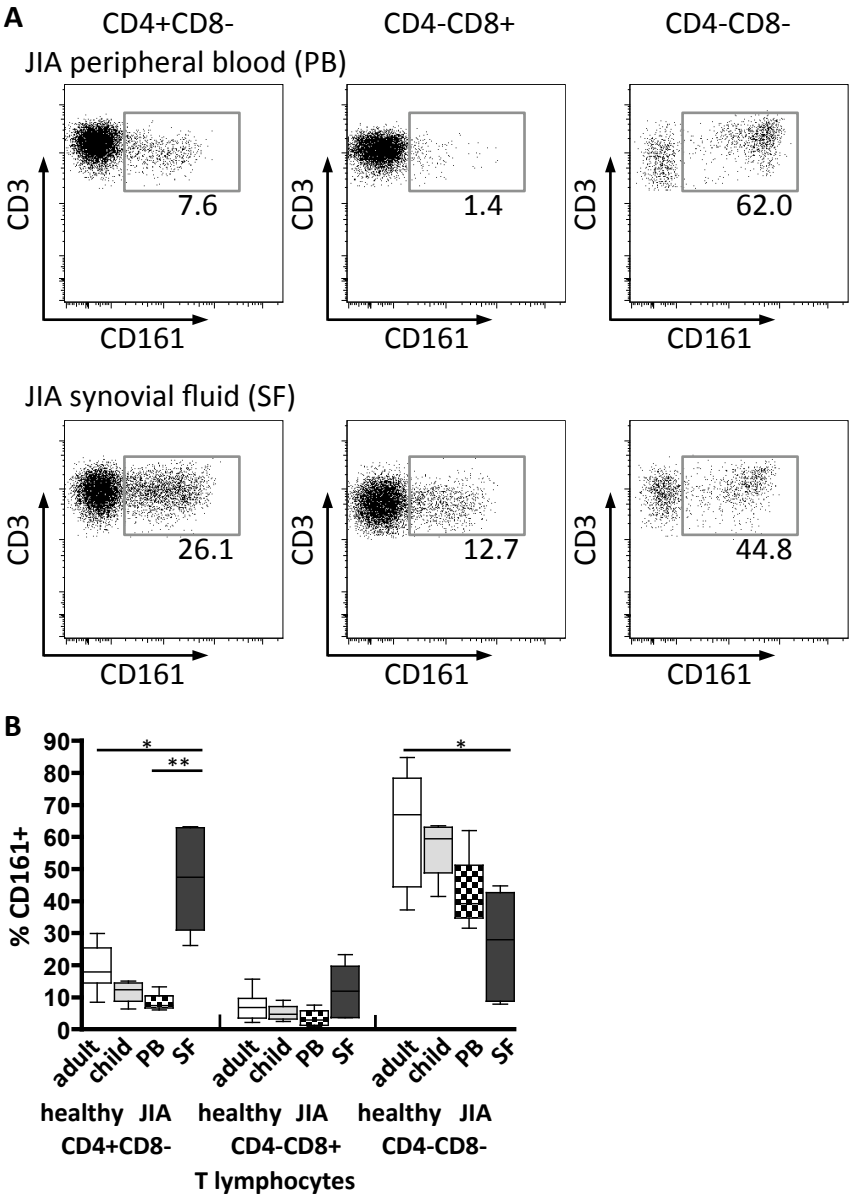

Figure 6.4: CD161 expression is highly enriched on CD4+ T cells in JIA synovial fluid (SF). CD161 expression on T (CD3+) lymphocyte subsets. (A) Representative flow cytometry plots of CD4+CD8- (left), CD4-CD8+ (middle) and CD4-CD8- (right) T cell subsets from peripheral blood (PB, checked n=4) and joint (SF, grey, n=6) of children with JIA with summary plot (B) compared to healthy adult (n=7) and child PB (n=4), horizontal lines represent median with Kruskal-Wallis test with Dunn's multiple comparison test, p values: **$\leq$0.01; *$\leq$0.05.

To further distinguish CD161+ CD4+ T cells, these were divided into CD161+ Tconv (FoxP3-) and CD161+ Treg (FoxP3+). In both healthy and JIA PBMC CD161+FoxP3+ Treg frequency correlated tightly with CD161+FoxP3- Tconv (Figure 6.5A top), suggesting that possibly development or expansion of CD161+ Treg may occur alongside that of CD161+ Tconv. However among cells from the inflamed joint this correlation was lost (Figure 6.5 bottom). Thus the increase of CD161 expressing Treg and Tconv does not appear linked in the joint of JIA. This suggests that CD161+ Treg might play a particular role and are not simply a 'bystander effect' secondary to the increased proportion of inflammatory or memory CD161+ effector Tconv.

Therefore enrichment of CD161+ cells in the joint of JIA is not a general phenomenon, but is selectively found in specific populations of cells. These data suggest that CD161+ are particular enriched and disassociated with CD161+ Tconv in the joint of JIA, and thus might be involved in JIA inflammation.

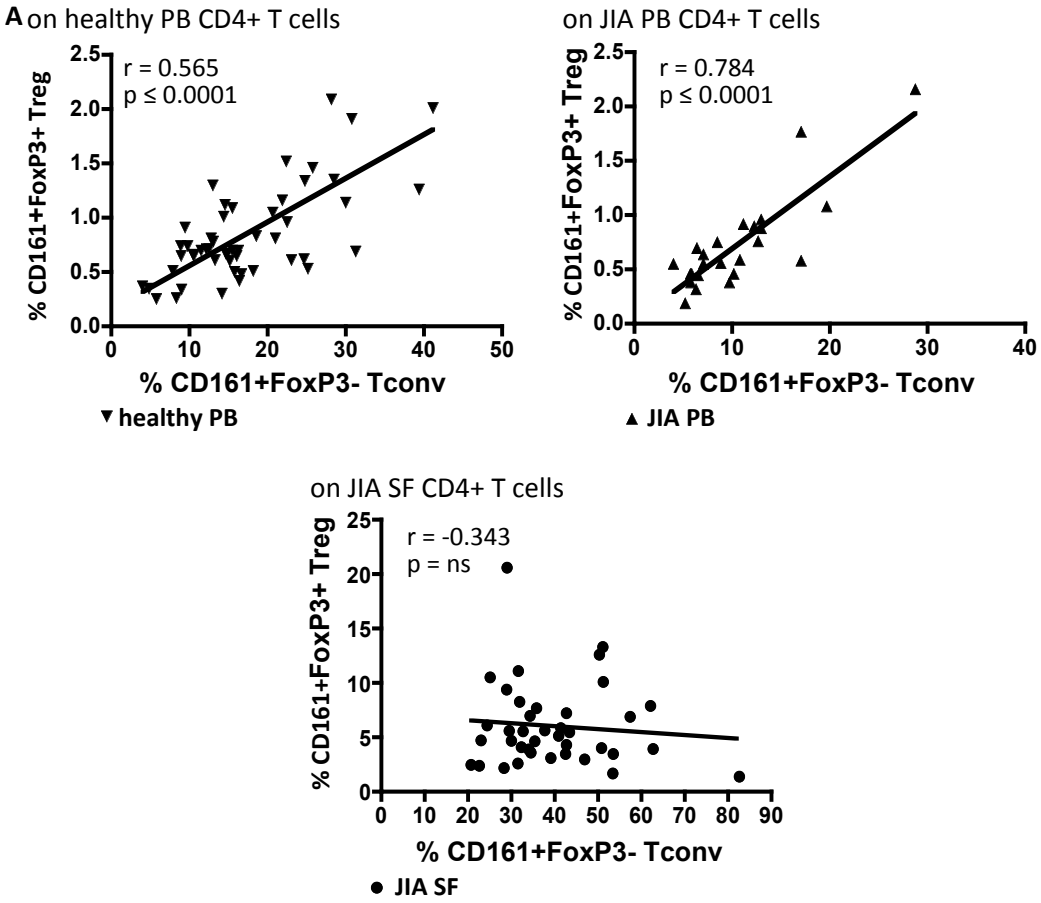

Figure 6.5: CD161+ Treg frequency is not associated with CD161+Tconv frequency in JIA synovial fluid (SF). Healthy PB (top left, filled down-pointing triangles, n=55) and JIA PB (top right, filled up-pointing triangle, n=24) not JIA SF (bottom, filled circles, n=39) CD161+ Treg correlate with CD161+ Tconv in the same sample, correlations by spearman.

6.2.4. Joint CD161+ Treg show distinct association to IL-17 producing T cells and clinical measurements

In a previous study, FoxP3+ Treg were shown to be present in a reciprocal relationship with IL-17A-producing CD4+ T lymphocytes in the inflammatory joint compartment [186]. Analysis of the data in this study for CD161- and CD161+FoxP3+ populations, compared to IL-17-producing CD4+ T cells, demonstrated that that only the CD161-FoxP3+ cells showed this reciprocal relationship ($r= -0.457$, $p=0.015$) but not the CD161+FoxP3+ population ($r= 0.179$, p=ns) (Figure 6.6A).

To assess whether CD161 frequency within the Treg population might be associated with disease severity, I next analysed the active joint count (as a measure of disease activity) on the day of sampling. Frequency of CD161+ in FoxP3+ Treg population correlated positively (although with a relatively weak correlation) with the active joint count (Figure 6.6B right). Consequently (as cells are either CD161+ or CD161-), CD161-cells of Treg correlated negatively with disease severity measured as active joint count on the day of sample (Figure 6.6B left). Correlation with the cumulative joint count (total number of different joints affected throughout one child's course of disease) showed the same trends. Correlation with clinical measures such as the erythrocyte sedimentation rate (ESR) and C-reactive protein (CRP) were non-significant due to clustering of samples within a small range of ESR/CRP.

These associations of CD161+ Treg with disease activity, and IL-17 give another insinuation for their involvement in JIA pathogenesis.

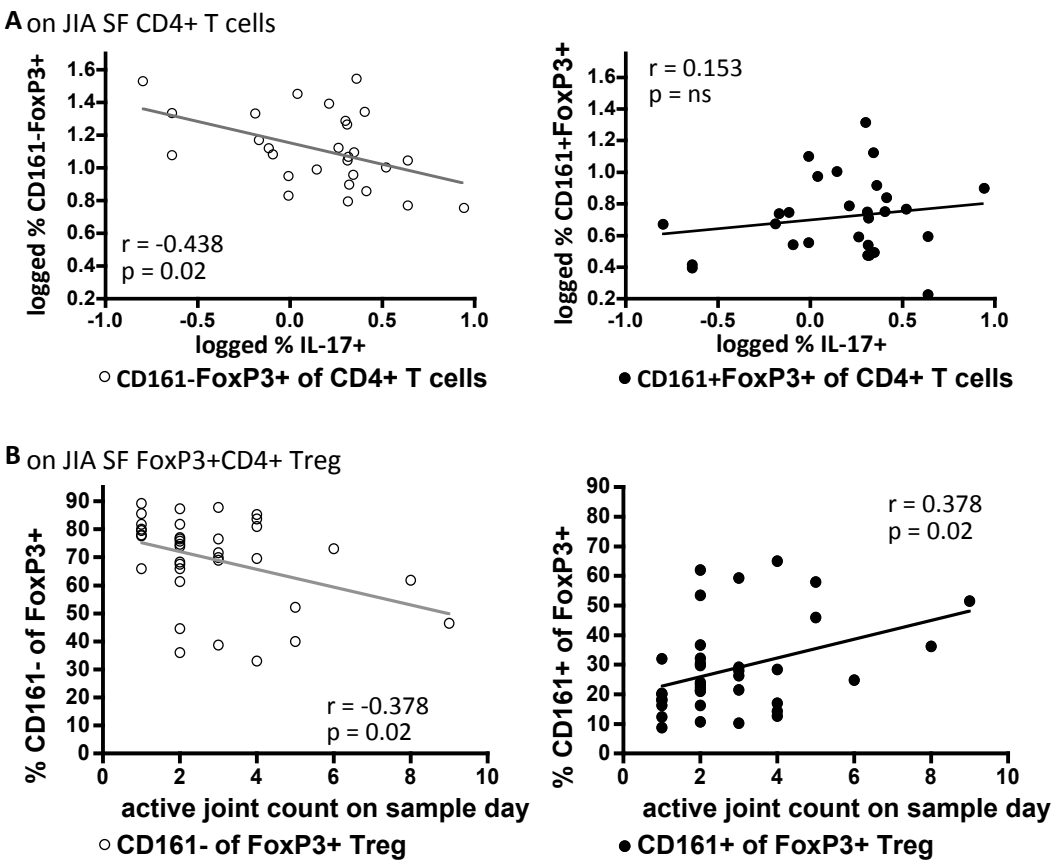

Figure 6.6: CD161+ and CD161- Treg frequencies have different correlations with Th17 frequencies and clinical disease activity. (A) The inverse relationship between Th17 and Treg in SF is specific to the CD161- Treg population. Correlation between SF CD161- Treg (left, clear circles), CD161+ Treg (right, filled circles) with IL-17A+ CD4+ T cells within the same sample (n=28). (B) SF CD161- frequency in the FoxP3+ population (left, clear circles) correlates negatively, and SF CD161+ frequency in the FoxP3+ population (left, filled circles) correlates positively with the number of active joints on the of sampling. All correlations by spearman.

6.2.5. The CD161 ligand LLT1 is expressed on JIA synovium

I hypothesized that the ligand of CD161 lectin like transcript 1 (LLT1) would be present in the synovium of JIA. Literature shows that LLT1 expression can be upregulated in many different cell types upon activation [279]. Initially a flow cytometry approach was tested, but due to technical gating difficulties this was not pursued. Synovial biopsy tissue from two individuals with JIA (O-JIA and P-JIA) was then stained for LLT1 for fluorescent microscopy (2.8) by Hemlata Varsani, a Research Assistant in the laboratory and analysed on the microscope by myself. In both individuals LLT1 staining (red) was found in the cytoplasm/cell surface (nucleus: DAPI, blue), 40x magnification was used. In one sample LLT1 was found with a circular cell formation (Figure 6.7 top), indicating the possibility of LLT1 being expressed in vessels. There have been reports that LLT1-CD161 interaction is critical with migration through vessels by $CD161^{high}$ CD8+ T cells [310]. The second example shows LLT1 staining on the tissue itself (Figure 6.7 bottom, zoomed in: in file). To further characterize where in the tissue LLT1 was expressed, optimization of a different LLT1 antibody for hematoxylin and eosin staining was attempted, but did not yield clear staining.

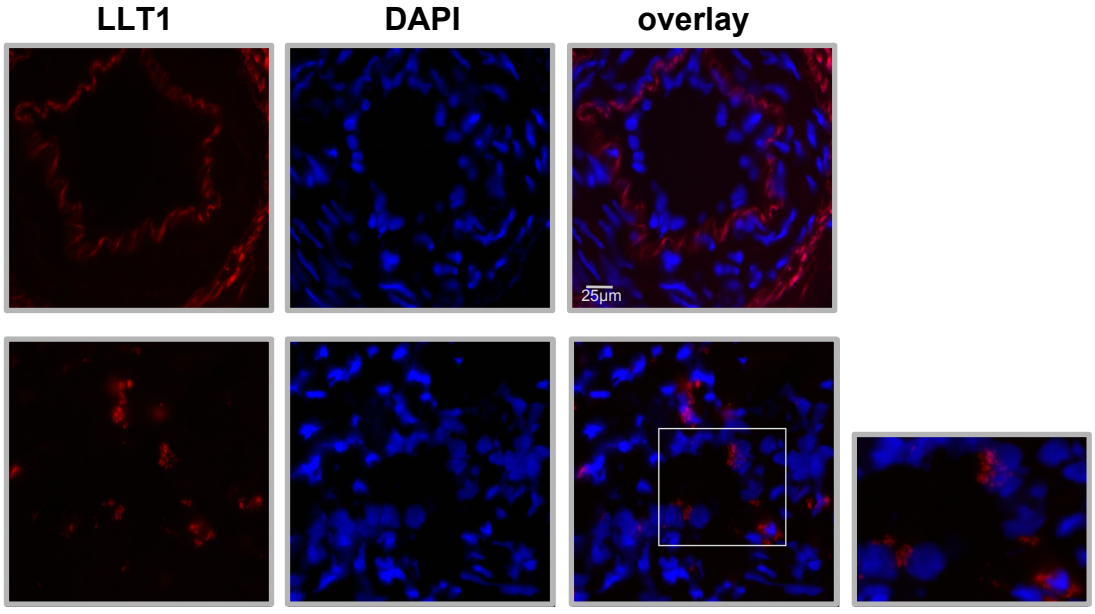

Figure 6.7: CD161 ligand LLT1 is expressed on the synovium of JIA. Representative staining of LLT1 (red, far left) and DAPI (blue, left) with an overlay (right) of two individual synovium biopsies (patient 1 top, patient 2 bottom panel) at 40x magnification, line in top right field marks 25µm. Far right bottom shows a zoomed in image of the square in right bottom picture, zoom done in file.

Consequently expression of CD161 ligand LLT1 in the synovium of JIA could lead to activation of CD161 and its subsequent signaling cascade. Even though the impact of CD161 ligation (especially on Treg) has not yet been clearly demonstrated, the prerequisite for such an interaction is the expression of both CD161 and ligand. Both of these molecules are clearly present in JIA, and CD161 is expressed at high frequency in SF Treg. Thus it would be very interesting to investigate the outcome of LLT1 and CD161 interaction in Treg, which will lead to further understanding of the potential role of CD161+ Treg in JIA joint inflammation.

6.3. Discussion

Previous data suggest that CD161 is enriched on T cells within a multitude of autoimmune conditions [83,93,302,311]. The data presented here now show that CD161+ Treg are enriched at the site of inflammation in childhood autoimmune arthritis. The persistence and over-representation of CD161+ Treg compared to CD161- Treg might be detrimental for the regulation of autoimmune responses, especially in view of their pro-inflammatory capacities.

This work demonstrates that besides high frequency of Tconv producing pro-inflammatory cytokines in the joint, there is a high frequency of FoxP3+ Treg staining positive for IL-17A, IFN-γ or IL-2. As with PB the majority of cytokine production from Treg lies within the CD161+ Treg population. However in addition SF CD161- Treg appear to have a slight higher frequency of IFN-γ producing cells compared to PB. This is the first work describing an enrichment of cytokine-producing Treg in JIA. Data from other studies corroborates a potential role for cytokine-producing Treg in autoimmune disease. IFN-γ+ Treg are enriched in multiples sclerosis patients [156], type 1 diabetes samples have a higher rate of IFN-γ+FoxP3+ cells during Treg expansion [152] and IL-17+FoxP3+ are increased at the site of inflammation in ulcerative colitis and colon carcinoma [155]. This is a new field of research suggesting involvement of a Treg, not just Tconv, subset in disease and will surely be expanded upon in the future.

Previous work has shown that the joint CD4+ T cells in JIA are mainly of a memory phenotype [188] and have high CCR6 [186] and CD39 [135] expression. This work concurs with these results. Additionally it also shows an increase in Helios+ Treg in the SF. CD161+ Treg hold their phenotype in the joint with high CD45RO, CCR6, IL-23R and CD39 and lower Helios expression compared to CD161- Treg. However the difference, except for IL-23R, is less marked than was found in PB Treg, because also SF CD161- Treg are enriched for expression of CD45RO, CCR6 and CD39. Thus similar to IFN-γ production, the phenotype difference between CD161- and CD161+ Treg has been shown to be less marked in the microenvironment of the JIA joint. This might be due to preferred infiltration of cells positive for these markers, especially with respect to

chemokine receptor CCR6 this seems plausible. On the other hand the environment of the joint might activate the Treg and induce upregulation of those surface molecules.

Recruitment of these pro-inflammatory Treg to inflammatory areas may be through CCR6, or for CD161+ Treg via CD161 itself [139,310,312]. However not all T cell subsets have an increased CD161 frequency in the joint. The relationship between CD161 frequency in Treg and Tconv is distorted in the joint, indicating a specific role for CD161+ Treg, not a generalized infiltration of CD161+ cells. Furthermore only CD161- Treg, not CD161+ Treg have a reciprocal relationship with IL-17 and disease severity on a population level within CD4+ T cells and within the FoxP3+ Treg as previously shown for the whole Treg population [186]. The fact that CD161+ Treg produce IL-17 themselves might contribute to the lack of correlation with total IL-17 producing CD4+ T cells. Thus high CD161+ frequency in Treg associates with more severe disease.

Additionally the CD161 ligand lectin like transcript 1 (LLT1) can be induced upon activation of many cell types [279]. And the preliminary study of synovial tissue shows LLT1 expression in the autoimmune inflamed joint. The upregulation of LLT1, possibly in response to inflammation, may equip such cells for activation of CD161 expressing T cells. Further studies in how CD161 ligation and the synovial microenvironment affect CD161+ Treg function, both in terms of regulatory capabilities and pro-inflammatory cytokine production will be necessary to ascertain their impact in JIA pathogenesis.

Taken together the data presented in this chapter suggests a potential role for CD161+ Treg in autoimmunity. Future investigations of JIA and other autoimmune conditions will further our understanding of their role.

Chapter 7

Discussion

7. Discussion

In this thesis, I have presented data that address aspects of immune regulation and how it may impact upon inflammation and the disease process in childhood autoimmune arthritis (JIA). Initially I studied molecules whose expression had been implicated by a gene expression analysis from inflammatory cells direct from the joint (Chapter 3). I showed that many genes involved in immune responses and immune regulation are differentially expressed between different subsets of oligoarticular JIA (O-JIA). The samples used to generate the expression data were from the inflamed site at the time of diagnosis, thus before extension to more severe disease, but for analysis the group was divided according to their one-year outcome [179]. In particular I focused on vasoactive peptide receptor one (VIPR1). The expression of VIPR1 was downregulated, showed a different sized protein and mRNA splicing at the inflamed site, compared to JIA and healthy peripheral blood samples. This was reflected in lower function, reducing IL-2 secretion, upon ligand binding.

Following this I turned my focus to a subset of FoxP3+ regulatory T cells (Treg), which express the surface protein CD161 (Chapter 4). I established that Treg positive for CD161 were enriched with cytokine-producing (IL-17A, IFN-γ and IL-2) cells. In addition CD161+ Treg share features of an effector Tconv phenotype in terms of their expression of chemokine and cytokine receptors, transcription factors and that they express markers of being memory T cells. CD161+ Treg also express the Treg associated ATPase CD39 at high levels, but only about half of this population express the transcription factor Helios. Furthermore CD161 expression on FoxP3+ Treg could be followed throughout development, from mature thymocytes, cord blood, healthy peadiatric and adult samples, increasing in frequency with age through childhood, until plateauing in adulthood.

Subsequently I investigated the function and epigenetic status of Treg expressing CD161 (Chapter 5). I showed that CD161+ Treg fulfill currently accepted criteria for bona-fide Treg. They are anergic to TCR stimuli when cultured alone *in vitro*, suppressive in co-cultures with Tconv and predominantly demethylated at the Treg specific demethylated region (TSDR) of the *FOXP3* locus. Furthermore the frequency

and cytokine-producing phenotype of CD161+ Treg was remarkably stable in *in vitro* culture, even with skewing conditions aimed to skew cells towards a more Th1 or Th17 phenotype. I also investigated specific functions of CD161+ Treg compared to CD161- Treg. Interestingly only CD161+ Treg made a proliferative and cytokine response to specific pathogenic antigens. CD161+ Treg had upon TCR stimulation increased phosphorylation levels of AKT. The specific regulation of CD161 expression and the result of ligating CD161 in Treg were also examined, however no clear conclusions could be drawn yet and further research is necessary.

In the final data section of this thesis, I focused upon Treg in relation to the chronic autoimmune disease of childhood arthritis, JIA (Chapter 6). In this work I found that CD161+ Treg are highly enriched in the synovial fluid of JIA, leading also to an increased frequency of cytokine+FoxP3+ cells among the SF CD4+ T cells. CD161+ Treg from the joint showed a similar phenotype to those in peripheral blood, although overall SF Treg are more activated, memory and Tconv like.

It has been previously shown that although Treg are enriched as a proportion of all CD4+ T cells in the joints of children with JIA, their relative frequency is significantly higher in those children with a very good prognostic outlook, so called persistent O-JIA compared to the more severe extended O-JIA [186,188]. However despite this the paradox remains that a large enrichment of a regulatory subset fails to prevent or resolve inflammation all together. It is therefore of particular interest to investigate the possible pro-inflammatory potential of Treg themselves in the context of JIA.

CD161+ Treg had a much greater fold increase in the joint compared to peripheral blood of the same patients than CD161- Treg. CD161 frequency did correlate with disease severity, measured as affected joints at day of sampling. Interestingly the previously described reciprocal relationship of IL-17A and Treg [186] did not hold true for the CD161+ Treg population, although in the same data set the reciprocal relationship was validated for CD161- Treg vs IL-17 producing CD4+ T cells. This might be due to the fact CD161+ Treg themselves can produce IL-17A.

I will now discuss some specific points raised by this body of work, in more detail in relation to the wider literature and set out some hypotheses to be considered and tested in future investigations.

7.1. Cytokine-producing Treg - what does this mean for our view on Treg?

Within this thesis I have defined cytokine-producing Treg as CD161 positive (Chapter 4). A classical defining feature of regulatory T cells has been thought to be that they do not produce cytokines upon TCR stimulation; evidence suggests that FoxP3 itself mediates suppression of genetic loci involved in cytokine production within Treg cells themselves [106]. In line with this, I have confirmed that only a very low proportion of CD161- Treg produce pro-inflammatory cytokines. This is especially true for IL-17A, which is negligible in CD161- Treg in any of the conditions tested. However this is clearly different in the Treg population expressing CD161.

There have been other reports of pro-inflammatory cytokine-producing Treg in mouse and man [152,153,155-157,159,160,164]. However, to the best of my knowledge, this is the first definite report linking cytokine production to the expression of CD161, following such a population throughout development and showing its functions. Some groups have observed CD161 expression on some Treg [155,159,313], but not characterized this population.

My investigation also showed that CD161+ Treg are suppressive and predominantly demethylated at the TSDR (Chapter 5). Other groups found similar results with the cytokine-producing Treg populations using clones, *ex-vivo* or cultured cells [153,155-157]. In contrast some studies, using Treg expansion to study IFN-γ+ Treg, have reported decreased levels of suppression and demethylation in these cytokine-producing Treg [152].

As mentioned in Chapter 5, analysis of individual DNA strands cloned and sequenced from the CD161+ Treg population showed some clones with a partly methylated TSDR at the *FOXP3* locus. Interestingly Baecher-Allan *et al* observed some IL-17+FoxP3+ Treg

clones with a similar methylation pattern, with specific CpG islands methylated whereas others are demethylated [303]. However it is important to note that in that study these cells had some CD127 expression, whereas sorting approaches used in this thesis always only included $CD127^{lo}$ cells. In knowledge of this data, I hypothesize that partially methylated clones originate from CD161+ Treg producing-cytokine at the time of sorting. This methylation pattern might be very relevant to the ability of those cells to produce cytokines, yet also show suppressive capacity. Whether cytokines can be produced at the very same time as suppressive function is exerted, by the same cell, or alternatively, whether a specific cell switches between one and the other function still needs to be further investigated.

Thus the question begs: Are cytokine-producing Treg 'damaging' for the immune system?

To address this question, I propose that Treg, which produce cytokines, may not be detrimental in all circumstances. Cytokine-producing Treg might be essential for immune homeostasis and specific responses. There has been some evidence that IFN-γ positive Treg are essential in transplant tolerance from two different mouse models. In a model of skin graft tolerance, where an allogeneic graft was introduced under the cover of anti-CD4 antibody, tolerized mice upregulated IFN-γ production by CD25+ Treg not CD25- Tconv upon an allogeneic challenge [164]. Furthermore, if IFN-γ was neutralized at the time of Treg and Tconv transfer into skin graft recipients (Rag-/-) the graft survival was dramatically reduced. Using Treg from IFN-γ knockout mice had the same effect. Koennecke *et al* showed in a graft-versus host disease (GVHD) model that IFN-γ produced by FoxP3+ cells was essential for preventing lethal GVHD [160]. Furthermore this study extended the knowledge about these Treg: they had stable expression of FoxP3, were highly demethylated at the TSDR and produced IFN-γ after antigen specific stimulation or IL-12. These murine cytokine positive Treg therefore share several key properties with the CD161+ Treg that I have characterized.

There is also some observational evidence that production of IFN-γ by Treg might be important in human transplantation. Daniel *et al* observed a higher frequency of IFN-γ+CD25+ Treg in patients with good kidney transplant functions [305]. In patients with

good graft function the frequency of IFN-γ+CD25+ cells correlated highly with the frequency of CD25+FoxP3+ cells, but this was not the case in samples from patients with low graft function. This indicates that in this study a stable frequency of IFN-γ+ cells among all Treg was associated with good graft function.

In addition to transplantation, there has been a link made between cytokine-producing Treg and infection. In a mouse model it was demonstrated that 10-15% of Treg produced IFN-γ after infection with *Listeria monocytogenes* upon PMA/ionomycin re-stimulation, but this was not the case in uninfected animals [160]. Furthermore *in vitro* culture with pathogenic antigens led to cytokine production by Treg. I showed that CD161+ Treg specifically (not CD161- Treg) responded to *C. albicans* and/or *hCMV* with proliferation and IL-17/ IFN-γ production, if the individual had responsive effector Tconv to said pathogens (Chapter 5). Duhen *et al* showed similar results with IL-17 and IFN-γ response to *C. albicans* and *hCMV* by some Treg [145].

Hence, taking these data together, I hypothesize that cytokine-producing Treg are important in enabling the immune system to fight pathogens and maybe set them in control of commensal organisms. That they may also play a role in graft survival is perhaps a bonus revealed by transplantation medicine although this latter phenomenon would not have been involved in the evolutionary selective pressure leading to these cells. It still remains to be investigated whether cytokine-producing Treg have an active role in tolerance to commensal bacteria. Thus far there is some evidence that commensals are important for Treg development [314,315]. Furthermore Treg specific for flagellin, a microbial protein, produce some cytokines [153]. These data encourage me to think that the relationship between commensals and cytokine-producing Treg might be bilateral. It would be very interesting to investigate the cytokine producing properties of FoxP3+ T cells in the gut immune system, where interactions with a large number of bacteria (commensal or pathogenic) are known to have a major impact on T cell biology.

But cytokine-producing Treg might be harmful in autoimmune conditions.

Autoimmune diseases show increased levels of cytokine-producing Treg. I have shown an enrichment of IL-17A+ and IFN-γ+ Treg, and of CD161+ Treg in childhood autoimmune arthritis (Chapter 6). IFN-γ producing Treg are enriched *ex-vivo* and in culture in multiple sclerosis [156] and upon Treg expansion from type I diabetes samples [152]. Furthermore IL-17+ Treg are increased in ulcerative colitis and inflammatory colon cancer (not other malignancies tested) [155].

Whether these cytokine-producing Treg are harmful or beneficial in these settings is not yet clear. In an animal model of colitis (induced by microbiota-specific effector Tconv) showed prevention of colitis by cytokine-producing Treg [153]. However it could also be that cytokine-producing Treg contribute to the possibly "vicious circle" of autoimmune diseases (see 7.3), by contributing to the inflammatory environment and potentially not recognizing the response to self as exacerbated.

Therefore cytokine positive Treg may not necessarily be detrimental: their effects might depend on the specific microenvironment or tissue. I propose that upon an acute insult, cytokine-producing Treg (CD161+FoxP3+ cells) may have a role in dictating the balance between tolerance and immunity, with the ability to produce pro-inflammatory cytokines, and also to suppress an overly active immune response. The link that I have established here between expression of CD161 and cytokines (especially IL-17A) in Treg, allows further research in different settings of health and disease like autoimmunity, different sites of inflammation, but also infection. Furthermore chronic vs acute states and clearing/remission vs ongoing/severity of disease can be assessed using the surface marker CD161.

7.2. Is CD161 essential for the full phenotype of CD161+ Treg?

My data suggest that CD161+ Treg population contains specific pathogen-reactive cells, while the CD161- Treg population did not (Chapter 5). Furthermore there appears to be a strong correlation of CD161+ Treg with CD161+ Tconv in blood, although this correlation was not observed at the autoimmune inflamed site (Chapter 6). This indicates that CD161+ Treg might develop alongside effector Tconv when acquiring immunity. The increasing frequency of these cells with age, throughout childhood, which then plateaus in adulthood, is further evidence for a link with immunological experience and memory. However CD161+ Treg are not simply 'induced' Treg, since I have also demonstrated that they are present in developing Treg in thymus and immunological inexperienced cord blood, albeit at low frequencies (Chapter 4).

CD161 can be further linked to different disease settings. I have shown that CD161 expression on Treg is increased at the site of inflammation of JIA (Chapter 6). Others have demonstrated that total CD161+ CD4+ T cells were associated with high ESR and CRP in JIA [83]. These correlations between CD161+ T cells and ESR and CRP were not apparent in my data set, which might be due to skewed ERS and CRP values in this data set. Analysis of synovial fluid and synovial membranes has revealed elevated levels of CD161 in rheumatoid and osteoarthritis [316]. While others had seen decreased CD161+CD8+ cells within PBMC from RA patients [317], the site of inflammation was not tested in that study. In psoriatic arthritis $CD161^{high}$CD8+ T cells preferentially home to the affected joint [310]. Furthermore IL-17 producing CD161+ Tconv [311] and CD161+ Tconv overall were increased in Crohn's disease and were decreased after anti-TNF-α treatment [318]. Likewise multiples sclerosis patients have increased gene expression of KLRB1 (CD161 gene) in whole blood, which was reduced after IFN-β treatment [319]. This study also observed a genetic association between a SNP in KLRB1 and multiple sclerosis, even though the p-value was relatively high. Multiples sclerosis patients showed elevated frequency of $CD161^{high}$CD8+ cells in blood and interestingly the site of inflammation, the brain (using post-mortem histology) [302].

Moreover in allergic rhinitis increased levels of CD161+ T cells (CD4+ and CD8+) were seen, additionally the frequency correlated positively with disease severity [320]. In addition CD161+ CD4+ T cells were more highly activated in active allergic asthma patients [321]. These data also suggest that CD161+ cells accumulate at the site of inflammation.

Interestingly in chronic infection, like HIV and AIDS both the frequency and the level per cell of CD161 is decreased in T cells [307,322] and NK cells, which correlated with increased viral load [306]. Another study showed preferred infection of CD161+ CD4+ T cells, with infection leading to decreased frequency of CD161+, Th17 cells and Treg (CD161 expression on Treg was however not measured) [323]. Furthermore in a humanized mouse model HIV infection led to depletion of double positive thymocytes and heavily reduced CD161+CD4+ cells leading on the other hand to increased frequency of CD161+CD4- thymocytes [324]. However no data on cell recovery or total numbers was given. Recently a population of CD8+ $CD161^{high}$ cells has been characterized, known as mucosal associated invariant T (MAIT) cells [325]. MAIT cells are lost in HIV infection and it is thought that their loss may correlate with susceptibility to opportunistic infections in HIV patients [326]. Interestingly, in Hepatitis C infected individuals more virus-specific CD161+ cells were found compared to other viral infections [327]. Additionally $CD161^{high}$CD8+ cells were tracked especially to the liver in Hepatitis C infections [310].

Thus there is some evidence linking CD161 with different disease settings. Furthermore CD161+ cells present in some diseases show specific activation and function. For example phosphorylation levels of STAT1 and STAT6 in CD161+ CD4+ T cells were dysregulated between allergic asthma, non-allergic asthma and healthy controlled samples [328]. In addition CD161+ cells have been linked with high cytokine production *in vitro* and *in vivo* [311,329]. CD161+ CD4+ Tconv also displayed high plasticity regarding their cytokine profile. CD161+ Th17 cells could switch to Th1-like cells *in vitro* upon culture in IL-12 and this effect was only partly prevented by addition of TGF-β and this phenomenon was also demonstrated in the inflamed joint of JIA [82,83]. In another study CD161+ Th17 cells from healthy individuals could also be

switched to IL-4 and IL-17 double producing cells under polarizing conditions [84]. These IL-4+IL-17+ cells were more abundant in samples from asthmatic patients.

The series of studies above give circumstantial evidence for an apparent link between the expression of CD161 and cytokine expression. However there is some support for a direct functional link through studies crosslinking CD161.

It has been observed that ligating CD161 increases IFN-γ production, when accompanied by a TCR stimulus in T cells, or Fc-R stimulus in NK cells [280-282,302]. However there are some differences between these studies, with Rosen *et al* not seeing IFN-γ increase in T cells, but only in NK cells [281]. Furthermore iNKT cells reacted with increased proliferation, IFN-γ and IL-4 when stimulated through TCR and CD161, but if iNKT cells were activated through CD1d and CD161 was ligated, inhibition in the above was observed [275]. However different anti-CD161 antibody clones were used in the different experiments.

Furthermore CD161 activity has been linked to acid sphingomyelinase activity in both NK cells and T cell clones [280]. This study observed that activation and CD161 ligation induced increased acid sphingomyelinase activity. Furthermore CD161 and acid sphingomyelinase co-precipitated in the membrane raft portion of cell lysates and an increase in pAKT, upstream phosphatidylinositide 3-kinases (PI3K) activity and extracellular-signal-regulated kinases (ERK) pathway were abolished by acid sphingomyelinase inhibitors.

Within my own studies, I showed a link between CD161 expression on Treg and increased pAKT response upon TCR stimulation (Chapter 5). This association is interesting considering the direct evidence from Pozo *et al*, which showed increased pAKT after CD161 ligation in T cell clones. It may be possible that acid sphingomyelinase and other kinases can be working with CD161 in partnership. Additionally I showed an increase of IFN-γ+ and TNF-α+ cells among Tconv after ligating CD161 in combination with a TCR stimulus. The data on Treg were less conclusive, probably due to the low frequency of CD161 (and of cytokine-producing

Treg) in healthy *ex-vivo* Treg (Chapter 5). It will be interesting to do further work on the effects of CD161 ligation on Treg in more roust *in vitro* assays. One possibility would be to generate CD161+ and CD161- Treg clones and repeat experiments to investigate the downstream effects of CD161 ligation and signaling. Another option would be to investigate CD161 function in animal models. However due to the lack of a mouse homologue to CD161 [286], humanized animal models would need to be explored, which in turn have separate limitations.

Furthermore I have demonstrated expression of CD161 ligand LLT1 on the synovium of JIA affected joints (Chapter 6). It is also know that upon activation of most cells LLT1 is upregulated [279].

For these reasons it remains possible and plausible that CD161 could be directly involved in cytokine production by Treg. Further work is required to investigate this, but the literature suggests strong ties between CD161, TCR signaling and cytokine production. Moreover the presence of LLT1 at the inflamed site is a prerequisite for an effect of CD161 within the joint, where there is an abundance of CD161+ Treg and overall cells are highly activated within the joint environment.

7.3. The environment of the arthritic joint as a factor for disease severity and progression - Is autoimmune inflammation a 'vicious circle'?

The synovial fluid (SF) of the arthritic joint in JIA has an enrichment of many pro-inflammatory cytokine (IL-17A, IFN-γ and IL-2) positive cells in both FoxP3+ and FoxP3- populations. Furthermore as I defined a link between CD161 expression and pro-inflammatory cytokine production, CD161 expression on CD4+ T cells and especially FoxP3+ Treg is highly enriched in the arthritic joint. More severe JIA cases (according to active joint count on day of sample) also have an increased frequency of CD161+ cells within the FoxP3+ population (Chapter 6). Thus there appears a clear enrichment of Treg with a pro-inflammatory potential in the joint of JIA. I also demonstrated that synovial fluid (SF) itself could favour CD161+ (FoxP3+ and FoxP3-) cells in *in vitro* culture systems. However in those pilot experiments, none of the cytokines tested by myself (IL-2, IL-6, IL-12, TGF-β or TNF-α) have proven the driving force for CD161 enrichment in culture. Moreover no cytokine, or stimulation was able to switch CD161- cells (Treg or Tconv) to CD161+ cells (Chapter5). This gives some evidence to the hypothesis that the inflammatory environment of the SF is a driving factor in favouring Treg with pro-inflammatory potential. I hypothesize now that the environment of the joint is a driving force in achieving and maintaining this state, and inflammation in the joint might be described as a 'vicious circle'.

Further support for this can be drawn from the literature. IL-12 (which is also increased in the SF of JIA [82]) can drive or enhance IFN-γ production by Treg [152,153,156]. In my studies also, there was a trend towards increased IFN-γ in CD161+ Treg with the addition of IL-12 (Chapter 5). Furthermore samples from multiples sclerosis and type one diabetes patients had significantly higher levels of IFN-γ+ Treg upon culture [152,156]. Similarly IL-17+ Treg are increased using different culture conditions. Antigen presenting cells or the presence of IL-2 and TGF-β [155], IL-1β and IL-6 [157] and IL-2 plus IL-1β, IL-6, IL-21 or IL-23 in various combinations [158] have been shown to enhance IL-17 in FoxP3+ cells or Treg clones in culture. In addition IL-17+ Treg are enriched at inflamed sites in the colon [155].

The joint of JIA is enriched for many pro-inflammatory cytokines like IL-12, IL-6 and TNF-α, whereas it is relatively low in TGF-β compared to matched serum from JIA patients or controls [82,206]. That these inflammatory cytokines influence the cytokine plasticity of effector Tconv has been shown previously. CD161+ IL-17 producing T cells convert through a double positive state of IFN-γ+ and IL-17+ to purely IFN-γ+ T cells. IL-12 could drive this *in vitro* and cells remained CD161+, even though they switched their profile from Th17 to Th1 cells. There was clear evidence that the same process might be occurring in the joint of JIA [82,83]. Furthermore there is now evidence that the cytokines IL-6 and TNF-α can make Tconv unresponsive, or resistant, to Treg suppression *in vitro*, and that Tconv from the highly inflamed joint are also resistant to Treg in *in vitro* systems [204,205].

Hence there is evidence to suggest the environment of the inflamed joint might be driving a 'vicious circle' of pro-inflammatory cytokines and other factors favouring CD161+ Treg with inflammatory potential, switching effector Tconv cytokine production, thus contributing to further the pro-inflammatory environment. In addition this environment then makes Tconv unresponsive to Treg suppression encouraging the 'vicious circle' of autoimmune arthritis to continue.

Moreover, additional processes are changed in the joint driven by the inflammatory environment. One such process affecting many proteins is altered splicing of mRNA. I have demonstrated that VIPR1 appears to be present at a different protein size and with a different mRNA sequence at the inflamed site (Chapter 3). Even though more work needs to be done to clearly identify the splice variant, its specific functional ability and to clarify if the variant (compared to the reference mRNA) is expressed at higher levels in more severe cases. In addition it needs to be considered that there is already less VIPR1 mRNA expression in SFMC compared to PBMC. Alterations in splicing have been observed in other studies of inflammation. For example IL-6 [330], T cell activation and TNF-α [331] shift expression ratios of functionally different isoforms of various proteins, often leading to a non-functional isoform being expressed under those conditions. These shifts can also be seen at the inflamed site, in this case the inflamed sarcoid lung, which is high in TNF-α [331]. IL-1β and IFN-γ as well as IFN-γ plus

TNF-α have shown to change splicing of many genes associated to type 1 diabetes. Ortis *et al* treated rat pancreatic islet β-cells with IL-1β and IFN-γ or IFN-γ and TNF-α and used RNA arrays to look at changes in expression and splicing of genes [332]. Besides changes in expression level of many functionally genes, about 50% genes were also expressed as splicing isoforms, NF-κB2 is one example. Similarly Eizirik *et al* treated langerhans cells from type 1 diabetes patients with IL-1β and IFN-γ. In this study 35% of diabetes associated genes showed altered in splicing in the presence of IL-1β and IFN-γ [333]. In another study, splice variants of deformed epidermal autoregulatory factor 1 (DEAF1) were found in peripheral lymph nodes of diabetic NOD mice and type 1 diabetes patients [334]. DEAF1 itself regulates expression of peripheral antigens in the peripheral lymph nodes to maintain tolerance against self. The DEAF1 variant however did inhibit the expression of peripheral antigens. Thus this alternate splicing might be an important mechanism in breaking tolerance towards β-cells in type 1 diabetes.

Thus these data give further evidence for a 'vicious circle' in autoimmune inflammation, as the inflammatory environment drives alternate splicing, which in turn results in proteins with altered, or opposite functions. In case of VIPR1, which imparts regulatory signals within a cell, this altered splicing might lead to abrogation of the dampening signals (e. g. inhibit pro-inflammatory cytokines), thus further enhancing the pro-inflammatory environment.

The notion of a 'window of opportunity' for treatment is emerging in the treatment of JIA. Some evidence shows that earlier aggressive treatment yields better outcome [335-339]; however aggressive treatment should only be administered to patients requiring it, since side effects can be detrimental in the long term [340,341] and the costs of for example biologics is relatively high. Moreover clinical trials and smaller drug response studies show that only some patients respond to specific treatments [341-343]. Therefore it would be highly advantageous if it were possible to predict which patients are likely to develop more severe disease and thus might benefit from early aggressive treatment. Prediction of response to treatment is another goal of current research. Both these potential sets of predictive measurements will help to

break the ‘vicious circle’ of autoimmune disease early and may provide the right mechanism for each patient.

8. References

1. Beutler B (2004) Innate immunity: an overview. Mol Immunol 40: 845-859.
2. Janeway CA, Jr., Medzhitov R (2002) Innate immune recognition. Annu Rev Immunol 20: 197-216.
3. Medzhitov R, Janeway CA, Jr. (2002) Decoding the patterns of self and nonself by the innate immune system. Science 296: 298-300.
4. Danilova N (2012) The evolution of adaptive immunity. Self and Nonself. 2012/03/09 ed: Landes Bioscience and Springer Science+Business Media, LLC. pp. 218-235.
5. Spits H, Cupedo T (2012) Innate lymphoid cells: emerging insights in development, lineage relationships, and function. Annu Rev Immunol 30: 647-675.
6. Magnani CF, Alberigo G, Bacchetta R, Serafini G, Andreani M*, et al.* (2011) Killing of myeloid APCs via HLA class I, CD2 and CD226 defines a novel mechanism of suppression by human Tr1 cells. Eur J Immunol 41: 1652-1662.
7. Meyers JH, Ryu A, Monney L, Nguyen K, Greenfield EA*, et al.* (2002) Cutting edge: CD94/NKG2 is expressed on Th1 but not Th2 cells and costimulates Th1 effector functions. J Immunol 169: 5382-5386.
8. Strid J, Sobolev O, Zafirova B, Polic B, Hayday A (2011) The intraepithelial T cell response to NKG2D-ligands links lymphoid stress surveillance to atopy. Science 334: 1293-1297.
9. Maggi L, Santarlasci V, Capone M, Peired A, Frosali F*, et al.* (2010) CD161 is a marker of all human IL-17-producing T-cell subsets and is induced by RORC. Eur J Immunol 40: 2174-2181.
10. Pesenacker AM, Bending D, Ursu S, Wu Q, Nistala K*, et al.* (2013) CD161 defines the subset of FoxP3+ T cells capable of producing pro-inflammatory cytokines. Blood 121: 2647-2658.
11. Fujinami RS, Oldstone MB (1985) Amino acid homology between the encephalitogenic site of myelin basic protein and virus: mechanism for autoimmunity. Science 230: 1043-1045.
12. Wucherpfennig KW (2001) Structural basis of molecular mimicry. J Autoimmun 16: 293-302.
13. Atassi MZ, Casali P (2008) Molecular mechanisms of autoimmunity. Autoimmunity 41: 123-132.
14. Doyle HA, Mamula MJ (2012) Autoantigenesis: the evolution of protein modifications in autoimmune disease. Curr Opin Immunol 24: 112-118.
15. Wucherpfennig KW (2001) Mechanisms for the induction of autoimmunity by infectious agents. J Clin Invest 108: 1097-1104.
16. Sprent J, Kishimoto H (2002) The thymus and negative selection. Immunol Rev 185: 126-135.
17. Kappler JW, Roehm N, Marrack P (1987) T cell tolerance by clonal elimination in the thymus. Cell 49: 273-280.
18. Gershon RK, Cohen P, Hencin R, Liebhaber SA (1972) Suppressor T cells. J Immunol 108: 586-590.
19. Herzenberg LA, Chan EL, Ravitch MM, Riblet RJ (1973) Active suppression of immunoglobulin allotype synthesis. 3. Identification of T cells as responsible for suppression by cells from spleen, thymus, lymph node, and bone marrow. J Exp Med 137: 1311-1324.

20. Anderson CF, Mosser DM (2002) A novel phenotype for an activated macrophage: the type 2 activated macrophage. J Leukoc Biol 72: 101-106.
21. Goerdt S, Orfanos CE (1999) Other functions, other genes: alternative activation of antigen-presenting cells. Immunity 10: 137-142.
22. Steinbrink K, WѴðlfl M, Jonuleit H, Knop J, Enk AH (1997) Induction of tolerance by IL-10-treated dendritic cells. The Journal of Immunology 159: 4772-4780.
23. Voisine Cc, Hubert F-X, TrinitѴ© B, Heslan Ml, Josien Rg (2002) Two Phenotypically Distinct Subsets of Spleen Dendritic Cells in Rats Exhibit Different Cytokine Production and T Cell Stimulatory Activity. The Journal of Immunology 169: 2284-2291.
24. Min W-P, Zhou D, Ichim TE, Strejan GH, Xia X*, et al.* (2003) Inhibitory Feedback Loop Between Tolerogenic Dendritic Cells and Regulatory T Cells in Transplant Tolerance. The Journal of Immunology 170: 1304-1312.
25. Mauri C, Bosma A (2012) Immune regulatory function of B cells. Annu Rev Immunol 30: 221-241.
26. Battaglia M, Gregori S, Bacchetta R, Roncarolo M-G. Tr1 cells: from discovery to their clinical application; 2006. Elsevier. pp. 120-127.
27. Hayden MS, Ghosh S (2008) Shared principles in NF-kappaB signaling. Cell 132: 344-362.
28. Moynagh PN (2005) The NF-kappaB pathway. J Cell Sci 118: 4589-4592.
29. Pasparakis M (2009) Regulation of tissue homeostasis by NF-kappaB signalling: implications for inflammatory diseases. Nat Rev Immunol 9: 778-788.
30. Wan F, Lenardo MJ (2010) The nuclear signaling of NF-kappaB: current knowledge, new insights, and future perspectives. Cell Res 20: 24-33.
31. Itoh S, Itoh F, Goumans MJ, Ten Dijke P (2000) Signaling of transforming growth factor-beta family members through Smad proteins. Eur J Biochem 267: 6954-6967.
32. Nagarajan RP, Chen F, Li W, Vig E, Harrington MA*, et al.* (2000) Repression of transforming-growth-factor-beta-mediated transcription by nuclear factor kappaB. Biochem J 348 Pt 3: 591-596.
33. Schiffer M, von Gersdorff G, Bitzer M, Susztak K, Bottinger EP (2000) Smad proteins and transforming growth factor-beta signaling. Kidney Int Suppl 77: S45-52.
34. Jana S, Jailwala P, Haribhai D, Waukau J, Glisic S*, et al.* (2009) The role of NF-kappaB and Smad3 in TGF-beta-mediated Foxp3 expression. Eur J Immunol 39: 2571-2583.
35. Ouyang W, Beckett O, Ma Q, Li MO (2010) Transforming growth factor-beta signaling curbs thymic negative selection promoting regulatory T cell development. Immunity 32: 642-653.
36. Xu L, Kitani A, Stuelten C, McGrady G, Fuss I*, et al.* (2010) Positive and negative transcriptional regulation of the Foxp3 gene is mediated by access and binding of the Smad3 protein to enhancer I. Immunity 33: 313-325.
37. Ishinaga H, Jono H, Lim JH, Kweon SM, Xu H*, et al.* (2007) TGF-beta induces p65 acetylation to enhance bacteria-induced NF-kappaB activation. Embo J 26: 1150-1162.
38. Lopez-Rovira T, Chalaux E, Rosa JL, Bartrons R, Ventura F (2000) Interaction and functional cooperation of NF-kappa B with Smads. Transcriptional regulation of the junB promoter. J Biol Chem 275: 28937-28946.

39. Ogawa K, Funaba M, Tsujimoto M (2008) Suppression of NF-kappaB and IRF-1-induced transcription of the murine IL-12 p40 by transforming growth factor-beta Smad pathway in macrophages. Mol Cell Biochem 308: 9-15.
40. Haller D, Holt L, Kim SC, Schwabe RF, Sartor RB*, et al.* (2003) Transforming growth factor-beta 1 inhibits non-pathogenic Gram negative bacteria-induced NF-kappa B recruitment to the interleukin-6 gene promoter in intestinal epithelial cells through modulation of histone acetylation. J Biol Chem 278: 23851-23860.
41. Le Y, Iribarren P, Gong W, Cui Y, Zhang X*, et al.* (2004) TGF-beta1 disrupts endotoxin signaling in microglial cells through Smad3 and MAPK pathways. J Immunol 173: 962-968.
42. Delgado M, Ganea D (2001) Cutting edge: is vasoactive intestinal peptide a type 2 cytokine? J Immunol 166: 2907-2912.
43. Delgado M, Martinez C, Leceta J, Garrido E, Gomariz RP (1996) Differential VIP and VIP1 receptor gene expression in rat thymocyte subsets. Peptides 17: 803-807.
44. Goetzl EJ, Sreedharan SP, Turck CW (1988) Structurally distinctive vasoactive intestinal peptides from rat basophilic leukemia cells. J Biol Chem 263: 9083-9086.
45. Martinez C, Delgado M, Abad C, Gomariz RP, Ganea D*, et al.* (1999) Regulation of VIP production and secretion by murine lymphocytes. J Neuroimmunol 93: 126-138.
46. Laburthe M, Couvineau A (2002) Molecular pharmacology and structure of VPAC Receptors for VIP and PACAP. Regul Pept 108: 165-173.
47. Johnson MC, McCormack RJ, Delgado M, Martinez C, Ganea D (1996) Murine T-lymphocytes express vasoactive intestinal peptide receptor 1 (VIP-R1) mRNA. J Neuroimmunol 68: 109-119.
48. Delgado M, Ganea D (2003) Vasoactive intestinal peptide inhibits IL-8 production in human monocytes by downregulating nuclear factor kappaB-dependent transcriptional activity. Biochem Biophys Res Commun 302: 275-283.
49. Ding W, Wagner JA, Granstein RD (2007) CGRP, PACAP, and VIP modulate Langerhans cell function by inhibiting NF-kappaB activation. J Invest Dermatol 127: 2357-2367.
50. Delgado M, Ganea D (2001) Vasoactive intestinal peptide and pituitary adenylate cyclase-activating polypeptide inhibit nuclear factor-kappa B-dependent gene activation at multiple levels in the human monocytic cell line THP-1. J Biol Chem 276: 369-380.
51. Ganea D, Delgado M (2001) Neuropeptides as modulators of macrophage functions. Regulation of cytokine production and antigen presentation by VIP and PACAP. Arch Immunol Ther Exp (Warsz) 49: 101-110.
52. Chorny A, Gonzalez-Rey E, Varela N, Robledo G, Delgado M (2006) Signaling mechanisms of vasoactive intestinal peptide in inflammatory conditions. Regul Pept 137: 67-74.
53. Gonzalez-Rey E, Chorny A, Delgado M (2007) Regulation of immune tolerance by anti-inflammatory neuropeptides. Nat Rev Immunol 7: 52-63.
54. Liu L, Yen JH, Ganea D (2007) A novel VIP signaling pathway in T cells cAMP-->protein tyrosine phosphatase (SHP-2?)-->JAK2/STAT4-->Th1 differentiation. Peptides 28: 1814-1824.

55. Jimeno R, Gomariz RP, Gutierrez-Canas I, Martinez C, Juarranz Y*, et al.* (2010) New insights into the role of VIP on the ratio of T-cell subsets during the development of autoimmune diabetes. Immunol Cell Biol 88: 734-745.
56. Yadav M, Rosenbaum J, Goetzl EJ (2008) Cutting edge: vasoactive intestinal peptide (VIP) induces differentiation of Th17 cells with a distinctive cytokine profile. J Immunol 180: 2772-2776.
57. Gonzalez-Rey E, Fernandez-Martin A, Chorny A, Delgado M (2006) Vasoactive intestinal peptide induces CD4+,CD25+ T regulatory cells with therapeutic effect in collagen-induced arthritis. Arthritis Rheum 54: 864-876.
58. Pozo D, Anderson P, Gonzalez-Rey E (2009) Induction of alloantigen-specific human T regulatory cells by vasoactive intestinal peptide. J Immunol 183: 4346-4359.
59. Delgado M, Toscano MG, Benabdellah K, Cobo M, O'Valle F*, et al.* (2008) In vivo delivery of lentiviral vectors expressing vasoactive intestinal peptide complementary DNA as gene therapy for collagen-induced arthritis. Arthritis Rheum 58: 1026-1037.
60. Delgado M, Chorny A, Gonzalez-Rey E, Ganea D (2005) Vasoactive intestinal peptide generates CD4+CD25+ regulatory T cells in vivo. J Leukoc Biol 78: 1327-1338.
61. Delgado M, Robledo G, Rueda B, Varela N, O'Valle F*, et al.* (2008) Genetic association of vasoactive intestinal peptide receptor with rheumatoid arthritis: altered expression and signal in immune cells. Arthritis Rheum 58: 1010-1019.
62. Grimm MC, Newman R, Hassim Z, Cuan N, Connor SJ*, et al.* (2003) Cutting edge: vasoactive intestinal peptide acts as a potent suppressor of inflammation in vivo by trans-deactivating chemokine receptors. J Immunol 171: 4990-4994.
63. Foey AD, Field S, Ahmed S, Jain A, Feldmann M*, et al.* (2003) Impact of VIP and cAMP on the regulation of TNF-alpha and IL-10 production: implications for rheumatoid arthritis. Arthritis Res Ther 5: R317-328.
64. Szliter EA, Lighvani S, Barrett RP, Hazlett LD (2007) Vasoactive intestinal peptide balances pro- and anti-inflammatory cytokines in the Pseudomonas aeruginosa-infected cornea and protects against corneal perforation. J Immunol 178: 1105-1114.
65. Delgado M, Munoz-Elias EJ, Gomariz RP, Ganea D (1999) VIP and PACAP inhibit IL-12 production in LPS-stimulated macrophages. Subsequent effect on IFNgamma synthesis by T cells. J Neuroimmunol 96: 167-181.
66. Ganea D (1996) Regulatory effects of vasoactive intestinal peptide on cytokine production in central and peripheral lymphoid organs. Adv Neuroimmunol 6: 61-74.
67. Anastasi S, Baietti MF, Frosi Y, Alema S, Segatto O (2007) The evolutionarily conserved EBR module of RALT/MIG6 mediates suppression of the EGFR catalytic activity. Oncogene 26: 7833-7846.
68. Anastasi S, Sala G, Huiping C, Caprini E, Russo G*, et al.* (2005) Loss of RALT/MIG-6 expression in ERBB2-amplified breast carcinomas enhances ErbB-2 oncogenic potency and favors resistance to Herceptin. Oncogene 24: 4540-4548.
69. Fiorini M, Ballaro C, Sala G, Falcone G, Alema S*, et al.* (2002) Expression of RALT, a feedback inhibitor of ErbB receptors, is subjected to an integrated transcriptional and post-translational control. Oncogene 21: 6530-6539.
70. Xu D, Patten RD, Force T, Kyriakis JM (2006) Gene 33/RALT is induced by hypoxia in cardiomyocytes, where it promotes cell death by suppressing

phosphatidylinositol 3-kinase and extracellular signal-regulated kinase survival signaling. Mol Cell Biol 26: 5043-5054.
71. Anastasi S, Fiorentino L, Fiorini M, Fraioli R, Sala G*, et al.* (2003) Feedback inhibition by RALT controls signal output by the ErbB network. Oncogene 22: 4221-4234.
72. Fiorentino L, Pertica C, Fiorini M, Talora C, Crescenzi M*, et al.* (2000) Inhibition of ErbB-2 mitogenic and transforming activity by RALT, a mitogen-induced signal transducer which binds to the ErbB-2 kinase domain. Mol Cell Biol 20: 7735-7750.
73. Xu D, Makkinje A, Kyriakis JM (2005) Gene 33 is an endogenous inhibitor of epidermal growth factor (EGF) receptor signaling and mediates dexamethasone-induced suppression of EGF function. J Biol Chem 280: 2924-2933.
74. Tsunoda T, Inokuchi J, Baba I, Okumura K, Naito S*, et al.* (2002) A novel mechanism of nuclear factor kappaB activation through the binding between inhibitor of nuclear factor-kappaBalpha and the processed NH(2)-terminal region of Mig-6. Cancer Res 62: 5668-5671.
75. Zhu J, Paul WE (2010) Heterogeneity and plasticity of T helper cells. Cell Res 20: 4-12.
76. Murphy KM, Stockinger B (2010) Effector T cell plasticity: flexibility in the face of changing circumstances. Nat Immunol 11: 674-680.
77. Bluestone JA, Mackay CR, O'Shea JJ, Stockinger B (2009) The functional plasticity of T cell subsets. Nat Rev Immunol 9: 811-816.
78. Takimoto T, Wakabayashi Y, Sekiya T, Inoue N, Morita R*, et al.* (2010) Smad2 and Smad3 are redundantly essential for the TGF-beta-mediated regulation of regulatory T plasticity and Th1 development. J Immunol 185: 842-855.
79. Zhu J, Paul WE (2010) Peripheral CD4+ T-cell differentiation regulated by networks of cytokines and transcription factors. Immunol Rev 238: 247-262.
80. Palmer MT, Weaver CT (2009) Autoimmunity: increasing suspects in the CD4+ T cell lineup. Nat Immunol 11: 36-40.
81. Weaver CT, Hatton RD (2009) Interplay between the TH17 and TReg cell lineages: a (co-)evolutionary perspective. Nat Rev Immunol 9: 883-889.
82. Nistala K, Adams S, Cambrook H, Ursu S, Olivito B*, et al.* (2010) Th17 plasticity in human autoimmune arthritis is driven by the inflammatory environment. Proc Natl Acad Sci U S A 107: 14751-14756.
83. Cosmi L, Cimaz R, Maggi L, Santarlasci V, Capone M*, et al.* (2011) Evidence of the transient nature of the Th17 phenotype of CD4+CD161+ T cells in the synovial fluid of patients with juvenile idiopathic arthritis. Arthritis Rheum 63: 2504-2515.
84. Cosmi L, Maggi L, Santarlasci V, Capone M, Cardilicchia E*, et al.* (2010) Identification of a novel subset of human circulating memory CD4(+) T cells that produce both IL-17A and IL-4. J Allergy Clin Immunol 125: 222-230 e221-224.
85. Huang W, Na L, Fidel PL, Schwarzenberger P (2004) Requirement of Interleukin-17A for Systemic Anti-Candida albicans Host Defense in Mice. Journal of Infectious Diseases 190: 624-631.
86. Kelly MN, Kolls JK, Happel K, Schwartzman JD, Schwarzenberger P*, et al.* (2005) Interleukin-17/interleukin-17 receptor-mediated signaling is important for generation of an optimal polymorphonuclear response against Toxoplasma gondii infection. Infection and immunity 73: 617-621.
87. O'Connor Jr W, Kamanaka M, Booth CJ, Town T, Nakae S*, et al.* (2009) A protective function for interleukin 17A in T cell,Äìmediated intestinal inflammation. Nat Immunol 10: 603-609.

88. Ogawa A, Andoh A, Araki Y, Bamba T, Fujiyama Y (2004) Neutralization of interleukin-17 aggravates dextran sulfate sodium-induced colitis in mice. Clinical immunology 110: 55-62.
89. Ivanov II, Atarashi K, Manel N, Brodie EL, Shima T*, et al.* (2009) Induction of intestinal Th17 cells by segmented filamentous bacteria. Cell 139: 485-498.
90. Ivanov II, Frutos RdL, Manel N, Yoshinaga K, Rifkin DB*, et al.* (2008) Specific microbiota direct the differentiation of IL-17-producing T-helper cells in the mucosa of the small intestine. Cell host & microbe 4: 337-349.
91. Esplugues E, Huber S, Gagliani N, Hauser AE, Town T*, et al.* (2011) Control of TH17 cells occurs in the small intestine. Nature 475: 514-518.
92. Kinugasa T, Sakaguchi T, Gu X, Reinecker HÄ (2000) Claudins regulate the intestinal barrier in response to immune mediators. Gastroenterology 118: 1001-1011.
93. Cosmi L, De Palma R, Santarlasci V, Maggi L, Capone M*, et al.* (2008) Human interleukin 17-producing cells originate from a CD161+CD4+ T cell precursor. J Exp Med 205: 1903-1916.
94. Sakaguchi S, Sakaguchi N, Asano M, Itoh M, Toda M (1995) Immunologic self-tolerance maintained by activated T cells expressing IL-2 receptor alpha-chains (CD25). Breakdown of a single mechanism of self-tolerance causes various autoimmune diseases. J Immunol 155: 1151-1164.
95. Thornton AM, Shevach EM (1998) CD4+CD25+ immunoregulatory T cells suppress polyclonal T cell activation in vitro by inhibiting interleukin 2 production. J Exp Med 188: 287-296.
96. Gavin MA, Clarke SR, Negrou E, Gallegos A, Rudensky A (2002) Homeostasis and anergy of CD4(+)CD25(+) suppressor T cells in vivo. Nat Immunol 3: 33-41.
97. Ng WF, Duggan PJ, Ponchel F, Matarese G, Lombardi G*, et al.* (2001) Human CD4(+)CD25(+) cells: a naturally occurring population of regulatory T cells. Blood 98: 2736-2744.
98. Baecher-Allan C, Viglietta V, Hafler DA (2002) Inhibition of human CD4(+)CD25(+high) regulatory T cell function. J Immunol 169: 6210-6217.
99. Dieckmann D, Plottner H, Dotterweich S, Schuler G (2005) Activated CD4+ CD25+ T cells suppress antigen-specific CD4+ and CD8+ T cells but induce a suppressive phenotype only in CD4+ T cells. Immunology 115: 305-314.
100. Levings MK, Sangregorio R, Sartirana C, Moschin AL, Battaglia M*, et al.* (2002) Human CD25+CD4+ T suppressor cell clones produce transforming growth factor beta, but not interleukin 10, and are distinct from type 1 T regulatory cells. J Exp Med 196: 1335-1346.
101. Brunkow ME, Jeffery EW, Hjerrild KA, Paeper B, Clark LB*, et al.* (2001) Disruption of a new forkhead/winged-helix protein, scurfin, results in the fatal lymphoproliferative disorder of the scurfy mouse. Nat Genet 27: 68-73.
102. Wildin RS, Smyk-Pearson S, Filipovich AH (2002) Clinical and molecular features of the immunodysregulation, polyendocrinopathy, enteropathy, X linked (IPEX) syndrome. J Med Genet 39: 537-545.
103. Hori S, Nomura T, Sakaguchi S (2003) Control of regulatory T cell development by the transcription factor Foxp3. Science 299: 1057-1061.
104. Fontenot JD, Gavin MA, Rudensky AY (2003) Foxp3 programs the development and function of CD4+CD25+ regulatory T cells. Nat Immunol 4: 330-336.
105. Khattri R, Cox T, Yasayko SA, Ramsdell F (2003) An essential role for Scurfin in CD4+CD25+ T regulatory cells. Nat Immunol 4: 337-342.

106. Yagi H, Nomura T, Nakamura K, Yamazaki S, Kitawaki T*, et al.* (2004) Crucial role of FOXP3 in the development and function of human CD25+CD4+ regulatory T cells. Int Immunol 16: 1643-1656.
107. Hartigan-O'Connor DJ, Poon C, Sinclair E, McCune JM (2007) Human CD4+ regulatory T cells express lower levels of the IL-7 receptor alpha chain (CD127), allowing consistent identification and sorting of live cells. J Immunol Methods 319: 41-52.
108. Baron U, Floess S, Wieczorek G, Baumann K, Grutzkau A*, et al.* (2007) DNA demethylation in the human FOXP3 locus discriminates regulatory T cells from activated FOXP3(+) conventional T cells. Eur J Immunol 37: 2378-2389.
109. Floess S, Freyer J, Siewert C, Baron U, Olek S*, et al.* (2007) Epigenetic control of the foxp3 locus in regulatory T cells. PLoS Biol 5: e38.
110. Polansky JK, Kretschmer K, Freyer J, Floess S, Garbe A*, et al.* (2008) DNA methylation controls Foxp3 gene expression. Eur J Immunol 38: 1654-1663.
111. Fontenot JD, Dooley JL, Farr AG, Rudensky AY (2005) Developmental regulation of Foxp3 expression during ontogeny. J Exp Med 202: 901-906.
112. Fontenot JD, Rasmussen JP, Williams LM, Dooley JL, Farr AG*, et al.* (2005) Regulatory T cell lineage specification by the forkhead transcription factor foxp3. Immunity 22: 329-341.
113. Thornton AM, Korty PE, Tran DQ, Wohlfert EA, Murray PE*, et al.* (2010) Expression of Helios, an Ikaros transcription factor family member, differentiates thymic-derived from peripherally induced Foxp3+ T regulatory cells. J Immunol 184: 3433-3441.
114. Verhagen J, Wraith DC (2010) Comment on "Expression of Helios, an Ikaros transcription factor family member, differentiates thymic-derived from peripherally induced Foxp3+ T regulatory cells". J Immunol 185: 7129; author reply 7130.
115. Gottschalk RA, Corse E, Allison JP (2012) Expression of Helios in peripherally induced Foxp3+ regulatory T cells. J Immunol 188: 976-980.
116. Himmel ME, Macdonald KG, Garcia RV, Steiner TS, Levings MK (2013) Helios+ and Helios- Cells Coexist within the Natural FOXP3+ T Regulatory Cell Subset in Humans. J Immunol.
117. Haribhai D, Williams JB, Jia S, Nickerson D, Schmitt EG*, et al.* (2011) A requisite role for induced regulatory T cells in tolerance based on expanding antigen receptor diversity. Immunity 35: 109-122.
118. Hippen KL, Merkel SC, Schirm DK, Nelson C, Tennis NC*, et al.* (2011) Generation and large-scale expansion of human inducible regulatory T cells that suppress graft-versus-host disease. Am J Transplant 11: 1148-1157.
119. Beres A, Komorowski R, Mihara M, Drobyski WR (2011) Instability of Foxp3 expression limits the ability of induced regulatory T cells to mitigate graft versus host disease. Clin Cancer Res 17: 3969-3983.
120. Kong N, Lan Q, Chen M, Wang J, Shi W*, et al.* (2012) Antigen-specific transforming growth factor beta-induced Treg cells, but not natural Treg cells, ameliorate autoimmune arthritis in mice by shifting the Th17/Treg cell balance from Th17 predominance to Treg cell predominance. Arthritis Rheum 64: 2548-2558.
121. Evans RL, Faldetta TJ, Humphreys RE, Pratt DM, Yunis EJ*, et al.* (1978) Peripheral human T cells sensitized in mixed leukocyte culture synthesize and express Ia-like antigens. J Exp Med 148: 1440-1445.

122. Ko HS, Fu SM, Winchester RJ, Yu DT, Kunkel HG (1979) Ia determinants on stimulated human T lymphocytes. Occurrence on mitogen- and antigen-activated T cells. J Exp Med 150: 246-255.
123. Baecher-Allan C, Brown JA, Freeman GJ, Hafler DA (2001) CD4+CD25high regulatory cells in human peripheral blood. J Immunol 167: 1245-1253.
124. Baecher-Allan C, Wolf E, Hafler DA (2006) MHC class II expression identifies functionally distinct human regulatory T cells. J Immunol 176: 4622-4631.
125. Kleinewietfeld M, Puentes F, Borsellino G, Battistini L, Rotzschke O*, et al.* (2005) CCR6 expression defines regulatory effector/memory-like cells within the CD25(+)CD4+ T-cell subset. Blood 105: 2877-2886.
126. Miyara M, Yoshioka Y, Kitoh A, Shima T, Wing K*, et al.* (2009) Functional delineation and differentiation dynamics of human CD4+ T cells expressing the FoxP3 transcription factor. Immunity 30: 899-911.
127. Booth NJ, McQuaid AJ, Sobande T, Kissane S, Agius E*, et al.* (2010) Different proliferative potential and migratory characteristics of human CD4+ regulatory T cells that express either CD45RA or CD45RO. J Immunol 184: 4317-4326.
128. Vukmanovic-Stejic M, Zhang Y, Cook JE, Fletcher JM, McQuaid A*, et al.* (2006) Human CD4+ CD25hi Foxp3+ regulatory T cells are derived by rapid turnover of memory populations in vivo. J Clin Invest 116: 2423-2433.
129. Takahashi T, Tagami T, Yamazaki S, Uede T, Shimizu J*, et al.* (2000) Immunologic self-tolerance maintained by CD25(+)CD4(+) regulatory T cells constitutively expressing cytotoxic T lymphocyte-associated antigen 4. J Exp Med 192: 303-310.
130. Deaglio S, Dwyer KM, Gao W, Friedman D, Usheva A*, et al.* (2007) Adenosine generation catalyzed by CD39 and CD73 expressed on regulatory T cells mediates immune suppression. J Exp Med 204: 1257-1265.
131. Borsellino G, Kleinewietfeld M, Di Mitri D, Sternjak A, Diamantini A*, et al.* (2007) Expression of ectonucleotidase CD39 by Foxp3+ Treg cells: hydrolysis of extracellular ATP and immune suppression. Blood 110: 1225-1232.
132. Walker LS, Sansom DM (2011) The emerging role of CTLA4 as a cell-extrinsic regulator of T cell responses. Nat Rev Immunol 11: 852-863.
133. Dwyer KM, Deaglio S, Gao W, Friedman D, Strom TB*, et al.* (2007) CD39 and control of cellular immune responses. Purinergic Signal 3: 171-180.
134. Mandapathil M, Hilldorfer B, Szczepanski MJ, Czystowska M, Szajnik M*, et al.* (2010) Generation and accumulation of immunosuppressive adenosine by human CD4+CD25highFOXP3+ regulatory T cells. J Biol Chem 285: 7176-7186.
135. Moncrieffe H, Nistala K, Kamhieh Y, Evans J, Eddaoudi A*, et al.* (2010) High expression of the ectonucleotidase CD39 on T cells from the inflamed site identifies two distinct populations, one regulatory and one memory T cell population. J Immunol 185: 134-143.
136. Ursu S, Pesenacker AM, Zheng D, Gordon-smith SB, Lerose A, et al. (2013) Autoimmune susceptibility gene critically influences CD39 T cell expression and function in modulating human inflammation. in preperation.
137. Wilkin F, Duhant X, Bruyns C, Suarez-Huerta N, Boeynaems JM*, et al.* (2001) The P2Y11 receptor mediates the ATP-induced maturation of human monocyte-derived dendritic cells. J Immunol 166: 7172-7177.
138. Hanley PJ, Musset B, Renigunta V, Limberg SH, Dalpke AH*, et al.* (2004) Extracellular ATP induces oscillations of intracellular Ca2+ and membrane

potential and promotes transcription of IL-6 in macrophages. Proc Natl Acad Sci U S A 101: 9479-9484.
139. Yamazaki T, Yang XO, Chung Y, Fukunaga A, Nurieva R*, et al.* (2008) CCR6 regulates the migration of inflammatory and regulatory T cells. J Immunol 181: 8391-8401.
140. Turner JE, Paust HJ, Steinmetz OM, Peters A, Riedel JH*, et al.* (2010) CCR6 recruits regulatory T cells and Th17 cells to the kidney in glomerulonephritis. J Am Soc Nephrol 21: 974-985.
141. Lim HW, Lee J, Hillsamer P, Kim CH (2008) Human Th17 cells share major trafficking receptors with both polarized effector T cells and FOXP3+ regulatory T cells. J Immunol 180: 122-129.
142. Tosello V, Odunsi K, Souleimanian NE, Lele S, Shrikant P*, et al.* (2008) Differential expression of CCR7 defines two distinct subsets of human memory CD4+CD25+ Tregs. Clin Immunol 126: 291-302.
143. Koch MA, Tucker-Heard G, Perdue NR, Killebrew JR, Urdahl KB*, et al.* (2009) The transcription factor T-bet controls regulatory T cell homeostasis and function during type 1 inflammation. Nat Immunol 10: 595-602.
144. Zheng J, Liu Y, Qin G, Lam KT, Guan J*, et al.* (2011) Generation of human Th1-like regulatory CD4+ T cells by an intrinsic IFN-gamma- and T-bet-dependent pathway. Eur J Immunol 41: 128-139.
145. Duhen T, Duhen R, Lanzavecchia A, Sallusto F, Campbell DJ (2012) Functionally distinct subsets of human FOXP3+ Treg cells that phenotypically mirror effector Th cells. Blood 119: 4430-4440.
146. Wang R, Kozhaya L, Mercer F, Khaitan A, Fujii H*, et al.* (2009) Expression of GARP selectively identifies activated human FOXP3+ regulatory T cells. Proc Natl Acad Sci U S A 106: 13439-13444.
147. Wang R, Wan Q, Kozhaya L, Fujii H, Unutmaz D (2008) Identification of a regulatory T cell specific cell surface molecule that mediates suppressive signals and induces Foxp3 expression. PLoS One 3: e2705.
148. Stockis J, Colau D, Coulie PG, Lucas S (2009) Membrane protein GARP is a receptor for latent TGF-beta on the surface of activated human Treg. Eur J Immunol 39: 3315-3322.
149. Kehrmann J, Zeschnigk M, Buer J, Probst-Kepper M (2011) FOXP3 Expression in GARP-Transduced Helper T Cells Is Not Associated with FOXP3 TSDR Demethylation. Transfus Med Hemother 38: 287-291.
150. Koenen HJ, Smeets RL, Vink PM, van Rijssen E, Boots AM*, et al.* (2008) Human CD25highFoxp3pos regulatory T cells differentiate into IL-17-producing cells. Blood 112: 2340-2352.
151. Nyirenda MH, Sanvito L, Darlington PJ, O'Brien K, Zhang GX*, et al.* (2011) TLR2 Stimulation Drives Human Naive and Effector Regulatory T Cells into a Th17-Like Phenotype with Reduced Suppressive Function. J Immunol.
152. McClymont SA, Putnam AL, Lee MR, Esensten JH, Liu W*, et al.* (2011) Plasticity of human regulatory T cells in healthy subjects and patients with type 1 diabetes. J Immunol 186: 3918-3926.
153. Feng T, Cao AT, Weaver CT, Elson CO, Cong Y (2011) Interleukin-12 converts Foxp3+ regulatory T cells to interferon-gamma-producing Foxp3+ T cells that inhibit colitis. Gastroenterology 140: 2031-2043.

154. Schadenberg AW, Vastert SJ, Evens FC, Kuis W, van Vught AJ*, et al.* (2011) FOXP3+ CD4+ Tregs lose suppressive potential but remain anergic during transient inflammation in human. Eur J Immunol 41: 1132-1142.
155. Kryczek I, Wu K, Zhao E, Wei S, Vatan L*, et al.* (2011) IL-17+ regulatory T cells in the microenvironments of chronic inflammation and cancer. J Immunol 186: 4388-4395.
156. Dominguez-Villar M, Baecher-Allan CM, Hafler DA (2011) Identification of T helper type 1-like, Foxp3+ regulatory T cells in human autoimmune disease. Nat Med 17: 673-675.
157. Beriou G, Costantino CM, Ashley CW, Yang L, Kuchroo VK*, et al.* (2009) IL-17-producing human peripheral regulatory T cells retain suppressive function. Blood 113: 4240-4249.
158. Voo KS, Wang YH, Santori FR, Boggiano C, Arima K*, et al.* (2009) Identification of IL-17-producing FOXP3+ regulatory T cells in humans. Proc Natl Acad Sci U S A 106: 4793-4798.
159. Ayyoub M, Deknuydt F, Raimbaud I, Dousset C, Leveque L*, et al.* (2009) Human memory FOXP3+ Tregs secrete IL-17 ex vivo and constitutively express the T(H)17 lineage-specific transcription factor RORgamma t. Proc Natl Acad Sci U S A 106: 8635-8640.
160. Koenecke C, Lee CW, Thamm K, Fohse L, Schafferus M*, et al.* (2012) IFN-gamma production by allogeneic Foxp3+ regulatory T cells is essential for preventing experimental graft-versus-host disease. J Immunol 189: 2890-2896.
161. Zheng Y, Chaudhry A, Kas A, deRoos P, Kim JM*, et al.* (2009) Regulatory T-cell suppressor program co-opts transcription factor IRF4 to control T(H)2 responses. Nature 458: 351-356.
162. Chaudhry A, Rudra D, Treuting P, Samstein RM, Liang Y*, et al.* (2009) CD4+ Regulatory T Cells Control TH17 Responses in a Stat3-Dependent Manner. Science 326: 986-991.
163. Chaudhry A, Samstein RM, Treuting P, Liang Y, Pils MC*, et al.* (2011) Interleukin-10 signaling in regulatory T cells is required for suppression of Th17 cell-mediated inflammation. Immunity 34: 566-578.
164. Sawitzki B, Kingsley CI, Oliveira V, Karim M, Herber M*, et al.* (2005) IFN-gamma production by alloantigen-reactive regulatory T cells is important for their regulatory function in vivo. J Exp Med 201: 1925-1935.
165. Hayward K, Wallace CA (2009) Recent developments in anti-rheumatic drugs in pediatrics: treatment of juvenile idiopathic arthritis. Arthritis Res Ther 11: 216.
166. Website.(2008) Juvenile idiopathic arthritis. American Academy of Pediatrics: http://www.pediatriccareonline.org/pco/ub/view/Point-of-Care-Quick-Reference/397191/0/Arthritis_juvenile.
167. Nistala K, Woo, P., Wedderburn, L. R. (2008) Juvenile idiopathic Arthritis. In: al Fe, editor. Kelly's Textbook of Rheumatology. 8th ed. pp. 1657-1676.
168. Forre O, Dobloug JH, Hoyeraal HM, Thorsby E (1983) HLA antigens in juvenile arthritis. Genetic basis for the different subtypes. Arthritis Rheum 26: 35-38.
169. Giannini EH, Malagon CN, Van Kerckhove C, Taylor J, Lovell DJ*, et al.* (1991) Longitudinal analysis of HLA associated risks for iridocyclitis in juvenile rheumatoid arthritis. J Rheumatol 18: 1394-1397.

170. Saila H, Pitkaniemi J, Tuomilehto J, Savolainen A, Alakulppi N*, et al.* (2004) HLA and susceptibility to juvenile idiopathic arthritis: a study of affected sibpairs in an isolated Finnish population. J Rheumatol 31: 2281-2285.
171. Smerdel A, Lie BA, Finholt C, Ploski R, Forre O*, et al.* (2003) An additional susceptibility gene for juvenile idiopathic arthritis in the HLA class I region on several DR-DQ haplotypes. Tissue Antigens 61: 80-84.
172. Smerdel A, Lie BA, Ploski R, Koeleman BP, Forre O*, et al.* (2002) A gene in the telomeric HLA complex distinct from HLA-A is involved in predisposition to juvenile idiopathic arthritis. Arthritis Rheum 46: 1614-1619.
173. Szer ISK, Y; Malleson, P N; Southwood, T R (2006) Arthritis in Children and Adolescents: Oxford University Press. 456 p.
174. Prahalad S, Glass DN (2008) A comprehensive review of the genetics of juvenile idiopathic arthritis. Pediatr Rheumatol Online J 6: 11.
175. Ravelli A, Martini A (2007) Juvenile idiopathic arthritis. Lancet 369: 767-778.
176. Wedderburn LR, Patel A, Varsani H, Woo P (2001) Divergence in the degree of clonal expansions in inflammatory T cell subpopulations mirrors HLA-associated risk alleles in genetically and clinically distinct subtypes of childhood arthritis. Int Immunol 13: 1541-1550.
177. Bupa (2008) Juvenile idiopathic arthritis. Bupa. pp. health fact sheet.
178. Southwood TR, Foster HE, Davidson JE, Hyrich KL, Cotter CB*, et al.* (2011) Duration of etanercept treatment and reasons for discontinuation in a cohort of juvenile idiopathic arthritis patients. Rheumatology (Oxford) 50: 189-195.
179. Hunter PJ, Nistala K, Jina N, Eddaoudi A, Thomson W*, et al.* (2010) Biologic predictors of extension of oligoarticular juvenile idiopathic arthritis as determined from synovial fluid cellular composition and gene expression. Arthritis Rheum 62: 896-907.
180. Pharoah DS, Varsani H, Tatham RW, Newton KR, de Jager W*, et al.* (2006) Expression of the inflammatory chemokines CCL5, CCL3 and CXCL10 in juvenile idiopathic arthritis, and demonstration of CCL5 production by an atypical subset of CD8+ T cells. Arthritis Res Ther 8: R50.
181. de Kleer IM, Kamphuis SM, Rijkers GT, Scholtens L, Gordon G*, et al.* (2003) The spontaneous remission of juvenile idiopathic arthritis is characterized by CD30+ T cells directed to human heat-shock protein 60 capable of producing the regulatory cytokine interleukin-10. Arthritis Rheum 48: 2001-2010.
182. Sedlackova L, Velek J, Vavrincova P, Hromadnikova I (2006) Peripheral blood mononuclear cell responses to heat shock proteins and their derived synthetic peptides in juvenile idiopathic arthritis patients. Inflamm Res 55: 153-159.
183. Kamphuis S, Kuis W, de Jager W, Teklenburg G, Massa M*, et al.* (2005) Tolerogenic immune responses to novel T-cell epitopes from heat-shock protein 60 in juvenile idiopathic arthritis. Lancet 366: 50-56.
184. Murray KJ, Luyrink L, Grom AA, Passo MH, Emery H*, et al.* (1996) Immunohistological characteristics of T cell infiltrates in different forms of childhood onset chronic arthritis. J Rheumatol 23: 2116-2124.
185. Wedderburn LR, Robinson N, Patel A, Varsani H, Woo P (2000) Selective recruitment of polarized T cells expressing CCR5 and CXCR3 to the inflamed joints of children with juvenile idiopathic arthritis. Arthritis Rheum 43: 765-774.
186. Nistala K, Moncrieffe H, Newton KR, Varsani H, Hunter P*, et al.* (2008) Interleukin-17-producing T cells are enriched in the joints of children with arthritis, but have

a reciprocal relationship to regulatory T cell numbers. Arthritis Rheum 58: 875-887.
187. Annunziato F, Cosmi L, Liotta F, Maggi E, Romagnani S (2009) Type 17 T helper cells-origins, features and possible roles in rheumatic disease. Nat Rev Rheumatol 5: 325-331.
188. de Kleer IM, Wedderburn LR, Taams LS, Patel A, Varsani H*, et al.* (2004) CD4+CD25bright regulatory T cells actively regulate inflammation in the joints of patients with the remitting form of juvenile idiopathic arthritis. J Immunol 172: 6435-6443.
189. Wei CM, Lee JH, Wang LC, Yang YH, Chang LY*, et al.* (2008) Frequency and phenotypic analysis of CD4+CD25+ regulatory T cells in children with juvenile idiopathic arthritis. J Microbiol Immunol Infect 41: 78-87.
190. Olivito B, Simonini G, Ciullini S, Moriondo M, Betti L*, et al.* (2009) Th17 transcription factor RORC2 is inversely correlated with FOXP3 expression in the joints of children with juvenile idiopathic arthritis. J Rheumatol 36: 2017-2024.
191. de Kleer I, Vastert B, Klein M, Teklenburg G, Arkesteijn G*, et al.* (2006) Autologous stem cell transplantation for autoimmunity induces immunologic self-tolerance by reprogramming autoreactive T cells and restoring the CD4+CD25+ immune regulatory network. Blood 107: 1696-1702.
192. Macaubas C, Nguyen K, Deshpande C, Phillips C, Peck A*, et al.* (2010) Distribution of circulating cells in systemic juvenile idiopathic arthritis across disease activity states. Clin Immunol 134: 206-216.
193. Nguyen KD, Macaubas C, Nadeau KC, Truong P, Yoon T*, et al.* (2011) Serum amyloid A overrides Treg anergy via monocyte-dependent and Treg-intrinsic, SOCS3-associated pathways. Blood 117: 3793-3798.
194. Thompson SD, Moroldo MB, Guyer L, Ryan M, Tombragel EM*, et al.* (2004) A genome-wide scan for juvenile rheumatoid arthritis in affected sibpair families provides evidence of linkage. Arthritis Rheum 50: 2920-2930.
195. Hinks A, Eyre S, Ke X, Barton A, Martin P*, et al.* (2010) Association of the AFF3 gene and IL2/IL21 gene region with juvenile idiopathic arthritis. Genes Immun 11: 194-198.
196. Hinks A, Ke X, Barton A, Eyre S, Bowes J*, et al.* (2009) Association of the IL2RA/CD25 gene with juvenile idiopathic arthritis. Arthritis Rheum 60: 251-257.
197. Omoyinmi E, Forabosco P, Hamaoui R, Bryant A, Hinks A*, et al.* (2012) Association of the IL-10 gene family locus on chromosome 1 with juvenile idiopathic arthritis (JIA). PLoS One 7: e47673.
198. Eastell T, Hinks A, Thomson W (2007) SNPs in the FOXP3 gene region show no association with Juvenile Idiopathic Arthritis in a UK Caucasian population. Rheumatology (Oxford) 46: 1263-1265.
199. Prahalad S, Bohnsack JF, Whiting A, Clifford B, Jorde LB*, et al.* (2008) Lack of association of functional CTLA4 polymorphisms with juvenile idiopathic arthritis. Arthritis Rheum 58: 2147-2152.
200. Hinks A, Cobb J, Marion MC, Prahalad S, Sudman M*, et al.* (2013) Dense genotyping of immune-related disease regions identifies 14 new susceptibility loci for juvenile idiopathic arthritis. Nat Genet.
201. Ruprecht CR, Gattorno M, Ferlito F, Gregorio A, Martini A*, et al.* (2005) Coexpression of CD25 and CD27 identifies FoxP3+ regulatory T cells in inflamed synovia. J Exp Med 201: 1793-1803.

202. Raghavan S, Cao D, Widhe M, Roth K, Herrath J*, et al.* (2009) FOXP3 expression in blood, synovial fluid and synovial tissue during inflammatory arthritis and intra-articular corticosteroid treatment. Ann Rheum Dis 68: 1908-1915.
203. Bendersky A, Marcu-Malina V, Berkun Y, Gerstein M, Nagar M*, et al.* (2012) Cellular interactions of synovial fluid gammadelta T cells in juvenile idiopathic arthritis. J Immunol 188: 4349-4359.
204. Wehrens EJ, Mijnheer G, Duurland CL, Klein M, Meerding J*, et al.* (2011) Functional human regulatory T cells fail to control autoimmune inflammation due to PKB/c-akt hyperactivation in effector cells. Blood 118: 3538-3548.
205. Haufe S, Haug M, Schepp C, Kuemmerle-Deschner J, Hansmann S*, et al.* (2011) Impaired suppression of synovial fluid CD4+CD25- T cells from patients with juvenile idiopathic arthritis by CD4+CD25+ Treg cells. Arthritis Rheum 63: 3153-3162.
206. de Jager W, Hoppenreijs EP, Wulffraat NM, Wedderburn LR, Kuis W*, et al.* (2007) Blood and synovial fluid cytokine signatures in patients with juvenile idiopathic arthritis: a cross-sectional study. Ann Rheum Dis 66: 589-598.
207. Ruperto N, Murray KJ, Gerloni V, Wulffraat N, de Oliveira SK*, et al.* (2004) A randomized trial of parenteral methotrexate comparing an intermediate dose with a higher dose in children with juvenile idiopathic arthritis who failed to respond to standard doses of methotrexate. Arthritis Rheum 50: 2191-2201.
208. Beresford MW, Baildam EM (2009) New advances in the management of juvenile idiopathic arthritis--2: the era of biologicals. Arch Dis Child Educ Pract Ed 94: 151-156.
209. Ravelli A (2004) Toward an understanding of the long-term outcome of juvenile idiopathic arthritis. Clin Exp Rheumatol 22: 271-275.
210. De Kleer IM, Brinkman DM, Ferster A, Abinun M, Quartier P*, et al.* (2004) Autologous stem cell transplantation for refractory juvenile idiopathic arthritis: analysis of clinical effects, mortality, and transplant related morbidity. Ann Rheum Dis 63: 1318-1326.
211. Wulffraat NM, Brinkman D, Ferster A, Opperman J, ten Cate R*, et al.* (2003) Long-term follow-up of autologous stem cell transplantation for refractory juvenile idiopathic arthritis. Bone Marrow Transplant 32 Suppl 1: S61-64.
212. Abinun M, Flood TJ, Cant AJ, Veys P, Gennery AR*, et al.* (2009) Autologous T cell depleted haematopoietic stem cell transplantation in children with severe juvenile idiopathic arthritis in the UK (2000-2007). Mol Immunol 47: 46-51.
213. Wu Q, Pesenacker AM, Stansfield A, King D, Barge D, et al. (2013) T cell depleted Autologous Stem Cell Transplantation Results in a Chimera of Clones from before and after Transplant in Systemic Juvenile Idiopathic Arthritis. Presented at Rheumatology 2013, Birmingham. Rheumatology (Oxford) 52 (suppl 1): i121.
214. Ruderman EM, Pope RM (2005) The evolving clinical profile of abatacept (CTLA4-Ig): a novel co-stimulatory modulator for the treatment of rheumatoid arthritis. Arthritis Res Ther 7 Suppl 2: S21-25.
215. Schiff M, Keiserman M, Codding C, Songcharoen S, Berman A*, et al.* (2008) Efficacy and safety of abatacept or infliximab vs placebo in ATTEST: a phase III, multi-centre, randomised, double-blind, placebo-controlled study in patients with rheumatoid arthritis and an inadequate response to methotrexate. Ann Rheum Dis 67: 1096-1103.

216. Ruperto N, Lovell DJ, Quartier P, Paz E, Rubio-Perez N*, et al.* (2008) Abatacept in children with juvenile idiopathic arthritis: a randomised, double-blind, placebo-controlled withdrawal trial. Lancet 372: 383-391.
217. Alvarez-Quiroga C, Abud-Mendoza C, Doniz-Padilla L, Juarez-Reyes A, Monsivais-Urenda A*, et al.* (2011) CTLA-4-Ig therapy diminishes the frequency but enhances the function of Treg cells in patients with rheumatoid arthritis. J Clin Immunol 31: 588-595.
218. Biton J, Semerano L, Delavallee L, Lemeiter D, Laborie M*, et al.* (2011) Interplay between TNF and regulatory T cells in a TNF-driven murine model of arthritis. J Immunol 186: 3899-3910.
219. Ehrenstein MR, Evans JG, Singh A, Moore S, Warnes G*, et al.* (2004) Compromised function of regulatory T cells in rheumatoid arthritis and reversal by anti-TNFalpha therapy. J Exp Med 200: 277-285.
220. Valencia X, Stephens G, Goldbach-Mansky R, Wilson M, Shevach EM*, et al.* (2006) TNF downmodulates the function of human CD4+CD25hi T-regulatory cells. Blood 108: 253-261.
221. Wang J, van Dongen H, Scherer HU, Huizinga TW, Toes RE (2008) Suppressor activity among CD4+,CD25++ T cells is discriminated by membrane-bound tumor necrosis factor alpha. Arthritis Rheum 58: 1609-1618.
222. Huang B, Wang QT, Song SS, Wu YJ, Ma YK*, et al.* (2012) Combined use of etanercept and MTX restores CD4(+)/CD8 (+) ratio and Tregs in spleen and thymus in collagen-induced arthritis. Inflamm Res 61: 1229-1239.
223. van der Heijde D, Klareskog L, Rodriguez-Valverde V, Codreanu C, Bolosiu H*, et al.* (2006) Comparison of etanercept and methotrexate, alone and combined, in the treatment of rheumatoid arthritis: two-year clinical and radiographic results from the TEMPO study, a double-blind, randomized trial. Arthritis Rheum 54: 1063-1074.
224. Antoni C, Kalden JR (1999) Combination therapy of the chimeric monoclonal anti-tumor necrosis factor alpha antibody (infliximab) with methotrexate in patients with rheumatoid arthritis. Clin Exp Rheumatol 17: S73-77.
225. Huang Z, Yang B, Shi Y, Cai B, Li Y*, et al.* (2012) Anti-TNF-alpha therapy improves Treg and suppresses Teff in patients with rheumatoid arthritis. Cell Immunol 279: 25-29.
226. Lina C, Conghua W, Nan L, Ping Z (2011) Combined Treatment of Etanercept and MTX Reverses Th1/Th2, Th17/Treg Imbalance in Patients with Rheumatoid Arthritis. J Clin Immunol.
227. Blache C, Lequerre T, Roucheux A, Beutheu S, Dedreux I*, et al.* (2011) Number and phenotype of rheumatoid arthritis patients' CD4+CD25hi regulatory T cells are not affected by adalimumab or etanercept. Rheumatology (Oxford) 50: 1814-1822.
228. Dige A, Hvas CL, Deleuran B, Kelsen J, Bendix-Struve M*, et al.* (2011) Adalimumab treatment in Crohn's disease does not induce early changes in regulatory T cells. Scand J Gastroenterol 46: 1206-1214.
229. McGovern JL, Nguyen DX, Notley CA, Mauri C, Isenberg DA*, et al.* (2012) Th17 cells are restrained by Treg cells via the inhibition of interleukin-6 in patients with rheumatoid arthritis responding to anti-tumor necrosis factor antibody therapy. Arthritis Rheum 64: 3129-3138.

230. de Gannes Gc GMPJ, et al. (2007) PSoriasis and pustular dermatitis triggered by tnf-Œ± inhibitors in patients with rheumatologic conditions. Archives of Dermatology 143: 223-231.
231. Ko JM, Gottlieb AB, Kerbleski JF (2009) Induction and exacerbation of psoriasis with TNF-blockade therapy: a review and analysis of 127 cases. J Dermatolog Treat 20: 100-108.
232. Ma HL, Napierata L, Stedman N, Benoit S, Collins M*, et al.* (2010) Tumor necrosis factor alpha blockade exacerbates murine psoriasis-like disease by enhancing Th17 function and decreasing expansion of Treg cells. Arthritis Rheum 62: 430-440.
233. Lara-Marquez M, O'Dorisio M, O'Dorisio T, Shah M, Karacay B (2001) Selective gene expression and activation-dependent regulation of vasoactive intestinal peptide receptor type 1 and type 2 in human T cells. J Immunol 166: 2522-2530.
234. Sreedharan SP, Huang JX, Cheung MC, Goetzl EJ (1995) Structure, expression, and chromosomal localization of the type I human vasoactive intestinal peptide receptor gene. Proc Natl Acad Sci U S A 92: 2939-2943.
235. Sreedharan SP, Patel DR, Huang JX, Goetzl EJ (1993) Cloning and functional expression of a human neuroendocrine vasoactive intestinal peptide receptor. Biochem Biophys Res Commun 193: 546-553.
236. Tang H, Sun L, Xin Z, Ganea D (1996) Down-regulation of cytokine expression in murine lymphocytes by PACAP and VIP. Ann N Y Acad Sci 805: 768-778.
237. Xin Z, Jiang X, Wang HY, Denny TN, Dittel BN*, et al.* (1997) Effect of vasoactive intestinal peptide (VIP) on cytokine production and expression of VIP receptors in thymocyte subsets. Regul Pept 72: 41-54.
238. Ganea D, Sun L (1993) Vasoactive intestinal peptide downregulates the expression of IL-2 but not of IFN gamma from stimulated murine T lymphocytes. J Neuroimmunol 47: 147-158.
239. Anderson P, Gonzalez-Rey E (2010) Vasoactive intestinal peptide induces cell cycle arrest and regulatory functions in human T cells at multiple levels. Mol Cell Biol 30: 2537-2551.
240. de Jager W, Prakken BJ, Bijlsma JW, Kuis W, Rijkers GT (2005) Improved multiplex immunoassay performance in human plasma and synovial fluid following removal of interfering heterophilic antibodies. J Immunol Methods 300: 124-135.
241. Sambrook J FE, Maniatis T (1989). Molecular Cloning A laboratory manual. Cold Spring Harbor: Cold Spring Harbor Laboratory Press. pp. pp 7: 19-17-22.
242. Rozen S (2000) Primer 3.
243. Rozen S, Skaletsky H (2000) Primer3 on the WWW for general users and for biologist programmers. Methods Mol Biol 132: 365-386.
244. NCBI NCBI Primer blast
245. Wedderburn LR, King DJ (2007) Analysis of the T-cell receptor repertoire of synovial T-cells. Methods Mol Med 136: 97-116.
246. Inc IS (2010) IPA. Ingenuity Systems Inc.
247. Dennis G, Jr., Sherman BT, Hosack DA, Yang J, Gao W*, et al.* (2003) DAVID: Database for Annotation, Visualization, and Integrated Discovery. Genome Biol 4: P3.
248. Huang da W, Sherman BT, Lempicki RA (2009) Systematic and integrative analysis of large gene lists using DAVID bioinformatics resources. Nat Protoc 4: 44-57.

249. Bopp T, Becker C, Klein M, Klein-Hessling S, Palmetshofer A*, et al.* (2007) Cyclic adenosine monophosphate is a key component of regulatory T cell-mediated suppression. J Exp Med 204: 1303-1310.
250. Chen G, Hao J, Xi Y, Wang W, Wang Z*, et al.* (2008) The therapeutic effect of vasoactive intestinal peptide on experimental arthritis is associated with CD4+CD25+ T regulatory cells. Scand J Immunol 68: 572-578.
251. Chorny A, Gonzalez-Rey E, Ganea D, Delgado M (2006) Vasoactive intestinal peptide generates CD4+CD25+ regulatory T cells in vivo: therapeutic applications in autoimmunity and transplantation. Ann N Y Acad Sci 1070: 190-195.
252. Gonzalez-Rey E, Chorny A, Fernandez-Martin A, Ganea D, Delgado M (2006) Vasoactive intestinal peptide generates human tolerogenic dendritic cells that induce CD4 and CD8 regulatory T cells. Blood 107: 3632-3638.
253. Yadav M, Goetzl EJ (2008) Vasoactive intestinal peptide-mediated Th17 differentiation: an expanding spectrum of vasoactive intestinal peptide effects in immunity and autoimmunity. Ann N Y Acad Sci 1144: 83-89.
254. Bokaei PB, Ma XZ, Byczynski B, Keller J, Sakac D*, et al.* (2006) Identification and characterization of five-transmembrane isoforms of human vasoactive intestinal peptide and pituitary adenylate cyclase-activating polypeptide receptors. Genomics 88: 791-800.
255. Thompson JD, Higgins DG, Gibson TJ (1994) CLUSTAL W: improving the sensitivity of progressive multiple sequence alignment through sequence weighting, position-specific gap penalties and weight matrix choice. Nucleic Acids Res 22: 4673-4680.
256. Sun L, Ganea D (1993) Vasoactive intestinal peptide inhibits interleukin (IL)-2 and IL-4 production through different molecular mechanisms in T cells activated via the T cell receptor/CD3 complex. J Neuroimmunol 48: 59-69.
257. Tang H, Welton A, Ganea D (1995) Neuropeptide regulation of cytokine expression: effects of VIP and Ro 25-1553. J Interferon Cytokine Res 15: 993-1003.
258. Geiss GK, Bumgarner RE, Birditt B, Dahl T, Dowidar N*, et al.* (2008) Direct multiplexed measurement of gene expression with color-coded probe pairs. Nat Biotechnol 26: 317-325.
259. Nistala K, Wedderburn LR (2009) Th17 and regulatory T cells: rebalancing pro- and anti-inflammatory forces in autoimmune arthritis. Rheumatology (Oxford) 48: 602-606.
260. Ferby I, Reschke M, Kudlacek O, Knyazev P, Pante G*, et al.* (2006) Mig6 is a negative regulator of EGF receptor-mediated skin morphogenesis and tumor formation. Nat Med 12: 568-573.
261. Juarranz MG, Santiago B, Torroba M, Gutierrez-Canas I, Palao G*, et al.* (2004) Vasoactive intestinal peptide modulates proinflammatory mediator synthesis in osteoarthritic and rheumatoid synovial cells. Rheumatology (Oxford) 43: 416-422.
262. Juarranz Y, Gutierrez-Canas I, Santiago B, Carrion M, Pablos JL*, et al.* (2008) Differential expression of vasoactive intestinal peptide and its functional receptors in human osteoarthritic and rheumatoid synovial fibroblasts. Arthritis Rheum 58: 1086-1095.
263. Laurenza A, Sutkowski EM, Seamon KB (1989) Forskolin: a specific stimulator of adenylyl cyclase or a diterpene with multiple sites of action? Trends Pharmacol Sci 10: 442-447.

264. Nagata A, Tanaka T, Minezawa A, Poyurovsky M, Mayama T*, et al.* (2009) cAMP activation by PACAP/VIP stimulates IL-6 release and inhibits osteoblastic differentiation through VPAC2 receptor in osteoblastic MC3T3 cells. J Cell Physiol 221: 75-83.
265. Nicole P, Lins L, Rouyer-Fessard C, Drouot C, Fulcrand P*, et al.* (2000) Identification of key residues for interaction of vasoactive intestinal peptide with human VPAC1 and VPAC2 receptors and development of a highly selective VPAC1 receptor agonist. Alanine scanning and molecular modeling of the peptide. J Biol Chem 275: 24003-24012.
266. Juarranz Y, Abad C, Martinez C, Arranz A, Gutierrez-Canas I*, et al.* (2005) Protective effect of vasoactive intestinal peptide on bone destruction in the collagen-induced arthritis model of rheumatoid arthritis. Arthritis Res Ther 7: R1034-1045.
267. Yin H, Cheng H, Yu M, Zhang F, Lin J*, et al.* (2005) Vasoactive intestinal peptide ameliorates synovial cell functions of collagen-induced arthritis rats by down-regulating NF-kappaB activity. Immunol Invest 34: 153-169.
268. Tran DQ, Ramsey H, Shevach EM (2007) Induction of FOXP3 expression in naive human CD4+FOXP3 T cells by T-cell receptor stimulation is transforming growth factor-beta dependent but does not confer a regulatory phenotype. Blood 110: 2983-2990.
269. Pillai V, Karandikar NJ (2008) Attack on the clones? Human FOXP3 detection by PCH101, 236A/E7, 206D, and 259D reveals 259D as the outlier with lower sensitivity. Blood 111: 463-464; author reply 464-466.
270. d'Hennezel E, Yurchenko E, Sgouroudis E, Hay V, Piccirillo CA (2011) Single-Cell Analysis of the Human T Regulatory Population Uncovers Functional Heterogeneity and Instability within FOXP3+ Cells. J Immunol 186: 6788-6797.
271. Liu W, Putnam AL, Xu-Yu Z, Szot GL, Lee MR*, et al.* (2006) CD127 expression inversely correlates with FoxP3 and suppressive function of human CD4+ T reg cells. J Exp Med 203: 1701-1711.
272. Annunziato F, Cosmi L, Santarlasci V, Maggi L, Liotta F*, et al.* (2007) Phenotypic and functional features of human Th17 cells. J Exp Med 204: 1849-1861.
273. Baine I, Basu S, Ames R, Sellers RS, Macian F (2012) Helios Induces Epigenetic Silencing of Il2 Gene Expression in Regulatory T Cells. J Immunol.
274. Getnet D, Grosso JF, Goldberg MV, Harris TJ, Yen HR*, et al.* (2010) A role for the transcription factor Helios in human CD4(+)CD25(+) regulatory T cells. Mol Immunol 47: 1595-1600.
275. Exley M, Porcelli S, Furman M, Garcia J, Balk S (1998) CD161 (NKR-P1A) costimulation of CD1d-dependent activation of human T cells expressing invariant V alpha 24 J alpha Q T cell receptor alpha chains. J Exp Med 188: 867-876.
276. Chen YT, Kung JT (2005) CD1d-independent developmental acquisition of prompt IL-4 gene inducibility in thymus CD161(NK1)-CD44lowCD4+CD8- T cells is associated with complementarity determining region 3-diverse and biased Vbeta2/Vbeta7/Vbeta8/Valpha3.2 T cell receptor usage. J Immunol 175: 6537-6550.
277. Kim YC, Bhairavabhotla R, Yoon J, Golding A, Thornton AM*, et al.* (2012) Oligodeoxynucleotides stabilize Helios-expressing Foxp3+ human T regulatory cells during in vitro expansion. Blood 119: 2810-2818.

278. Germain C, Bihl F, Zahn S, Poupon G, Dumaurier MJ*, et al.* (2010) Characterization of alternatively spliced transcript variants of CLEC2D gene. J Biol Chem 285: 36207-36215.
279. Germain C, Meier A, Jensen T, Knapnougel P, Poupon G*, et al.* (2011) Induction of lectin-like transcript 1 (LLT1) protein cell surface expression by pathogens and interferon-gamma contributes to modulate immune responses. J Biol Chem 286: 37964-37975.
280. Pozo D, Vales-Gomez M, Mavaddat N, Williamson SC, Chisholm SE*, et al.* (2006) CD161 (human NKR-P1A) signaling in NK cells involves the activation of acid sphingomyelinase. J Immunol 176: 2397-2406.
281. Rosen DB, Cao W, Avery DT, Tangye SG, Liu YJ*, et al.* (2008) Functional consequences of interactions between human NKR-P1A and its ligand LLT1 expressed on activated dendritic cells and B cells. J Immunol 180: 6508-6517.
282. Aldemir H, Prod'homme V, Dumaurier MJ, Retiere C, Poupon G*, et al.* (2005) Cutting edge: lectin-like transcript 1 is a ligand for the CD161 receptor. J Immunol 175: 7791-7795.
283. Poggi A, Costa P, Morelli L, Cantoni C, Pella N*, et al.* (1996) Expression of human NKRP1A by CD34+ immature thymocytes: NKRP1A-mediated regulation of proliferation and cytolytic activity. Eur J Immunol 26: 1266-1272.
284. Poggi A, Costa P, Zocchi MR, Moretta L (1997) Phenotypic and functional analysis of CD4+ NKRP1A+ human T lymphocytes. Direct evidence that the NKRP1A molecule is involved in transendothelial migration. Eur J Immunol 27: 2345-2350.
285. Rosen DB, Bettadapura J, Alsharifi M, Mathew PA, Warren HS*, et al.* (2005) Cutting edge: lectin-like transcript-1 is a ligand for the inhibitory human NKR-P1A receptor. J Immunol 175: 7796-7799.
286. Yokoyama WM, Plougastel BF (2003) Immune functions encoded by the natural killer gene complex. Nat Rev Immunol 3: 304-316.
287. Carlyle JR, Martin A, Mehra A, Attisano L, Tsui FW*, et al.* (1999) Mouse NKR-P1B, a novel NK1.1 antigen with inhibitory function. J Immunol 162: 5917-5923.
288. Ljutic B, Carlyle JR, Filipp D, Nakagawa R, Julius M*, et al.* (2005) Functional requirements for signaling through the stimulatory and inhibitory mouse NKR-P1 (CD161) NK cell receptors. J Immunol 174: 4789-4796.
289. Dieckmann D, Plottner H, Berchtold S, Berger T, Schuler G (2001) Ex vivo isolation and characterization of CD4(+)CD25(+) T cells with regulatory properties from human blood. J Exp Med 193: 1303-1310.
290. Crome SQ, Clive B, Wang AY, Kang CY, Chow V*, et al.* (2010) Inflammatory effects of ex vivo human Th17 cells are suppressed by regulatory T cells. J Immunol 185: 3199-3208.
291. Ohkura N, Hamaguchi M, Morikawa H, Sugimura K, Tanaka A*, et al.* (2012) T Cell Receptor Stimulation-Induced Epigenetic Changes and Foxp3 Expression Are Independent and Complementary Events Required for Treg Cell Development. Immunity 37: 785-799.
292. Furtado GC, Curotto de Lafaille MA, Kutchukhidze N, Lafaille JJ (2002) Interleukin 2 signaling is required for CD4(+) regulatory T cell function. J Exp Med 196: 851-857.
293. de la Rosa M, Rutz S, Dorninger H, Scheffold A (2004) Interleukin-2 is essential for CD4+CD25+ regulatory T cell function. Eur J Immunol 34: 2480-2488.

294. Chen W, Jin W, Hardegen N, Lei KJ, Li L*, et al.* (2003) Conversion of peripheral CD4+CD25- naive T cells to CD4+CD25+ regulatory T cells by TGF-beta induction of transcription factor Foxp3. J Exp Med 198: 1875-1886.
295. Huter EN, Punkosdy GA, Glass DD, Cheng LI, Ward JM*, et al.* (2008) TGF-beta-induced Foxp3+ regulatory T cells rescue scurfy mice. Eur J Immunol 38: 1814-1821.
296. Azzoni L, Zatsepina O, Abebe B, Bennett IM, Kanakaraj P*, et al.* (1998) Differential transcriptional regulation of CD161 and a novel gene, 197/15a, by IL-2, IL-15, and IL-12 in NK and T cells. J Immunol 161: 3493-3500.
297. Poggi A, Costa P, Tomasello E, Moretta L (1998) IL-12-induced up-regulation of NKRP1A expression in human NK cells and consequent NKRP1A-mediated down-regulation of NK cell activation. Eur J Immunol 28: 1611-1616.
298. Chan SH, Kobayashi M, Santoli D, Perussia B, Trinchieri G (1992) Mechanisms of IFN-gamma induction by natural killer cell stimulatory factor (NKSF/IL-12). Role of transcription and mRNA stability in the synergistic interaction between NKSF and IL-2. J Immunol 148: 92-98.
299. Bettelli E, Carrier Y, Gao W, Korn T, Strom TB*, et al.* (2006) Reciprocal developmental pathways for the generation of pathogenic effector TH17 and regulatory T cells. Nature 441: 235-238.
300. Veldhoen M, Hocking RJ, Atkins CJ, Locksley RM, Stockinger B (2006) TGFbeta in the context of an inflammatory cytokine milieu supports de novo differentiation of IL-17-producing T cells. Immunity 24: 179-189.
301. Crellin NK, Garcia RV, Levings MK (2007) Altered activation of AKT is required for the suppressive function of human CD4+CD25+ T regulatory cells. Blood 109: 2014-2022.
302. Annibali V, Ristori G, Angelini DF, Serafini B, Mechelli R*, et al.* (2011) CD161(high)CD8+T cells bear pathogenetic potential in multiple sclerosis. Brain 134: 542-554.
303. Baecher-Allan CM, Costantino CM, Cvetanovich GL, Ashley CW, Beriou G*, et al.* (2011) CD2 costimulation reveals defective activity by human CD4+CD25(hi) regulatory cells in patients with multiple sclerosis. J Immunol 186: 3317-3326.
304. Campbell DJ, Koch MA (2011) Phenotypical and functional specialization of FOXP3+ regulatory T cells. Nat Rev Immunol 11: 119-130.
305. Daniel V, Naujokat C, Sadeghi M, Weimer R, Renner F*, et al.* (2008) Observational support for an immunoregulatory role of CD3+CD4+CD25+IFN-gamma+ blood lymphocytes in kidney transplant recipients with good long-term graft outcome. Transpl Int 21: 646-660.
306. Kulkarni A, Paranjape R, Thakar M (2012) Expansion of Defective NK Cells in Early HIV Type 1C Infection: A Consequence of Reduced CD161 Expression. AIDS Res Hum Retroviruses 28: 100-105.
307. Singleterry WL, Henderson H, Cruse JM (2012) Depletion of pro-inflammatory CD161(+) double negative (CD3(+)CD4(-)CD8(-)) T cells in AIDS patients is ameliorated by expansion of the gammadelta T cell population. Exp Mol Pathol 92: 155-159.
308. Petty RE (2001) Growing pains: the ILAR classification of juvenile idiopathic arthritis. J Rheumatol 28: 927-928.

309. Lanier LL, Chang C, Phillips JH (1994) Human NKR-P1A. A disulfide-linked homodimer of the C-type lectin superfamily expressed by a subset of NK and T lymphocytes. J Immunol 153: 2417-2428.
310. Billerbeck E, Kang YH, Walker L, Lockstone H, Grafmueller S*, et al.* (2010) Analysis of CD161 expression on human CD8+ T cells defines a distinct functional subset with tissue-homing properties. Proc Natl Acad Sci U S A 107: 3006-3011.
311. Kleinschek MA, Boniface K, Sadekova S, Grein J, Murphy EE*, et al.* (2009) Circulating and gut-resident human Th17 cells express CD161 and promote intestinal inflammation. J Exp Med 206: 525-534.
312. Poggi A, Costa P, Zocchi MR, Moretta L (1997) NKRP1A molecule is involved in transendothelial migration of CD4+ human T lymphocytes. Immunol Lett 57: 121-123.
313. Fogal B, Yi T, Wang C, Rao DA, Lebastchi A*, et al.* (2011) Neutralizing IL-6 reduces human arterial allograft rejection by allowing emergence of CD161(+) CD4(+) regulatory T cells. J Immunol 187: 6268-6280.
314. Round JL, Mazmanian SK (2010) Inducible Foxp3+ regulatory T-cell development by a commensal bacterium of the intestinal microbiota. Proceedings of the National Academy of Sciences 107: 12204-12209.
315. Ostman S, Rask C, Wold AE, Hultkrantz S, Telemo E (2006) Impaired regulatory T cell function in germ-free mice. Eur J Immunol 36: 2336-2346.
316. Yamada H, Nakashima Y, Okazaki K, Mawatari T, Fukushi JI*, et al.* (2011) Preferential Accumulation of Activated Th1 Cells Not Only in Rheumatoid Arthritis But Also in Osteoarthritis Joints. J Rheumatol.
317. Mitsuo A, Morimoto S, Nakiri Y, Suzuki J, Kaneko H*, et al.* (2006) Decreased CD161+CD8+ T cells in the peripheral blood of patients suffering from rheumatic diseases. Rheumatology (Oxford) 45: 1477-1484.
318. Maggi L, Capone M, Giudici F, Santarlasci V, Querci V*, et al.* (2012) CD4+CD161+ T Lymphocytes Infiltrate Crohn's Disease-Associated Perianal Fistulas and Are Reduced by Anti-TNF-alpha Local Therapy. Int Arch Allergy Immunol 161: 81-86.
319. Sondergaard HB, Sellebjerg F, Hillert J, Olsson T, Kockum I*, et al.* (2011) Alterations in KLRB1 gene expression and a Scandinavian multiple sclerosis association study of the KLRB1 SNP rs4763655. Eur J Hum Genet.
320. Poggi A, Canevali P, Contatore M, Ciprandi G (2012) Higher Frequencies of CD161 Circulating T Lymphocytes in Allergic Rhinitis Patients Compared to Healthy Donors. Int Arch Allergy Immunol 158: 151-156.
321. Gonzalez-Hernandez Y, Pedraza-Sanchez S, Blandon-Vijil V, del Rio-Navarro BE, Vaughan G*, et al.* (2007) Peripheral blood CD161+ T cells from asthmatic patients are activated during asthma attack and predominantly produce IFN-gamma. Scand J Immunol 65: 368-375.
322. Jacobs R, Weber K, Wendt K, Heiken H, Schmidt RE (2004) Altered coexpression of lectin-like receptors CD94 and CD161 on NK and T cells in HIV patients. J Clin Immunol 24: 281-286.
323. Prendergast A, Prado JG, Kang YH, Chen F, Riddell LA*, et al.* (2010) HIV-1 infection is characterized by profound depletion of CD161+ Th17 cells and gradual decline in regulatory T cells. Aids 24: 491-502.
324. Gurney KB, Yang OO, Wilson SB, Uittenbogaart CH (2002) TCR gamma delta+ and CD161+ thymocytes express HIV-1 in the SCID-hu mouse, potentially contributing to immune dysfunction in HIV infection. J Immunol 169: 5338-5346.

325. Walker LJ, Kang YH, Smith MO, Tharmalingham H, Ramamurthy N*, et al.* (2012) Human MAIT and CD8alphaalpha cells develop from a pool of type-17 precommitted CD8+ T cells. Blood 119: 422-433.
326. Cosgrove C, Ussher JE, Rauch A, Gartner K, Kurioka A*, et al.* (2013) Early and nonreversible decrease of CD161++ /MAIT cells in HIV infection. Blood 121: 951-961.
327. Northfield JW, Kasprowicz V, Lucas M, Kersting N, Bengsch B*, et al.* (2008) CD161 expression on hepatitis C virus-specific CD8+ T cells suggests a distinct pathway of T cell differentiation. Hepatology 47: 396-406.
328. Gernez Y, Tirouvanziam R, Nguyen KD, Herzenberg LA, Krensky AM*, et al.* (2007) Altered phosphorylated signal transducer and activator of transcription profile of CD4+CD161+ T cells in asthma: modulation by allergic status and oral corticosteroids. J Allergy Clin Immunol 120: 1441-1448.
329. Takahashi T, Dejbakhsh-Jones S, Strober S (2006) Expression of CD161 (NKR-P1A) defines subsets of human CD4 and CD8 T cells with different functional activities. J Immunol 176: 211-216.
330. Kalsheker N, Swanson T (1990) Exclusion of an exon in monocyte alpha-1-antitrypsin mRNA after stimulation of U937 cells by interleukin-6. Biochem Biophys Res Commun 172: 1116-1121.
331. Ford NR, Miller HE, Reeme AE, Waukau J, Bengtson C*, et al.* (2012) Inflammatory Signals Direct Expression of Human IL12RB1 into Multiple Distinct Isoforms. The Journal of Immunology 189: 4684-4694.
332. Ortis F, Naamane N, Flamez D, LadriV®re L, Moore F*, et al.* (2010) Cytokines Interleukin-1Œ≤ and Tumor Necrosis Factor-Œ± Regulate Different Transcriptional and Alternative Splicing Networks in Primary Œ≤-Cells. Diabetes 59: 358-374.
333. Eizirik DcL, Sammeth M, Bouckenooghe T, Bottu G, Sisino G*, et al.* (2012) The human pancreatic islet transcriptome: expression of candidate genes for type 1 diabetes and the impact of pro-inflammatory cytokines. PLoS genetics 8: e1002552.
334. Yip L, Su L, Sheng D, Chang P, Atkinson M*, et al.* (2009) Deaf1 isoforms control the expression of genes encoding peripheral tissue antigens in the pancreatic lymph nodes during type 1 diabetes. Nat Immunol 10: 1026-1033.
335. Bartoli M, Taro M, Magni-Manzoni S, Pistorio A, Traverso F*, et al.* (2008) The magnitude of early response to methotrexate therapy predicts long-term outcome of patients with juvenile idiopathic arthritis. Ann Rheum Dis 67: 370-374.
336. Shenoi S, Wallace CA (2010) Remission in juvenile idiopathic arthritis: current facts. Curr Rheumatol Rep 12: 80-86.
337. Tynjala P, Vahasalo P, Tarkiainen M, Kroger L, Aalto K*, et al.* (2011) Aggressive combination drug therapy in very early polyarticular juvenile idiopathic arthritis (ACUTE-JIA): a multicentre randomised open-label clinical trial. Ann Rheum Dis 70: 1605-1612.
338. Wallace CA, Giannini EH, Spalding SJ, Hashkes PJ, O'Neil KM*, et al.* (2012) Trial of early aggressive therapy in polyarticular juvenile idiopathic arthritis. Arthritis Rheum 64: 2012-2021.

339. Albers HM, Wessels JA, van der Straaten RJ, Brinkman DM, Suijlekom-Smit LW*, et al.* (2009) Time to treatment as an important factor for the response to methotrexate in juvenile idiopathic arthritis. Arthritis Rheum 61: 46-51.
340. Packham JC, Hall MA (2002) Long-term follow-up of 246 adults with juvenile idiopathic arthritis: functional outcome. Rheumatology (Oxford) 41: 1428-1435.
341. Hashkes PJ, Laxer RM (2006) Update on the medical treatment of juvenile idiopathic arthritis. Curr Rheumatol Rep 8: 450-458.
342. Ungar WJ, Costa V, Burnett HF, Feldman BM, Laxer RM (2013) The use of biologic response modifiers in polyarticular-course juvenile idiopathic arthritis: A systematic review. Semin Arthritis Rheum.
343. Moncrieffe H, Ursu S, Holzinger D, Patrick F, Kassoumeri L*, et al.* (2013) A subgroup of juvenile idiopathic arthritis patients who respond well to methotrexate are identified by the serum biomarker MRP8/14 protein. Rheumatology (Oxford).

9. List of publications arising from this work or contributed to during this PhD programme

*: joint first authors

Published:

Pesenacker A M, Bending D, Ursu S, Wu Q, Nistala K, Wedderburn L R. **CD161 defines the subset of FoxP3+ T cells capable of producing pro-inflammatory cytokines** (2013), *Blood,* 121(14), 2647-2658

Omoyinmi E*, Hamaoui R*, Pesenacker A, Nistala K, Moncrieffe H, Ursu S, Wedderburn L R, and Woo P. **Th1 and Th17 cell subpopulations are enriched in the peripheral blood of patients with systemic juvenile idiopathic arthritis.** (2012), *Rheumatology*; 51(10), 1881-6

Under review:

Pesenacker A M and Wedderburn L R. **T regulatory cells in childhood arthritis - novel insights.** *Expert Reviews in Molecular Medicine*

In preparation:

Wu Q*, Pesenacker A M*, Stansfield A, King D, Barge D, Abinun M, Foster H E, Wedderburn L R. **Immune reconstitution and T cell receptor clonal diversity in children with systemic juvenile idiopathic arthritis undergoing T cell depleted autologous stem cell transplantation.** in preparation

Piper C*, Pesenacker A M*, Varsani H, Wedderburn L R, Nistala K. **GM-CSF expression within the inflamed joint is explained by the enrichment of ex-Th17 cells.** in preparation

Ursu S, Pesenacker A M, Zheng D, Gordon-smith S B, Lerose A, Eaton S, Wedderburn L R, Moncrieffe H. **Autoimmune susceptibility gene critically influences CD39 T cell expression and function in modulating human inflammation**. in preparation

10. Appendices

Appendix I: VIPR1 isoform sequence alignment

Using Biology WorkBench 3.2 (workbench.sdc.edu); CLUSTAL W (1.81) multiple sequence alignment[255]

key : */blue letters: single, fully conserved residue, consensus
space: no consensus
| vertical line + residue ~~strikethrough~~: EXON EXON BREAK
BOLD + underlined: ATG: start of protein translation, TGA: stop of translation
Numbers above each sequence: position from start of sequence
Below: protein sequence
Highlighted: VIPR1 primers: FW: forward, RV: reverse, RT: used for real-time PCR

Primer 1: grey FW	Primer 2: pink FW	Primer 3: red FW	Primer 4: green FW
Primer 5: turquoise FW	Primer 6,7: yellow FW + RV	Primer 8: tile RT FW	Primer 9: tile RT RV
Primer 10: turquoise RV	Primer 11: yellow RV	Primer 12: green RV	

```
VIPR1_Ref_seq_mRNA      --------------------------------------------------
VIPR1_202_by_ensembl    --------------------------------------------------
                        1                                                50
VIPR1_002_by_ensembl    ATTTTCCCAGCTTACTAGTGGAAAAGCAGCTTCTTTCCCACAGTTCCAGC

VIPR1_Ref_seq_mRNA      --------------------------------------------------
VIPR1_202_by_ensembl    --------------------------------------------------
                                                                        100
VIPR1_002_by_ensembl    AAAAGCCCCAGGGCTGATGCTCATTGGCCCAGGTTGGGGCATGTGACCAT

VIPR1_Ref_seq_mRNA      --------------------------------------------------
VIPR1_202_by_ensembl    --------------------------------------------------
                                                                        150
VIPR1_002_by_ensembl    TGGCAAGACTCCCATTGGCCAGGCCTGGGGCAGGTGCTCACTACTGGAGC

VIPR1_Ref_seq_mRNA      --------------------------------------------------
VIPR1_202_by_ensembl    --------------------------------------------------
                                                                        200
VIPR1_002_by_ensembl    CAGAGCGGAGTATAAGCCCTACCCAATCACTGAACTACGTGGGTCAAGAG

VIPR1_Ref_seq_mRNA      --------------------------------------------------
VIPR1_202_by_ensembl    --------------------------------------------------
                                                                        250
VIPR1_002_by_ensembl    TAAAGGAGCTGTGGCTTCCCCCCAATCAGAAGGGCACTGGATGATGGATG

VIPR1_Ref_seq_mRNA      --------------------------------------------------
VIPR1_202_by_ensembl    --------------------------------------------------
                                                                        300
VIPR1_002_by_ensembl    AACTCTGTGTGGTGCGTCTTCACACTGACACCAGGAGGATAAGGAAGTGA

VIPR1_Ref_seq_mRNA      --------------------------------------------------
VIPR1_202_by_ensembl    --------------------------------------------------
                                                                        350
VIPR1_002_by_ensembl    CTCCCTCAGCTGAGTGGCTGGCATGTGCCAGGCTAGAGCAGCTTGGCTAT

                                          Exon 1
                                          1                           36
VIPR1_Ref_seq_mRNA      ----------CTCTTAGCTCTGGGGCCACAGCGCCAGCGCCACTC-T
                                          1                           36
VIPR1_202_by_ensembl    ----------CTCTTAGCTCTGGGGCCACAGCGCCAGCGCCACTC-T
                                                                        400
VIPR1_002_by_ensembl    GGCAGAACATCCAGCCCCACCGTGTGGACGGCAGAGATGAGGAAACTGGT
                                  *  * *    ** * | *** *     *  ***  *
```

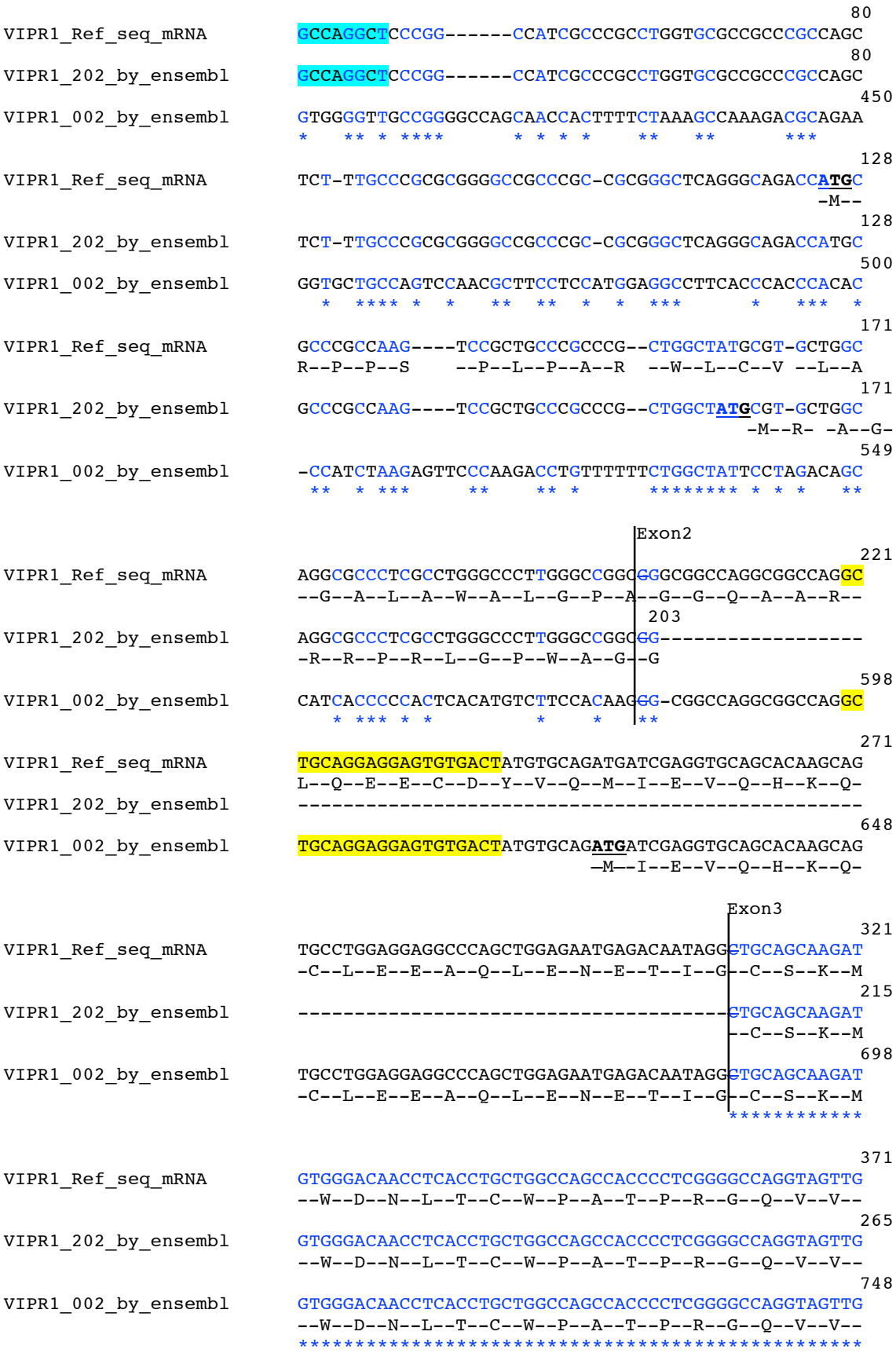
VIPR1_Ref_seq_mRNA
VIPR1_202_by_ensembl
VIPR1_002_by_ensembl
Exon2
Exon3

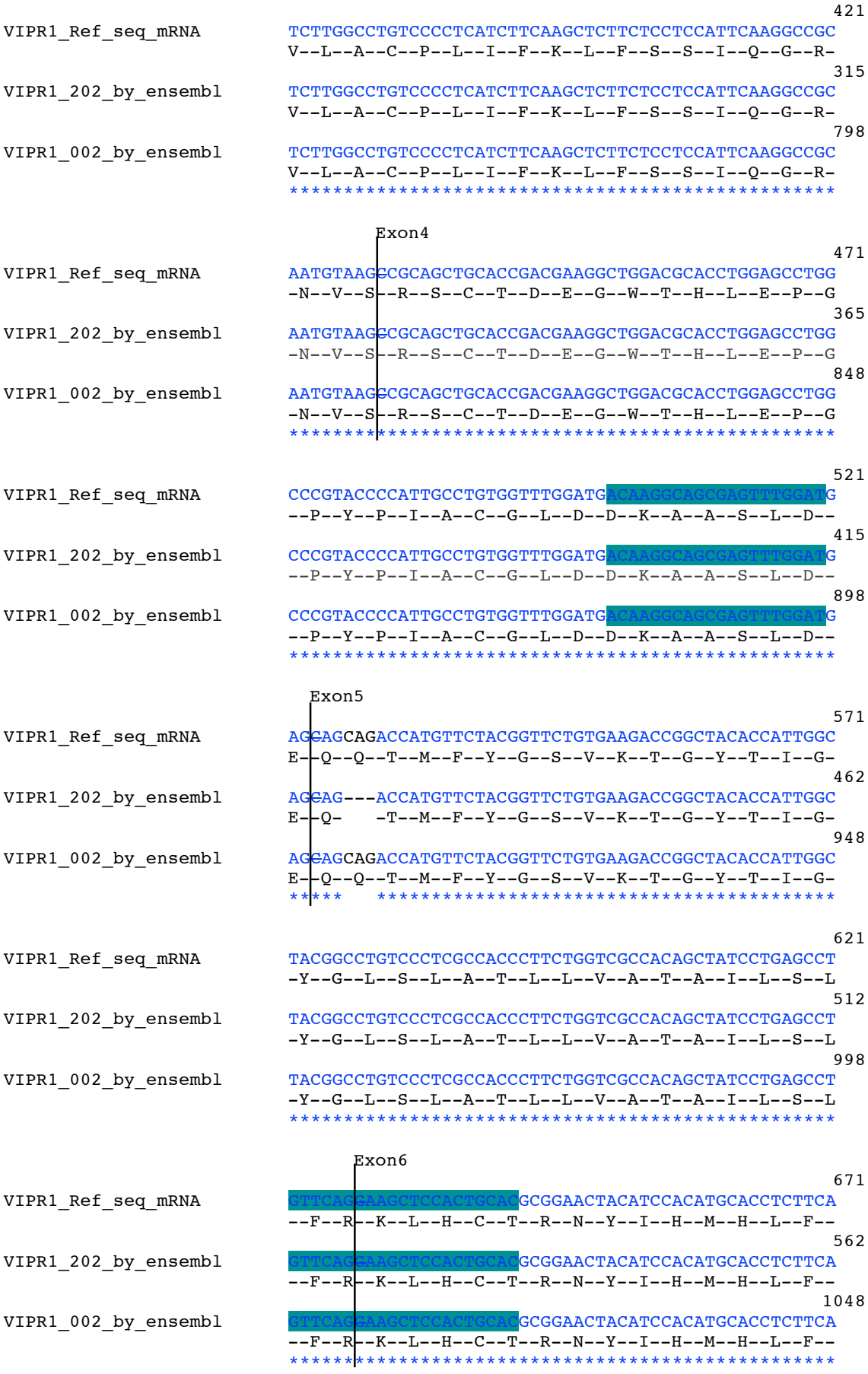
421
VIPR1_Ref_seq_mRNA TCTTGGCCTGTCCCCTCATCTTCAAGCTCTTCTCCTCCATTCAAGGCCGC
V--L--A--C--P--L--I--F--K--L--F--S--S--I--Q--G--R-
315
VIPR1_202_by_ensembl TCTTGGCCTGTCCCCTCATCTTCAAGCTCTTCTCCTCCATTCAAGGCCGC
V--L--A--C--P--L--I--F--K--L--F--S--S--I--Q--G--R-
798
VIPR1_002_by_ensembl TCTTGGCCTGTCCCCTCATCTTCAAGCTCTTCTCCTCCATTCAAGGCCGC
V--L--A--C--P--L--I--F--K--L--F--S--S--I--Q--G--R-
****
Exon4
471
VIPR1_Ref_seq_mRNA AATGTAAGCCGCAGCTGCACCGACGAAGGCTGGACGCACCTGGAGCCTGG
-N--V--S--R--S--C--T--D--E--G--W--T--H--L--E--P--G
365
VIPR1_202_by_ensembl AATGTAAGCCGCAGCTGCACCGACGAAGGCTGGACGCACCTGGAGCCTGG
-N--V--S--R--S--C--T--D--E--G--W--T--H--L--E--P--G
848
VIPR1_002_by_ensembl AATGTAAGCCGCAGCTGCACCGACGAAGGCTGGACGCACCTGGAGCCTGG
-N--V--S--R--S--C--T--D--E--G--W--T--H--L--E--P--G
****
521
VIPR1_Ref_seq_mRNA CCCGTACCCCATTGCCTGTGGTTTGGATGACAAGGCAGCGAGTTTGGATG
--P--Y--P--I--A--C--G--L--D--D--K--A--A--S--L--D--
415
VIPR1_202_by_ensembl CCCGTACCCCATTGCCTGTGGTTTGGATGACAAGGCAGCGAGTTTGGATG
--P--Y--P--I--A--C--G--L--D--D--K--A--A--S--L--D--
898
VIPR1_002_by_ensembl CCCGTACCCCATTGCCTGTGGTTTGGATGACAAGGCAGCGAGTTTGGATG
--P--Y--P--I--A--C--G--L--D--D--K--A--A--S--L--D--
****
Exon5
571
VIPR1_Ref_seq_mRNA AGCCAGCAGACCATGTTCTACGGTTCTGTGAAGACCGGCTACACCATTGGC
E--Q--Q--T--M--F--Y--G--S--V--K--T--G--Y--T--I--G-
462
VIPR1_202_by_ensembl AGCCAG---ACCATGTTCTACGGTTCTGTGAAGACCGGCTACACCATTGGC
E--Q- -T--M--F--Y--G--S--V--K--T--G--Y--T--I--G-
948
VIPR1_002_by_ensembl AGCCAGCAGACCATGTTCTACGGTTCTGTGAAGACCGGCTACACCATTGGC
E--Q--Q--T--M--F--Y--G--S--V--K--T--G--Y--T--I--G-
***** **********
621
VIPR1_Ref_seq_mRNA TACGGCCTGTCCCTCGCCACCCTTCTGGTCGCCACAGCTATCCTGAGCCT
-Y--G--L--S--L--A--T--L--L--V--A--T--A--I--L--S--L
512
VIPR1_202_by_ensembl TACGGCCTGTCCCTCGCCACCCTTCTGGTCGCCACAGCTATCCTGAGCCT
-Y--G--L--S--L--A--T--L--L--V--A--T--A--I--L--S--L
998
VIPR1_002_by_ensembl TACGGCCTGTCCCTCGCCACCCTTCTGGTCGCCACAGCTATCCTGAGCCT
-Y--G--L--S--L--A--T--L--L--V--A--T--A--I--L--S--L
****
Exon6
671
VIPR1_Ref_seq_mRNA GTTCAGGAAGCTCCACTGCACGCGGAACTACATCCACATGCACCTCTTCA
--F--R--K--L--H--C--T--R--N--Y--I--H--M--H--L--F--
562
VIPR1_202_by_ensembl GTTCAGGAAGCTCCACTGCACGCGGAACTACATCCACATGCACCTCTTCA
--F--R--K--L--H--C--T--R--N--Y--I--H--M--H--L--F--
1048
VIPR1_002_by_ensembl GTTCAGGAAGCTCCACTGCACGCGGAACTACATCCACATGCACCTCTTCA
--F--R--K--L--H--C--T--R--N--Y--I--H--M--H--L--F--
****

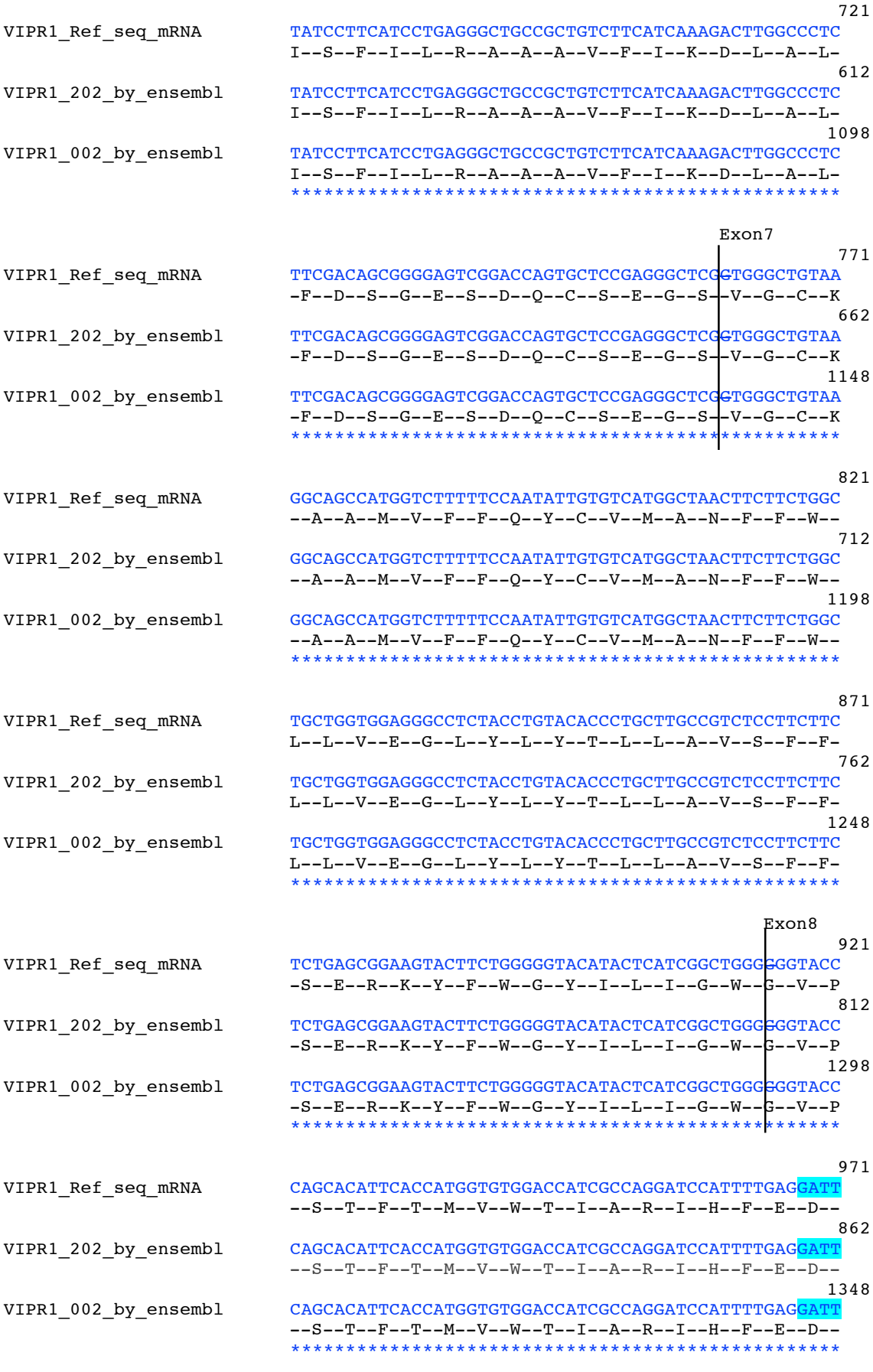
721
VIPR1_Ref_seq_mRNA
TATCCTTCATCCTGAGGGCTGCCGCTGTCTTCATCAAAGACTTGGCCCTC
I--S--F--I--L--R--A--A--A--V--F--I--K--D--L--A--L-
612
VIPR1_202_by_ensembl
TATCCTTCATCCTGAGGGCTGCCGCTGTCTTCATCAAAGACTTGGCCCTC
I--S--F--I--L--R--A--A--A--V--F--I--K--D--L--A--L-
1098
VIPR1_002_by_ensembl
TATCCTTCATCCTGAGGGCTGCCGCTGTCTTCATCAAAGACTTGGCCCTC
I--S--F--I--L--R--A--A--A--V--F--I--K--D--L--A--L-
****
Exon7
771
VIPR1_Ref_seq_mRNA
TTCGACAGCGGGGAGTCGGACCAGTGCTCCGAGGGCTCGGTGGGCTGTAA
-F--D--S--G--E--S--D--Q--C--S--E--G--S--V--G--C--K
662
VIPR1_202_by_ensembl
TTCGACAGCGGGGAGTCGGACCAGTGCTCCGAGGGCTCGGTGGGCTGTAA
-F--D--S--G--E--S--D--Q--C--S--E--G--S--V--G--C--K
1148
VIPR1_002_by_ensembl
TTCGACAGCGGGGAGTCGGACCAGTGCTCCGAGGGCTCGGTGGGCTGTAA
-F--D--S--G--E--S--D--Q--C--S--E--G--S--V--G--C--K
****
821
VIPR1_Ref_seq_mRNA
GGCAGCCATGGTCTTTTTCCAATATTGTGTCATGGCTAACTTCTTCTGGC
--A--A--M--V--F--F--Q--Y--C--V--M--A--N--F--F--W--
712
VIPR1_202_by_ensembl
GGCAGCCATGGTCTTTTTCCAATATTGTGTCATGGCTAACTTCTTCTGGC
--A--A--M--V--F--F--Q--Y--C--V--M--A--N--F--F--W--
1198
VIPR1_002_by_ensembl
GGCAGCCATGGTCTTTTTCCAATATTGTGTCATGGCTAACTTCTTCTGGC
--A--A--M--V--F--F--Q--Y--C--V--M--A--N--F--F--W--
****
871
VIPR1_Ref_seq_mRNA
TGCTGGTGGAGGGCCTCTACCTGTACACCCTGCTTGCCGTCTCCTTCTTC
L--L--V--E--G--L--Y--L--Y--T--L--L--A--V--S--F--F-
762
VIPR1_202_by_ensembl
TGCTGGTGGAGGGCCTCTACCTGTACACCCTGCTTGCCGTCTCCTTCTTC
L--L--V--E--G--L--Y--L--Y--T--L--L--A--V--S--F--F-
1248
VIPR1_002_by_ensembl
TGCTGGTGGAGGGCCTCTACCTGTACACCCTGCTTGCCGTCTCCTTCTTC
L--L--V--E--G--L--Y--L--Y--T--L--L--A--V--S--F--F-
****
Exon8
921
VIPR1_Ref_seq_mRNA
TCTGAGCGGAAGTACTTCTGGGGGTACATACTCATCGGCTGGGGGGTACC
-S--E--R--K--Y--F--W--G--Y--I--L--I--G--W--G--V--P
812
VIPR1_202_by_ensembl
TCTGAGCGGAAGTACTTCTGGGGGTACATACTCATCGGCTGGGGGGTACC
-S--E--R--K--Y--F--W--G--Y--I--L--I--G--W--G--V--P
1298
VIPR1_002_by_ensembl
TCTGAGCGGAAGTACTTCTGGGGGTACATACTCATCGGCTGGGGGGTACC
-S--E--R--K--Y--F--W--G--Y--I--L--I--G--W--G--V--P
****
971
VIPR1_Ref_seq_mRNA
CAGCACATTCACCATGGTGTGGACCATCGCCAGGATCCATTTTGAGGATT
--S--T--F--T--M--V--W--T--I--A--R--I--H--F--E--D--
862
VIPR1_202_by_ensembl
CAGCACATTCACCATGGTGTGGACCATCGCCAGGATCCATTTTGAGGATT
--S--T--F--T--M--V--W--T--I--A--R--I--H--F--E--D--
1348
VIPR1_002_by_ensembl
CAGCACATTCACCATGGTGTGGACCATCGCCAGGATCCATTTTGAGGATT
--S--T--F--T--M--V--W--T--I--A--R--I--H--F--E--D--
****

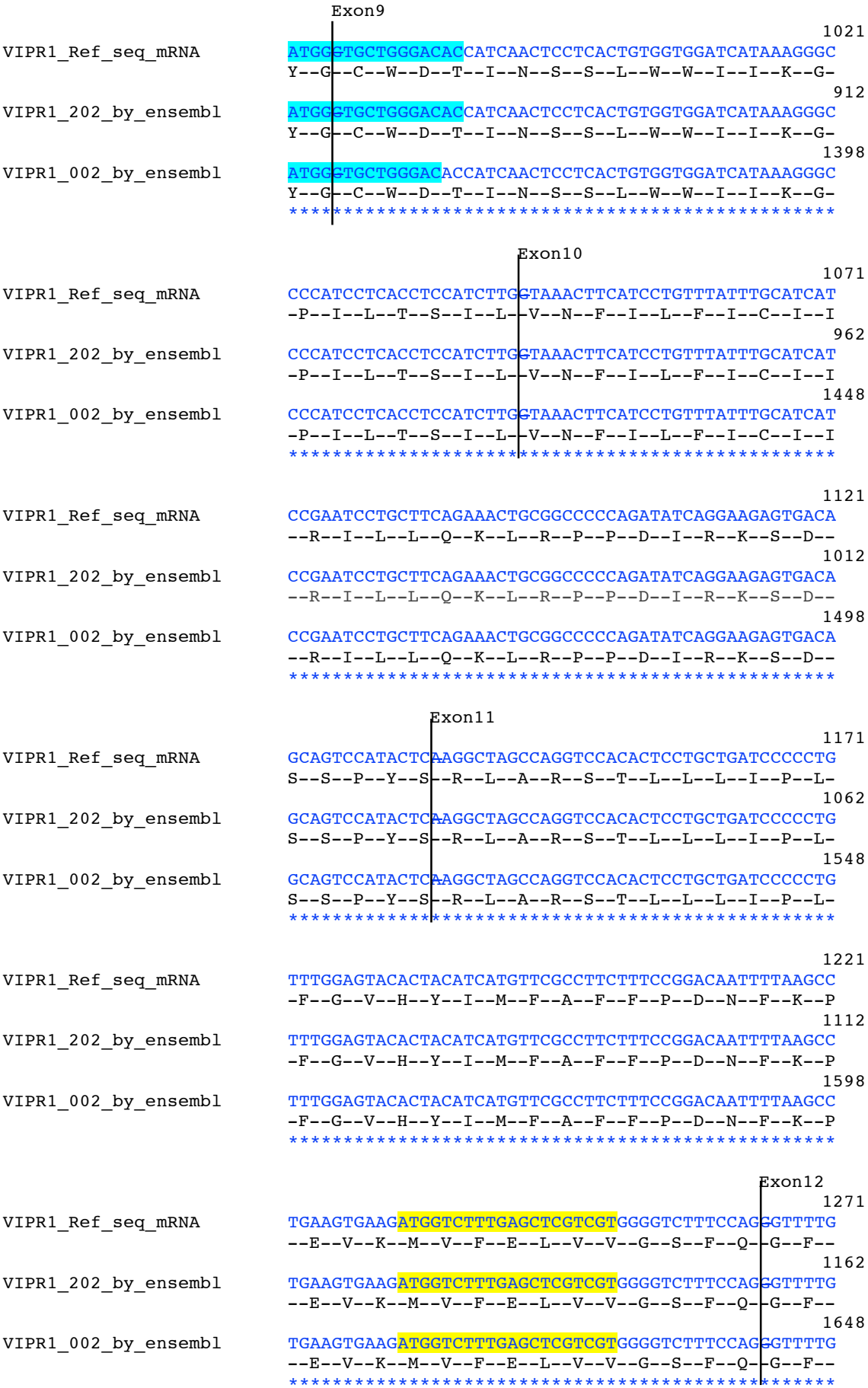
Exon9
1021
VIPR1_Ref_seq_mRNA
ATGGGTGCTGGGACACCATCAACTCCTCACTGTGGTGGATCATAAAGGGC
Y--G--C--W--D--T--I--N--S--S--L--W--W--I--I--K--G-
912
VIPR1_202_by_ensembl
ATGGGTGCTGGGACACCATCAACTCCTCACTGTGGTGGATCATAAAGGGC
Y--G--C--W--D--T--I--N--S--S--L--W--W--I--I--K--G-
1398
VIPR1_002_by_ensembl
ATGGGTGCTGGGACACCATCAACTCCTCACTGTGGTGGATCATAAAGGGC
Y--G--C--W--D--T--I--N--S--S--L--W--W--I--I--K--G-
Exon10
1071
VIPR1_Ref_seq_mRNA
CCCATCCTCACCTCCATCTTGGTAAACTTCATCCTGTTTATTTGCATCAT
-P--I--L--T--S--I--L--V--N--F--I--L--F--I--C--I--I
962
VIPR1_202_by_ensembl
CCCATCCTCACCTCCATCTTGGTAAACTTCATCCTGTTTATTTGCATCAT
-P--I--L--T--S--I--L--V--N--F--I--L--F--I--C--I--I
1448
VIPR1_002_by_ensembl
CCCATCCTCACCTCCATCTTGGTAAACTTCATCCTGTTTATTTGCATCAT
-P--I--L--T--S--I--L--V--N--F--I--L--F--I--C--I--I
1121
VIPR1_Ref_seq_mRNA
CCGAATCCTGCTTCAGAAACTGCGGCCCCCAGATATCAGGAAGAGTGACA
--R--I--L--L--Q--K--L--R--P--P--D--I--R--K--S--D--
1012
VIPR1_202_by_ensembl
CCGAATCCTGCTTCAGAAACTGCGGCCCCCAGATATCAGGAAGAGTGACA
--R--I--L--L--Q--K--L--R--P--P--D--I--R--K--S--D--
1498
VIPR1_002_by_ensembl
CCGAATCCTGCTTCAGAAACTGCGGCCCCCAGATATCAGGAAGAGTGACA
--R--I--L--L--Q--K--L--R--P--P--D--I--R--K--S--D--
Exon11
1171
VIPR1_Ref_seq_mRNA
GCAGTCCATACTCAAGGCTAGCCAGGTCCACACTCCTGCTGATCCCCCTG
S--S--P--Y--S--R--L--A--R--S--T--L--L--L--I--P--L-
1062
VIPR1_202_by_ensembl
GCAGTCCATACTCAAGGCTAGCCAGGTCCACACTCCTGCTGATCCCCCTG
S--S--P--Y--S--R--L--A--R--S--T--L--L--L--I--P--L-
1548
VIPR1_002_by_ensembl
GCAGTCCATACTCAAGGCTAGCCAGGTCCACACTCCTGCTGATCCCCCTG
S--S--P--Y--S--R--L--A--R--S--T--L--L--L--I--P--L-
1221
VIPR1_Ref_seq_mRNA
TTTGGAGTACACTACATCATGTTCGCCTTCTTTCCGGACAATTTTAAGCC
-F--G--V--H--Y--I--M--F--A--F--F--P--D--N--F--K--P
1112
VIPR1_202_by_ensembl
TTTGGAGTACACTACATCATGTTCGCCTTCTTTCCGGACAATTTTAAGCC
-F--G--V--H--Y--I--M--F--A--F--F--P--D--N--F--K--P
1598
VIPR1_002_by_ensembl
TTTGGAGTACACTACATCATGTTCGCCTTCTTTCCGGACAATTTTAAGCC
-F--G--V--H--Y--I--M--F--A--F--F--P--D--N--F--K--P
Exon12
1271
VIPR1_Ref_seq_mRNA
TGAAGTGAAGATGGTCTTTGAGCTCGTCGTGGGGTCTTTCCAGGGTTTTG
--E--V--K--M--V--F--E--L--V--V--G--S--F--Q--G--F--
1162
VIPR1_202_by_ensembl
TGAAGTGAAGATGGTCTTTGAGCTCGTCGTGGGGTCTTTCCAGGGTTTTG
--E--V--K--M--V--F--E--L--V--V--G--S--F--Q--G--F--
1648
VIPR1_002_by_ensembl
TGAAGTGAAGATGGTCTTTGAGCTCGTCGTGGGGTCTTTCCAGGGTTTTG
--E--V--K--M--V--F--E--L--V--V--G--S--F--Q--G--F--

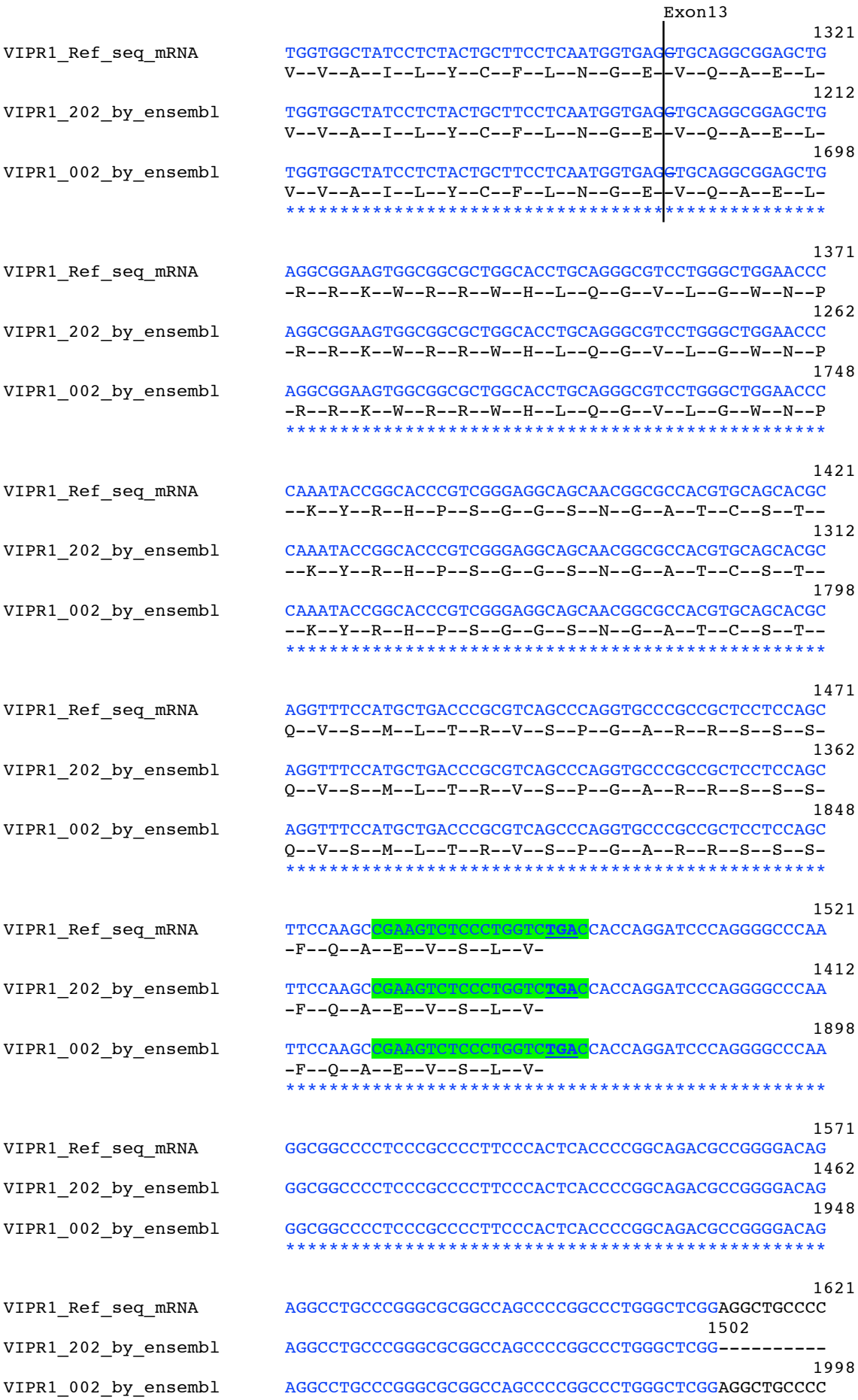
Exon13
1321
VIPR1_Ref_seq_mRNA TGGTGGCTATCCTCTACTGCTTCCTCAATGGTGAGGTGCAGGCGGAGCTG
V--V--A--I--L--Y--C--F--L--N--G--E--V--Q--A--E--L-
1212
VIPR1_202_by_ensembl TGGTGGCTATCCTCTACTGCTTCCTCAATGGTGAGGTGCAGGCGGAGCTG
V--V--A--I--L--Y--C--F--L--N--G--E--V--Q--A--E--L-
1698
VIPR1_002_by_ensembl TGGTGGCTATCCTCTACTGCTTCCTCAATGGTGAGGTGCAGGCGGAGCTG
V--V--A--I--L--Y--C--F--L--N--G--E--V--Q--A--E--L-
1371
VIPR1_Ref_seq_mRNA AGGCGGAAGTGGCGGCGCTGGCACCTGCAGGGCGTCCTGGGCTGGAACCC
-R--R--K--W--R--R--W--H--L--Q--G--V--L--G--W--N--P
1262
VIPR1_202_by_ensembl AGGCGGAAGTGGCGGCGCTGGCACCTGCAGGGCGTCCTGGGCTGGAACCC
-R--R--K--W--R--R--W--H--L--Q--G--V--L--G--W--N--P
1748
VIPR1_002_by_ensembl AGGCGGAAGTGGCGGCGCTGGCACCTGCAGGGCGTCCTGGGCTGGAACCC
-R--R--K--W--R--R--W--H--L--Q--G--V--L--G--W--N--P
1421
VIPR1_Ref_seq_mRNA CAAATACCGGCACCCGTCGGGAGGCAGCAACGGCGCCACGTGCAGCACGC
--K--Y--R--H--P--S--G--G--S--N--G--A--T--C--S--T--
1312
VIPR1_202_by_ensembl CAAATACCGGCACCCGTCGGGAGGCAGCAACGGCGCCACGTGCAGCACGC
--K--Y--R--H--P--S--G--G--S--N--G--A--T--C--S--T--
1798
VIPR1_002_by_ensembl CAAATACCGGCACCCGTCGGGAGGCAGCAACGGCGCCACGTGCAGCACGC
--K--Y--R--H--P--S--G--G--S--N--G--A--T--C--S--T--
1471
VIPR1_Ref_seq_mRNA AGGTTTCCATGCTGACCCGCGTCAGCCCAGGTGCCCGCCGCTCCTCCAGC
Q--V--S--M--L--T--R--V--S--P--G--A--R--R--S--S--S-
1362
VIPR1_202_by_ensembl AGGTTTCCATGCTGACCCGCGTCAGCCCAGGTGCCCGCCGCTCCTCCAGC
Q--V--S--M--L--T--R--V--S--P--G--A--R--R--S--S--S-
1848
VIPR1_002_by_ensembl AGGTTTCCATGCTGACCCGCGTCAGCCCAGGTGCCCGCCGCTCCTCCAGC
Q--V--S--M--L--T--R--V--S--P--G--A--R--R--S--S--S-
1521
VIPR1_Ref_seq_mRNA TTCCAAGCCGAAGTCTCCCTGGTCTGACCACCAGGATCCCAGGGGCCCAA
-F--Q--A--E--V--S--L--V-
1412
VIPR1_202_by_ensembl TTCCAAGCCGAAGTCTCCCTGGTCTGACCACCAGGATCCCAGGGGCCCAA
-F--Q--A--E--V--S--L--V-
1898
VIPR1_002_by_ensembl TTCCAAGCCGAAGTCTCCCTGGTCTGACCACCAGGATCCCAGGGGCCCAA
-F--Q--A--E--V--S--L--V-
1571
VIPR1_Ref_seq_mRNA GGCGGCCCCTCCCGCCCCTTCCCACTCACCCCGGCAGACGCCGGGGACAG
1462
VIPR1_202_by_ensembl GGCGGCCCCTCCCGCCCCTTCCCACTCACCCCGGCAGACGCCGGGGACAG
1948
VIPR1_002_by_ensembl GGCGGCCCCTCCCGCCCCTTCCCACTCACCCCGGCAGACGCCGGGGACAG
1621
VIPR1_Ref_seq_mRNA AGGCCTGCCCGGGCGCGGCCAGCCCCGGCCCTGGGCTCGGAGGCTGCCCC
1502
VIPR1_202_by_ensembl AGGCCTGCCCGGGCGCGGCCAGCCCCGGCCCTGGGCTCGG----------
1998
VIPR1_002_by_ensembl AGGCCTGCCCGGGCGCGGCCAGCCCCGGCCCTGGGCTCGGAGGCTGCCCC

```
                                                                    1671
VIPR1_Ref_seq_mRNA        CGGCCCCCTGGTCTCTGGTCCGGACACTCCTAGAGAACGCAGCCCTAGAG
VIPR1_202_by_ensembl      ------------------------------------------------
                                                                    2048
VIPR1_002_by_ensembl      CGGCCCCCTGGTCTCTGGTCCGGACACTCCTAGAGAACGCAGCCCTAGAG

                                                                    1721
VIPR1_Ref_seq_mRNA        CCTGCCTGGAGCGTTTCTAGCAAGTGAGAGAGATGGGAGCTCCTCTCCTG
VIPR1_202_by_ensembl      ------------------------------------------------
                                                                    2098
VIPR1_002_by_ensembl      CCTGCCTGGAGCGTTTCTAGCAAGTGAGAGAGATGGGAGCTCCTCTCCTG

                                                                    1771
VIPR1_Ref_seq_mRNA        GAGGATTGCAGGTGGAACTCAGTCATTAGACTCCTCCTCCAAAGGCCCCC
VIPR1_202_by_ensembl      ------------------------------------------------
                                                                    2148
VIPR1_002_by_ensembl      GAGGATTGCAGGTGGAACTCAGTCATTAGACTCCTCCTCCAAAGGCCCCC

                                                                    1821
VIPR1_Ref_seq_mRNA        TACGCCAATCAAGGGCAAAAAGTCTACATACTTTCATCCTGACTCTGCCC
VIPR1_202_by_ensembl      ------------------------------------------------
                                                                    2198
VIPR1_002_by_ensembl      TACGCCAATCAAGGGCAAAAAGTCTACATACTTTCATCCTGACTCTGCCC

                                                                    1871
VIPR1_Ref_seq_mRNA        CCTGCTGGCTCTTCTGCCCAATTGGAGGAAAGCAACCGGTGGATCCTCAA
VIPR1_202_by_ensembl      ------------------------------------------------
                                                                    2248
VIPR1_002_by_ensembl      CCTGCTGGCTCTTCTGCCCAATTGGAGGAAAGCAACCGGTGGATCCTCAA

                                                                    1921
VIPR1_Ref_seq_mRNA        ACAACACTGGTGTGACCTGAGGGCAGAAAGGTTCTGCCCGGGAAGGTCAC
VIPR1_202_by_ensembl      ------------------------------------------------
                                                                    2298
VIPR1_002_by_ensembl      ACAACACTGGTGTGACCTGAGGGCAGAAAGGTTCTGCCCGGGAAGGTCAC

                                                                    1971
VIPR1_Ref_seq_mRNA        CAGCACCAACACCACGGTAGTGCCTGAAATTTCACCATTGCTGTCAAGTT
VIPR1_202_by_ensembl      ------------------------------------------------
                                                                    2348
VIPR1_002_by_ensembl      CAGCACCAACACCACGGTAGTGCCTGAAATTTCACCATTGCTGTCAAGTT

                                                                    2021
VIPR1_Ref_seq_mRNA        CCTTTGGGTTAAGCATTACCACTCAGGCATTTGACTGAAGATGCAGCTCA
VIPR1_202_by_ensembl      ------------------------------------------------
                                                                    2398
VIPR1_002_by_ensembl      CCTTTGGGTTAAGCATTACCACTCAGGCATTTGACTGAAGATGCAGCTCA

                                                                    2071
VIPR1_Ref_seq_mRNA        CTACCCTATTCTCTCTTTACGCTTAGTTATCAGCTTTTTAAAGTGGGTTA
VIPR1_202_by_ensembl      ------------------------------------------------
                                                                    2448
VIPR1_002_by_ensembl      CTACCCTATTCTCTCTTTACGCTTAGTTATCAGCTTTTTAAAGTGGGTTA

                                                                    2121
VIPR1_Ref_seq_mRNA        TTCTGGAGTTTTTGTTTGGAGAGCACACCTATCTTAGTGGTTCCCCACCG
VIPR1_202_by_ensembl      ------------------------------------------------
                                                                    2498
VIPR1_002_by_ensembl      TTCTGGAGTTTTTGTTTGGAGAGCACACCTATCTTAGTGGTTCCCCACCG
```

```
                                                                    2171
VIPR1_Ref_seq_mRNA        AAGTGGACTGGCCCCTGGGTCAGTCTGGTGGGAGGACGGTGCAACCCAAG
VIPR1_202_by_ensembl      ------------------------------------------------
                                                                    2548
VIPR1_002_by_ensembl      AAGTGGACTGGCCCCTGGGTCAGTCTGGTGGGAGGACGGTGCAACCCAAG


                                                                    2221
VIPR1_Ref_seq_mRNA        GACTGAGGGACTCTGAAGCCTCTGGGAAATGAGAAGGCAGCCACCAGCGA
VIPR1_202_by_ensembl      ------------------------------------------------
                                                                    2598
VIPR1_002_by_ensembl      GACTGAGGGACTCTGAAGCCTCTGGGAAATGAGAAGGCAGCCACCAGCGA


                                                                    2271
VIPR1_Ref_seq_mRNA        ATGCTAGGTCTCGGACTAAGCCTACCTGCTCTCCAAGTCTCAGTGGCTTC
VIPR1_202_by_ensembl      ------------------------------------------------
                                                                    2648
VIPR1_002_by_ensembl      ATGCTAGGTCTCGGACTAAGCCTACCTGCTCTCCAAGTCTCAGTGGCTTC


                                                                    2321
VIPR1_Ref_seq_mRNA        ATCTGTCAAGTGGGATCTGTCACACCAGCCATACTTATCTCTCTGTGCTG
VIPR1_202_by_ensembl      ------------------------------------------------
                                                                    2698
VIPR1_002_by_ensembl      ATCTGTCAAGTGGGATCTGTCACACCAGCCATACTTATCTCTCTGTGCTG


                                                                    2371
VIPR1_Ref_seq_mRNA        TGGAAGCAACAGGAATCAAGAGCTGCCCTCCTTGTCCACCCACCTATGTG
VIPR1_202_by_ensembl      ------------------------------------------------
                                                                    2748
VIPR1_002_by_ensembl      TGGAAGCAACAGGAATCAAGAGCTGCCCTCCTTGTCCACCCACCTATGTG


                                                                    2421
VIPR1_Ref_seq_mRNA        CCAACTGTTGTAACTAGGCTCAGAGATGTGCACCCATGGGCTCTGACAGA
VIPR1_202_by_ensembl      ------------------------------------------------
                                                                    2798
VIPR1_002_by_ensembl      CCAACTGTTGTAACTAGGCTCAGAGATGTGCACCCATGGGCTCTGACAGA


                                                                    2471
VIPR1_Ref_seq_mRNA        AAGCAGATACCTCACCCTGCTACACATACAGGATTTGAACTCAGATCTGT
VIPR1_202_by_ensembl      ------------------------------------------------
                                                                    2848
VIPR1_002_by_ensembl      AAGCAGATACCTCACCCTGCTACACATACAGGATTTGAACTCAGATCTGT


                                                                    2521
VIPR1_Ref_seq_mRNA        CTGATAGGAATGTGAAAGCACGGACTCTTACTGCTAACTTTTGTGTATCG
VIPR1_202_by_ensembl      ------------------------------------------------
                                                                    2898
VIPR1_002_by_ensembl      CTGATAGGAATGTGAAAGCACGGACTCTTACTGCTAACTTTTGTGTATCG


                                                                    2571
VIPR1_Ref_seq_mRNA        TAACCAGCCAGATCCTCTTGGTTATTTGTTTACCACTTGTATTATTAATG
VIPR1_202_by_ensembl      ------------------------------------------------
                                                                    2948
VIPR1_002_by_ensembl      TAACCAGCCAGATCCTCTTGGTTATTTGTTTACCACTTGTATTATTAATG


                                                                    2621
VIPR1_Ref_seq_mRNA        CCATTATCCCTGAATCCCCCTTGCCACCCCACCCTCCCTGGAGTGTGGCT
VIPR1_202_by_ensembl      ------------------------------------------------
                                                                    2998
VIPR1_002_by_ensembl      CCATTATCCCTGAATCCCCCTTGCCACCCCACCCTCCCTGGAGTGTGGCT
```

```
                                                                      2671
VIPR1_Ref_seq_mRNA        GAGGAGGCCTCCATCTCATGTATCATCTGGATAGGAGCCTGCTGGTCACA
VIPR1_202_by_ensembl      --------------------------------------------------
                                                                      3048
VIPR1_002_by_ensembl      GAGGAGGCCTCCATCTCATGTATCATCTGGATAGGAGCCTGCTGGTCACA


                                                                      2721
VIPR1_Ref_seq_mRNA        GCCTCCTCTGTCTGCCCTTCACCCCAGTGGCCACTCAGCTTCCTACCCAC
VIPR1_202_by_ensembl      --------------------------------------------------
                                                                      3098
VIPR1_002_by_ensembl      GCCTCCTCTGTCTGCCCTTCACCCCAGTGGCCACTCAGCTTCCTACCCAC


                                                                      2771
VIPR1_Ref_seq_mRNA        ACCTCTGCCAGAAGATCCCCTCAGGACTGCAACAGGCTTGTGCAACAATA
VIPR1_202_by_ensembl      --------------------------------------------------
                                                                      3148
VIPR1_002_by_ensembl      ACCTCTGCCAGAAGATCCCCTCAGGACTGCAACAGGCTTGTGCAACAATA


                           2773 + poly-A tail signal and tail
VIPR1_Ref_seq_mRNA        AA|TGTTGGCTTGGATTGGCAAAAAAAAAAAAAAAAAA
VIPR1_202_by_ensembl      ---------------------------------------
                                     3161
VIPR1_002_by_ensembl      AATGTTGGCTTGG-------------------------
```

Appendix II: Full list of pathways identified by IPA and DAVID

Ingenuity Pathway Analysis (IPA):

Ingenuity Canonical Pathways	-Log (P-value)	Ratio
Complement System	4.1E00	1.52E-01
VDR/RXR Activation	1.67E00	5.19E-02
Pantothenate and CoA Biosynthesis	1.65E00	9.09E-02
Starch and Sucrose Metabolism	1.65E00	4.65E-02
Hepatic Fibrosis / Hepatic Stellate Cell Activation	1.55E00	3.97E-02
Riboflavin Metabolism	1.52E00	8E-02
Cell Cycle: G1/S Checkpoint Regulation	1.42E00	5.56E-02
Wnt/β-catenin Signaling	1.23E00	3.12E-02
Role of Pattern Recognition Receptors in Recognition of Bacteria and Viruses	1.04E00	3.85E-02
Galactose Metabolism	9.82E-01	6.12E-02
Pentose and Glucuronate Interconversions	9.82E-01	4.44E-02
Nucleotide Sugars Metabolism	8.16E-01	6.67E-02
Human Embryonic Stem Cell Pluripotency	7.01E-01	2.5E-02
Basal Cell Carcinoma Signaling	6.8E-01	3.08E-02
GM-CSF Signaling	6.8E-01	3.23E-02
Androgen and Estrogen Metabolism	6.59E-01	3.75E-02
Small Cell Lung Cancer Signaling	6.12E-01	2.9E-02
Aminophosphonate Metabolism	5.99E-01	6.25E-02
Acute Myeloid Leukemia Signaling	5.94E-01	2.74E-02
Pyrimidine Metabolism	5.66E-01	1.97E-02
TGF-β Signaling	5.22E-01	2.5E-02
Biosynthesis of Steroids	5.2E-01	3.33E-02
Sonic Hedgehog Signaling	4.93E-01	3.45E-02
Interferon Signaling	4.81E-01	3.45E-02
Neuregulin Signaling	4.8E-01	2.3E-02
Fcγ Receptor-mediated Phagocytosis in Macrophages and Monocytes	4.55E-01	2.13E-02
PTEN Signaling	4.55E-01	2.17E-02
Nicotinate and Nicotinamide Metabolism	4.49E-01	2.06E-02
Glycosaminoglycan Degradation	4.47E-01	5.56E-02
cAMP-mediated Signaling	4.46E-01	1.9E-02
Chronic Myeloid Leukemia Signaling	4.43E-01	2.17E-02
Cell Cycle Regulation by BTG Family Proteins	4.26E-01	2.86E-02
Notch Signaling	4.26E-01	2.7E-02
Glioma Signaling	4.25E-01	2.11E-02
Allograft Rejection Signaling	4.16E-01	2.7E-02
Retinol Metabolism	4.16E-01	2.56E-02
IL-8 Signaling	4.11E-01	1.82E-02
Calcium Signaling	3.99E-01	1.75E-02
T Helper Cell Differentiation	3.97E-01	2.63E-02
Oncostatin M Signaling	3.97E-01	2.7E-02
Autoimmune Thyroid Disease Signaling	3.97E-01	2.56E-02
Acute Phase Response Signaling	3.95E-01	1.79E-02

Thyroid Cancer Signaling	3.88E-01	2.33E-02
Graft-versus-Host Disease Signaling	3.8E-01	2.5E-02
Glucocorticoid Receptor Signaling	3.68E-01	1.6E-02
Role of PKR in Interferon Induction and Antiviral Response	3.64E-01	2.44E-02
Melanoma Signaling	3.56E-01	2.38E-02
Type II Diabetes Mellitus Signaling	3.5E-01	1.8E-02
Chondroitin Sulfate Biosynthesis	3.48E-01	2.13E-02
Role of RIG1-like Receptors in Antiviral Innate Immunity	3.48E-01	2.27E-02
Fructose and Mannose Metabolism	3.48E-01	1.92E-02
Androgen Signaling	3.36E-01	1.74E-02
Integrin Signaling	3.33E-01	1.57E-02
LPS/IL-1 Mediated Inhibition of RXR Function	3.3E-01	1.61E-02
Glycerophospholipid Metabolism	3.28E-01	1.55E-02
Cardiac β-adrenergic Signaling	3.28E-01	1.68E-02
Molecular Mechanisms of Cancer	3.21E-01	1.49E-02
β-alanine Metabolism	3.01E-01	2E-02
Role of Cytokines in Mediating Communication between Immune Cells	2.9E-01	1.89E-02
Endometrial Cancer Signaling	2.9E-01	1.92E-02
Semaphorin Signaling in Neurons	2.79E-01	1.82E-02
Aryl Hydrocarbon Receptor Signaling	2.62E-01	1.5E-02
Aminosugars Metabolism	2.58E-01	1.56E-02
Death Receptor Signaling	2.53E-01	1.69E-02
Ubiquinone Biosynthesis	2.48E-01	2.82E-02
Activation of IRF by Cytosolic Pattern Recognition Receptors	2.39E-01	1.59E-02
Tight Junction Signaling	2.37E-01	1.3E-02
Non-Small Cell Lung Cancer Signaling	2.27E-01	1.54E-02
Growth Hormone Signaling	2.22E-01	1.52E-02
LXR/RXR Activation	2.15E-01	1.45E-02
Agrin Interactions at Neuromuscular Junction	2.11E-01	1.45E-02
Sphingolipid Metabolism	2.07E-01	2.41E-02
Melatonin Signaling	2.03E-01	1.41E-02

Database for Annotation, Visualization and Integrated Discovery (DAVID)

Term	Count	ratio	p Value
complement activation, classical pathway	5	0.02439	0.00099
humoral immune response mediated by circulating immunoglobulin	5	0.02439	0.00130
immunoglobulin mediated immune response	6	0.02927	0.00159
B cell mediated immunity	6	0.02927	0.00188
negative regulation of granulocyte differentiation	3	0.01463	0.00251
complement activation	5	0.02439	0.00316
activation of plasma proteins involved in acute inflammatory response	5	0.02439	0.00348
acute inflammatory response	7	0.03415	0.00370
membrane depolarization	5	0.02439	0.00497
lymphocyte mediated immunity	6	0.02927	0.00507
regulation of granulocyte differentiation	3	0.01463	0.00516
positive regulation of protein kinase cascade	9	0.04390	0.00550
response to nutrient	8	0.03902	0.00731

adaptive immune response	6	0.02927	0.00762
adaptive immune response based on somatic recombination of immune receptors built from immunoglobulin superfamily domains	6	0.02927	0.00762
response to extracellular stimulus	10	0.04878	0.00895
locomotory behavior	11	0.05366	0.01064
leukocyte mediated immunity	6	0.02927	0.01205
inflammatory response	12	0.05854	0.01366
response to nutrient levels	9	0.04390	0.01382
defense response	18	0.08780	0.01423
activation of immune response	6	0.02927	0.01514
regulation of cell proliferation	22	0.10732	0.01517
negative regulation of defense response	4	0.01951	0.01854
positive regulation of signal transduction	11	0.05366	0.01987
negative regulation of smooth muscle cell proliferation	3	0.01463	0.02075
response to vitamin	5	0.02439	0.02180
innate immune response	7	0.03415	0.02215
response to organic substance	20	0.09756	0.02230
regulation of transcription	53	0.25854	0.02242
regulation of hormone secretion	5	0.02439	0.02290
monosaccharide metabolic process	9	0.04390	0.02527
positive regulation of transport	9	0.04390	0.02700
regulation of insulin secretion	4	0.01951	0.02815
protein processing	6	0.02927	0.02948
negative regulation of myeloid leukocyte differentiation	3	0.01463	0.03005
negative regulation of cell proliferation	12	0.05854	0.03130
humoral immune response	5	0.02439	0.03291
positive regulation of insulin secretion	3	0.01463	0.03345
positive regulation of response to stimulus	9	0.04390	0.03467
regulation of homeostatic process	6	0.02927	0.03608
regulation of locomotion	8	0.03902	0.03614
positive regulation of cell communication	11	0.05366	0.03692
chemotaxis	7	0.03415	0.03867
taxis	7	0.03415	0.03867
regulation of peptide secretion	4	0.01951	0.03994
regulation of interleukin-1 beta production	3	0.01463	0.04068
protein maturation	6	0.02927	0.04094
response to wounding	15	0.07317	0.04116
protein maturation by peptide bond cleavage	5	0.02439	0.04185
negative regulation of cell communication	9	0.04390	0.04290
transcription	43	0.20976	0.04486
regulation of protein kinase cascade	9	0.04390	0.04709
regulation of interleukin-1 production	3	0.01463	0.04843
positive regulation of glucose transport	3	0.01463	0.04843
positive regulation of glucose import	3	0.01463	0.04843
negative regulation of multicellular organismal process	7	0.03415	0.04981
immune response	17	0.08293	0.04983
protein heterooligomerization	4	0.01951	0.05138
positive regulation of peptide secretion	3	0.01463	0.05250

immune effector process	6	0.02927	0.05781
negative regulation of secretion	4	0.01951	0.05893
regulation of cell morphogenesis	6	0.02927	0.05937
negative regulation of signal transduction	8	0.03902	0.05988
response to drug	8	0.03902	0.05988
UDP-glucuronate metabolic process	2	0.00976	0.06300
response to endogenous stimulus	12	0.05854	0.06309
positive regulation of phosphorylation	5	0.02439	0.06549
response to hypoxia	6	0.02927	0.06754
positive regulation of phosphorus metabolic process	5	0.02439	0.07176
positive regulation of phosphate metabolic process	5	0.02439	0.07176
positive regulation of I-kappaB kinase/NF-kappaB cascade	5	0.02439	0.07176
cellular defense response	4	0.01951	0.07258
regulation of multicellular organism growth	4	0.01951	0.07258
negative regulation of locomotion	4	0.01951	0.07546
positive regulation of immune response	6	0.02927	0.07812
response to oxygen levels	6	0.02927	0.07812
uronic acid metabolic process	2	0.00976	0.07812
glucuronate metabolic process	2	0.00976	0.07812
negative regulation of macrophage differentiation	2	0.00976	0.07812
negative regulation of myeloid cell differentiation	3	0.01463	0.07916
regulation of epithelial cell differentiation	3	0.01463	0.07916
negative regulation of cell motion	4	0.01951	0.08138
negative regulation of inflammatory response	3	0.01463	0.08394
positive regulation of immune system process	8	0.03902	0.08503
hexose metabolic process	7	0.03415	0.08504
cell cycle arrest	5	0.02439	0.08517
response to steroid hormone stimulus	7	0.03415	0.08905
regulation of cell motion	7	0.03415	0.09284
regulation of myelination	2	0.00976	0.09300
positive regulation of growth hormone secretion	2	0.00976	0.09300
regulation of I-kappaB kinase/NF-kappaB cascade	5	0.02439	0.09475
response to retinoic acid	3	0.01463	0.09879
regulation of glucose import	3	0.01463	0.09879

Appendix III: List of clone sequences found in CD161- and/or CD161+ Treg by CDR3 cloning and sequencing of TCR-Vβ2

(nucleotide over protein sequence), first bold sequence: end of TCR-Vβ2 specific region in bold, then non-bold N region, followed by specific J region (TRBJ, annotated in bold and C region (TRBC, annotated) non-bold.

TCR-VB2 N-Region	J region (TRBJ)	C region (TCRBC)	161- Treg	161+ Treg
ATC TGC AGT GCG TAC CCG GGA CTA GCG GGA GGG CAA AGG CGG GAC	**GAG CAG TAC TTC GGG CCG GGC** G^	**CC AGG CTC ACG GTC ACA** GAG GAC CTG AAA AAC	3 ^	
-I- -C- -S- -A- -Y- -P- -G- -L- -A- -G- -G- -Q- -R- -R- -D-	**-E- -Q- -Y- -F- -G- -P- -G-** -A-^	**-R- -L- -T- -V- -T-** -E- -D- -L- -K- -N-		
ACC TGC AGT GCG TAC CCG GGA CTA GCG GGA GGG CAA AGG CGG GAC	**GAG CAG TAC TTC GGG CCG GGC** G^	**CC AGG CTC ACG GTC ACA** GAG GAC CTG AAA AAC	2 ^	
-T- -C- -S- -A- -Y- -P- -G- -L- -A- -G- -G- -Q- -R- -R- -D-	**-E- -Q- -Y- -F- -G- -P- -G-** -A-^	**-R- -L- -T- -V- -T-** -E- -D- -L- -K- -N-		
ATC TGC AGT GCG TAC CCG TGA$ CTA GCG GGA GGG CAA AGG CGG GAC	**GAG CAG TAC TTC GGG CCG GGC ACC AGG CTC ACG GTC ACA**	GAG GAC CTG AAA AAC	4 $	
-I- -C- -S- -A- -Y- -P- -*-$ -L- -A- -G- -G- -Q- -R- -R- -D-	**-E- -Q- -Y- -F- -G- -P- -G- -T- -R- -L- -T- -V- -T-**	-E- -D- -L- -K- -N-		
ATC TGC AGT GCG GAT CCC GGG ACT AGC GGG ACC	**AAT GAG CAG TTC TTC GGG CCA GGG ACA CGG CTC ACC GTG CTA**	GAG GAC CTG AAA AAC		3
-I- -C- -S- -A- -D- -P- -G- -T- -S- -G- -T-	**-N- -E- -Q- -F- -F- -G- -P- -G- -T- -R- -L- -T- -V- -L-**	-E- -D- -L- -K- -N-		
ATG TGC AGT GCT AGA GAC ACA GGG GGC TGG GGG	**TAC GAG CAG TAC TTC GGG CCG GGC ACC AGG CTC ACG GTC ACA**	GAG GAC CTG AAA AAC		4
-I- -C- -S- -A- -R- -D- -T- -G- -G- -W- -G-	**-Y- -E- -Q- -Y- -F- -G- -P- -G- -T- -R- -L- -T- -V- -T-**	-E- -D- -L- -K- -N-		
ATC TGC AGT GCT AAG GGC CAG CGA TCG AGG	**AGC TAC GAG CAG TAC TTC GGG CCG GGC ACC AGG CTC ACG GTC ACA**	GAG GAC CTG AAA AAC		8
-I- -C- -S- -A- -K- -G- -Q- -R- -S- -R-	**-S- -Y- -E- -Q- -Y- -F- -G- -P- -G- -T- -R- -L- -T- -V- -T-**	-E- -D- -L- -K- -N-		
ATC TGC AGT GCT AGA CAT GAC CTT GAT GTC	**TAC GAG CAG TAC TTC GGG CCG GGC ACC AGG CTC ACG GTC ACA**	GAG GAC CTG AAA AAC		2
-I- -C- -S- -A- -R- -H- -D- -L- -D- -V-	**-Y- -E- -Q- -Y- -F- -G- -P- -G- -T- -R- -L- -T- -V- -T-**	-E- -D- -L- -K- -N-		
ATC TGC AGT GCT AGA GAG GGT TTC ATG TTA	**TAT GGC TAV ACC TTC GGT TCG GGG ACC AGG TTA ACC GTT GTA**	GAG GAC CTA AAC AAG	4	
-I- -C- -S- -A- -R- -E- -G- -F- -M- -L-	**-Y- -G- -Y- -T- -F- -G- -S- -G- -T- -R- -L- -T- -V- -V-**	-E- -D- -L- -K- -N-		
ATC TGC AGT GCC AGA GAT ACC ATT	**TAT GGC TAC ACC TTC GGT TCG GGG ACC AGG TTA ACC GTT GTA**	GAG GAC CTG AAC AAG	4	
-I- -C- -S- -A- -R- -D- -T- -I-	**-Y- -G- -Y- -T- -F- -G- -S- -G- -T- -R- -L- -T- -V- -V-**	-E- -D- -L- -N- -K-		
ATC TGC AGT GCT AGT TCC ACC GGG TCC CTT	**GGC TAC ACC TTC GGT TCG GGG ACC AGG TTA ACC GTT GTA**	GAG GAC CTG AAC AAG	6	
-I- -C- -S- -A- -S- -S- -T- -G- -S- -L-	**-G- -Y- -T- -F- -G- -S- -G- -T- -R- -L- -T- -V- -V-**	-E- -D- -L- -N- -K-		
ATC TGC AGT GCT AGA ACA GGA GCC	**AAT GAA AAA CTG TTT TTT GGC AGT GGA ACC CAG CTC TCT GTC TTG**	GAG GAC CTG AAC AAG	6	
-I- -C- -S- -A- -R- -T- -G- -A-	**-N- -E- -K- -L- -F- -F- -G- -S- -G- -T- -Q- -L- -S- -V- -L-**	-E- -D- -L- -N- -K-		
ATC TGC AGT GCT GGC CTT AAA GTC CCG TCC GAT	**GAG CAG TTC TTC GGG CCA GGG ACA CGC CTC ACC GTG CTA**	GAG GAC CTG AAA AAC		4
-I- -C- -S- -A- -G- -L- -K- -V- -P- -S- -D-	**-E- -Q- -F- -F- -G- -P- -G- -T- -R- -L- -T- -V- -L-**	-E- -D- -L- -K- -N-		
ATC TGC AGT GCC AGA GAT ACC ATT	**TAT GGC TAC ACC TTC GGT TCG GGG ACC AGG TTA ACC GTT GTA**	GAG GAC CTG AAC AAG	3	
-I- -C- -S- -A- -R- -D- -T- -I-	**-Y- -G- -Y- -T- -F- -G- -S- -G- -T- -R- -L- -T- -V- -V-**	-E- -D- -L- -K- -N-		
ATC TGC AGT GCT ATT TCA GGG ACC AAG AAT	**GGC TAC ACC TTC GGT TCG GGG ACC AGG TTA ACG GTT GTA**	GAG GAC CTG AAC AAG		4
-I- -C- -S- -A- -I- -S- -G- -T- -K- -N-	**-G- -Y- -T- -F- -G- -S- -G- -T- -R- -L- -T- -V- -V-**	-E- -D- -L- -N- -K-		
ATC TGC AGT GCA GCG GGG ACA GCC	**TAT GGC TAC ACC TTC GGT TCG GGG ACC AGG TTA ACC GTT GTA**	GAG GAC CTG AAC AAG		4
-I- -C- -S- -A- -A- -G- -T- -A-	**-Y- -G- -Y- -T- -F- -G- -S- -G- -T- -R- -L- -T- -V- -V-**	-E- -D- -L- -N- -K-		
ATC TGC AGT CTC CCT CCG GGC AGG	**AGC AAT CAG CCC CAG CAT TTT GGT GAT GGG ACT CGA CTC TCC ATC CYA**	GAG GAC CTG AAC AAG		5
-I- -C- -S- -L- -P- -P- -G- -R-	**-S- -N- -Q- -P- -Q- -H- -F- -G- -D- -G- -T- -R- -L- -S- -I- -L-**	-E- -D- -L- -N- -K-		
ATC TGC AGT GCT AGA GGA GGT CCC	**ACA GAT ACG CAG TAT TTT GGC CCA GGC ACC CGG CTG ACA GTG CTC**	GAG GAC CTG AAA AAC	3	
-I- -C- -S- -A- -R- -G- -G- -P-	**-T- -D- -T- -Q- -Y- -F- -G- -P- -G- -T- -R- -L- -T- -V- -L-**	-E- -D- -L- -K- -N-		
ATC TGC AGT GCT AGA GCG ACA GGG CCA	**GAT ACG CAG TAT TTT GGC CCA GGC ACC CGG CTG ACA GTG CTC**	GAG GAC CTG AAA AAC		4
-I- -C- -S- -A- -R- -A- -T- -G- -P-	**-D- -T- -Q- -Y- -F- -G- -P- -G- -T- -R- -L- -T- -V- -L-**	-E- -D- -L- -K- -N-		
ATC TGC AGT TGG ACT AGC GGG AGG GCC CGC	**ACA GAT ACG CAG TAT TTT GGC CCA GGC ACC CGG CTG ACA GTG CTC**	GAG GAC CTG AAA AAC		2
-I- -C- -S- -W- -T- -S- -G- -R- -A- -R-	**-T- -D- -T- -Q- -Y- -F- -G- -P- -G- -T- -R- -L- -T- -V- -L-**	-E- -D- -L- -K- -N-		
ATC TGC AGT GCT GGT AGC GGG CGG GGC GTC	**TAC AAT GAG CAG TTC TTC GGG CCA GGG ACA CGG CTC ACC GTG CTA**	GAG GAC CTG AAA AAC		3
-I- -C- -S- -A- -G- -S- -G- -R- -G- -V-	**-Y- -N- -E- -Q- -F- -F- -G- -P- -G- -T- -R- -L- -T- -V- -L-**	-E- -D- -L- -K- -N-		
ATC TGC AGT GCT AGC ACT AGC GGG AGA GGG	**ACA GAT ACG CAG TAT TTT GGC CCA GGC ACC CGG CTG ACA GTG CTC**	GAG GAC CTG AAA AAC	8	
-I- -C- -S- -A- -S- -T- -S- -G- -R- -G-	**-T- -D- -T- -Q- -Y- -F- -G- -P- -G- -T- -R- -L- -T- -V- -L-**	-E- -D- -L- -K- -N-		
ATC TGC AGT GCT TCC CTA GGA TCT TTA CGT AAA	**GAT ACG CAG TAT TTT GGC CCA GGC ACC CGG CTG ACA GTG CTC**	GAG GAC CTG AAA AAC	4	
-I- -C- -S- -A- -S- -L- -G- -S- -L- -R- -K-	**-D- -T- -Q- -Y- -F- -G- -P- -G- -T- -R- -L- -T- -V- -L-**	-E- -D- -L- -K- -N-		
ATC TGC AGT GCT ATT CTC GGA GCG AGT	**AGC ACA GAT ACG CAG TAT TTT GGC CCA GGC ACC CGG CTG ACA GTG CTC**	GAG GAC CTG AAA AAC	2	
-I- -C- -S- -A- -I- -L- -G- -A- -S-	**-S- -T- -D- -T- -Q- -Y- -F- -G- -P- -G- -T- -R- -L- -T- -V- -L-**	-E- -D- -L- -K- -N-		
ATC TGC AGT GCT CGG ACA CTA GCG GGA GGC	**ACA GAT ACG CAG TAT TTT GGC CCA GGC ACC CGG CTG ACA GTG CTC**	GAG GAC CTG AAA AAC	6	
-I- -C- -S- -A- -R- -T- -L- -A- -G- -G-	**-T- -D- -T- -Q- -Y- -F- -G- -P- -G- -T- -R- -L- -T- -V- -L-**	-E- -D- -L- -K- -N-		
ATC TGC AGT GCC GAA GCG CCG GGA CGA	**AAA AAC ATT CAG TAC TTC GGC GCC GGG ACC CGG CTC TCA GTG CTG**	GAG GAC CTG AAA AAC	4	
-I- -C- -S- -A- -E- -A- -P- -G- -R-	**-K- -N- -I- -Q- -Y- -F- -G- -A- -G- -T- -R- -L- -S- -V- -L-**	-E- -D- -L- -K- -N-		

^ apparent allelic polymorphism; alternative PCR error

$ possible non-coding transcript; alternative PCR error

TCR-VB2 N-Region	J region (TRBJ) C region (TCRBC)	161- Treg	161+ Treg
ATC TGC AGT GCC GAA GCG CCG GGA CGA AAA AAC GTT **CAG TAC TTC GGC GCC GGG ACC CGG CTC TCA GTG CTG** GAG GAC CTG AAA AAC **-I- -C- -S- -A-** -E- -A- -P- -G- -R- -K- -N- -V- **-Q- -Y- -F- -G- -A- -G- -T- -R- -L- -S- -V- -L-** -E- -D- -L- -K- -N-	**TRBJ2.4** TCRBC2	2	
ATC TGC AGT GCT GGC CTT AAA GTC CCG TCC GAT **GAG CAG TTC TTC GGG CCA GGG ACA CGG CTC ACC GTG CTA** GAG GAC CTG AAA AAC **-I- -C- -S- -A-** -G- -L- -K- -V- -P- -S- -D- **-E- -Q- -F- -F- -G- -P- -G- -T- -R- -L- -T- -V- -L-** -E- -D- -L- -K- -N-	**TRBJ2.1** TCRBC2		4
ATC TGC AGT GCT AGA GAC CAC GGG ACT AGC ATC **AAT GAG CAG TTC TTC GGG CCA GGG ACA CGG CTC ACC GTG CTA** GAG GAC CTG AAA AAC **-I- -C- -S- -A- -R-** -D- -H- -G- -T- -S- -I- **-N- -E- -Q- -F- -F- -G- -P- -G- -T- -R- -L- -T- -V- -L-** -E- -D- -L- -K- -N-	**TRBJ2.1** TCRBC2	3	
ATC TGC AGT GCC CCG ACG GGG GGA **TAC GAG CAG TAC TTC GGG CCG GGC ACC AGG CYC ACG GTC ACA** GAG GAC CTG AAA AAC **-I- -C- -S- -A-** -P- -T- -G- -G- **-Y- -E- -Q- -Y- -F- -G- -P- -G- -T- -R- -L- -T- -V- -T-** -E- -D- -L- -K- -N-	**TRBJ2.7** TCRBC2	1*	5*
ATC TGC AGT GCT CCC GAG CCC TCC AAC CCC CGA **GAT ACG CAG TAT TTT GGC CCA GGC ACC CGG CTG ACA GTG CTC** GAG GAC CTG AAA AAC **-I- -C- -S- -A-** -P- -E- -P- -S- -N- -P- -R- **-D- -T- -Q- -Y- -F- -G- -P- -G- -T- -R- -L- -T- -V- -L-** -E- -D- -L- -K- -N-	**TRBJ2.3** TCRBC2	3*	2*
ATC TGC AGT GCT AGA GCC GTC CCA GTC ATG **AAC ACT GAA GCT TTC TTT GGA CAA GGC ACC A**A^**A CTC ACA GTT GTA** GAG GAC CTG AAC AAG **-I- -C- -S- -A- -R-** -A- -V- -P- -V- -M- **-N- -T- -E- -A- -F- -F- -G- -Q- -G- -T-** -K-^ **-L- -T- -V- -V-** -E- -D- -L- -N- -K-	**TRBJ1.1** TCRBC1		2 ^
ATC TGC AAT GCG AGC GGG GTC TTG **AAC ACT GAA GCT TTC TTT GGA CAA GGC ACC AGA CTC ACA G**A^**T GTA** GAG GAC CTG AAC AAG **-I- -C-** -N- -A- -S- -G- -V- -L- **-N- -T- -E- -A- -F- -F- -G- -Q- -G- -T- -R- -L- -T-** -D-^ **-V-** -E- -D- -L- -N- -K-	**TRBJ1.1** TCRBC1	2 ^	
ATC TGC AGT GCT GGT AGC GGG CGG GGC GTC **TAC AAT GAG CAG TTC TTC GGG CCA GGG ACA CGG CTC ACC GTG CTA** GAG GAC CTG AAA AAC **-I- -C- -S- -A-** -G- -S- -G- -R- -G- -V- **-Y- -N- -E- -Q- -F- -F- -G- -P- -G- -T- -R- -L- -T- -V- -L-** -E- -D- -L- -K- -N-	**TRBJ2.1** TCRBC2		3
ATC TGC AGT GCG AGC GGG GTC TTG **AAC ACT GAA GCT TTC TTT GGA CAA GGC ACC AGA CTC ACA GTT GTA** GAG GAC CTG AAC AAG **-I- -C- -S- -A-** -S- -G- -V- -L- **-N- -T- -E- -A- -F- -F- -G- -Q- -G- -T- -R- -L- -T- -V- -V-** -E- -D- -L- -N- -K-	**TRBJ1.1** TCRBC1	5	
ATC TGC AGT GCT TTC GGA CAG GGG **AAC ACT GAA GCT** C^**TC TTT GGA CAA GGC ACC AGA CTC ACA GTT GTA** GAG GAC CTG AAC AAG **-I- -C- -S- -A-** -F- -G- -Q- -G- **-N- -T- -E- -A-** -L-^ **-F- -G- -Q- -G- -T- -R- -L- -T- -V- -V-** -E- -D- -L- -N- -K-	**TRBJ1.1** TCRBC1		4 ^
ATC TGC AGT GCT AGA TCC GCT AGC GGG GCC **TAC AAT GAG CAG TTC TTC GGG CCA GGG ACA CGG CTC ACC GTG CTA** GAG GAC CTG AAA AAC **-I- -C- -S- -A- -R-** -S- -A- -S- -G- -A- **-Y- -N- -E- -Q- -F- -F- -G- -P- -G- -T- -R- -L- -T- -V- -L-** -E- -D- -L- -K- -N-	**TRBJ2.1** TCRBC2		4
ATC TGC AGT GCT AGA GAC CAC GGG ACT AGC ATC **AAT GAG CAG TTC TTC GGG CCA GGG ACA CGG CTC ACC GTG CTA** GAG GAC CTG AAA AAC **-I- -C- -S- -A- -R-** -D- -H- -G- -T- -S- -I- **-N- -E- -Q- -F- -F- -G- -P- -G- -T- -R- -L- -T- -V- -L-** -E- -D- -L- -K- -N-	**TRBJ2.1** TCRBC2	4	
ATC TGC AGC GAG CAA CGG GAG GTC AAC **AAT GAG CAG TTC TTC GGG CCA GGG ACA CGG CTC ACC GTG CTA** GAG GAC CTG AAA AAC **-I- -C- -S-** -E- -Q- -R- -E- -V- -N- **-N- -E- -Q- -F- -F- -G- -P- -G- -T- -R- -L- -T- -V- -L-** -E- -D- -L- -K- -N-	**TRBJ2.1** TCRBC2		7
ATC TGC AGT GCT GCC AAG CGG GAG GGC CAC TTC **TCT GGG GCC AAC GTC CTG ACT TTC GGG GCC GGC AGC AGG CTG ACC GTG CTG** GAG GAC CTG AAA AAC **-I- -C- -S- -A-** -A- -K- -R- -E- -G- -H- -F- **-S- -G- -A- -N- -V- -L- -T- -F- -G- -A- -G- -S- -R- -L- -T- -V- -L-** -E- -D- -L- -K- -N-	**TRBJ2.6** TCRBC2		2
ATC TGC AGT GCT AGT ACT AGC GGG AGG GCA AGG GTG **AAC ACC GGG GAG CTG TTT TTT GGA GAA GGC TCT AGG CTG ACC GTA CTG** GAG GAC CTG AAA AAC **-I- -C- -S- -A-** -S- -T- -S- -G- -R- -A- -R- -V- **-N- -T- -G- -E- -L- -F- -F- -G- -E- -G- -S- -R- -L- -T- -V- -L-** -E- -D- -L- -K- -N-	**TRBJ2.2** TCRBC2		4
ATC TGC AGT GCT AGA GCA GCC GGG GGA CGG ACA GGG GTT **ACC GGG GAG CTG TTT TTT GGA GAA GGC TCT AGG CTG ACC GTA CTG** GAG GAC CTG AAA AAC **-I- -C- -S- -A- -R-** -A- -A- -G- -G- -R- -T- -G- -V- **-T- -G- -E- -L- -F- -F- -G- -E- -G- -S- -R- -L- -T- -V- -L-** -E- -D- -L- -K- -N-	**TRBJ2.2** TCRBC2	3	
ATC TGC AGT GCT AGA CAT GAC CTT GAT GTC **TAC GAG CAG TAC TTC GGG CCG GGC ACC AGG CTC ACG GTC ACA** GAG GAC CTG AAA AAC **-I- -C- -S- -A- -R-** -H- -D- -L- -D- -V- **-Y- -E- -Q- -Y- -F- -G- -P- -G- -T- -R- -L- -T- -V- -T-** -E- -D- -L- -K- -N-	**TRBJ2.7** TCRBC2		2
ATC TGC AGT GCG TAC CCG TGA$ CTA GCG GGA GGG CAA AGG CGG GAC **GAG CAG TAC TTC GGG CCG GGC ACC AGG CTC ACG GTC ACA** GAG GAC CTG AAA AAC **-I- -C- -S- -A-** -Y- -P- -*-$ -L- -A- -G- -G- -Q- -R- -R- -D- **-E- -Q- -Y- -F- -G- -P- -G- -T- -R- -L- -T- -V- -T-** -E- -D- -L- -K- -N-	**TRBJ2.7** TCRBC2	4 $	
ATC TGC AGT GCG TACCCG GGA CTA GCG GGA GGG CAA AGG CGG GAC **GAG CAG TAC TTC GGG CCG GGC** G^**CC AGG CTC ACG GTC ACA** GAG GAC CTG AAA AAC **-I- -C- -S- -A-** -Y- -P- -G- -L- -A- -G- -G- -Q- -R- -R- -D- **-E- -Q- -Y- -F- -G- -P- -G-** -A-^ **-R- -L- -T- -V- -T-** -E- -D- -L- -K- -N-	**TRBJ2.7** TCRBC2	2 ^	
ATC TGC AGT GCT AGA GCC CGT GCC **TAC GAG CAG TAC TTC GGG CCG GGC ACC AGG CTC ACG GTC ACA** GAG GAC CTG AAA AAC **-I- -C- -S- -A- -R-** -A- -R- -A- **-Y- -E- -Q- -Y- -F- -G- -P- -G- -T- -R- -L- -T- -V- -T-** -E- -D- -L- -K- -N-	**TRBJ2.7** TCRBC2	12	
ATC TGC AGT GCT AGA GAA GCG GGA GGG TGG GCA **GAT ACG CAG TAT TTT GGC CCA GGC ACC CGG CTG ACA GTG CTC** GAG GAC CTG AAA AAC **-I- -C- -S- -A- -R-** -E- -A- -G- -G- -W- -A- **-D- -T- -Q- -Y- -F- -G- -P- -G- -T- -R- -L- -T- -V- -L-** -E- -D- -L- -K- -N-	**TRBJ2.3** TCRBC2		7
ATC TGC AGT GCC GTA GAG ACA GGG GCC CTC **ACA GAT ACG CAG TAT TTT GGC CCA GGC ACC CGG CTG ACA GTG CTC** GAG GAC CTG AAA AAC **-I- -C- -S- -A-** -V- -E- -T- -G- -A- -L- **-T- -D- -T- -Q- -Y- -F- -G- -P- -G- -T- -R- -L- -T- -V- -L-** -E- -D- -L- -K- -N-	**TRBJ2.3** TCRBC2	6	
ATC TGC AGT GCC CCG ACG GGG GGA TAC GAG **CAG TAC TTC GGG CCA GGG ACA CGG CTC ACC GTG CTA** GAG GAC CTG AAA AAC **-I- -C- -S- -A-** -P- -T- -G- -G- -Y- -E- **-Q- -Y- -F- -G- -P- -G- -T- -R- -L- -T- -V- -L-** -E- -D- -L- -K- -N-	**TRBJ2.3** TCRBC2		2
ATC TGC AGT GCT CAG GGG GGG TCC CTC **CAA GAG ACC CAG TAC TTC GGG CCA GGC ACG CGG CTC CTG GTG CTC** GAG GAC CTG AAA AAC **-I- -C- -S- -A-** -Q- -G- -G- -S- -L- **-Q- -E- -T- -Q- -Y- -F- -G- -P- -G- -T- -R- -L- -L- -V- -L-** -E- -D- -L- -K- -N-	**TRBJ2.5** TCRBC2	2	
ATC TGC AGT GCC ACC ACA GGG ATA CCT **GGA AAC ACC ATA TAT TTT GGA GAG GGA AGT TGG CTC ACT GTT GTA** GAG GAC CTG AAC AAG **-I- -C- -S- -A-** -T- -T- -G- -I- -P- **-G- -N- -T- -I- -Y- -F- -G- -E- -G- -S- -W- -L- -T- -V- -V-** -E- -D- -L- -N- -K-	**TRBJ1.3** TCRBC1		3
ATC TGC AGT GCT AGA CAT GAC CTT GAT GTC **TAC GAG CAG TAC TTC GGG CCG GGC ACC AGG CTC ACG GTC ACA** GAG GAC CTG AAA AAC **-I- -C- -S- -A- -R-** -H- -D- -L- -D- -V- **-Y- -E- -Q- -Y- -F- -G- -P- -G- -T- -R- -L- -T- -V- -T-** -E- -D- -L- -K- -N-	**TRBJ2.7** TCRBC2		2
ATC TGC AGT GCT GCC AAG CGG GAG GGC CAC TTC **TCT GGG GCC AAC GTC CTG ACT TTC GGG GCC GGC AGC AGG CTG ACC GTG CTG** GAG GAC CTG AAA AAC **-I- -C- -S- -A-** -A- -K- -R- -E- -G- -H- -F- **-S- -G- -A- -N- -V- -L- -T- -F- -G- -A- -G- -S- -R- -L- -T- -V- -L-** -E- -D- -L- -K- -N-	**TRBJ2.6** TCRBC2		2
ATC TGC AGT GCT TTC CGC CTC AAA AAT GCT **AAC TAT GGC TAC ACC TTC GGT TCG GGG ACC AGG TTA ACC GTT GTA** GAG GAC CTG AAC AAG **-I- -C- -S- -A-** -F- -R- -L- -K- -N- -A- **-N- -Y- -G- -Y- -T- -F- -G- -S- -G- -T- -R- -L- -T- -V- -V-** -E- -D- -L- -N- -K-	**TRBJ1.2** TCRBC1		2

^ apparent allelic polymorphism ; alternative PCR error

$ possible non-coding transcript; alternative PCR error

* sequence found in cDNA from both CD161- and CD161+ Treg

TCR-VB2 N-Region J region (TRBJ) C region (TCRBC)	161- Treg	161+ Treg
TRBJ2.5 TCRBC2 **ATC TGC AGT GCT AGA** GAT CAG GGG GAG TCC GTA **GAG ACC CAG TAC T**C^**C GGG CCA GGC ACG CGG CTC CTG GTG CTC** GAG GAC CTG AAA AAC -I- -C- -S- -A- -R- -D- -Q- -G- -E- -S- -V- -E- -T- -Q- -Y- -S-^ -G- -P- -G- -T- -R- -L- -L- -V- -L- -E- -D- -L- -K- -N-	2 ^	
TRBJ1.1 TCRBC1 **ATC TGC AGT GCT AGA** GCC GTC CCA GTC ATG **AAC ACT GAA GCT TTC TTT GGA CAA GGC ACC AGA CTC ACA GTT GTA** GAG GAC CTG AAC AAG -I- -C- -S- -A- -R- -A- -V- -P- -V- -M- -N- -T- -E- -A- -F- -F- -G- -Q- -G- -T- -R- -L- -T- -V- -V- -E- -D- -L- -N- -K-		3
TRBJ1.1 TCRBC1 **ATC TGC AGT GCT** ATA CCC TCC GGG ACT AGG GAC **ACT GAA GCT TTC TTT GGA CAA GGC ACC AGA CTC ACA GTT GTA** GAG GAC CTG AAC AAG -I- -C- -S- -A- -I- -P- -S- -G- -T- -R- -D- -T- -E- -A- -F- -F- -G- -Q- -G- -T- -R- -L- -T- -V- -V- -E- -D- -L- -N- -K-		2
TRBJ1.1 TCRBC1 **ATC TGC AGT GCT AGA** GAC ATG GGG ACA GGG TCC GTC **AAC ACT GAA GCT TTC TTT GGA CAA GGC ACC AGA CTC ACA GTT GTA** GAG GAC CTG AAC AAG -I- -C- -S- -A- -R- -D- -M- -G- -T- -G- -S- -V- -N- -T- -E- -A- -F- -F- -G- -Q- -G- -T- -R- -L- -T- -V- -V- -E- -D- -L- -N- -K-		3
TRBJ1.1 TCRBC1 **ATC TGC AGT GCT** AGG GCG ACG GTG **AAC ACT GAA GCT TTC TTT GGA CAA GGC ACC AGA CTC ACA GTT GTA** GAG GAC CTG AAC AAG -I- -C- -S- -A- -R- -A- -T- -V- -N- -T- -E- -A- -F- -F- -G- -Q- -G- -T- -R- -L- -T- -V- -V- -E- -D- -L- -N- -K-		4
TRBJ2.3 TCRBC2 **ATC TGC AGT GCT AGA** CCC CAG TTG AAG **ACG CAG TAT TTT GGC CCA GGC ACC CGG CTG ACA GTG CTC** GAG GAC CTG AAA AAC -I- -C- -S- -A- -R- -P- -Q- -L- -K- -T- -Q- -Y- -F- -G- -P- -G- -T- -R- -L- -T- -V- -L- -E- -D- -L- -K- -N-		4
TRBJ2.3 TCRBC2 **ATC TGC AGT GCT** AGG AGG GCA GGA AAC **ACA GAT ACG CAG TAT TTT GGC CCA GGC ACC CGG CTG ACA GTG CTC** GAG GAC CTG AAA AAC -I- -C- -S- -A- -R- -R- -A- -G- -N- -T- -D- -T- -Q- -Y- -F- -G- -P- -G- -T- -R- -L- -T- -V- -L- -E- -D- -L- -K- -N-		2
TRBJ2.7 TCRBC2 **ATC TGC AGT GCC** GGG ACT AGC GGC CTC **TAC GAG CAG TAC TTC GGG CCG GGC ACC AGG CTC ACG GTC ACA** GAG GAC CTG AAA AAC -I- -C- -S- -A- -G- -T- -S- -G- -L- -Y- -E- -Q- -Y- -F- -G- -P- -G- -T- -R- -L- -T- -V- -T- -E- -D- -L- -K- -N-	2	
TRBJ2.1 TCRBC2 **ATC TGC AGT GCT AGA** CAA ACC GGA CTA GCG GGA GCG AAA **AAT GAG CAG TTC TTC GGG CCA GGG ACA CGG CTC ACC GTG CTA** GAG GAC CTG AAA AAC -I- -C- -S- -A- -R- -Q- -T- -G- -L- -A- -G- -A- -K- -N- -E- -Q- -F- -F- -G- -P- -G- -T- -R- -L- -T- -V- -L- -E- -D- -L- -K- -N-	5	
TRBJ2.3 TCRBC2 **ATC TGC AGT GCT** CGC AGA CTA GCG GGG CTA TCT **AGC ACA GAT ACG CAG TAT TTT GGC CCA GGC ACC CGG CTG ACA GTG CTC** GAG GAC CTG AAA AAC -I- -C- -S- -A- -R- -R- -L- -A- -G- -L- -S- -S- -T- -D- -T- -Q- -Y- -F- -G- -P- -G- -T- -R- -L- -T- -V- -L- -E- -D- -L- -K- -N-	2	
TRBJ2.1 TCRBC2 **ATC TGC AGT GTC** CTC CGA TCA GGG TTA AGG AAT GAT **GAG CAG TTC TTC GGG CCA GGG ACA CGC CTC ACC GTG CTA** GAG GAC CTG AAA AAC -I- -C- -S- -A- -L- -R- -S- -G- -L- -R- -N- -D- -E- -Q- -F- -F- -G- -P- -G- -T- -R- -L- -T- -V- -L- -E- -D- -L- -K- -N-	3	
Total	122	118
additional unique sequences	48	57

^ apparent allelic polymorphism ; alternative PCR error